

**MODELLING, SIMULATION, OPTIMISATION  
AND THERMODYNAMIC ANALYSIS OF  
MULTISTAGE REVERSE OSMOSIS PROCESS  
BASED BRACKISH WATER DESALINATION**

**A. A. Alsarayreh**

**PHD**

**2020**



# **Modelling, Simulation, Optimisation and Thermodynamic Analysis of Multistage Reverse Osmosis Process based Brackish Water Desalination**

Investigates multistage multi pass reverse osmosis process for brackish water desalination using modelling, simulation and optimisation to sustain high performance process with thermodynamic analysis

**Alanood Abdelmajid ALSARAYREH**

Submitted for the Degree of  
Doctor of Philosophy

Faculty of Engineering and Informatics  
University of Bradford  
United Kingdom

*2020*

**Alanood Abdelmajid Alsarayreh**

**Modelling, Simulation, Optimisation and Thermodynamic Analysis of Multistage Reverse Osmosis Process based Brackish Water Desalination**

Investigates multistage multi pass reverse osmosis process for brackish water desalination using modelling, simulation and optimisation to sustain high performance process with thermodynamic analysis

**Keywords:** *Brackish Water Desalination; Multistage Reverse Osmosis; Permeate Reprocessing; Retentate Reprocessing; Modelling; Simulation; Optimisation; Total Energy Consumption; Membrane Type; Thermodynamic analysis.*

**ABSTRACT**

The Reverse Osmosis (RO) process has been considered to be one of the most widely utilised techniques for brackish water desalination for its capabilities to produce high-quality water. The RO process characterised by its low energy consumption compared to thermal distillation processes, leading to reduced overall water production cost.

To systematically understand the transport phenomena of solvent and solutes via the membrane texture, several mathematical models were developed. This interestingly aids to conduct a huge amount of simulation and optimisation studies to judge the influence of control variables on the performance indexes and to adjust the key variables at optimum values to realise optimum production indexes. In this research, a specific accurate model for a single spiral wound RO process has been successfully developed and used to build accurate models for the multistage brackish water RO desalination process of two different designs. The robustness of the model developed was confirmed via validation against the experimental data collected from simple design of RO system and complicated design of RO system of Arab Potash Company (APC). This is followed by a thorough simulation of the RO process to explore the influence of operating conditions on the process performance indicators. Recently, several contributions were made in this thesis that specifically comprises the improvement of the original design of brackish water RO desalination process. The influence of a retentate recycle design is investigated on the process performance. Moreover, evaluation and minimisation of specific energy consumption (expressed in kWh/m<sup>3</sup> of freshwater production) is carried out on the simple and complicated designs of RO process by implementing an energy recovery device. Also, the most suitable brand of membranes was explored for the RO system from a set of different brands of membrane to attain the highest-performance rejection at lowest energy consumption compared to the

original membrane. Furthermore, a single optimisation framework was developed to mitigate the specific energy consumption of simple and complicated designs of brackish water RO desalination process. Finally, a thermodynamic limitations and exergy analysis of the complicated design of RO system are outlined via a thoroughly study to investigate the locations of high exergy destruction. These contributions were verified as they promoted the separation performance at a significant energy saving.

## **Acknowledgment**

**Gratitude is the ground where the seeds of peace grow.**

**To the memory of my father, this thesis is affectionately dedicated.**

Firstly, I am very much grateful to almighty Allah for giving me courage and good health for completing the venture.

I would like to express my sincere gratitude to my supervisor Professor I.M. Mujtaba for his invaluable guidance and advice, continuous co-operation, valuable comments, suggestions, unlimited help and support, and most of all his wisdom, made this project a pleasure to complete. Also, my sincere thanks and appreciation my deepest gratitude goes to my co-supervisor Professor R. Patel and Dr. M. A. Al-Obaidi for their academic guidance, constructive comments, and for wonderful guidance, encouragement.

I acknowledge the financial support provided by the MUTAH UNIVERSITY /Jordan for the professional development opportunities to execute this project.

I am grateful to THE ARAB POTASH COMPANY for supplying me with data for my project, without its precious support it would not be possible to conduct this research.

I want to express my endless gratitude to my mother for her unconditional, spiritual, and moral support, prayers, and encouragement. I also want to appreciate my brothers, sisters, my husband family, and all my friends for their words of encouragement and moral support.

Last but not at the least, I would like to dedicate this work to my husband Dr. Abdullah and my daughters Rafeef & Zaina for their love, support, understanding, and patience, during my study without which I could have never completed this work.

## Table of Contents

ABSTRACT .....	i
Acknowledgment .....	iii
Table of Contents .....	iv
List of Tables .....	viii
List of Figures .....	ix
List of Nomenclature.....	xii
CHAPTER ONE.....	1
Introduction .....	1
1.1 Water and perspective fact .....	1
1.2 Background of desalination.....	3
1.3 Water desalination in the Middle East countries .....	3
1.3.1 Brackish water desalination.....	4
1.4 Desalination technologies.....	5
1.5 Principles and description of RO process.....	8
1.5.1 Theory of water and solute transport in RO membranes.....	10
1.6 Characteristics of RO process .....	11
1.7 Limitations of RO membrane process .....	12
1.7.1 Membrane Fouling .....	12
1.7.2 Concentration polarisation .....	13
1.8 Membrane modules .....	13
1.8.1 Spiral Wound.....	14
1.9 Simple design of RO desalination plant .....	16
1.10 Knowledge gap .....	18
1.11 Limitations of this research .....	19
1.12 Research aim and objectives .....	19
1.12.1 Aim of research .....	19
1.12.2 Objectives of the research .....	19
1.13 Thesis structure.....	20
CHAPTER TWO.....	23
Literature Review .....	23
2.1 Introduction .....	23
2.2 Overview of modelling of a spiral wound RO module .....	27
2.2.1 Model of Lonsdale et al. (1965) .....	28

2.2.2 Model of Boudinar et al. (1992).....	29
2.2.3 Model of Avlonitis et al. (1991), Avlonitis et al. (1993) and Avlonitis et al. (2007) .....	30
2.2.4 Model of Abbas and Al-Bastaki (2001) .....	31
2.2.5 Model of Marriott and Sørensen (2003).....	32
2.2.6 Model of Abbas (2005) .....	33
2.2.7 Model of Geraldès et al. (2005).....	34
2.2.8 Model of Avlonitis et al. (2007).....	35
2.2.9 Model of Majali et al. (2008) .....	35
2.2.10 Model of Oh et al. (2009).....	37
2.2.11 Model of Lee et al. (2010).....	37
2.2.12 Model of Kaghazchi et al. (2010).....	38
2.2.13 Model of Ruiz-Saavedra et al. (2015) .....	38
2.2.14 Model of Kotb et al. (2015).....	39
2.2.15 Model of Dimitriou et al. (2017).....	40
2.3 Overview of simulation of a spiral wound RO process.....	44
2.4 Overview of optimisation a spiral wound RO process .....	50
2.5 Overview of thermodynamic aspect of RO process .....	59
2.6 Modelling and Optimisation Software .....	67
2.6.1 Modelling and simulation in gPROMS .....	67
2.7 Conclusions .....	71
CHAPTER THREE.....	73
Modeling of a Spiral Wound Reverse Osmosis Desalination System .....	73
3.1 Introduction .....	73
3.2 Modelling of a single spiral wound RO process .....	73
3.3 Model validation against two different sizes of brackish water RO desalination systems .....	78
3.3.1 Description of a simple design of RO system .....	78
3.3.2 Model validation.....	79
3.3.3 Description of a complicated design of RO system .....	81
3.3.4 Model validation.....	82
3.4 Further simulation for a simple design of RO system.....	85
3.4.1 Impact of feed salinity .....	85
3.4.2 Impact of feed water flow rate .....	87
3.4.3 Impact of inlet feed pressure .....	89
3.4.4 Impact of inlet feed temperature .....	90

3.5 Conclusions .....	91
CHAPTER FOUR .....	93
Performance Evaluation of Reverse Osmosis Brackish Water Desalination Plant with Recycled Retentate Design.....	93
4.1 Introduction .....	93
4.2 Performance evaluation of retentate recycle mode for a simple design of brackish water RO process.....	95
4.2.1 Description of a simple design RO desalination plant with retentate recycle mode .....	95
4.2.2 Impact of retentate recycling scheme on the RO process performance .....	96
4.3 Performance evaluation of retentate recycle mode for a complicated design of brackish water RO process .....	101
4.3.1 Description of a complicated design of RO desalination plant of APC with retentate recycle mode.....	101
4.3.2 Impact of retentate recycling scheme of 1 <sup>st</sup> pass on the RO process performance .....	104
4.4 Evaluation of retentate recycle mode on the performance of simple and complicated designs of brackish water RO desalination process .....	113
4.5 Conclusions .....	113
CHAPTER FIVE .....	115
Evaluation and Minimisation of Energy Consumption of Reverse Osmosis Brackish Water Desalination Plant.....	115
5.1 Introduction .....	115
5.2 Model development.....	119
5.3 Case Study 1: Minimisation of energy consumption of a simple RO brackish water desalination plant.....	121
5.3.1 Description of a simple RO brackish water desalination plant with an ERD .....	121
5.3.2 Process simulation: Impact of operating parameters of a simple multistage RO system.....	122
5.4 Case Study 2: Minimisation of energy consumption of a complicated RO brackish water desalination plant of APC.....	127
5.4.1 Description of the complicated design of multistage brackish water RO desalination plant of APC with an ERD .....	127
5.4.2 Process simulation: Impact of operating parameters.....	130
5.4.3 Expected merits of the advanced design of APC .....	138
5.5 Critique of specific energy consumption of simple and complicated designs of brackish water RO process .....	140
5.6 Conclusions .....	142
CHAPTER SIX .....	143
Performance evaluation of a reverse osmosis brackish water desalination plant with different brands of membranes .....	143

6.1 Introduction .....	143
6.2 Case study 1. Performance evaluation of a simple multistage RO brackish water desalination plant with different brands of membranes .....	146
6.2.1 Simulation results and discussion.....	147
6.3 Case study 2. Performance evaluation of a complicated multistage RO brackish water desalination plant of APC with different brands of membranes .....	154
6.3.1 Simulation results and discussion.....	155
6.4 Critique of performance indicators of simple and complicated brackish water RO desalination systems based on the best brand of membranes.....	162
6.5 Conclusions .....	163
CHAPTER SEVEN .....	165
Optimisation of energy consumption in a reverse osmosis brackish water desalination plant .....	165
7.1 Introduction .....	165
7.2 Case Study 1: Optimisation of energy consumption of a simple RO brackish water desalination plant.....	166
7.2.1 Mathematical optimisation problem.....	167
7.3 Case Study 2: Optimisation of energy consumption of a complicated RO brackish water desalination plant of APC.....	168
7.3.1 Mathematical optimisation problem.....	169
7.3.2 Optimisation results.....	170
7.4 Evaluation of optimisation of two different sizes of brackish water RO desalination systems .....	171
7.5 Conclusions .....	172
CHAPTER EIGHT .....	174
Thermodynamic limitations and exergy analysis of reverse osmosis brackish water desalination plant .....	174
8.1 Introduction .....	174
8.2 Thermodynamic limitations and exergy analysis of brackish water RO desalination plant of APC .....	177
8.2.1 General overview of the RO system of APC and tested locations .....	178
8.2.2 Exergy analysis.....	180
8.2.3 Discussion of exergy distribution of the RO system .....	182
8.3 Conclusions .....	188
CHAPTER NINE .....	189
Conclusions and Recommendations for Future Work .....	189
9.1 Introduction .....	189
9.2 Conclusions .....	189

9.3 Recommendations for Future Work .....	192
References .....	193
List of Publications.....	203

## List of Tables

<b>Table 1.1.</b> Brackish water composition of Arab Potash Company .....	5
<b>Table 2.1.</b> Summary of the models developed for spiral wound RO process .....	42
<b>Table 2.2.</b> Summary of the previous work of RO simulation .....	48
<b>Table 2.3.</b> Summary of the previous work of RO optimisation .....	55
<b>Table 2.4.</b> Summary of the past work of RO thermodynamic and exergy analysis .....	64
<b>Table 3.1.</b> Design specification for a simple RO system .....	80
<b>Table 3.2.</b> Specifications of the membrane element and transport parameters .....	80
<b>Table 3.3.</b> Comparison of simple design RO plant of Abbas (2005) and the model predictions multistage model predictions.....	80
<b>Table 3.4.</b> Design specification for an industrial brackish water RO system of APC.....	84
<b>Table 3.5.</b> Specifications of the membrane element and transport parameters (Adapted from Al- Obaidi et al., 2018a) .....	84
<b>Table 3.6.</b> Comparison of the experimental results of RO system of APC and the model predictions .....	85
<b>Table 4.1.</b> Effect of recycle ratio on the overall product flow rate and product salinity (Al-Bastaki and Abbas, 2003).....	94
<b>Table 4.2.</b> Specific energy consumption vs feed salinity (Sarkar et al., 2008) .....	94
<b>Table 4.3.</b> Simulation results of three schemes of partial recycle on the product phenol concentration .....	95
<b>Table 4.4.</b> Simulation results of process performance indicators with 0% (without recycle mode), 80% and 100% percentages of retentate recycle for simple RO system.....	101
<b>Table 4.5.</b> The simulation results of several operating conditions and process performance indicators with variable recycle percentage of the 1st pass retentate stream.....	111
<b>Table 4.6.</b> Simulation results of process performance indicators with 0% (without recycle mode), 40% and 100% percentages of retentate recycle .....	112
<b>Table 5.1.</b> Summary of studies on the energy consumption of RO process.....	117
<b>Table 5.2.</b> Simulation results of specific energy consumption of two sizes of brackish water RO desalination systems .....	141
<b>Table 6.1.</b> Input operating conditions of RO system of APC .....	147
<b>Table 6.2.</b> Simulation results of different brands of spiral wound membrane in a simple RO system with characterizing the performance indicators.....	148
<b>Table 6.3.</b> Characteristics of the membrane used in the RO system of APC and transport parameters .....	155
<b>Table 6.4.</b> Input operating conditions of a complicated RO system of APC .....	155
<b>Table 6.5.</b> Simulation results of different brands of membranes in the complicated design of RO system with characterising the performance indicators.....	156
<b>Table 6.6.</b> Comparison of performance indicators of two selected RO systems.....	163
<b>Table 7.1.</b> Simulation and optimisation results of a simple RO system at base case conditions.....	168
<b>Table 7.2.</b> Simulation and optimisation results of RO system of APC at base case operating conditions .....	171
<b>Table 8.1.</b> The dead state operating conditions of RO desalination plant of APC.....	181
<b>Table 8.2</b> Rate of exergy change of major components of RO of APC desalination plant.....	186

## List of Figures

<b>Fig. 1.1.</b> Projected water scarcity in 2025 (I.W.M.I., 2001).....	2
<b>Fig. 1.2.</b> The future of water stress over the world in 2040 (Andrew Maddocks, 2015).....	2
<b>Fig. 1.3.</b> The total global desalinated water capacity (market share) of operational desalination in term of feed water type (Adapted from Jones et al., 2018).....	6
<b>Fig. 1.4.</b> The total global desalinated water capacity (market share) of operational desalination in term of technology type (Adapted from Jones et al., 2018).....	7
<b>Fig. 1.5.</b> Number of publications by type of desalination technology Reverse Osmosis (RO), Multi-Effect Distillation (MED), Multi-Stage Flash (MSF), and others (Adapted from Jones et al., 2018)	8
<b>Fig. 1.6.</b> Schematic diagram for representing the RO theory .....	10
<b>Fig. 1.7.</b> Schematic diagram of a spiral wound membrane element.....	15
<b>Fig. 1.8.</b> Diagram of a flat membrane envelope (Adapted from Marriott and Sørensen, 2003) .....	16
<b>Fig. 1.9.</b> Schematic diagram of the brackish water RO desalination plant.....	17
<b>Fig. 2.1.</b> The desalination capacity over the worldwide based on the region .....	24
<b>Fig. 2.2.</b> Platform of gPROMS model builder.....	68
<b>Fig. 2.3.</b> The model entity .....	69
<b>Fig. 2.4.</b> The model equations .....	70
<b>Fig. 2.5.</b> The process entity .....	71
<b>Fig. 3.1.</b> Flowsheet of a simple design of RO brackish water desalination system .....	79
<b>Fig. 3.2.</b> Flowsheet of brackish water RO desalination plant of APC .....	82
<b>Fig. 3.3.</b> Impact of feed water salinity on total recovery and solute rejection.....	86
<b>Fig. 3.4.</b> Impact of feed water salinity on product and retentate salinities .....	87
<b>Fig. 3.5.</b> Impact of feed flow rate on total recovery and solute rejection .....	88
<b>Fig. 3.6.</b> Impact of feed flow rate on product and retentate salinities .....	88
<b>Fig. 3.7.</b> Impact of feed pressure on total water recovery and solute rejection .....	89
<b>Fig. 3.8.</b> Impact of feed pressure on product and retentate salinities .....	90
<b>Fig. 3.9.</b> Impact of feed temperature on water recovery and solute rejection.....	91
<b>Fig. 3.10.</b> Impact of feed temperature on product and retentate salinities.....	91
<b>Fig. 4.1.</b> Schematic diagram of a simple RO desalination plant.....	96
<b>Fig. 4.2.</b> Effect of retentate recycle percentage of the last stage on the water recovery and solute rejection.....	98
<b>Fig. 4.3.</b> Effect of retentate recycle percentage of the last stage on the product and retentate salinities on product and retentate flowrates .....	98
<b>Fig. 4.4.</b> Effect of retentate recycle percentage of the last stage on the product and retentate salinities.....	99
<b>Fig. 4.5.</b> Effect of retentate recycle percentage of the last stage on the specific energy consumption .....	100
<b>Fig. 4.6.</b> Schematic diagram of brackish water RO desalination plant of APC with 1 <sup>st</sup> pass retentate recycled mode (Adapted from Al-Obaidi et al., 2018a) .....	103
<b>Fig. 4.7.</b> Effect of different recycle percentage of the 1 <sup>st</sup> pass retentate stream on plant recovery and solute rejection .....	105
<b>Fig. 4.8.</b> Effect of different recycle percentage of the 1 <sup>st</sup> pass retentate stream on product and retentate plant flowrate .....	106
<b>Fig. 4.9.</b> Effect of different recycle percentage of the 1 <sup>st</sup> pass retentate stream on product and retentate salinities .....	107

<b>Fig. 4.10.</b> Effect of different recycle percentage of the 1st pass retentate stream on the 1st and 2nd passes water recovery .....	108
<b>Fig. 4.11.</b> Effect of different recycle percentage of the 1st pass retentate stream on the 1st and 2nd passes mass transfer coefficient.....	109
<b>Fig. 4.12.</b> Effect of different recycle percentage of the 1st pass retentate stream on the total energy consumption .....	110
<b>Fig. 5.1.</b> Schematic diagram of multistage, multi pass simple BWRO desalination plant with adding of an ERD.....	121
<b>Fig. 5.2.</b> Specific energy consumption and total water recovery of a small brackish water RO desalination plant with and without an ERD (at different efficiencies) against plant feed flow rate .....	123
<b>Fig. 5.3.</b> Specific energy consumption and total water recovery of a small brackish water RO desalination plant with and without an ERD (at different efficiencies) against plant pressure .....	125
<b>Fig. 5.4.</b> Specific energy consumption and total water recovery of a small brackish water RO desalination plant with and without an ERD (at different efficiencies) against plant temperature..	126
<b>Fig. 5.5.</b> Schematic diagram of multistage, multi-pass BWRO desalination plant of APC with adding of an ERD and booster pump.....	129
<b>Fig. 5.6.</b> Specific energy consumption and water recovery of brackish water RO desalination plant of APC with and without an ERD (at different efficiencies) against plant feed flow rate.....	132
<b>Fig. 5.7.</b> Specific energy consumption and total water recovery of BWRO desalination plant of APC with and without an ERD (at different efficiencies) against operating feed pressure .....	135
<b>Fig. 5.8.</b> Specific energy consumption and total recovery of brackish water RO desalination plant of APC without and with an ERD (at different efficiencies) against feed temperature .....	137
<b>Fig. 6.1.</b> Impact of membrane brands on solute rejection of a simple design of brackish water RO desalination system .....	150
<b>Fig. 6.2.</b> Impact of membrane brands on total water recovery of a simple design of a brackish water RO desalination system .....	151
<b>Fig. 6.3.</b> Impact of membrane brands on total product flowrate of a simple design of brackish water RO desalination system .....	151
<b>Fig. 6.4.</b> Impact of membrane brands on total water salinity of a simple design of brackish water RO desalination system .....	152
<b>Fig. 6.5.</b> Impact of membrane brands on plant energy consumption of a simple design of brackish water RO desalination system .....	153
<b>Fig. 6.6.</b> Impact of membrane brands on solute rejection of a complicated brackish water RO desalination system .....	158
<b>Fig. 6.7.</b> Impact of membrane brands on total water recovery of a complicated brackish water RO desalination system .....	159
<b>Fig. 6.8.</b> Impact of membrane brands on total product flow rate of a complicated brackish water RO desalination system .....	160
<b>Fig. 6.9.</b> Impact of membrane brands on product salinity of a complicated brackish water RO desalination system .....	161
<b>Fig. 6.10.</b> Impact of membrane brands on plant energy consumption of a complicated brackish water RO desalination system .....	162
<b>Fig. 8. 1.</b> Schematic diagram of the RO desalination plant of APC .....	179

## List of Nomenclature

$A_w$	Water (solvent) transport coefficient of the membrane for solution diffusion model, water permeability coefficient, (m/atm s)
$A_m$	Effective area of the membrane (m <sup>2</sup> )
$A_{w(T)}$	Water transport coefficient at operating temperature (m/atm s)
$A^*$ and $n$	The feed spacer characteristic (dimensionless)
$B_s$	The solute transport parameter at operating temperature, salt permeability coefficient, (m/s)
$B_{s0}$	The intrinsic solute transport parameter (dimensionless)
$B_{s(25\text{ }^\circ\text{C})}$	The transport parameter of solute (at 25 °C) (m/s)
$C_f$	Feed concentration (ppm)
$C_b$	The solute concentration in the bulk solution (ppm)
$C_r$	Retentate (brine) concentration (ppm)
$C_p$	Solute concentration at permeate side (ppm)
$C_w$	The solute salinity at the membrane wall (ppm)
$C_{p_s}$	The specific heat of salt at 25 °C (kJ/kg K)
$C_{p_w}$	The specific heat of water at 25 °C (kJ/kg K)
$D_s$	The solute diffusion coefficient (m <sup>2</sup> /s)
$Dh$	Hydraulic diameter of the flow channel (m)
$d_{ch}$	The membrane channel diameter (m)
$E_{HPP}$	Specific energy consumption of high-pressure pump (kWh/m <sup>3</sup> )
$E_{ERD}$	Specific energy consumption of ERD (kWh/m <sup>3</sup> )
$Ex_{gy}$	The exergy (kJ/kg)
$F_f$	The fouling factor (dimensionless)
$H$	Height (m)
$h_w$	the specific enthalpy of water (kJ/kg)
$h_s$	The specific enthalpy of salt (kJ/kg)
$J_s$	Solute molar flux through the membrane (kmol/m <sup>2</sup> s) or (mol/m <sup>2</sup> s)
$J_w$	Water (solvent) flux at the feed channel (m/s)
$k_{fp}$	Permeate friction parameter (m <sup>-2</sup> )
$k_{fr}$	Retentate (brine) friction parameter (m <sup>-2</sup> )
$K$	Mass transfer coefficient (m/s)
$K_{1m}$	Constant depends on membrane type (dimensionless)
$K_{2m}$	Constant depends on membrane type (dimensionless)
$K_{1.0}$	Water permeability coefficient at zero pressure (m/s Pa)
$k_{dc}$	The feed spacer characteristic (dimensionless)
$L$	Membrane length (m)
$L_f$	The length of filament in the spacer mesh (m)
$mf$	The mass fraction (dimensionless)
$n_s$	The number of ions per salt molecule
$NDP_{fb}$	The net driving pressure of feed and brine (atm)
$\Delta p$	Pressure drop of the membrane (atm)
$P_{out(MODULE)}$	Outlet pressure of membrane module (atm)
$P_{out(ERD)}$	Outlet pressure of an ERD (atm)
$Pf_{(in-plant)}$	Inlet feed pressure (atm)

$Pf_{(pass1)}$	Inlet feed pressure of 1 <sup>st</sup> pass (atm)
$Pf_{(BPump)}$	Outlet booster pump pressure (atm)
$Pf_{(plant)}$	The operating feed pressure (atm)
$P_{eff}$	The residual trans-membrane pressure (atm)
$P_b$	Bulk pressure (atm)
	Feed retentate pressure (atm)
$P_f$	Feed pressure (atm)
$P_p$	Permeate pressure (atm)
$P_r$	Retentate (brine) pressure (atm)
$P_{fb}$	The pressure for feed brine (atm)
$\Delta P_{ef}$	Driving pressure (atm)
$P_{drop}$	The pressure drop along a RO system (atm)
$P_{loss}$	Pressure loss in an RO system (atm)
$Qr_{(pass 1)}$	Retentate flow rate of 1 <sup>st</sup> pass (m <sup>3</sup> /s)
$Qp_{(total plant)}$	Plant permeate flow rate (m <sup>3</sup> /s)
$Qf_{(pass 2)}$	Inlet feed flow rate of 2 <sup>nd</sup> pass (m <sup>3</sup> /s)
$Qf_{(in\_plant)}$	Plant feed flow rate (m <sup>3</sup> /s)
$Qf_{(plant)}$	The applied feed flow rate (m <sup>3</sup> /s),
$Q_r$	Retentate flowrate (m <sup>3</sup> /s) or (m <sup>3</sup> /day)
$Q_f$	Feed flowrate (m <sup>3</sup> /s) or (m <sup>3</sup> /day)
$Q_b$	Bulk flowrate (m <sup>3</sup> /s) or (m <sup>3</sup> /day)
$Q_p$	The total permeate production capacity (m <sup>3</sup> /s) or (m <sup>3</sup> /day)
$R$	Universal Gas constant ( $R = 0.082 \frac{\text{atm m}^3}{\text{K kmol}}$ ), (8.314 J/mol K)
$R_r$	Retentate resistance (s/m)
$Re_p$	The Reynolds Number at permeate (dimensionless)
$Re_r$	The Reynolds Number at retentate (brine) (dimensionless)
$Re, Re_b$	Reynolds Number ( $Re = \rho u d_h / \mu$ ) (dimensionless)
$Re_f$	The Reynolds Number at feed (dimensionless)
$R_p$	Permeate resistance (Pa s/m)
$R^o$	Fibre outer radius (m)
$Sc$	Schmidt number (dimensionless)
$Sh$	Sherwood number (dimensionless)
$s_s$	The specific entropy of salt (kJ/kg K)
$s_w$	specific entropy of water (kJ/kg K)
$T_o$	The absolute temperature (°C)
$T_b$	Bulk temperature (°C)
$T$	Temperature (K)
$TCF_s$	The temperature correction factor of solute at standard conditions (dimensionless)
$TCF_p$	The temperature correction factor of permeate at standard conditions (dimensionless)
$T$	The operating time in (day)
$u_f$	Feed velocity (m/s)
$U_b$	expresses the bulk velocity (m/s)
$W$	Membrane width (m)

$X_p$	The outlet salinity of permeate stream from membrane module (ppm)
$X_f$	Feed salinity entering membrane module (ppm)

### ***Greek letters***

$\rho$	Water density (kg/m <sup>3</sup> )
$\beta_1$	Constant for solute transport (dimensionless)
$\emptyset$	The concentration polarisation (dimensionless)
$M$	Viscosity (g/cm. s) or (kg/m s)
$\mu_b$	The kinematic viscosity (kg/m s)
$\Delta\pi_m$	Osmotic pressure drop across the membrane (kPa)
$\Delta\pi$	Total osmotic pressure difference of the membrane (atm)
$\pi_p$	Permeate osmotic pressure (bar)
$\pi_{T_i}$	The osmotic pressure at operating temperature (Pa)
$\pi_B$	Brine osmotic pressure (bar)
$\pi_b$	The osmotic pressure of bulk brine (atm)
$\pi_r$	Brine (retentate) osmotic pressure (atm)
$\pi_m$	The local osmotic pressures of the solutions adjacent to the membrane surfaces in feed side (atm)
$\pi_w$	The osmotic pressure at the membrane wall (Pa)
$\pi_f$	Feed osmotic pressure (atm)
$\rho_p$	Permeate density (kg/m <sup>3</sup> )
$\rho_b$	Bulk density (kg/m <sup>3</sup> )
$\varepsilon_{Bpump}$	Efficiency of booster pump (dimensionless)
$\varepsilon_{ERD}$	Efficiency of an ERD (dimensionless)
$\varepsilon_{HPpump}$	Efficiency of high-pressure pump (dimensionless)
$\epsilon$	Feed spacer void fraction (dimensionless)
$\nu$	kinematic viscosity (cm <sup>2</sup> /s)

### ***LIST OF ABBREVIATION***

APC	Arab Potash Company
BWRO	Brackish water reverse osmosis
CP	Concentration polarisation (dimensionless).
ERD	Energy recovery device
ED	Electrodialysis
GA	Genetic algorithm
GCC	Gulf Cooperation Council
gPROMS	general PROcess Modelling System
HER	Hydraulic energy recovery
IEA	International Energy Agency
MW	Salt molecular weight (kg/kmole)
MED	Multi-effect distillation

MSF	Multistage flash distillation
MEE	Multi Effect Evaporation
NLP	Non-linear optimisation problems
OER	Osmotic energy recovery
PRO	Pressure retarded osmosis process
RO	Reverse osmosis
RR	Retentate ratio
RED	Reverse Electrodialysis process
SR	Salt rejection (dimensionless)
SEC	Specific energy consumption (kWh/m <sup>3</sup> )
SWRO	Sea water reverse osmosis
SQP	Successive quadratic programming
TDS	Total dissolved solids
UNDESA	United Nations Department of Economic and Social Affairs
UAE	United Arab Emirates
VDS	Visual Design and Simulation package software
VC	Vapour-compression distillation
WR	Water permeate recovery (dimensionless)
WHO	World Health Organization

### ***Subscripts***

B or b	Brine
BW	brine wall
fb	brine friction
fp	permeate friction
F	Feed
m	Membrane
P	Permeate
PW	permeate wall
S	Salt
W	Wall

# CHAPTER ONE

## Introduction

### 1.1 Water and perspective fact

Water is very important for life as an essential constitutes for growing populations who require a clean water for drinking, as well as for industrial and agriculture fields. In spite of 71% of the earth surface is covered by water, but the majority of this water is not suitable for human use. The oceans account for about 97% of the total water in the earth which are undrinkable and salty water, and 2% of ice caps and glaciers are not easily accessible, while the rest about 1% in rivers, underground and lakes. Therefore, the fresh water natural sources are inadequate to meet the growing demand of fresh water around the globe. Moreover, increased salinity of aquifers will continuously exacerbate the problem of water scarcity in many regions of the world especially for the areas completely dependent on these non-renewable sources. Basically, when the water demand exceeds the available resources, this would result in water scarcity. The problem of water shortage is one of the most common and widespread problems in the world. It is expected that this problem will spread widely in the future (2025) as depicted in Fig. 1.1. Fig 1.1 indicates the expected increase of water scarcity on a large scale in the world, especially in most countries of the Middle East and North Africa. Moreover, it is expected that around 1.8 billion of the population of these areas will be affected by absolute water scarcity.

Fig. 1.2 shows an increase of areas exposed to water shortage between 2025 to 2040 compare to those areas exposed to water shortage presented in Fig. 1.1. The future water stress is scored and ranked by world resources institute for 167 countries and shows that 33 countries face extremely high-water stress in 2040, which are mainly located in the Middle East. In this respect, Jordan, occupies a strategic location in the Middle East, is considered as one of the ten most water countries in the world suffering from water scarcity. Specifically, Jordan is expected to score the 14<sup>th</sup> rank in water stress by 2040 (Andrew Maddocks, 2015).

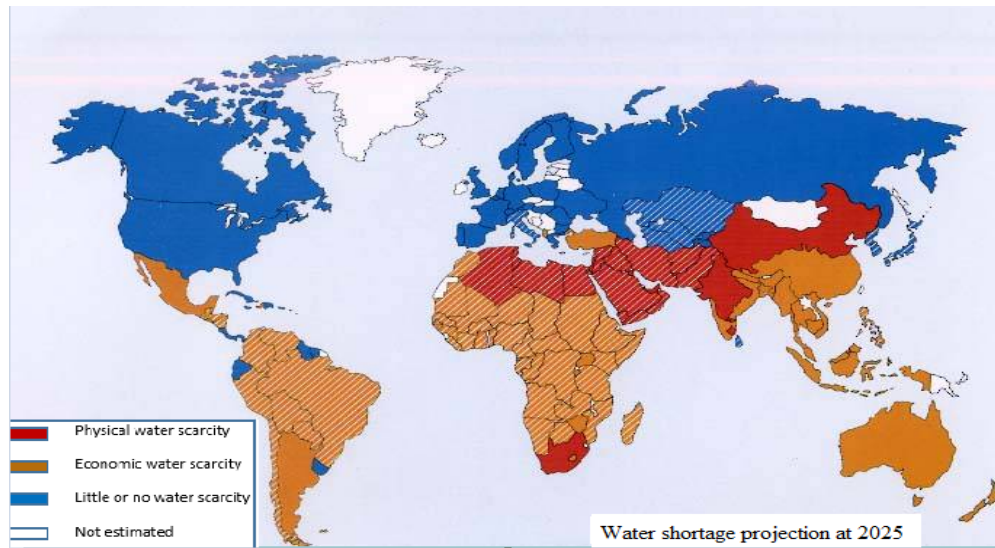


**Fig. 1.1.** Projected water scarcity in 2025 (I.W.M.I., 2001)

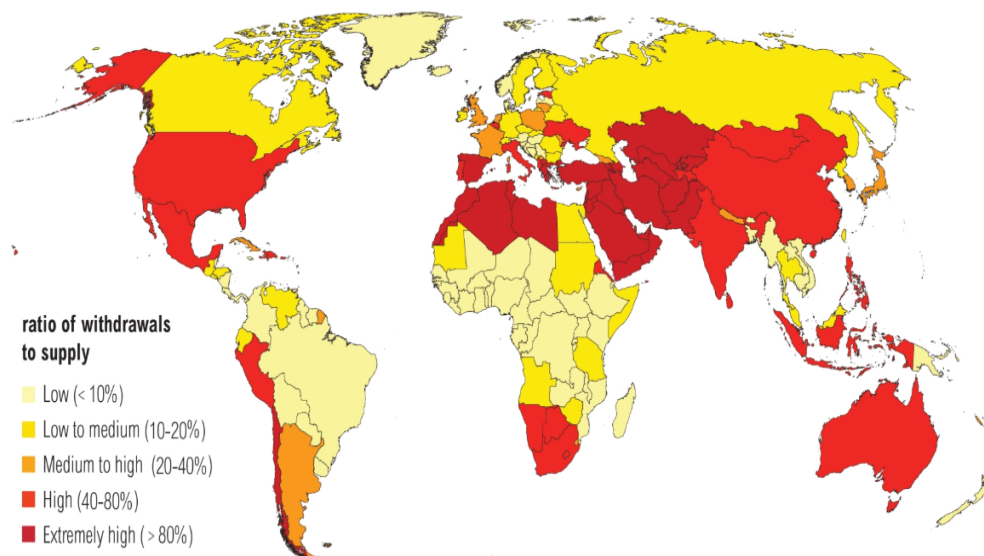


**Fig. 1.2.** The future of water stress over the world in 2040 (Andrew Maddocks, 2015)

For the above discussed reason, it was necessary to search for other sources of fresh water to compensate the water shortage, and therefore the solution was accomplished via the desalination and treatment of seawater and brackish water (Temperely, 1995). Recently, there are more than 16,000 desalination plants in operation worldwide and the total global capacity of all plants is around 74.8 million m<sup>3</sup>/day (Bennett, 2013).

## **1.2 Background of desalination**

The reliance on desalination technology to produce fresh water has been extensively increased due to the shortage of fresh water with progressive line of industry. Therefore, there were intensive efforts to invent proper desalination technologies to compensate the freshwater scarcity, which explicitly comes with developing thermal and membrane processes.

Desalination is a physical separation process of a saline water to separate salts from water which in turn obtaining fresh water with low salinity and concentrated brine. This mainly includes seawater, and brackish water (Al-Zahrani et al., 2012). However, desalination has been widely used in the provision of water for industrial and agricultural uses, which entirely aided the setting up of numerous arid regions around the world, especially in the Middle East.

Selection of the desalination method mainly depends on the salinity of water resource. This is referred to the concentration of dissolved salts in water, which is presented in Mass/Volume or Mass/Mass unit ratios. The total dissolved solids (TDS) is reported in the most desalination industries as the standard indicator measured by part per million (ppm) (mg/l). Thereby, the water can be classified based on its salinity into low salinity water (brackish water) and high salinity water (seawater) (El-Dessouky and Ettouney, 2002, El-Manharawy and Hafez, 2001). In this respect, the allowed upper and lower concentration limits of TDS in drinking water are 1000 ppm and 500 ppm, respectively. Therefore, TDS more than 1000 ppm would make foul-tasting water. These limits are reported by the World Health Organization (WHO) on their guidelines of drinking-water quality (WHO, 2003). Occasionally, the salinity of seawater ranges between 35,000 to 45,000 ppm of TDS (Eltawil et al., 2009). Therefore, the desalination plants are constructed based on the quality of feed water, i.e, seawater and brackish water, which in turn would explain the reason of simple and complicated designs of the desalination plants.

## **1.3 Water desalination in the Middle East countries**

Over the past few years, desalination has become an integral part of water management strategies in several countries across the world including the Middle east countries. In fact,

the resources of natural fresh water are not distributed equally around the world. Therefore, there are many countries suffering from water scarcity despite having sufficient water to support their residents.

The demand of fresh water has been exponentially increased due to the growth of pollution with employing water in a variety of industries. This is specially noticed in the Middle East countries, which made the desalination technology as the most important fresh water source of potable, agriculture, and industrial uses.

The increase of population and economic development in the Middle East countries has led to an imbalance between supply and demand of freshwater. These countries depend essentially on desalination to meet the growing of water demands (Nair and Kumar, 2013). This would interpret the expansion of water desalination plants in this region that confirmed the appropriateness of desalination as the most expedient solution to water scarcity compared to other parts of the globe (Khan et al., 2017).

Generally, water scarcity is a major environmental challenge facing Jordan since the early 1960s until these days. In fact, Jordan occupies the 10<sup>th</sup> rank in the world in terms of the shortage and insufficient of water resources (Hadadin et al., 2010). Thus, it is important to exploit the brackish water besides seawater to be used as a main source of drinking water, agriculture, and industrial requirements. This in turn would aid to resolve the challenge of water shortage in this country by employing the desalination technologies.

This thesis focuses on desalinating the brackish water and therefore, the next section will illustrate more details of brackish water and their characteristics with desalination plants in Jordan.

### ***1.3.1 Brackish water desalination***

The brackish water has a concentration limit of TDS about (<10,000 ppm) and includes components that basically dependent on the present minerals of the ground where it is sourced. For instance, the composition of brackish water used in Arab Potash Company (APC) desalination plant (located in Jordan) before desalinated with RO process are given in Table 1.1. It is noteworthy to mention that the characteristics of brackish water including TDS might differ as a result to continuous and intensive desalination operation. Therefore, this would negatively increase the osmotic pressure that requires a substantial

increase of operating pressure to maintain fixed quantity and quality of fresh water produced by RO process.

**Table 1.1.** Brackish water composition of Arab Potash Company

Parameter composition	Unit	Value
Calcium (Ca)	ppm	134
Chloride (Cl)	ppm	344
Fluoride (F)	ppm	0.394
Iron (Fe)	ppm	<0.10
Magnesium (Mg)	ppm	68.2
Manganese (Mn)	ppm	<0.05
Nitrate (NO <sub>3</sub> )	ppm	30.2
Potassium (K)	ppm	12.3
Sodium (Na)	ppm	151
Sulphate (SO <sub>4</sub> )	ppm	267
Total hardness (CaCO <sub>3</sub> )	ppm	615
PH	-	7.27
Conductivity	ppm	1.2352
Turbidity	NTU	0.6

Occasionally, the largest brackish water desalination plant in the world is located in Yuma, AZ, USA with a total capacity of 275,000 m<sup>3</sup>/day. It uses spiral wound cellulose acetate RO membranes to treat raw water with TDS about 3100 ppm and produces fresh water with TDS less than 200 ppm (Lohman, 1994).

#### **1.4 Desalination technologies**

Indeed, the spread of desalination technologies has caused an increase in fresh water supply over worldwide. Desalination technologies can be classified into two processes; thermal processes and membrane separation processes as follows,

1. Desalination process with phase change, which includes three main methods: Multi-effect distillation (MED), Multistage flash distillation (MSF), and Vapour-compression distillation (VC).
2. Desalination process with no phase change, which includes two main methods: Reverse osmosis (RO), and Electrodialysis (ED).

The selection of desalination method is strictly associated with the requested quality and quantity of produced water.

Thermal processes can be considered as one of the most widely used methods for seawater desalination of high salinity. The basics of thermal process are the distillation (boiling and evaporation) with expensing energy to operate the boilers as steam generators. This is quite different than the membrane technology that entails the separation of salts from water via a semipermeable membrane. The main widely used membrane processes are including the reverse osmosis (RO) process and Electrodialysis (ED) process. RO process uses high-pressure to separate dissolved salts from water while ED process uses the electricity as the driving force of salt separation. However, the RO process can be considered as a superior and efficient technology for both brackish and seawater desalination. Fig. 1.3 depicts that both seawater and brackish water are the largest water resources of fresh water with market share account for 61%, and 21%, respectively. These sources together with river water constitute 90% of the total produced volume of desalinated water.

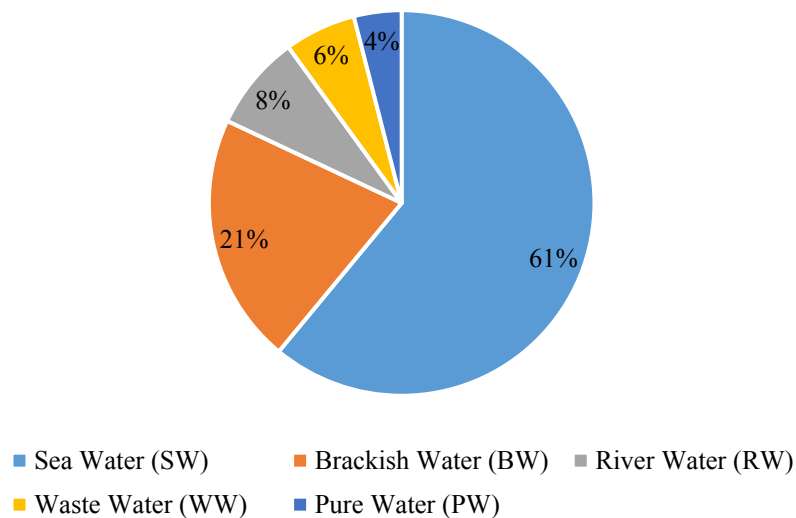


**Fig. 1.3.** The total global desalinated water capacity (market share) of operational desalination in term of feed water type (Adapted from Jones et al., 2018)

In this regard, the RO capacity producing about 69% (65.5 million m<sup>3</sup>/day) of the total global desalinated water. This means that RO process accounting for 84% of the total number of operational desalination plants, as shown in Fig. 1.4.

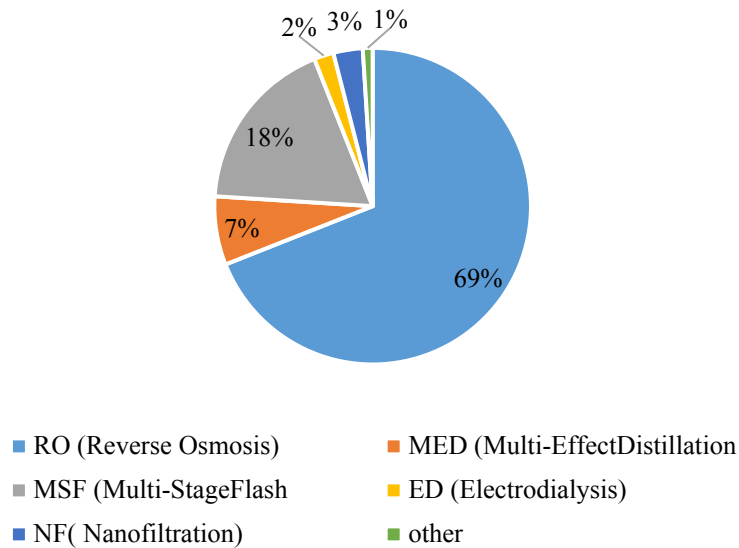


**Fig. 1.4.** The total global desalinated water capacity (market share) of operational desalination in term of technology type (Adapted from Jones et al., 2018)

Moreover, the number of publications of RO process are twofold of thermal process each five-year period as depicted in Fig. 1.5. Fig. 1.5 shows a high and rapid increase over the period from 1980 to 2020 and it is expected to increase in the following years. Consequently, the progressive of RO desalination research is attributed to its critical advantages if compared to thermal process. Fundamentally, a significant reduction in total water production cost was affirmed in the RO membrane technology compared to thermal technologies. Specifically, the thermal technologies such as MSF and MED necessitate electricity and heating steam which are more expensive than RO process, and therefore less reliable. Furthermore, thermal technologies are inadequate based on transportation of water from different areas than RO process (Al-bahou et al., 2007).

The next section will present in details the RO process (the target of this thesis) in more details.

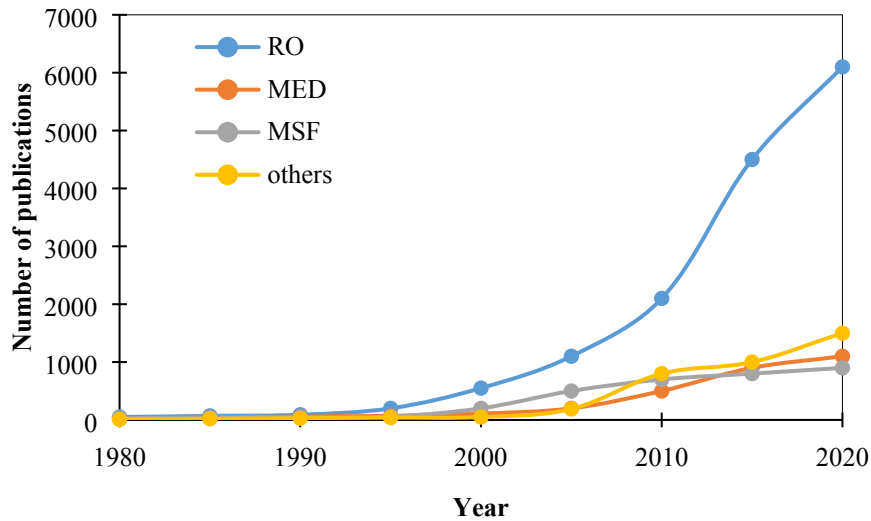


**Fig. 1.5.** Number of publications by type of desalination technology Reverse Osmosis (RO), Multi-Effect Distillation (MED), Multi-Stage Flash (MSF), and others (Adapted from Jones et al., 2018)

Today, the installations of RO desalination process have been significantly increased and comprises about 80% of the total desalination plants over the worldwide. The RO membrane technique can be considered as the most promising technology for seawater and brackish water desalination (Mehdizadeh, 2006).

### 1.5 Principles and description of RO process

There are several invented membrane technologies of water desalination. Among these technologies, the Reverse Osmosis (RO) process is one of the best invented technologies that uses partially membranes to reject a wide range of impurities from treated water.

In fact, the RO process falls under the membrane process category, which is devised based on the theory of solvent and solute fluxes via a semi-permeable medium. This theory constitutes the fact of natural osmosis, which refers to the net movement of water from a lower concentration medium to a higher concentration medium.

RO is the opposite phenomenon of osmosis. The osmosis process is a natural flow of water through a semipermeable membrane from the dilute solution (low concentration areas) to the more concentrated areas (Fig. 1.6.A). The osmotic flow is attributed to the tendency to equalise both the membrane sides with same solute concentrations. As schematically represented in (Fig. 1.6.B), the pressure on the dilute side drops and for that the

concentrated solution rises. This osmotic flux continuously occurs until the equilibrium between the two sides is reached, where the net water flux through the membrane becomes zero (Rao, 2011). If excess pressure is applied on the higher concentration, the water would reversely move from the higher concentration medium to the lower concentration one across a partially permeable membrane. This in turn would interpret the denoting of RO process. Specifically, The RO process is operated by pressurising the saline feed water into a closed vessel using high-pressure pumps above the osmotic pressure, which is proportional to the concentration of the solutes in the feed water. Therefore, the water would pass through the membrane towards the low concentration side, which particularly produces fresh water at the permeate channel and brine (high concentration) leaving the unit. It is important to know that the feed water is progressively concentrated along the membrane channel as a result to the water permeation becomes more and more concentrated. Moreover, the performance of RO system is quite sensitive to the quality of the feed water and operating conditions. In overall, the two characteristics of water quantity and quality need to be maximised for the most efficient and economical desalination technology. In RO systems these two characteristics are adversely affected by membrane fouling, compaction, and hydrolysis. In practice, the RO process requires high operating pressure to overcome the reduction in productivity and maintain a constant production rate. However, this would lead to a higher cost of water production. Moreover, the prediction of a long-term performance is essential for a successful operation of the RO system (Abbas and Al-Bastaki, 2001).

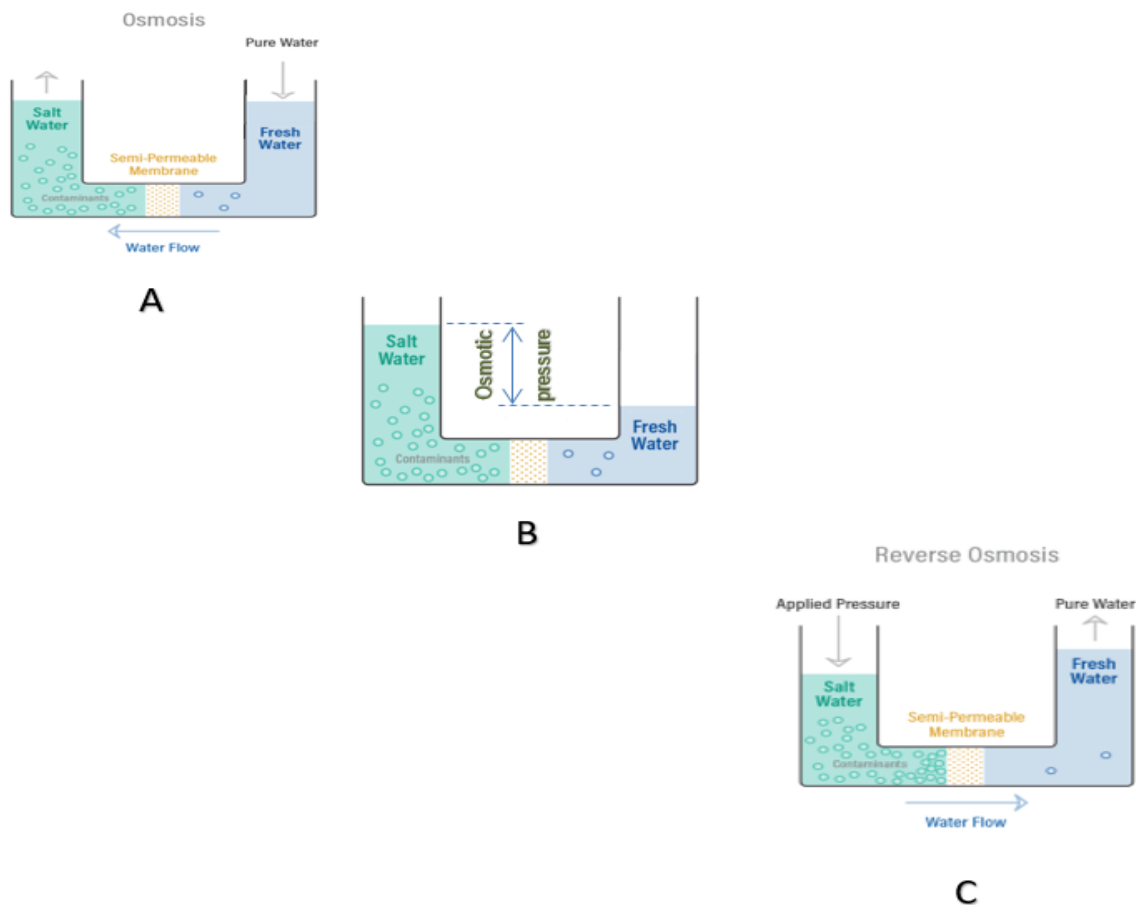


**Fig. 1.6.** Schematic diagram for representing the RO theory

### ***1.5.1 Theory of water and solute transport in RO membranes***

The RO process classified as a pressure driven membrane separation process due to the use of driving force to carry out the filtration. In this aspect, the osmotic pressure of the feed solution is justified by applying high pressure using pumps. Specifically, the hydrostatic pressure difference between the two solutions and the concentration difference in the feed and permeate channels drive the water to flow from the high concentration side to the lower one across the membrane matrix. In other words, a pressure must be applied to the concentrated solution to overcome the osmotic pressure and to force the solvent to cross the membrane towards the low concentration side. However, the solvent flux in RO process is associated with some solute flux as they diffuse through the membrane but at different diffusivities. This in turn would aid to reject the salt on the membrane surface. This is mainly pictured in Fig. 1.6.C.

## **1.6 Characteristics of RO process**

RO process has several merits including its reliability and maturity at low investment costs at low capacities, low maintenance cost. Interestingly, deteriorated and aging or excessive fouling RO membrane modules can be easily replaced besides the flexibility of adding new modules to suit any required water quantity and quality with its short construction periods (Nooijen and Wouters, 1992). Moreover, the RO process operates at ambient temperature compared to thermal desalination processes (Alghoul et al., 2009). Also, RO process has a high quality of simultaneous removal of both organic and inorganic impurities, low discharge in the purge stream, and energy savings. The RO process was the most widely used technology accounting for over 60% of the market share in 2017 (Islam et al., 2018). RO membranes were used in seawater and brackish water desalination and affirmed its successfulness to produce water with high-quality by removing most of the salts and other impurities from water sources (Sourirajan and Matsuura, 1985).

More importantly, the RO process consumes a considerable amount of energy as a result to the necessity of electric power to drive the high-pressure pumps to pressurise the high concentration feed. However, the RO process has been proved to consume lower energy compared to other thermal desalination processes such as MSF or MED. Bouguecha et al. (2004) concluded that RO process consumes half of the energy needed for the thermal desalination process. Statistically, the requirement of electrical energy of RO process is 3 to 4 kWh/m<sup>3</sup> in comparison to MSF and MED of 5.5 to 16 kWh/m<sup>3</sup> (Global Water Desalination Market 2018-2025 Current Trends 2018). Interestingly, the energy consumption of RO process can be also reduced by 30% by adding an energy recovery unit to the brine discharge. In this regard, seawater and brackish water require a range of pressures of 55 to 68 atm, and 17 to 27 atm, respectively (Abdallah et al., 2005, Mohsen and Jaber, 2001).

The expansion of RO desalination plants can also be attributed to the significant improvements of membrane synthesis that comprehensively employed novel materials with advantages of high-resistance to high-operating temperature, low energy requirements, low water production costs, and compact design (Senthilmurugan et al., 2005). Recently, the aromatic polyamide membranes type is one of the most types used due to its several advantages of more stability, high resistivity to fouling, and its ability of

high solute rejection. In this regard, this type is largely acceptable in real applications than the cellulose acetate type which been used in the past (Mallevalle et al., 1996). The advantages of RO process are apparently beyond the one provided by thermal processes, which in turn aid to a wide market of RO process (Kaghazchi et al., 2010). Therefore, RO process has been used in different industrial desalination plant of small, medium and large size because of its plausible energy consumption compared to other thermal processes (Oh et al., 2009).

The successive operation of RO process aided to develop several effective hybrid systems with other feasible processes to attain high water quality and quantity besides achieving economic aspects. For instance, the RO plants have adapted a renewable energy supply to reduce the total energy consumption that entirely mitigates the total production cost. As reported by Subramani et al. (2011), the use of traditional fossil fuel as an energy source to desalinate the seawater for RO system, the CO<sub>2</sub> and NO<sub>x</sub> emissions were 1.78 kg/m<sup>3</sup>, and 4.05 g/m<sup>3</sup>, respectively. However, the CO<sub>2</sub> emissions were 0.6–0.9 kg/m<sup>3</sup> and NO<sub>x</sub> emissions were 1.8–2.1 g/m<sup>3</sup> by using solar photovoltaic energy resource. Consequently, the using of renewable energy as a source of energy in an RO desalination system would reduce the water production cost.

## **1.7 Limitations of RO membrane process**

The RO process has disadvantages of a limited retardation of water recovery especially for treating of high salinity water. For instance, seawater can be recovered with around 35-40% compared to 90% water recovery for brackish water (Abdallah et al., 2005, Mohsen and Jaber, 2001). The low water recovery of RO process is attributed to its propensity of fouling. The membrane fouling and concentration polarisation are the two main limitation of RO process as described below.

### ***1.7.1 Membrane Fouling***

Fouling is the major obstacle that affects the operation of the RO systems by shortening the membrane life, reducing the water flux through a membrane, and increasing the pressure loss along the feed channel. It is well-known that the membrane fouling of the RO process is specifically related to the type of feed water and requires a careful

monitoring of the operating conditions. Therefore, it is fair to claim that membrane fouling can deteriorate the whole performance of the RO desalination plant (Tran et al., 2007). In this respect, there are two common fouling mechanisms can be detected. This includes the membrane surface fouling and the pores fouling. The first surface fouling can be considered as the most affected one that causes a decline in the filtration performance as a result to the accumulation of rejected salts on the membrane surface. The detected surface fouling mechanisms include the cake formation, scale formation and biofilm formation (Speth et al., 2000). Thus, it is crucial to predict the RO process performance and understanding the surface fouling phenomena (Hoek and Elimelech, 2003).

The membrane fouling can be limited by feed pre-treatment, periodic membrane cleaning, and using of fouling inhibitors (Al-Bastaki and Abbas, 1999, Winzeler and Belfort, 1993). Generally, fouling in brackish water RO is more complex than seawater RO desalination. This is due to the variability of feed water characteristics compared to seawater (Ruiz-García et al., 2018).

#### ***1.7.2 Concentration polarisation***

Concentration polarisation is another important factor affecting the membrane performance in the desalination plants (Staude, 1992). The concentration polarisation results from the interactions of the fluid flow and solute mass transfer through the membrane as well as the permeation properties through the membrane (Staude, 1992). Zhang et al. (2019) confirmed that the concentration polarisation depends on the solute properties, hydrodynamics, and the membrane properties.

The accurate prediction of solute concentration polarisation phenomena is an important target in designing of RO process due to its relationship to increase the osmotic pressure, surface fouling and scaling, as well as the solute passage (Kim and Hoek, 2005).

The problem of concentration polarisation can be reduced by amending the hydrodynamics conditions inside the feed channel. For instance, the use of feed spacer can improve the mass transfer of the spiral wound module.

### **1.8 Membrane modules**

Several types of RO membrane modules have been synthesised by the membranes manufacturers to suit various purposes, such as the spiral wound module, hollow-fibre,

tubular and plate and frame. The membrane modules are characterised by different membrane area and design specifications (Baker and ProQuest, 2012). The spiral wound module is one of the most economic modules of RO process compared to other modules. Also, the membranes are designed as high flux membranes (suitable for brackish water), high rejection membranes (suitable for seawater) and fouling resistant membranes (suitable for feed waters leading to excessive fouling). In this regard, the spiral wound membrane modules (the aim of this thesis) have affirmed its consistency in both seawater and brackish water desalination.

The most important characteristics that must be provided in an ideal membrane are

- High salt rejection and freshwater productivity.
- Low intensity of fouling.
- Consistent and chemically and physically stable.
- Providing high membrane area against its volume.
- Low and reasonable price.
- Hold feed water of high temperatures.
- Long and reliable life.

The next section discusses the most promising features of the spiral wound module and discussing its limitations.

### ***1.8.1 Spiral Wound***

Among the synthesised membrane modules, the spiral wound module occupies the largest market share. This is due to its characteristics of simple fabrication technology of ease of operation and compact size and easier to clean (Zhu et al., 2010, Bhattacharyya and Williams, 1992). Also, the spiral wound module is cheap with high packing density  $>1000 \text{ m}^2/\text{m}^3$ , and high mass transfer rates due to feed spacers (Kaghazchi et al., 2010). Moreover, this module has higher permeation rates compared to hollow-fibre module (Bhattacharyya and Williams, 1992). More importantly, it has a good balance between fouling resistance and ease of operation. This might be the reason for nominating spiral wound modules to be used for water desalination in remote areas (Ahmad and Schmid, 2002).

Fig. 1.7 shows a basic assembly of an RO spiral wound module. Spiral-wound membrane elements are made from flat membrane envelopes (sheets), which are wrapped around a central perforated permeate collection tube. These flat sheets are separated by high porous spacer materials allowing product water to transfer to the central collection tube. The advantage of these spacers is to keep the layer of membrane apart and promotes the turbulence and mixing inside the feed channel. This in turn would promote the mass transport near the surface of the membrane and reduce the concentration polarisation (Marriott and Sørensen, 2003). In other words, this would minimise the boundary layer of membrane with a penalty of a slight increase in the pressure drop. However, the presence of feed spacer would also mitigate the fouling potential. Fig. 1.8 shows a schematically representation of a flat membrane envelope and the direction of water flow from x to y-axis and z-axis as the direction of flowing fresh water through the membrane.

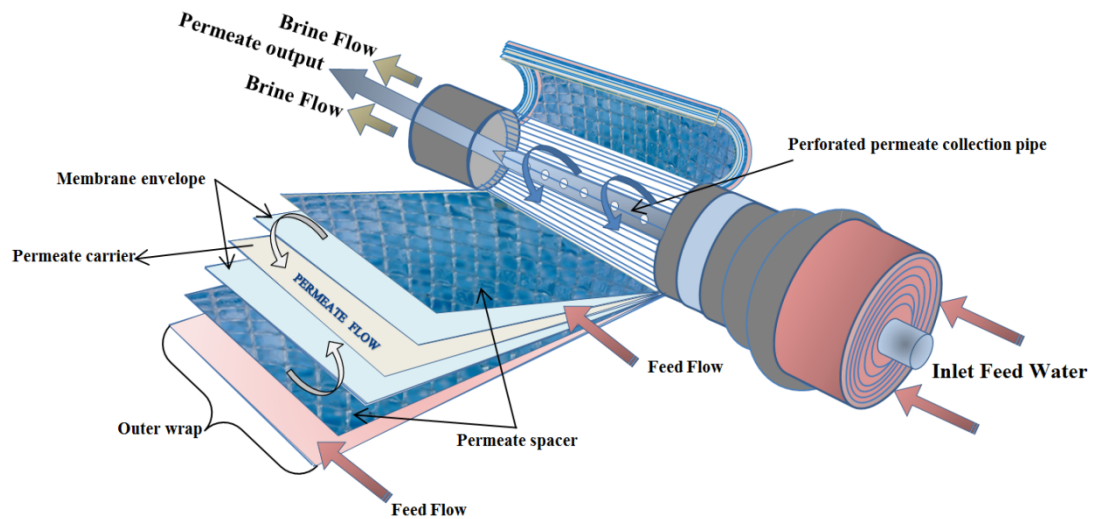


**Fig. 1.7.** Schematic diagram of a spiral wound membrane element

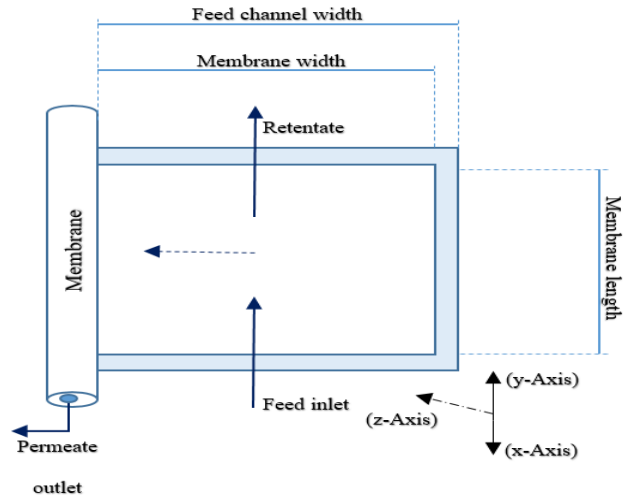


**Fig. 1.8.** Diagram of a flat membrane envelope (Adapted from Marriott and Sørensen, 2003)

The spiral wound RO process module occupies the largest market share with a noticeable growth of its use in different filtration fields such as wastewater treatment and beverage production besides seawater and brackish water desalination due to its aforementioned techno-economic factors (Kaghazchi et al., 2010; Al-Obaidi et al., 2017b). However, the spiral wound as any module has disadvantages which can be summarised by its pressure loss, susceptible to fouling.

### 1.9 Simple design of RO desalination plant

The RO desalination plants are essentially made with different designs. However, the desalination plants are mostly operated with the same approach of water filtration to produce high quality water. The feed water is fed and pressurised by high pressure pump to pass through a membrane of enclosed vessel which allow the passage of pure water and retaining salts on the membrane surface. However, the quantity and quality of produced water are dependent on the salt content of the feed water and the pressure applied. Moreover, the RO process efficiency depends on the type of membrane used that control the passage of water and solutes through the membrane's pores and its resistance towards the chemical and environmental impacts.

Basically, any practical RO plant has to have essential components including the membrane modules, high-pressure pumps, and energy-recovery devices (Abdallah et al.,

2005, Mohsen and Jaber, 2001). However, the site location and the start-up and shut-off have to be considered (Herold et al., 1998).

In the field of industrial seawater and brackish water desalination (such as APC, Jordan), a typical RO desalination plant consists of several stages as presented in Fig. 1.9. This includes five major sub-systems that professionally arranged, water abstraction (intake), pre-treatment, pumping system, RO membrane separation units, and post-treatment (Fritzmman et al., 2007).

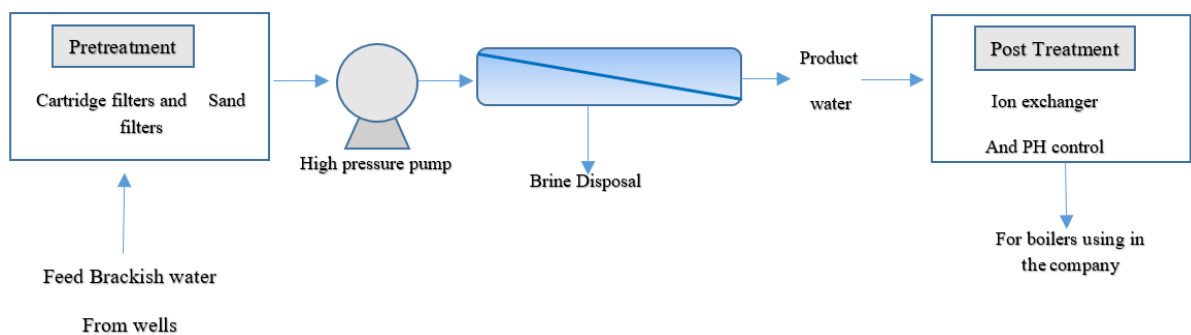


**Fig. 1.9.** Schematic diagram of the brackish water RO desalination plant

The intake feed water can be abstracted from wells in brackish water desalination case or open seawater intake systems. However, the wells provide water of less turbidity compared to open seawater intakes (Veza, 2001). In pre-treatment stage, the feed water is filtrated from sand and any particulate matter to protect membrane blockage as large debris can be found. Also, some chemicals are added to control the fouling and scaling intensity, which aid to increase the lifespan of membranes. The pre-treatment stage is the key to produce high-quality water and its complexity depend on the quality of feed water used. The next stage is the RO membrane units. In this stage, the water and salts are separated and the rejection of membrane depending on the type of membrane used that ranges between 98% to 99.5%. The pumping system is compulsory in this stage to apply the required pressure to overcome the osmotic pressure. This in turn allows fresh water to pass through the membrane's pores and reject concentrated discharge. Afterwards, the freshwater flows into the post-treatment stage to guarantee safe water while concentrated

saline water is discharged. In the post-treatment stage, the product fresh water can be re-mineralised, PH adjusted, di-ionisation, disinfected by chlorine injection to prevent bacterial growth and to be adjusted to suit the drinking water standards (Fritzmann et al., 2007).

### **1.10 Knowledge gap**

Several simulation and optimisation studies can be found in the open literature that elaborated methods of enhancement for process performance of brackish water desalination systems. However, critical and thorough studies to enhance the process performance indicators, specifically the specific energy consumption, of simple and complicated designs of brackish water multistage RO desalination plants were not achieved yet. Therefore, the recent research focuses on exploring several strategies to improve the performance of multistage brackish water RO desalination process considering different sizes of simple and complicated configurations. The multistage retentate reprocessing (simple) design of RO process and the multistage multi pass (complicated) design of RO process based brackish water desalination are considered in this research. To systematically conduct this goal, a specific model for a single RO process was developed and used to derive two models to characterise two different sizes of multistage RO brackish water desalination plants. Firstly, assessing the utilisation of an improved design of the RO system of retentate recycle mode to sustain the process at higher product capacity within acceptable specific energy consumption and freshwater salinity will be achieved. This is followed by applying methods of improvement included practical ideas of a novel design of RO system and implementing an energy recovery system to attain the process at a low energy consumption. This is basically carried out via analysing the performance of the desalination plant under a wide range of operating conditions. Then, investigating the most suitable brand of membranes for a RO plant from a set of different brands of membrane that would attain the highest-performance rejection at lowest energy consumption compared to the original membrane. Furthermore, exploring the lower energy consumption of the simple and complicated designs of RO process via optimisation. Finally, analysing the thermodynamic limitations including the assessment exergy will be addressed in this thesis.

### **1.11 Limitations of this research**

Several contributions were made in this this research (mentioned above). However, the research shortcomings are presented in the following.

- The recent research is basically built on a simple model developed to predict the performance indicators of a single spiral wound RO process. The influence of membrane fouling has not been critically involved in this model where a fixed value of fouling factor was considered. In fact, a fixed fouling factor will not practically characterise the real operation of RO process. Therefore, the prediction of the model will be less accurate after a long time of operation due to the possibility of fouling and scaling formations.
- The model developed of a single spiral wound RO process is basically a steady state model. Thus, the dynamic behaviour of the RO process has not been analysed.

### **1.12 Research aim and objectives**

#### ***1.12.1 Aim of research***

The overall aim of this research is to produce a reliable operation of the multistage brackish water RO desalination system via modelling, simulation, and optimisation.

#### ***1.12.2 Objectives of the research***

The objectives of the thesis included the following:

- (a) To carry out a literature review on the modelling, simulation, and optimisation of spiral wound RO process besides analysing the thermodynamic limitations and specific energy consumption.
- (b) To implement a novel edition of retentate recycle to the main design of multistage brackish water RO desalination system and investigate its contribution on the process performance via simulation based on the model developed for the multistage RO process.

- (c) To analyse the influence of adding an energy recovery device to the main design of RO system and explore its contribution on mitigating the specific energy consumption.
- (d) To investigate the most suitable brand of membranes for a RO plant from a set of different brands of membrane that would attain the highest-performance rejection at lowest specific energy consumption compared to the original membrane.
- (e) To optimise the operation of the simple and complicated designs of brackish water RO desalination process by exploring the optimal operating conditions that would ensure the lowest specific energy consumption with fulfilling the highest performance of the RO process.
- (f) To carry out an intensive analysis of exergy and thermodynamic limitations in several locations of the complicated design of brackish water RO desalination system of APC.

### **1.13 Thesis structure**

This research has been carried out in different stages and covered several tasks that are reported in different chapters. The thesis consists of **nine chapters** that are presented as follows:

#### **Chapter One: Introduction**

In this chapter, desalination background information and the classifications of desalination technologies are presented. Also, the principles of RO process are described in detail. After that, the scope of the thesis is introduced followed by a description of the aim and objectives of the research. The objectives, further, are broken down into specific points.

#### **Chapter Two: Literature Review**

In this chapter, a literature review of previous work on simple and detailed steady state and dynamic modelling, simulation, and optimisation of the spiral wound module are presented. Also, the thermodynamic limitations of RO based on the

desalination process and overview of energy consumption will be discussed in detail in this chapter.

**Chapter Three: Modelling of a Spiral Wound Reverse Osmosis Desalination System**

This chapter shows the development of a steady-state model for an individual spiral wound RO process that used to characterise the complete mathematical modelling of multistage brackish water RO plant.

**Chapter Four: Performance Evaluation of Reverse Osmosis Brackish Water Desalination Plant with Recycled Retentate Design**

The performance of multistage simple and complicated designs of brackish water RO desalination plants with a new design of different recycled ratios of the retentate is investigated via simulation.

**Chapter Five: Evaluation and Minimisation of Energy Consumption of Reverse Osmosis Brackish Water Desalination Plant**

In this chapter, the impact of implementing an energy recovery device at different efficiencies on the specific energy consumption and water recovery of simple and complicated designs of brackish water RO desalination is studied.

**Chapter Six: Performance evaluation of a reverse osmosis brackish water desalination plant with different brands of membranes**

In this chapter, the most suitable brand of membranes for two different designs of brackish water RO desalination plants from a set of different brands of membrane are investigated to attain the highest-performance rejection at lowest specific energy consumption compared to the original membrane.

**Chapter Seven: Optimisation of energy consumption in a reverse osmosis brackish water desalination plant**

An optimisation framework was embedded in the process model to reduce the specific energy consumption of simple and complicated designs of brackish water RO desalination plants.

**Chapter Eight: Thermodynamic limitations and exergy analysis of reverse osmosis brackish water desalination plant**

This chapter characterises by conducting a comprehensive study to analyse the exergy and thermodynamic limitations of a complicated design of brackish water RO desalination plant. Several locations of the RO process were tested to explore the one of the highest exergy destruction.

**Chapter Nine: Conclusions and Recommendations for future work**

Final conclusions and recommendations for future work that need to be done are presented.

## **CHAPTER TWO**

### **Literature Review**

#### **2.1 Introduction**

The 21<sup>st</sup> century has been termed as the “century of water shortage”, and its 1<sup>st</sup> and 2<sup>nd</sup> decades have been called “water crisis decades” (Kim et al., 2009). This is associated with a progressive increase of population growth and elevated levels of freshwater demand. According to some reports issued by World Health Organization (WHO), it is predicted that the half of population in the world will live in water-stressed regions by 2025. This means that about 2.1 billion people in the world will find it difficult to have access to safe drinking water (WHO, 2018). Another report from the United Nations World Water Assessment Program confirmed that one-fifth of the world's inhabitants are facing shortage of freshwater resources. In the meantime, several Middle Eastern, South East Asia and North Africa countries are struggling from water shortage and classified as water-stressed areas due to a lack of rainwater and water resources pollution (Mancosu et al., 2015). Accordingly, this scarcity is expected to affect up to 40% of the world's population by 2030. The improvement of seawater and brackish water desalination technologies is thus a pressing need. Basically, desalination is a water treatment process to produce fresh water from high salinity water by removing the dissolved salts and other contaminants. Therefore, desalination is widely deployed to enhance the quality of high-salinity seawater and low-salinity brackish water. Specifically, the desalination process involves the filtration of feed saline water that produces low-salinity water and brine (very concentrated water) (Alghoul et al., 2009).

Indeed, there was a clear incline and increased application of seawater and brackish water desalination in the world and especially in the Gulf region as the main technology for supplying fresh water. The Middle East has thus prevailed the global desalination market along the last decades (Fig. 2.1). Many of the world's desalination plants are situated in the Gulf Cooperation Council (GCC) countries that comprise Qatar, Saudi Arabia, UAE, Kuwait, Oman, and Bahrain. Based on the statistical data presented by the International

Energy Agency (IEA), about 58% of total desalination capacity in the world's lies in the Middle East and North Africa as shown in the Fig. 2.1 (Greenlee et al., 2009). Specifically, RO desalination projects have been remarkably increased and expanded especially between 2014 and 2016. For instance, the RO desalination plant of Ras Al-Khair located in Saudi Arabia associated with freshwater capacity of 1,025,000 m<sup>3</sup>/day in 2014 (Global Water Desalination Market 2018-2025 Current Trends 2018). Undoubtedly, the progressive increased line of water shortage would contribute to grow up the Global Desalination Market by 2025 as expected by the United Nations Department of Economic and Social Affairs (UNDESA). Historically, the first large scale desalination unit was installed in the Middle East in Kuwait in the 1950's. The world's biggest RO plant at a capacity of 274,000 m<sup>3</sup>/d was constructed in southern Arizona (Burgi et al., 2010).

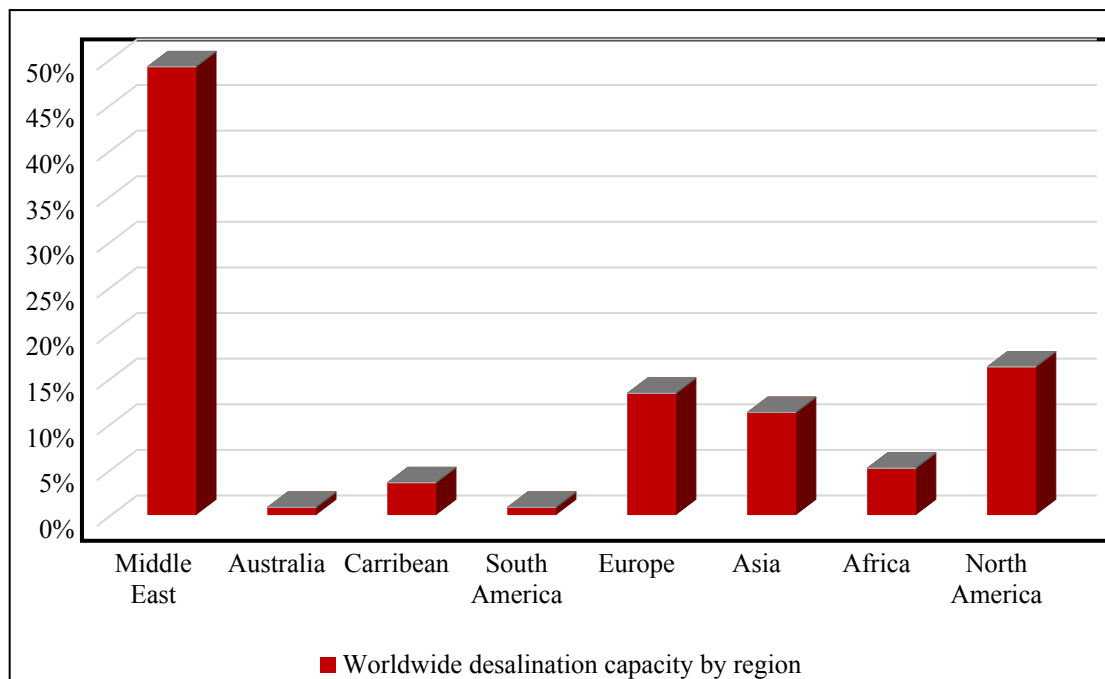


**Fig. 2.1.** The desalination capacity over the worldwide based on the region

According to the level of salinity, the water can be classified into three types of (El-Manharawy and Hafez, 2001);

- Seawater (high-salinity water) with a concentration of 35,000 mg/l of total dissolved solids (TDS) or more.

- Brackish water (medium-salinity water) with concentration between 1,000 – 15,000 mg/l of TDS.
- Fresh water (low-salinity water) with concentration below 500 mg/l of TDS.

The application of spiral wound module in the water treatment has initiated with understanding the transport phenomena of solvent and solute transport the membrane pores. This is originally required the development of accurate models to assess the performance of RO membrane via correlating the main operating conditions and the performance indicators. Basically, modelling of any RO process has a vital role to understand the transport phenomenon inside the module which helps to implement an optimum process design. Moreover, it aids to carry out a comprehensive simulation to specify the influence of each operating variable on the process outputs. Therefore, the operator can determine the best operating conditions to guarantee the optimum operation of RO process. In other words, the practical controlling variables can be obtained and leading to maximum performance. Interestingly, the modelling of a spiral wound module has a positive contribution to carry out process simulation and optimisation. The merits of RO process modelling, simulation and optimisation are summarised in the following.

***a. The importance of RO process modelling***

- A paramount tool to analysis and design the RO system.
- To forecast the long-term performance using the dynamic modelling version. Thus, the decision-makers can predict when to change the membrane elements.
- To predict the performance of different designs of RO systems.
- To be combined with the cost functions to assess the water production cost of different designs of RO systems (small, medium, and large sizes).
- To carry out extensive simulation and optimisation studies to improve the process performance.

***b. The importance of simulation***

- To conceive the power of operating conditions on the performance indicators of solute removal and water recovery.
- To analysis the effect of operating conditions of RO system on the specific energy consumption.
- A simulator tool can be used for process training and examining without the risk of damaging the equipment.
- To obtain suitable operating conditions to maintain the highest performance.
- To aid the process designer and select the best membrane area to achieve highest recovery.
- To carry out the process optimisation to progress the process operation and selecting the optimal operating conditions and process control.

***c. The importance of optimisation***

- To forecast the appropriate values of the control variables of the RO process that would attain the highest water recovery and lowest freshwater concentration.
- To obtain the optimal configuration of the multistage RO process by considering a set of several constraints communicated to the unit's equations or including inequalities to yield the favorite optimum responses.
- To minimise the total freshwater production cost whilst maintaining maximum quantity and quality of product water.
- To improve the design, operation, and assembly of multistage RO process at different periods of its life cycle.
- To reduce the total energy consumption of RO process with delivering a high-performance ratio and stable operation.
- To mitigate the fouling propensity of RO process by selecting the optimum control variables and process design.

An overview of the modelling, simulation, and optimisation of the SWRO process is thoroughly outlined in the following sections.

Up to this point, this chapter focuses on carrying out a critical review of the past work regarding the modelling, simulation, and optimisation considering the spiral wound module RO process. Moreover, the thermodynamic limitations based on the RO desalination process will be utilised in details including the energy consumption. Finally, the review of methodology of gPROMS will be outlined.

## **2.2 Overview of modelling of a spiral wound RO module**

Modelling of industrial processes is essential since it recognises the process mechanism and realises the intercorrelation between the process variables and its responses. This in turn enables the assessment of the influence of each control variable, which aids to allocating the objective functions through process simulation and optimisation. For instance, the modelling of RO process helps to understand the contribution of all control variables that control the process performance without resorting to carrying out extensive, expensive, and complicated experiments. Therefore, the relationship between the relevant RO process indicators, such as water recovery ratio, energy consumption and solute rejection, with the control variables of feed flow rate, pressure, temperature and designing variables of the membrane module dimensions can be outlined via simulation. Furthermore, the process variables can be optimised without applying any changes in the real plant via optimisation. Therefore, it is not surprising to find many serious attempts of modelling the RO process in the open literature. In this aspect, Oh et al., (2009) reported that the obtainability of a consistent RO model is of pronounced status for process design and operation. Therefore, generating rigorous models that could efficiently forecast the process mechanism was the main aim. However, several mathematical models were developed based on strict assumptions or relaxing reliable assumptions that entailed with a noticeable simplicity or difficulty of process modelling. Specifically, the complex models of the RO process have included membrane fouling, concentration polarisation, pressure drop and membrane aging. On the other hand, the simple models have relaxed the membrane fouling and ignoring the concentration polarisation. In addition, several models have been proposed with fixed mass transfer and permeate pressure at the permeate channel.

The earliest mathematical models (~1965) were developed to specify the transport phenomena of the RO process including both water and solute permeation via the membrane structure. This was specifically carried out by the investigation of two parental theories of the solution-diffusion model (homogeneous membrane model), and the irreversible thermodynamic model (Abbas, 2005, Senthilmurugan et al., 2005, Oh et al., 2009, Kaghazchi et al., 2010, Al-Obaidi et al., 2017a). This is followed by the development of several models to represent different complexity of transport phenomena for different RO process modules and feed type (seawater, brackish water, wastewater) based on the original basic models.

The next section presents in detail the state-of-the-art of modelling of the RO desalination process.

### ***2.2.1 Model of Lonsdale et al. (1965)***

Lonsdale et al. (1965) developed the basic solution-diffusion model (homogeneous or non-porous membrane model). They assumed that both solvent and solute are separately diffused from the high-concentration and pressure side to the low-concentration and pressure side, at different rates of diffusion, via the membrane texture due to the pressure and concentration gradient along the feed and permeate channels. In this regard, the total water flux ( $J_w$ ) (m/s) and solute flux ( $J_s$ ) (kmol/m<sup>2</sup>.s) are determined based on their diffusion mechanism, which are related to their solubility and solute mobility

$$J_w = A_w (\Delta p - \Delta \pi) = A_w ((P_r - P_p) - RT (C_r - C_p)) \quad (2.1)$$

$$J_s = B_s (C_r - C_p) \quad (2.2)$$

Water permeability coefficients (m/s atm) is  $A_w$ . Moreover,  $\Delta p, \Delta \pi, P_r, P_p, R, T, C_p, C_r$ , and  $B_s$  express the hydraulic pressure difference (atm), osmotic pressure difference (atm), the brine pressure (atm), the permeate pressure (atm), gas law constant (8.314 J/mol K), temperature (K), permeate concentration (kmol/m<sup>3</sup>), retentate concentration (kmol/m<sup>3</sup>) and salt permeability coefficient (m/s), respectively. It is worth noting that Lonsdale et al. (1965) assumed that solute flux does not rely on the pressure difference (Eq. 2.2). Interestingly, realising of water and solute transport parameters is critical to

predict the solvent and solute fluxes. However, ignoring both the pressure influence on the solute flux and the membrane characteristics are the main disadvantages of this model.

### **2.2.2 Model of Boudinar et al. (1992)**

Boudinar et al. (1992) established a mathematical model for an RO module considering the main parameters, which affect its performance based on the solution-diffusion model. The model considered the pressure loss in the feed and permeate channels is controlled by feed and permeate friction parameters based on the theory of Darcy for porous media. The features of the model developed are as follows:

#### **2.2.2.1 Assumptions**

- Validity of the solution-diffusion model to specify the solvent and solute transport mechanisms.
- Ignoring the variation of brine and permeate along axial and radial directions.
- Fixed fluid physical properties such as density and viscosity.
- The pressure change is neglected at the permeate collector tube.

#### **2.2.2.2 Model equations**

The solvent and solute fluxes via the membrane are measured using Eqs. (2.3) and (2.4), respectively. However, the water and solute permeability constants are estimated as

$$A_w = K_{1.0} \times 10^{-5} \exp^{-1.701 \times 10^2 P_f} \quad (2.3)$$

$$B_s = 1.112 \times 10^{-6} \exp^{274.15 \times 10^{-2} T} \quad (2.4)$$

Water permeability coefficient at zero pressure (m/s Pa) is  $K_{1.0}$ , while  $P_f$  and  $T$  are the feed pressure (Pa) and temperature (K), respectively. Eq. (2.5) expresses the correlation between water flux and solute flux to calculate the permeate concentration

$$C_p = \frac{J_s}{J_w + J_s} = \frac{J_s}{J_w} = \frac{B_s (C_r - C_p)}{J_w} \quad (2.5)$$

The retentate concentration  $C_r$  (kmol/m<sup>3</sup>) is estimated by a material balance equation as follows

$$C_r = \frac{C_f Q_f - C_p Q_p}{Q_r} \quad (2.6)$$

The feed concentration is  $C_f$  (kmol/m<sup>3</sup>), and  $Q_f$ ,  $Q_p$ ,  $Q_r$  represent the feed flow rate (m<sup>3</sup>/s), product flow rate (m<sup>3</sup>/s), and retentate flow rate (m<sup>3</sup>/s), respectively. The mass transfer coefficient  $k$  (m/s) and solute concentration at the membrane wall  $C_w$  (kmol/m<sup>3</sup>) are involved in Eq. (2.7)

$$J_w = k \ln \left[ \frac{C_w - C_p}{C_r - C_p} \right] \quad (2.7)$$

The osmotic pressure at operating temperature  $\pi_{T_i}$  (Pa) is calculated based on osmotic pressure at 25 °C ( $\pi_{T_{25}}$ ) as

$$\frac{\pi_{T_i}}{T_i} = \frac{\pi_{T_{25}}}{T_{25}} \quad (2.8)$$

$$\pi_{T_{25}} = 0.23745 + 6.4784 \times 10^{-4} C_b + 1.7753 \times 10^{-9} C_b^2 \quad (2.9)$$

The bulk concentration is  $C_b$  (kmol/m<sup>3</sup>). The physical properties of viscosity  $\mu$  (kg/m s) and diffusion coefficient  $D_s$  (m<sup>2</sup>/s) correlations are calculated using Eqs. (2.10) to (2.12), respectively.

$$\mu = 0.1 \mu_0 \exp^{-2.008 \times 10^{-2} T} \quad (2.10)$$

$$\mu_0 = 1.4757 \times 10^{-2} + 2.4817 \times 10^{-8} C_b + 9.3287 \times 10^{-14} C_b^2 \quad (2.11)$$

$$D_s = (0.72598 + 2.3087 \times 10^{-2} T + 2.7657 \times 10^{-4} T^2) \times 10^{-9} \quad (2.12)$$

### **2.2.3 Model of Avlonitis et al. (1991), Avlonitis et al. (1993) and Avlonitis et al. (2007)**

Avlonitis et al. (1991), Avlonitis et al. (1993) and Avlonitis et al. (2007) presented steady state distributed models instituted on the solution-diffusion model and the thin film theory to study the performance of a spiral wound RO module.

#### **2.2.3.1 Assumptions**

- The module is made up of a flat channel with fixed geometry.

- Variable fluid flow rate along the x-axis of feed channel and y-axis of permeate channel.
- Fixed fluid flow rate across the y-axis of feed side and x-axis of permeate side.
- Fixed mass transfer coefficient and physical properties.
- Fixed permeate concentration at the permeate channel.
- Fluid velocity specifies the friction parameters of the feed and permeate channels.

### 2.2.3.2 Model equations

The brine and the permeate friction parameters at different Reynolds numbers can be calculated using Eqs. (2.13) and (2.14), respectively.

$$K_{fr} = 0.309 R_{er}^{0.83} \quad (2.13)$$

$$K_{fp} = 46.2915 R_{ep}^{0.26} \quad (2.14)$$

The retentate and permeate friction parameters ( $m^2$ ) are represented as  $K_{fr}$  and  $K_{fp}$ , respectively and  $R_{er}$  and  $R_{ep}$  (dimensionless) are the Reynolds Number at retentate and permeate channels respectively. The water permeability coefficient  $A_w$  depends on the operating temperature and applied pressure

$$A_w = 2.955 \times 10^{-5} \exp^{(10.27 \frac{T - T_{293.15}}{T_{293.15}} - 0.0015 P_f)} \quad (2.15)$$

The solute transport parameter is expressed as a function of the applied temperature as depicted in Eq. (2.16).  $T_{293.15}$  is the operating temperature at 20 °C

$$B_s = 9.54 \times 10^{-7} \exp^{14.648 \frac{T - T_0}{T_0}} \quad (2.16)$$

The absolute temperature is  $T_o$  (K) at 20 °C.

#### **2.2.4 Model of Abbas and Al-Bastaki (2001)**

Abbas and Al-Bastaki (2001) presented a complete model to expect the performance of a spiral wound membrane module. Both turbulent and laminar flow regimes were considered in the model. However, the diffusivity is assumed constant.

##### **2.2.4.1 Model equations**

Eqs. (2.17) and (2.18) are used to assess turbulent and laminar flow regimes (Wilf and Klinko 1994)

$$Sh = 0.04 Re^{0.75} Sc^{0.33} \quad \text{for turbulent flow} \quad (2.17)$$

$$Sh = 1.86 (Re Sc d_h/L)^{0.33} \quad \text{for laminar flow} \quad (2.18)$$

Sherwood number is  $Sh$  (dimensionless), while  $Sc$ ,  $L$ , and  $d_h$  are Schmidt number (dimensionless), membrane length (m), and hydraulic diameter of the flow channel (m), respectively. The water  $A_w''$  (m/s.Pa) and solute  $B_s''$  (kg/m<sup>2</sup>.s Pa) permeability constants were determined based on the operating time  $t$  (day)

$$A_w'' = \frac{168 + 0.68 t}{166.3 + t} \times 10^{-5} \quad (2.19)$$

$$B_s'' = 0.68 \times 10^{-5} \exp\left(\frac{79}{t + 201.1}\right) \quad (2.20)$$

The water flux and mass transfer coefficient are the same as those used by (Boudinar et al. 1992).

#### **2.2.5 Model of Marriott and Sørensen (2003)**

Marriott and Sørensen (2003) established a distributed dynamic model for a spiral wound RO module by implementing mass balance, momentum, and energy equations and disregarded some mutual assumptions. This model describes the flow patterns inside the module and can be applied to any membrane separation. However, the variation of bulk concentration inside the feed channel due to solvent flux through the membrane was not entirely considered.

### 2.2.5.1 Assumptions

- The flow behavior in the module is not affected significantly by the bent channel.
- The channel curvature is negligible.
- The stagnant model describes the concentration polarisation.
- The friction parameter signifies the pressure drop along the feed channel.
- The pressure and temperature in feed channel are assumed constant.
- Fixed physical properties of the fluid.
- Steady state plug flow (no concentration variation in the perpendicular direction) inside the feed channel.

### 2.2.5.2 Model equations

Water (permeate) and solute (retentate) fluxes are represented as

$$J_w = A_w C_p (\Delta P - \Delta\pi) \quad (2.21)$$

$$J_s = B_s (C_f - C_p) \quad (2.22)$$

### 2.2.6 Model of Abbas (2005)

Abbas (2005) proposed a semi-rigorous model to inspect the performance of a RO desalination plant designed in three tapered stages. The model developed can predict the future plant performance.

#### 2.2.6.1 Model equations

The water and salt fluxes are calculated based on Sourirajan (1970) relationships as follows

$$Q_p = J_w A_m = A_m \frac{\Delta p - \Delta\pi}{(1.142 \times 10^{-10} R_p)} \quad (2.23)$$

$$J_s = \frac{C_w - C_p}{R_r} \quad (2.24)$$

Total production capacity is  $Q_p$  (m<sup>3</sup>/s), and  $A_m$ ,  $R_p$ , and  $R_r$  are the effective membrane area (m<sup>2</sup>), permeate membrane resistance which is relevant to  $(\frac{1}{B_s})$  (s/m), and retentate

membrane resistance (s/m), respectively. The bulk concentration  $C_b$  (kmol/m<sup>3</sup>) and bulk flow rate  $Q_b$  (m<sup>3</sup>/s) can be calculated based on their relative values on the feed and retentate sides

$$C_b = \frac{C_f + C_r}{2} \quad (2.25)$$

$$Q_b = \frac{Q_f - Q_r}{2} \quad (2.26)$$

Water recovery and solute rejection (dimensionless) are used to evaluate the performance of RO process as follow

$$WR = \frac{Q_p}{Q_f} \times 100 \quad (2.27)$$

$$SR = \frac{C_f - C_p}{C_f} \times 100 \quad (2.28)$$

### **2.2.7 Model of Geraldles et al. (2005)**

Geraldles et al. (2005) improved a steady state distributed model for a spiral wound RO process considering the mass and momentum transport inside the membrane modules. The model is substantially settled based on the solution-diffusion and ignores the diffusion flow in the feed channel and the pressure variation along the permeate channel.

#### **2.2.7.1 Assumptions**

Plug flow happens in the feed channel.

- Concentration polarisation is considered based on the film theory.
- The decrease of pressure inside the permeate channel is neglected.
- Physical properties of seawater are correlated based on temperature and concentration.

#### **2.2.7.2 Model equations**

Water and solute fluxes are expressed in Eqs (2.29) and (2.30)

$$J_w = A_w [P_f - \pi_m + \pi_p] \quad (2.29)$$

$$J_s = B_s (C_r - C_p) \quad (2.30)$$

The osmotic pressures of the feed water at high-concentration and low-concentration channels are denoted as  $\pi_m$  and  $\pi_p$  (Pa), respectively. Moreover,  $C_p$  is the permeate concentration which is calculated via Eq. (2.31)

$$C_p = \frac{J_s}{J_w} \quad (2.31)$$

The mass transfer coefficient  $k$  (m/s) is derived from the following correlation

$$Sh = 0.065 Re^{0.875} Sc^{0.25} = k 6.23 Re^{-0.3} \quad (2.32)$$

### 2.2.8 Model of Avlonitis et al. (2007)

Avlonitis et al. (2007) developed an extensive mathematical model to calculate the performance of any type of RO membrane modules. Their model considered both axial and tangential dimensions of RO membrane to determine the quality of the produced water.

#### 2.2.8.1 Model equations

Eqs. (2.33), (2.34), and (2.35) are used to estimate the brine friction parameter, water permeability coefficient, and salt permeability coefficient, respectively.

$$k_{fr} = 309 \times Re_f^{0.83} \quad (2.33)$$

$$A_w = K_{1m} \exp^{8.6464 \left( \frac{T - T_{20}}{T_{20}} \right) - 0.0028 P_f} \quad (2.34)$$

$$B_s = K_{2m} \exp^{14.648 \left( \frac{T - T_0}{T_0} \right)} \quad (2.35)$$

Two symbols of  $K_{1m}$  and  $K_{2m}$  are constants that depend on membrane type.

### 2.2.9 Model of Majali et al. (2008)

Majali et al. (2008) developed two models for two pilot-scale RO plants to analyse their performances. Firstly, a semi-empirical simple model was developed for a RO Sharjah plant used to desalinate brackish water. This model predicts the flow rate, concentration, and pressure profiles but ignored the membrane area. Secondly, a

permeability model was proposed to predict the performance of RO plant in Qatar that desalinates high salinity seawater. Interestingly, the model predicts the membrane area. The model's assumptions are as follows.

#### 2.2.9.1 Assumptions

- Steady state and isothermal operation.
- Fixed salt rejection and recovery for each membrane module for the semi-empirical model.
- Fixed water and salt transfer parameters along the membrane for the permeability model.
- Atmospheric pressure inside the permeate channel.

#### 2.2.9.2 Model equations of a semi-empirical simple model (Majali et al. 2008)

Eqs. (2.36) and (2.37) show the mass and salt balances on the SW membrane module for both semi-empirical and permeability models

$$Q_f = Q_r + Q_p \quad (2.36)$$

$$Q_f C_f = Q_r C_r + Q_p C_p \quad (2.37)$$

The product recovery and salt rejection represent the most necessary performance indicators,

$$Q_p = WR Q_f \quad (2.38)$$

$$C_p = C_f (1 - SR) \quad (2.39)$$

The pressure drop and the osmotic pressure are given in Eqs. (2.40) and (2.41), respectively.

$$\Delta p = 0.5 (P_f + P_r) - P_p \quad (2.40)$$

$$\Delta \pi = RT \frac{\rho}{MW} \left( \frac{C_f Q_f + C_r Q_r}{Q_f + Q_r} - C_p \right) \quad (2.41)$$

The water density is  $\rho$  (kg/m<sup>3</sup>) and  $MW$  is the salt molecular weight (kg/kmole).

#### 2.2.9.3 Model equations of an advanced model of Majali et al. (2008)

The permeability model was developed based on the mechanical-statistical model basically established by Mason and Lonsdale (1990). This model included the mass and

salt balances equations of Eqs. (2.42) and (2.43), and the following relations give the water and salt fluxes.

$$Q_p = (\Delta P - \Delta \pi) A_w A_m \quad (2.42)$$

$$C_p Q_p \rho = \left( \frac{C_f Q_f + C_r Q_r}{Q_f + Q_r} - C_p \right) B_s A_m \quad (2.43)$$

### **2.2.10 Model of Oh et al. (2009)**

Oh et al. (2009) improved a simple mathematical model based on the solution-diffusion principles and considering the impact of multiple fouling of spiral wound RO system.

#### **2.2.10.1 Assumptions**

- Constant water flux and mass transfer coefficient after varying inlet feed flow rate.
- Constant permeate pressure at the permeate channel.
- The osmotic pressure is proportionated to the solute concentration.

#### **2.2.10.2 Model equations**

Water permeation through the membrane structure is formulated to consider the pressure loss along the membrane feed channel

$$J_w = A_w (P_f - P_{loss}) \quad (2.44)$$

The pressure loss is  $P_{loss}$  (Pa). However, the solute flux equation of Lonsdale et al. (1965) has been used. The osmotic pressure is expressed as

$$\Delta \pi = (C_r - C_p) R T \quad (2.45)$$

### **2.2.11 Model of Lee et al. (2010)**

A complete dynamic model was developed by Lee et al. (2010) based on the work of (Lee and Lueptow, 2001; Marriott and Sørensen, 2003; Oh et al., 2009). Lee et al. (2010) investigated the dynamic features and process design and operation of the Jeddah large-scaled RO desalination plant of production capacity of 56800 m<sup>3</sup>/day and located in the Kingdom of Saudi Arabia. The applied assumptions were the same as the previous models except RO process was considered as a dynamic operation.

### 2.2.11.1 Model equations

Based on steady-state membrane transport, the solvent flux equation is depicted as

$$J_w = A_w (P_f - P_{loss}) = A_w [P_f - (\Delta\pi + P_{drop})] \quad (2.46)$$

The pressure drop along the x-axis of feed side is  $P_{drop}$  (atm). The solute transport parameter is obtained from

$$B_s = B_{s0} \exp^{\frac{\beta_1(T-273)}{273}} \quad (2.47)$$

The intrinsic and fixed solute transport parameters are  $B_{s0}$  and  $\beta_1$  (dimensionless), respectively. The concentration polarisation  $\phi$  (dimensionless) is given by Eq. (2.48).

$$\phi = \frac{C_w - C_p}{C_r - C_p} = \exp^{\frac{B_s}{k}} \quad (2.48)$$

The mass transfer coefficient  $k$  (m/s) for the bulk diffusion of the solute is expressed as

$$k = 0.551 \left( \frac{u_f d_h}{v} \right)^{0.4} \left( \frac{v}{D_s} \right)^{0.17} \left( \frac{C_r}{\rho} \right)^{-0.77} \left( \frac{D_s}{d_h} \right) \quad (2.49)$$

The feed solution velocity on the bulk high-concentration side  $u_f$  (m/s) and  $v$  denotes the kinematic viscosity (cm<sup>2</sup>/s). The dynamic equation of retentate concentration ( $C_r$ ) along the length membrane (x\_ dimension (m)) is derived as

$$\frac{\partial C_r}{\partial t} = - \frac{\partial}{\partial x} \left( C_r u_f - D_s \frac{\partial C_r}{\partial x} \right) - \frac{1}{d_h} J_s \quad (2.50)$$

### 2.2.12 Model of Kaghazchi et al. (2010)

Kaghazchi et al. (2010) utilised a steady state model grounded on the theory of the solution-diffusion model for the spiral wound membrane module to examine the performance of two industrial seawater RO plants. The equations of Abbas (2005) have been used to forecast the water and salt fluxes, and consequently the water recovery and salt rejection were estimated. Interestingly, Kaghazchi et al. (2010) considered the variation of operating conditions along the feed channel axis.

### 2.2.13 Model of Ruiz-Saavedra et al. (2015)

A simple model was invented by Ruiz-Saavedra et al. (2015) for a spiral wound brackish water RO plant located in Spain. The model included the fundamental operational data of

the plant such as the chemical composition, pH, silt density index (SDI) <sup>1</sup> and temperature. It can calculate the product concentration and quantity, considering the manufacturer's membrane design guidelines. The model assumptions considered were similar to those that have been presented in the previously developed models.

### 2.2.13.1 Model equations

The water flow rate  $Q_{pi}$  (m<sup>3</sup>/s) through a membrane element  $i$  in a series of membrane elements stuffed in a pressure vessel is calculated as

$$Q_{pi} = A_{wi} (\Delta P_i - \Delta \pi_i) A_{mi} \quad (2.51)$$

Water permeability constant of the membrane element  $i$  is  $A_{wi}$  (m/Pa s), and  $\Delta P_i$ ,  $\Delta \pi_i$ , and  $A_{mi}$ , are the pressure drop across the membrane element  $i$  (Pa), the differential osmotic pressure along the membrane element  $i$  (Pa), and the membrane surface area (m<sup>2</sup>) of the membrane element  $i$ , respectively. The salt flux  $J_{si}$  (kmol/m<sup>2</sup> s) via the membrane element  $i$  is formulated as

$$J_{si} = B_{si} \Delta C_i A_{mi} \quad (2.52)$$

The salt permeability constant of the membrane element  $i$  (m/s) and the differential solute concentration along the membrane element  $i$  (kmol/m<sup>3</sup>) are expressed as  $B_{si}$ , and  $\Delta C_i$ , respectively. The osmotic pressure of the average concentration of the RO element  $i$   $\pi_{fri}$  (Pa) is expressed as

$$\pi_{fri} = \pi_{fi} WR_i CP_i \quad (2.53)$$

The osmotic pressure of the feed concentration of membrane element  $i$   $\pi_{fi}$  (Pa). Moreover,  $WR_i$ , and  $CP_i$  are the water recovery of membrane element  $i$ , and the concentration polarisation of  $i$ , respectively.

---

<sup>1</sup>Silt density index (SDI) is expressed as the flux decline calculated by differentiating the initial flux to the flux after a constant time.

#### 2.2.14 Model of Kotb et al. (2015)

Kotb et al. (2015) developed a simple model by considering several layouts for two modules of RO systems to study concentration polarisation. The model developed was based on the same set of assumptions as those made by Boudinar et al. (1992) with ignored the module pressure drop.

##### 2.2.14.1 Model equations

The volumetric brine flow rate and concentration are calculated based on Eqs. (2.7), and (2.36), respectively.

The water flux via a membrane is estimated based on Wiley et al. (1985). However, the solute flux has been calculated by Eq. (2.30)

$$J_w = A_w P_{eff} \quad (2.54)$$

The residual transmembrane pressure is  $P_{eff}$  (Pa).

$$P_{eff} = (P_f - P_p - \Delta P - \frac{\Delta p_f}{2}) - (\pi_w - \pi_p) \quad (2.55)$$

The pressure drop in membrane module channel  $\Delta p_f$  (Pa) consists of pressure losses in the inlet and outlet module manifolds ( $\Delta p_{in}$  and  $\Delta p_{out}$ ) (Pa). The osmotic pressure at the membrane wall and permeate channel are  $\pi_w$  and  $\pi_p$  (Pa). The correlation of Maskan et al. (2000) has been deployed to guess the mass transfer coefficient

$$k = 1.62 \left( \frac{Re Sc d_{ch}}{L} \right)^{0.33} \frac{D_s}{d_{ch}} \quad Re \leq 2100 \quad (2.56)$$

$$k = 0.023 Re^{0.875} Sc^{0.25} \frac{D_s}{d_{ch}} \quad Re > 2100 \quad (2.57)$$

The membrane channel diameter is  $d_{ch}$  (m).

#### 2.2.15 Model of Dimitriou et al. (2017)

Dimitriou et al. (2017) established a model based on the solution-diffusion and film theory for a spiral wound RO membrane module. Several parameters along the x-axis of feed channel are explored including the solute and solvent fluxes, concentration at the retentate and permeate sides and pressure drop in the membrane element under different pressure and flow rate operation. Therefore, variable values of the solute concentration, pressure

and fluid velocity at feed and permeate sides are evaluated at each point along the x-direction.

#### **2.2.15.1 Assumptions**

- The physical properties of fluid are a function of the salinity and temperature.
- Flat feed and permeate channel profiles. Specifically, the channel thickness is apparently lower than the radius of the module.
- Plug flow in both feed and permeate channels.

#### **2.2.15.2 Model equations**

The total water flux  $J_{total}$  (kg/m<sup>2</sup>.s) via the membrane structure is simultaneously represented as the summation of water  $J_w$  and solute  $J_s$  fluxes

$$J_{total} = J_w + J_s \quad (2.58)$$

The solvent and solute fluxes have been considered the same as those presented by Lonsdale et al. (1965). The pressure and osmotic pressure variances along the membrane are defined in Eqs. (2.59) and (2.60), respectively.

$$\Delta P = P_r - P_p \quad (2.59)$$

$$\Delta \pi = n_s R T (C_w - C_p) \quad (2.60)$$

The number of ions per salt molecule is  $n_s$  (e.g.  $n_s = 2$  for NaCl).

**Table 2.1.** Summary of the models developed for spiral wound RO process

Author and year	Main characteristics	Shortcomings
<i>(Lonsdale et al., 1965)</i>	<ul style="list-style-type: none"> <li>• A homogeneous diffusion model for cellulose acetate membrane.</li> <li>• Explained the transport phenomena through membrane films in the RO process.</li> <li>• Solvent and solute are dissolved in the nonporous surface layers of the membrane.</li> </ul>	<ul style="list-style-type: none"> <li>• Constant pressure throughout the membrane channels.</li> </ul>
<i>(Avlonitis et al., 1991)</i>	<ul style="list-style-type: none"> <li>• Considering the pressure loss occurred in brine and permeate channels.</li> <li>• Brine and permeate friction parameters, and membrane water permeability constant were integrated.</li> </ul>	<ul style="list-style-type: none"> <li>• The osmotic pressure and the concentration polarisation were ignored.</li> </ul>
<i>(Boudinar et al., 1992)</i>	<ul style="list-style-type: none"> <li>• Involved the main parameters affecting the performance of a SW module.</li> </ul>	<ul style="list-style-type: none"> <li>• Constant fluid density.</li> <li>• Neglected the pressure drop along the permeate tube.</li> </ul>
<i>(Avlonitis et al., 1993)</i>	<ul style="list-style-type: none"> <li>• Considered the thin film theory to characterise concentration polarisation.</li> <li>• The concentration gradient along the membrane feed channel was embedded.</li> </ul>	<ul style="list-style-type: none"> <li>• Neglected the solute–solute interaction in multi-component solutions.</li> </ul>
<i>(Abbas and Al-Bastaki, 2001)</i>	<ul style="list-style-type: none"> <li>• Turbulent and laminar flow regimes were considered.</li> <li>• Represented a decay in water flux because of membrane fouling.</li> </ul>	<ul style="list-style-type: none"> <li>• Ignored the solute–solute interaction.</li> <li>• Eliminated the description of the membrane transport mechanism.</li> </ul>
<i>(Marriott and Sørensen, 2003)</i>	<ul style="list-style-type: none"> <li>• Described the flow patterns inside a SW module and characterised the main features of the membrane.</li> <li>• The pressure drop of flow was characterised by the friction parameter.</li> <li>• The stagnant film model presented the concentration polarisation.</li> </ul>	<ul style="list-style-type: none"> <li>• The permeate flow area was assumed constant.</li> </ul>
<i>(Abbas, 2005)</i>	<ul style="list-style-type: none"> <li>• Investigated a neural network model (NNM) to guess the RO performance.</li> </ul>	<ul style="list-style-type: none"> <li>• The diffusivity, viscosity, and density were assumed constant.</li> </ul>
<i>(Geraldes et al., 2005)</i>	<ul style="list-style-type: none"> <li>• Improved a steady state distributed model for a SW RO process.</li> <li>• Mass and momentum transport inside the membrane modules were realised.</li> </ul>	<ul style="list-style-type: none"> <li>• Ignored the pressure change inside the permeate channels.</li> <li>• Ignored diffusion flow inside the feed side.</li> </ul>
<i>(Avlonitis et al., 2007)</i>	<ul style="list-style-type: none"> <li>• Two-dimensional flow equations were developed.</li> <li>• Easy to be used for any membrane with a bit modification for the water and solute permeability constants.</li> </ul>	<ul style="list-style-type: none"> <li>• Ignored the permeate concentration compared to the feed concentration.</li> </ul>
<i>(Majali et al., 2008)</i>	<ul style="list-style-type: none"> <li>• Developed semi-empirical and permeability models for two types of pilot scale RO plants.</li> </ul>	<ul style="list-style-type: none"> <li>• Comprehensive mixing conditions were presumed in the feed and permeate channels.</li> <li>• The semi-empirical model assumed fixed salt retention and water recovery.</li> </ul>

		<ul style="list-style-type: none"> <li>Fixed permeability coefficients for water and salt fluxes across the membrane are assumed.</li> </ul>
<i>(Oh et al., 2009)</i>	<ul style="list-style-type: none"> <li>A simple model relying on the solution-diffusion principles was developed that signifies the mechanisms of multiple fouling of a SW RO system.</li> </ul>	<ul style="list-style-type: none"> <li>The diffusion coefficient was unrelated to solute concentration.</li> <li>Fixed mass transfer parameter for a specified fluid condition.</li> </ul>
<i>(Lee et al., 2010)</i>	<ul style="list-style-type: none"> <li>A dynamic model was developed to explore the dynamic features and process operation of a large-scale RO desalination plant.</li> </ul>	<ul style="list-style-type: none"> <li>Dynamic fouling was not involved.</li> </ul>
<i>(Kaghazchi et al., 2010)</i>	<ul style="list-style-type: none"> <li>A steady state model was provided for a SW membrane module to examine the performance of two industrial seawater RO plants.</li> </ul>	<ul style="list-style-type: none"> <li>Ignored the effect of surface charge, pore length, tortuosity, bound water, and molecular shape.</li> </ul>
<i>(Ruiz-Saavedra et al., 2015)</i>	<ul style="list-style-type: none"> <li>A modest model for the SW membrane RO process was investigated relying on the solution-diffusion model.</li> </ul>	<ul style="list-style-type: none"> <li>Ignored the solute–solute interaction.</li> </ul>
<i>(Kotb et al., 2016)</i>	<ul style="list-style-type: none"> <li>A simple model for RO system was developed to study the concentration polarisation.</li> </ul>	<ul style="list-style-type: none"> <li>Fouling propensity was not precisely involved.</li> </ul>
<i>(Dimitriou et al., 2017)</i>	<ul style="list-style-type: none"> <li>A dynamic model for a SW RO process was established under a non-constant operating condition of pressure and flow rate.</li> </ul>	<ul style="list-style-type: none"> <li>Plug flow was assumed in both feed and permeate sides.</li> </ul>
<i>This work</i>	<ul style="list-style-type: none"> <li>A mathematical model for the multistage multi-pass medium-sized SW brackish water RO process was presented.</li> <li>Highlighted the fouling factor.</li> </ul>	<ul style="list-style-type: none"> <li>Absence of a specific formula to signify the membrane retardation due to fouling for a long operation time.</li> </ul>

### 2.3 Overview of simulation of a spiral wound RO process

To obtain higher efficiency and economical use of the RO seawater desalination process, two important parameters must be maximised: the product water quality and quantity. These parameters are adversely impacted by the operating conditions, membrane fouling, hydrolysis, and compaction in the RO unit. Raising the feed pressure is one of the probable solutions to maintain constant productivity. However, this would cause a **increase** in production cost as a result to a higher constraint of energy for filtration. Therefore, it is crucial to assess the process performance against the control variables via simulation to operate a RO plant efficiently. Basically, the process parameters are mainly affected by the characteristics of raw water and the efficiency of the pre-treatment scheme (Abbas and Al-Bastaki, 2001). This section highlights an overview of the many simulation studies that have been carried out and deployed to predict the performance of RO desalination system. Costa and Dickson (1991) used their model, which is based on Kimura Sourirajan fundamentals, to conduct a simulation to investigate the performance of a spiral wound RO membrane element under different control variables for a single solute system and with a different number of RO membrane modules in series. They included the influence of operating pressure, feed flow rate, and the number of modules arranged in a series configuration. Their simulation results showed that the recovery rate is increased with increasing pressure but dropped dramatically with increasing feed flow rate. The recovery rate is increased by about 10 times at a pressure of 29.6 atm when increasing the number of modules from 1 to 10.

Boudinar et al. (1992) improved the performance of a spiral wound module based on physical transportation phenomena via simulation. A wide range of feed conditions including concentration, pressure and flow rate of the brine and permeate streams were considered. Their results showed that the brine velocity, pressure, and water flux have a significant role in limiting the thickness of the mass transfer boundary layer at the membrane wall, that in turn improves the spiral wound membrane performance.

Abbas (2005) explored the performance of an industrial medium-scale brackish water spiral wound RO desalination plant (40 m<sup>3</sup>/day), which was designed in three tapered stages using their semi-rigorous steady-state model. Specifically, the influence of feed flow rate and operating pressure have been tested on the plant performance for different

membrane modules arrangement. The simulation results showed a deterioration of the product quality as a result of increasing pressure and feed flow rate. This is attributed to a decrease in the net transmembrane pressure difference caused by the high-frictional pressure drop. However, both solute rejection and water production were improved at low to moderate feed pressures and feed flow rates. The influence of feed spacer on the calculation of pressure drop was also evaluated. This is basically carried out by including the total drag force of the feed spacer to calculate the pressure drop along the membrane length using the relationship of Da Costa et al. (1994).

Hyung and Kim (2006) appraised the consequence of feed parameters including temperature and pH on boron rejection on the performance of a seawater RO process based on their mechanistic predictive developed model. They confirmed that boron rejection could be improved due to increasing pH, decreasing temperature, and increasing pressure. Pais and Ferreira (2007) evaluated the performance of spiral wound membranes based industrial desalination plant over a working time of 454 days based on the solution-diffusion model. They demonstrated that water and solute permeability constants are important pointers in assessing the membrane performance. The simulation results showed a decrease in water permeability coefficient due to the absence of membrane cleaning during a given period. On the other hand, salt permeability had significantly enlarged during the summer season as a result to the temperature impact.

Oh et al. (2009) analysed the effect of several parameters including the water flux, temperature, and fouling mechanism on the efficiency of a RO system over a wide set of feed conditions. Also, the impact of feed water temperature on the boron concentration and energy consumption in permeate was explored. They showed that the recovery ratio increased with increasing feed pressure. However, the energy consumption decreases with decreasing water flux despite the improvement of solute rejection. Furthermore, raising the feed temperature would decrease the specific energy and boron rejection due to increasing boron concentration in the permeate channel. An optimum permeate flux and recovery ratio for a specific condition of boron concentration in permeate and energy consumption were investigated.

Mane et al. (2009) simulated boron removal in pilot and full-scale, single-stage, single-pass RO processes and based on 6 and 8 spiral wound membrane elements in a series to

treat seawater. The model considered different water quality and operating conditions. Their results showed that boron rejection decreases due to a decrease in pressure and pH or an increase in temperature. Moreover, boron removal is mainly influenced by the overall water recovery.

Kaghazchi et al. (2010) simulated two industrial seawater RO desalination plants utilising spiral wound membrane modules. A semi-rigorous mathematical model was used to examine their performance under various feed conditions of feed pressure and flow rate. Results exhibited that any growing of feed flow rate would cause a decrease in the permeate concentration due to increasing mass transfer coefficient and concentration polarisation. Also, increasing the operating pressure increases the water flux with non-linear behavior despite increasing the salt concentration along the feed channel that promotes the osmotic pressure.

Farhat et al. (2013) investigated the performance of a new cohort of RO membranes of two-pass configuration to remove boron from seawater of Arabian Gulf. Specifically, the impact of operational parameters of the second pass including feed water concentration, pressure, bulk velocity, temperature on boron removal was assessed. Their simulation results show that 96% of boron removal from brackish water can be achieved with low temperatures, high feed flow velocities and high pressures. However, with high feed temperatures boron removal decreased markedly.

Kotb et al. (2015) studied the influence of feed characteristics and membrane module sizes on the salt concentration at the membrane surface using a simple model. They examined the effect of feed features (feed concentration and feed flow rate), control variables (feed temperature and feed pressure) and membrane dimensions on the salt concentration at the surface of each membrane. Results showed a decrease in the wall concentration as a result to increasing feed flow rate and feed temperature while it is increased with increasing feed pressure, feed concentration and membrane area. Also, increasing the feed temperature is more practicable to reduce the wall concentration than decreasing the feed pressure and increasing the feed flow rate. This is attributed to high energy consumption in case of increasing pressure. More specifically, raising the temperature from 25 to 50 °C would reduce the membrane surface concentration by 23%. They concluded that the wall concentration is nearly double the feed concentration as a result of growing the

temperature from 25 to 35 °C. Consequently, the wall concentration was condensed by 7% while the flow rate and pressure are increased by 2%.

Al-Obaidi et al. (2018a) simulated the operating conditions of TDS of lower than 2 ppm multistage, multi-pass medium-sized spiral wound brackish water RO desalination system of the Arab Potash Company (APC). Simulations were carried out to study the effect of increasing by 20% the operating conditions from the base case of actual plant data against numerous operating parameters including feed concentration, feed flow rate, feed pressure, and feed temperature. Results confirmed that both feed flow rate and pressure have a positive contribution on the product salinity.

Table 2.2 summarises the simulation results of the selected literature of spiral wound RO system.

**Table 2.2.** Summary of the previous work of RO simulation

Authors and year	Highlighted characteristics	Simulation results
<i>(Costa and Dickson, 1991)</i>	<ul style="list-style-type: none"> <li>Predicted the performance of a spiral wound RO membrane element based on various feed conditions for a single solute system.</li> </ul>	<ul style="list-style-type: none"> <li>Recovery rate increased with increasing the pressure.</li> <li>Recovery rate decreased with increasing flow rate.</li> </ul>
<i>(Boudinar et al., 1992)</i>	<ul style="list-style-type: none"> <li>Investigated the performance of two types spiral wound modules against the concentration, pressure and flow rate of the brine and permeate streams.</li> </ul>	<ul style="list-style-type: none"> <li>The thickness of the mass transfer boundary layer was affected by the brine velocity, flux, concentration, and pressure.</li> </ul>
<i>(Abbas, 2005)</i>	<ul style="list-style-type: none"> <li>Explored the performance of a spiral wound membrane of a medium-scale brackish water RO desalination system based on the feed flow rate, pressures, and the membrane modules arrangement.</li> </ul>	<ul style="list-style-type: none"> <li>High operating pressures leads to a weakening in product quality.</li> <li>High flow feed rates drive to a drop in the water production and permeate quality.</li> </ul>
<i>(Hyung and Kim, 2006)</i>	<ul style="list-style-type: none"> <li>Estimated the performance of full-scale spiral wound RO processes based on studying the influence of pH and temperature on boron removal.</li> </ul>	<ul style="list-style-type: none"> <li>Boron rejection decreased as a result to a decrease in pH or an increase in temperature.</li> </ul>
<i>(Pais and Ferreira, 2007)</i>	<ul style="list-style-type: none"> <li>Studied the performance of a spiral wound membrane desalination system based on water and solute permeability coefficients evolution.</li> </ul>	<ul style="list-style-type: none"> <li>Water permeability coefficient was decreased due to the absence of membranes cleaning during the considered period.</li> <li>Salt permeability has enlarged during the summer due to temperature increases.</li> </ul>
<i>(Oh et al., 2009)</i>	<ul style="list-style-type: none"> <li>Simulation study was achieved to predict the performance of RO plant at any operating conditions.</li> </ul>	<ul style="list-style-type: none"> <li>Recovery ratio increased with increasing feed pressure.</li> <li>Specific energy consumption decreased with decreasing water flux.</li> <li>Increasing the feed temperature would decrease the specific energy and boron rejection due to increasing the boron concentration in the permeate channel.</li> </ul>
<i>(Mane et al., 2009)</i>	<ul style="list-style-type: none"> <li>Analysed the boron rejection of a pilot- and full-scale for single-stage single-pass RO processed based on 6 and 8 spiral wound elements to treat seawater.</li> </ul>	<ul style="list-style-type: none"> <li>Boron rejection decreased due to a decrease in pressure and pH or an increase in temperature.</li> <li>Boron rejection was mainly affected by the overall process recovery.</li> </ul>
<i>Kaghazchi et al., 2010)</i>	<ul style="list-style-type: none"> <li>Investigated the operation and performance of two industrial seawater RO plants based on spiral wound membrane modules.</li> </ul>	<ul style="list-style-type: none"> <li>At higher feed flow rate, concentration polarisation was neglected.</li> </ul>

		<ul style="list-style-type: none"> <li>Increasing feed flow rate caused a decrease in the permeate concentration.</li> <li>Increasing operating pressure has increased the water flux with non-linearly behaviour.</li> </ul>
<i>(Farhat et al., 2013)</i>	<ul style="list-style-type: none"> <li>Studied the performance of a new group of RO membranes under a two-pass arrangement and without any pH alteration to remove boron from seawater.</li> </ul>	<ul style="list-style-type: none"> <li>Lower boron removal was obtained with high feed temperatures.</li> <li>Boron elimination was influenced by feed concentration, membrane material, pH, bulk velocity, feed pressure, and temperature.</li> </ul>
<i>(Kotb et al., 2015)</i>	<ul style="list-style-type: none"> <li>A considerable range of control variables was investigated on the concentration polarisation of a spiral wound module.</li> </ul>	<ul style="list-style-type: none"> <li>Increasing the module area, feed concentration, and feed pressure would increase the concentration at the membrane wall.</li> <li>Increasing feed temperature and flow rate would decrease the wall concentration.</li> </ul>
<i>Al-Obaidi et al. (2018a)</i>	<ul style="list-style-type: none"> <li>Simulated the performance of a low-salinity multistage multi-pass medium-sized spiral wound brackish water RO desalination plant.</li> </ul>	<ul style="list-style-type: none"> <li>The feed flow rate and feed pressure have positively affected the permeate salinity.</li> </ul>
<i>This work</i>	<ul style="list-style-type: none"> <li>Simulated the small-scale multistage RO brackish water desalination system.</li> </ul>	<ul style="list-style-type: none"> <li>The feed flow rate, pressure, and temperature have positively affected the permeate salinity.</li> </ul>

## **2.4 Overview of optimisation a spiral wound RO process**

Optimisation of RO process has been presented with less attention in the last few decades if compared to modelling and simulation studies. Following to the modern progresses in advanced numerical approaches, optimisation methods can hold complex problems in the operation and/or design of different manufacturing processes (Edgar et al. 2001). Implementation of the operating variables set and designed values at plant start-up time would not assure the predictable productivity due to operational instabilities. Therefore, it is important to set an amended set of optimal points of the specified operating conditions compared to employing of designed and real plant data (Tanvir and Mujtaba 2008).

The optimisation studies of (Hatfield and Graves, 1970; van der Meer and van Dijk, 1997) focused on maximising the permeate production and specific productivity in order to reduce the operational cost by manipulating the water recovery, feed flow rate, and pressure. Moreover, the arrangement of RO modules has also contributed to attaining the objective function. Specifically, the optimum design of RO process would guarantee the best connection between the feed and product streams of different stages. Many studies have also been carried out to diminish specific energy consumption by refining membrane permeability and based on varying the recovery ratio, salinity, membrane configuration, existence of energy recovery device, feed pressure, flow rate and temperature ( Wilf and Schierach, 2001; Oh et al., 2009; Zhu et al., 2009; Li, 2010;). Previous studies on optimisation of RO processes using spiral wound RO membranes are reviewed in the following.

Hatfield and Graves (1970) formulated a nonlinear programming problem for a mathematical model of a RO system based on brackish water desalination to optimise the product flux and predict the optimal configuration of modules regarding to construction temperature. They affirmed that the cost of produced water can be condensed by reducing the size of RO systems.

Boudinar et al. (1992) predicted the improvement in performance of spiral wound RO modules based on optimising the geometrical parameters at given operating conditions. They developed a computer simulation program considering the physical phenomena inside the module and the module geometry. The geometrical optimisation of the ROGA

module was maximised at a set of operating conditions, which included the permeate flow per unit volume and the driving force.

van der Meer and van Dijk (1997) used two mathematical models to simulate capillary and spiral wound modules in order to optimise the module design parameters including the feed and permeate channel porosity, capillary diameter, and height. They also optimised the feed pressure and flow rate. A growth in the water production of 100% was realised by optimising the capillary module configuration and operation conditions compared to spiral wound module.

Nemeth (1998) Optimised the performance of ultra-low-pressure RO membranes of an advanced hybrid system of ultra-low and standard RO membranes. The optimisation methodology led to around 30% higher permeate productivity of ultra-low-pressure membranes compared to standard membranes. Also, the permeate indicators are meaningfully upgraded from the low-pressure systems.

Wilf and Schierach (2001) improved the long-term performance of RO membranes to attain high recovery and high flux operation that satisfies the reduction of water production cost via optimising the operating conditions. A successful reduction of around 10% in water cost was obtained.

Villafafila and Mujtaba (2003) developed an optimisation framework, subjected to general constraints for the RO process to maximise the recovery ratio using different energy recovery devices. The optimisation problem of the highest recovery ratio was solved using an effectual successive quadratic programming (SQP) based method that included the determination of optimal control variables (feed flow rate and pressure) and design factors (total number of tubes, and internal diameter). They included, in the optimisation problem, the choices of energy recovery with various devices include an improved Energy Recovery Device (ERD), turbines, and pressure exchangers. Results showed an improvement on freshwater recovery by connecting a number of RO membranes in a series. They affirmed that including of ERD would reduce the operating costs and the energy consumption by more than 50%.

Bouguecha et al. (2004) optimised the operation of a desalination plant coupled with a source of solar energy that operates itself in an intermittent mode with the aim of

minimising the energy consumption related to water production cost. Results showed the contribution of the solar energy system.

Wilf and Bartels (2005) optimised the design of a large-scale seawater RO desalination plant and decreased the freshwater production cost. They proved that the use of specific RO configurations such as one-stage array configuration, two-pass, and split partial permeate treatment, and elevated pH seawater are essential to increasing boron removal capacity. However, this causes an increase in operating cost. In this regard, the freshwater production cost has been reduced due to applying high-efficiency ERDs or high-permeability membranes. Also, the increase of water permeability coefficient and decrease in the salt passage would contribute to the reduction of water production cost.

Geraldes et al. (2005) optimised a single stage arrangement and the control variables of a medium-sized SWRO (1000 m<sup>3</sup>/day) with two stage spiral wound modules to obtain the optimum design of a minimum specific freshwater production cost (objective function). In this regard, the optimum design of a single stage with 7 membrane modules in a series reduced the freshwater production cost by 13.5% when compared to a typical system design (single stage of four membrane modules). They also claimed that the specific freshwater production cost could be further condensed by utilising two stages in a series structure, with 7 membrane modules per pressure vessel. Specifically, a two-stage seawater RO has decreased the freshwater production cost by around 5.5% compared to a single stage configuration.

Guria et al. (2005) achieved a multi objective optimisation based on a genetic algorithm (GA) for brackish and seawater desalination using tubular and spiral wound modules. The optimisation aimed to minimise the cost of desalination while maximising the permeate flow rate. Results showed that the membrane area was the most vital decision variable for spiral wound modules whilst the pressure was the important variable for tubular modules. Gilau and Small (2008) used the model developed by Hyun et al. (2009) to optimise the performance of a small-scale seawater RO process connected to a renewable energy system. The optimisation targeted two objective function of maximising the water productivity and minimising the specific energy consumption besides attaining a high boron removal. They looked at achieving the lowest specific energy consumption.

Vince et al. (2008) optimised the brackish water RO process within an environmental and economical method based on a flexible superstructure optimization i.e. taking into consideration the arrangement of membrane modules and the number of membranes in each module. Their simulation results showed that employing 7 membranes for both 1<sup>st</sup> and 2<sup>nd</sup> stages would have water recovery rate of 82%. In this respect, the performances of the RO process configurations are appraised by updated cost models, including electricity consumption and total recovery rate.

Djebedjian et al. (2008) developed a methodology to optimise the performance of a RO desalination system by the employment of the Genetic Algorithms (GA) technique. They concluded that an optimal pressure variance along the membrane aids to maximise the permeate flux and satisfy the permeate concentration limitation.

Zhu et al. (2009a) optimised the energy consumption of a simple sweeter RO desalination process by constraining a fixed permeate flow in the presence of a fluctuating feed salinity. The analysis confirmed the possibility of predicting the optimal pressure operation to increase the energy savings of the proposed system. In other words, the total energy consumption can be decreased by deploying the same permeate flow due to pressure fluctuation despite the variation of feed concentration. Also, the impact of ERD, membrane hydraulic permeability, brine disposal cost, and pressure drop are outlined for one-stage system. More importantly, the possible highest water recovery is recommended especially when the cost of disposed brine is high.

Oh et al. (2009) applied a simple model to explore the optimum operating conditions of a RO process including the water recovery, water flux, temperature, and fouling mechanism to predict the lowest energy consumption and at the same time enhancing the permeate quality. The feasibility of water recovery was explored via optimisation that reduced the energy consumption at the highest solute rejection. Moreover, the feed temperature was found to have a significant impact on the RO process performance.

The minimisation of specific energy consumption for three different RO modules (one stage, one stage with ERD and two stages) was investigated by Li (2010). The models were formulated as non-linear optimisation problems. Li (2010) introduced a set of dimensionless parameters which signified the coupling between membrane properties and operating variables. The optimal solution to specific energy consumption normalised by

the seawater concentration was merely dependent on a dimensionless parameter, which is a function of the hydraulic permeability, membrane area, feed flowrate and concentration. Kotb et al. (2016) minimised the total operational cost of general superstructures of single stage, two-stages and three stage RO system via optimisation considering various operating conditions. They specifically recommended the application of a single-stage configuration to achieve permeate flow rates below 6 m<sup>3</sup>/h whilst minimising freshwater production cost. For freshwater flow rates of up to 12 m<sup>3</sup>/h, they recommend two-stage configuration whilst three-stage configuration is useful for production of higher flow rates. Table 2.3 summarises the characteristics of the discussed optimisation research of RO processes.

**Table 2.3.** Summary of the previous work of RO optimisation

Authors and year	Objective function	Control variables	Constraints	Results
<i>(Hatfield and Graves, 1970)</i>	<ul style="list-style-type: none"> <li>Maximised the product flux.</li> </ul>	<ul style="list-style-type: none"> <li>Operating temperature.</li> </ul>	<ul style="list-style-type: none"> <li>Maximum number of modules per pressure vessel.</li> </ul>	<ul style="list-style-type: none"> <li>The cost of produced water is reduced as a result of reducing the size of RO systems.</li> <li>Predicted the optimal arrangement of modules in a specific stage.</li> </ul>
<i>(Boudinar et al., 1992)</i>	<ul style="list-style-type: none"> <li>Optimised the geometrical parameters of a spiral wound RO process.</li> </ul>	<ul style="list-style-type: none"> <li>Flow rates, pressures, and concentrations in the brine and permeate channels.</li> </ul>	<ul style="list-style-type: none"> <li>Adopting a more realistic model which considers the spiral geometry.</li> </ul>	<ul style="list-style-type: none"> <li>A set of operating conditions has been maximised including the permeate flow per unit volume and driving force.</li> </ul>
<i>(van der Meer and van Dijk, 1997)</i>	<ul style="list-style-type: none"> <li>Maximising the permeate productivity per module and minimising the losses in high-concentration and permeate channels and hydraulic pressure (minimising energy consumption).</li> </ul>	<ul style="list-style-type: none"> <li>The operating conditions of feed pressure, and feed flowrate.</li> </ul>	<ul style="list-style-type: none"> <li>Water production per module.</li> <li>Pressure losses in feed and permeate sides.</li> </ul>	<ul style="list-style-type: none"> <li>Improved the performance of the spiral wound (productivity).</li> <li>An additional increase in performance of 100% can be obtained by optimising the arrangement and control variables of a capillary module.</li> </ul>
<i>(Nemeth, 1998)</i>	<ul style="list-style-type: none"> <li>Optimised the performance of ultra-low pressure RO membranes in a novel system design.</li> </ul>	<ul style="list-style-type: none"> <li>Pressure boosting</li> <li>Utilising permeates throttling at the 1<sup>st</sup> stage.</li> </ul>	<ul style="list-style-type: none"> <li>The hydraulic behavior of the full-scale membrane water treatment system.</li> </ul>	<ul style="list-style-type: none"> <li>The obtained cost savings by the ultra-low-pressure membranes are noteworthy.</li> <li>The cost savings principally originate from energy savings.</li> </ul>
<i>(Wilf and Schierach, 2001)</i>	<ul style="list-style-type: none"> <li>Improved the long-term performance of RO seawater and the cost discount of systems using UF pretreatment.</li> </ul>	<ul style="list-style-type: none"> <li>Recovery rate.</li> <li>Permeate flux.</li> </ul>	<ul style="list-style-type: none"> <li>Deployment of high-water recovery and flux operation needs an improved quality of the feed seawater.</li> </ul>	<ul style="list-style-type: none"> <li>The economics of the desalting process is improved by increasing the recovery rate and water flux in seawater systems.</li> <li>The collective savings due to operating cost, lower investment and capability to optimise system control variables as a result to better seawater quality would cause around 10% decrease in total water production cost.</li> </ul>

<i>(Villafafila and Mujtaba, 2003)</i>	<ul style="list-style-type: none"> <li>Optimised the recovery ratio.</li> </ul>	<ul style="list-style-type: none"> <li>Feed flowrate and pressure.</li> <li>Total number of tubes and internal diameter are the design parameters.</li> </ul>	<ul style="list-style-type: none"> <li>Optimised control variables are dependent on the constraints presented.</li> <li>The optimal values are high-sensitive to changes in water and energy prices, in addition to seawater salinity.</li> </ul>	<ul style="list-style-type: none"> <li>The energy consumption is reduced by up to 50% by using a pressure exchanger device.</li> </ul>
<i>(Bouguecha et al., 2004)</i>	<ul style="list-style-type: none"> <li>Assessed the performances of a desalination plant with the aim of optimising its operation in terms of energy accessibility.</li> </ul>	<ul style="list-style-type: none"> <li>A continuous operating mode was utilised by eliminating the impacts of source variations.</li> </ul>	<ul style="list-style-type: none"> <li>Represent the time limit of the autonomous operating pilot.</li> </ul>	<ul style="list-style-type: none"> <li>The participation of the storage dissipation unit by means of solar energy.</li> </ul>
<i>(Wilf and Bartels, 2005)</i>	<ul style="list-style-type: none"> <li>Optimised the design of large-scale seawater RO desalination systems to evaluate the decreasing of desalted water costs.</li> </ul>	<ul style="list-style-type: none"> <li>The arrangement and control variables of current large seawater desalination systems.</li> </ul>	<ul style="list-style-type: none"> <li>No constraints</li> </ul>	<ul style="list-style-type: none"> <li>A notable reduction of freshwater cost is obtained as a result to high-permeability, high-rejection membranes, and high-efficiency ERDs.</li> </ul>
<i>(Gerald et al., 2005)</i>	<ul style="list-style-type: none"> <li>Minimise the cost of water production.</li> </ul>	<ul style="list-style-type: none"> <li>Number of membrane modules in pressure vessel.</li> <li>Feed pressure and velocity.</li> </ul>	<ul style="list-style-type: none"> <li>Maximum concentration polarisation.</li> <li>Maximum permeate salt concentration.</li> </ul>	<ul style="list-style-type: none"> <li>The water cost can be condensed to 66.7 eurocent/m<sup>3</sup>, for a two-stage spiral wound RO unit compared to 81.4 eurocent/m<sup>3</sup> compared to a single-stage and 4 membrane modules (FilmTecSW30HR-380) per pressure vessel.</li> </ul>
<i>(Guria et al., 2005)</i>	<ul style="list-style-type: none"> <li>Maximise the permeate, minimise the cost of desalination, and minimise the permeate concentration.</li> </ul>	<ul style="list-style-type: none"> <li>The pressure difference along the membrane, the active membrane area.</li> <li>The membrane types.</li> </ul>	<ul style="list-style-type: none"> <li>Maximum throughput</li> <li>Maximum permissible permeability coefficients.</li> </ul>	<ul style="list-style-type: none"> <li>To attain a maximum throughput, the permeability factor of water must be at the highest one.</li> </ul>
<i>(Gilau and Small, 2008)</i>	<ul style="list-style-type: none"> <li>Optimise the performance of RO process for high boron</li> </ul>	<ul style="list-style-type: none"> <li>Specific energy.</li> <li>Boron concentration.</li> </ul>	<ul style="list-style-type: none"> <li>No constraints</li> </ul>	<ul style="list-style-type: none"> <li>Total energy consumption was lessened by 70% by using an energy recovery turbine, a</li> </ul>

	elimination and minimum specific energy consumption.			booster pump, and a suitable membrane. <ul style="list-style-type: none"> <li>Water cost was reduced by 41% by using ERD.</li> </ul>
<i>(Vince et al., 2008)</i>	<ul style="list-style-type: none"> <li>Optimised the brackish water RO process within an economical and environmental approach based on the flexible superstructure.</li> </ul>	<ul style="list-style-type: none"> <li>The arrangement of the membrane module.</li> <li>The number of membranes in a module.</li> </ul>	<ul style="list-style-type: none"> <li>Number of membranes used in the module configuration.</li> </ul>	<ul style="list-style-type: none"> <li>Low total costs can be obtained at high-water flux; however, desalination environmental effects and electricity consumption are still high.</li> <li>Low water flux allows lower electricity consumption using larger membranes area (higher cost).</li> </ul>
<i>(Djebedjian et al., 2008)</i>	<ul style="list-style-type: none"> <li>Optimise the performance of RO desalination plant by the genetic algorithms (GA) to maximise permeate volumetric flow rate and satisfy the permeate concentration.</li> </ul>	<ul style="list-style-type: none"> <li>The pressure variance across the membrane.</li> </ul>	<ul style="list-style-type: none"> <li>The permeate concentration.</li> </ul>	<ul style="list-style-type: none"> <li>Permeate concentration reduces with increasing in water flux and the membrane pressure difference.</li> </ul>
<i>(Zhu et al., 2009a)</i>	<ul style="list-style-type: none"> <li>Optimise the energy consumption for a simple model of RO water desalination process by creating a fixed water flux in the occurrence of fluctuating in the feed concentration of seawater and brackish water.</li> </ul>	<ul style="list-style-type: none"> <li>Feed pressure.</li> <li>Feed concentration.</li> </ul>	<ul style="list-style-type: none"> <li>Membrane hydraulic permeability.</li> </ul>	<ul style="list-style-type: none"> <li>Specific energy consumption can be markedly condensed, providing the same water flux.</li> <li>Higher water recovery can be obtained particularly when the brine stream disposal cost is high.</li> </ul>
<i>(Oh et al., 2009)</i>	<ul style="list-style-type: none"> <li>Optimising the design of a simple model of RO process for low energy requirement.</li> </ul>	<ul style="list-style-type: none"> <li>Recovery ratio.</li> <li>Permeate flux.</li> <li>Temperature.</li> <li>Fouling mechanism.</li> </ul>	<ul style="list-style-type: none"> <li>No constraints</li> </ul>	<ul style="list-style-type: none"> <li>Higher flux increases the solute retention but grows the specific energy consumption.</li> <li>Increased temperature would cut the specific energy but worsens the rejection.</li> </ul>
<i>(Li, 2010)</i>	<ul style="list-style-type: none"> <li>Minimisation of specific energy consumption.</li> </ul>	<ul style="list-style-type: none"> <li>Several fixed RO configurations.</li> <li>Energy recovery efficiency.</li> <li>Driving force.</li> </ul>	<ul style="list-style-type: none"> <li>Minimum recovery is constant.</li> </ul>	<ul style="list-style-type: none"> <li>Specific energy consumption was reduced with a much better water recovery by using ERD.</li> </ul>

<i>(Kotb et al., 2016)</i>	<ul style="list-style-type: none"> <li>Minimisation of total cost of freshwater production for a RO system.</li> </ul>	<ul style="list-style-type: none"> <li>Feed pressure.</li> <li>Membrane area.</li> <li>Feed flow rate.</li> </ul>	<ul style="list-style-type: none"> <li>No constraints</li> </ul>	<ul style="list-style-type: none"> <li>Single-stage layout can cause a minimum cost of freshwater production.</li> <li>Two-stage layout was endorsed for the directed water production of less than 12 m<sup>3</sup>/h.</li> <li>Three-stage layout was endorsed for higher water production rates.</li> </ul>
<i>This work</i>	<ul style="list-style-type: none"> <li>Minimise the specific energy consumption of simple and complicated designs of RO brackish water desalination systems.</li> </ul>	<ul style="list-style-type: none"> <li>Feed pressure.</li> <li>Feed flowrate.</li> </ul>	<ul style="list-style-type: none"> <li>No constraints</li> </ul>	<ul style="list-style-type: none"> <li>The specific energy consumption for a simple and complicated designs of RO brackish water desalination systems saved by 37.3%, and 35%, respectively.</li> </ul>

## **2.5 Overview of thermodynamic aspect of RO process**

One of the most important concerns related to thermodynamics of seawater RO desalination process is the high requirements of energy (Miller et al. 2015). Therefore, minimising the energy consumption has attracted the attention of several researchers. It is noteworthy to mention that exergy is that part of energy that is convertible into all other forms of energy and considered as a useful part of energy for any system. The exergy can be expressed in term of Second Law of Thermodynamics to specify the irreversible losses that occur within any thermal or power cycle (the exergy destroyed when the heat transfer from high to low temperature source). Basically, the RO process has various thermodynamic limitations that necessitates applying operating pressures higher than the summation of both osmotic pressure and frictional pressure losses to carry out successful filtration. This is basically required to maintain the water permeation through the membrane. Therefore, the feed pressure always should be higher than the retentate pressure to guarantee the filtration process (water flux) and that denoted as the thermodynamic restriction of crossflow membrane water desalination. In this aspect, a critical review of the open literature confirmed several successful attempts of the RO thermodynamics analysis as discussed below.

Cerci et al. (2003) developed a general relationship to anticipate the minimum work required for RO desalination processes using the second law of thermodynamics. Specifically, the minimum input work per unit mass of fresh water produced for various feed water salinities has been recognised. It is concluded that the minimum energy consumption for the separation of a saline solution into pure water and concentrated brine is independent of the process configuration. This also confirmed an increase of the energy consumption as a result to increase the feed water salinity for a fixed product quality and a recovery ratio.

Song et al. (2003a) formulated several equations to analyse the performance of RO process and demonstrate the thermodynamic restriction as a limiting factor for full-scale RO process under common conditions. The thermodynamic restriction arises from a significant increase in the osmotic pressure downstream of the membrane channel due to the accumulation of rejected salt on the membrane wall because of water permeation. This

affirmed that the thermodynamic restriction has a stronger influence on the full-scale RO process performance than the concentration polarisation.

Song et al. (2003b) examined the transport mechanism that control the performance of a full-scale RO process under various operating conditions. This showed that the thermodynamic equilibrium can impose a strong restriction on the performance of RO membrane under certain conditions. In other words, the performance of RO process is entirely affected by the thermodynamic restriction as a controlling mechanism. Moreover, the mass transfer correlation is not enough to describe the RO process. However, the average permeate flux has significantly deviated from a linear dependence on the trans-membrane pressure close to thermodynamic equilibrium.

Mehdizadeh (2006) developed a simple and practical mathematical model for multi-solute fluid processed into industrial membrane modules to predict the plant performance under various operating conditions. Mehdizadeh (2006) combined the thermodynamic property of exergy with a mathematical model to determine the optimum operating conditions. The studied performance indicators are the recovery, solute rejection, and entropy production. The simulation analysis offered a higher recovery, higher solute rejection, and lower entropy production for the RO plant.

Mabrouk et al. (2007) presented a thermo-economic analysis for RO process, MSF (Multistage Flash), and MEE (Multi Effect Evaporation). The thermo-economic of these processes has been evaluated and compared using a developed Visual Design and Simulation package (VDS) software. The thermo-economic results showed that the RO process provided a lowest unit product cost. Moreover, the RO process obtained the maximum exergetic efficiency due to the using of recovery turbine.

The effect of the thermodynamic restriction on the cost minimisation of the RO/nanofiltration membrane desalination processes has been studied by Zhu et al. (2008). They assessed numerous parameters associated with the water production cost such as energy, membrane area and permeability, brine management, and pressure drop, the thermodynamic cross-flow restriction, operational feed and permeate flow rate constraints, and applying energy recovery devices. The optimisation problem of the RO process has been formulated to maximise the water recovery and minimise the energy consumption, while constraining the thermodynamic crossflow restriction and feed or

permeate flow rate. The optimisation results showed the best conditions to satisfy the minimum energy consumption with lower water production cost. However, the multistage RO process can save more energy with the penalty of a greater membrane area.

Zhu et al. (2009a) investigated the energy optimisation of a two-pass membrane of RO desalination process at a limit imposed by thermodynamic restriction. This is readily compared to the energy optimisation of single-pass membrane RO desalination. The impact of pump and energy recovery devices, membrane rejection, and retentate recycling from the second to the first-pass based on the limitations imposed by the thermodynamic cross flow restriction on the minimum achievable specific energy consumption has been studied. This showed that the two-pass process consumes lower energy compared to the single pass. Moreover, recycling of the second pass retentate to the first pass feed in the two-pass process can mainly reduce the specific energy consumption.

Zhu et al. (2009b) studied the impact of increasing the permeability of the RO membrane on the reduction of water production cost at the limit imposed by thermodynamic restriction. The thermodynamic limit has been expressed by the ratio of membrane to energy cost as a function of the water recovery level and a dimensionless cost parameter that accounts for the purchase of electrical energy and membrane area. Also, the feed water salinity, salt rejection and membrane permeability were considered. This showed that the water permeability constant is the most significant parameter to reduce the water production cost.

Al-Zahrani et al. (2012) used the second thermodynamic law to carry out a thermodynamic analysis for three configurations of RO process by calculating the total energy consumption with and without an energy recovery device (ERD). The performance indicators such as specific energy and the recovery ratio for these configurations over a wide range of feed salinity, temperature and applied pressure are investigated and compared. The results illustrated that the specific energy consumption behavior depends on the feed salinity. It increases with the applied pressure almost linearly when the feed salinity is low. Moreover, the importance of employing ERD when the salinity is high has been verified.

Qi et al. (2012) presented a theoretical analysis for both single-stage and two-stage RO desalination processes at the limit imposed by thermodynamic restriction. This aided to

study the impact of RO response parameters including the water recovery, ERDs efficiency leakage ratio, and pump efficiency on the specific energy consumption. By the presence of ERDs, the water recovery has visibly reduced at higher ERD efficiency and became more sensitive to the leakage ratio. Moreover, the specific energy consumption affected by the leakage at lower water recoveries compared to the higher one.

Banchik and Lienhard (2012) applied a thermodynamic analysis of RO desalination system to evaluate the energy efficiency of hybrid desalination cycles that are driven by simultaneous mixed inputs, including electrical work, heat, and chemical energy. The study confirmed that the energy attained by adding of the chemical input stream can be served to the lower amount of electrical work required for operation. Moreover, the significant reduction in work can be obtained by using an ERD.

Feinberg et al. (2013) applied a thermodynamic analysis to evaluate the potential of pressure retarded osmosis PRO and Reverse Electrodialysis (RED) processes coupled to a typical seawater RO plant. The possibility of osmotic energy recovery from both the RO feed stream and the RO brine are assessed. They provided insight into various process parameters that affect the optimal Specific Energy Consumption (SEC) for a hybrid reverse osmosis- Hydraulic Energy Recovery- Osmotic Energy Recovery (RO-HER-OER) plant configuration. In this regard, the process potential through the thermodynamically available work produced by each OER technology is theoretically probed by ignoring system-specific losses, for example, hydraulic losses pumps, piping, modules etc.), membrane losses and other sources of inefficiency. They affirmed that a coupled system of RO-RED could significantly reduce the net SEC of RO process.

El-Emam and Dincer (2014) investigated the performance of an SWRO desalination plant involving a comprehensive thermo-economic analysis (based on the first and second laws of thermodynamics) at different seawater salinities. Specifically, the effects of the system components irreversibilities on the economics and cost of product water based on the thermo-economic analysis was carried out. The exergy destruction results showed that the large irreversibilities occurred in the RO module of 67.8% and 17.16% of a high-pressure pump. Moreover, an increase in the recovery ratio would decrease the water production cost. Furthermore, the exergy destruction by using a Pelton turbine as an energy recovery device has been reduced by about 35.5%, compared to the use of an expansion valve.

Haluch et al. (2017) assessed and improved the performance of a small capacity RO desalination systems on thermodynamic grounds. The research has utilised a semi-empirical model to predict the thermodynamic (exergy) efficiency, the permeate volumetric flow rate, and the salt rejection as functions of the feed water salinity, pump and the membrane characteristics. They found that the feed water concentration is the most important factor that affects all the studied parameters. An optimal feed concentration has been obtained to maximise the salt rejection. However, increasing the feed water concentration caused an increase of exergy efficiency, which is attributed to increasing of work besides diminishing the permeate flow rate.

Table 2.4 presents a summary of all the previous work that carried out in thermodynamic of RO process.

**Table 2.4.** Summary of the past work of RO thermodynamic and exergy analysis

Authors and year	Main objectives	Results
<i>Cerci et al. (2003)</i>	<ul style="list-style-type: none"> <li>Developed a general relation for the minimum work required per unit mass of fresh water for the desalination process using the second law of thermodynamics with various feed water salinities and produced freshwater salinities</li> </ul>	<ul style="list-style-type: none"> <li>Minimum energy consumption was independent of the process configuration.</li> <li>Increasing the energy consumption as a result to increase the feed water salinity for a fixed product quality and a recovery ratio</li> </ul>
<i>Song et al. (2003a)</i>	<ul style="list-style-type: none"> <li>Demonstrate the thermodynamic restriction as a limiting factor for full-scale RO processes under common conditions</li> <li>The effect of concentration polarisation on the recovery is practically negligible for all conditions except for a few combinations of very high salt concentrations and pressures. Therefore, there is no need to consider the effect of concentration polarisation on mass transfer.</li> <li>Considered the thermodynamic restricted regime shifts remarkably to a higher pressure when concentration polarisation without considering thermodynamic restriction, the operating pressures for the second and third stages could be substantially underestimated.</li> </ul>	<ul style="list-style-type: none"> <li>The thermodynamic restriction has a stronger influence on the full-scale RO process performance than the concentration polarisation.</li> </ul>
<i>Song et al. (2003b)</i>	<ul style="list-style-type: none"> <li>Examined the mechanisms controlling the performance of a full-scale RO process under various operating conditions without need to consider thermodynamic restriction for RO processes employing an old generation of RO membranes.</li> </ul>	<ul style="list-style-type: none"> <li>The thermodynamic equilibrium can impose a strong restriction on the performance of RO membrane under certain conditions.</li> <li>The average permeate flux has significantly deviated from a linear dependence on the trans-membrane pressure close to thermodynamic equilibrium.</li> </ul>
<i>Mehdizadeh (2006)</i>	<ul style="list-style-type: none"> <li>Predicted the plant performance under operating conditions of the plant based on the exergy variations for a desalination plant with changes in these conditions by combining the thermodynamic property of exergy with a mathematical model for multi-solute RO systems to determine the optimum operating condition for an integrated RO seawater desalination plant.</li> <li>The performance is studied based on the recovery, solute rejection, and the entropy production with variation in applied pressure for the RO plant.</li> </ul>	<ul style="list-style-type: none"> <li>The simulation analysis offered a higher recovery, higher solute rejection, and lower entropy production for the RO plant.</li> </ul>
<i>Mabrouk et al. (2007)</i>	<ul style="list-style-type: none"> <li>Presented a thermo-economic analysis for a widely used desalination processes based on thermodynamic evaluation.</li> <li>The RO process is in competition with other desalination processes if the reliability and long life of the heating surface are taken into consideration.</li> </ul>	<ul style="list-style-type: none"> <li>The RO process provided a lowest unit product cost.</li> <li>The RO process obtained the maximum exergetic efficiency due to the using of the recovery turbine.</li> </ul>
<i>Zhu et al. (2008)</i>	<ul style="list-style-type: none"> <li>They optimised the RO membrane process with respect to product water recovery and considering thermodynamic crossflow constraints. Considering the limitations due to the mineral scaling and fouling which impose additional constraints.</li> </ul>	<ul style="list-style-type: none"> <li>Minimise the water production cost.</li> <li>High recovery operations at lower pressures for the newer generation of RO membranes.</li> </ul>
<i>Zhu et al. (2009a)</i>	<ul style="list-style-type: none"> <li>Minimise the energy consumption of the two-pass membrane desalination process relative to a single-pass process operating at the limit of the thermodynamic restriction and concluded that two-pass membrane desalination is less energy efficient than single pass.</li> </ul>	<ul style="list-style-type: none"> <li>The two-pass process consumes lower energy compared to the single pass.</li> </ul>

	<ul style="list-style-type: none"> <li>• Considered the energy cost which is a major direct factor affecting water production cost.</li> <li>• Considered a product water recovery constraints that imposed by mineral scaling, fouling and operational pressure limits, membrane, and brine management costs.</li> <li>• The cost associated with feed pre-treatment and post-treatment and investment costs.</li> </ul>	<ul style="list-style-type: none"> <li>• Recycling of the second pass retentate to the first pass feed in the two-pass process can mainly reduce the specific energy consumption.</li> </ul>
<i>Zhu et al. (2009b)</i>	<ul style="list-style-type: none"> <li>• Minimise the production water desalination cost up to the thermodynamic restriction limit by carrying out a simple analysis of the specific membrane cost that relative to specific energy cost for RO desalination over membrane permeability improvements.</li> <li>• Considered the fouling resistant membranes.</li> <li>• Considered more effective and lower feed pre-treatment.</li> <li>• Considered the brine management costs.</li> <li>• Considered the optimisation of process configuration and control schemes.</li> <li>• Considered the utilization of low-cost renewable energy sources.</li> </ul>	<ul style="list-style-type: none"> <li>• The water permeability constant is the most significant parameter to reduce the water production cost.</li> </ul>
<i>Al-Zahrani et al. (2012)</i>	<ul style="list-style-type: none"> <li>• Investigated the RO process performance in term of specific energy consumption and the recovery ratio for three modelled configurations of the desalination unit with and without energy recovery device (ERD) using thermodynamic laws.</li> <li>• The concentration polarisation and pressure losses are not considered.</li> <li>• The membrane is considered as a porous environment.</li> <li>• The spacers help not only on promoting mixing but also have a depolarisation effect.</li> </ul>	<ul style="list-style-type: none"> <li>• The specific energy consumption behaviour depends on the feed salinity. It increases with the applied pressure almost linearly when the feed salinity is low.</li> </ul>
<i>Qi et al. (2012)</i>	<ul style="list-style-type: none"> <li>• Studied the impact of ERD performance variables (efficiency and leakage ratio) on the specific energy consumption of RO process at the limitation imposed by thermodynamic for both single-stage and two-stage cross flow RO processes.</li> <li>• Considered the pressure drop in the feed channel.</li> <li>• Considered varying rejection along the RO channel.</li> <li>• Considered the concentration polarisation.</li> </ul>	<ul style="list-style-type: none"> <li>• The water recovery has visibly reduced at higher ERD efficiency and became more sensitive to the leakage ratio.</li> <li>• The specific energy consumption affected by the leakage at lower water recoveries compared to the higher one.</li> </ul>
<i>Banchik and Lienhard (2012)</i>	<ul style="list-style-type: none"> <li>• Applied a thermodynamic analysis of RO desalination system to evaluate the energy efficiency of hybrid desalination cycles that are driven by simultaneous mixed inputs, including electrical work, heat, and chemical energy. They assumed the wastewater is only used to recover energy for the desalination process. This might represent a case where the policy does not allow for the human consumption of treated wastewater.</li> </ul>	<ul style="list-style-type: none"> <li>• The energy attained by adding of the chemical input stream can be served to the lower amount of electrical work required for operation.</li> <li>• The significant reduction in work can be obtained by using an ERD.</li> </ul>
<i>Feinberg et al. (2013)</i>	<ul style="list-style-type: none"> <li>• Applied a thermodynamic analysis to evaluate the potential of PRO and RED processes coupled to typical seawater RO plant. The currently accepted configuration used for the operation of PRO the incoming high-concentration feed is pressurised prior to the membrane-mediated mixing process. The reasoning behind this configuration is based on efficiency</li> </ul>	<ul style="list-style-type: none"> <li>• The coupled system of RO-RED could significantly reduce the net SEC of RO process.</li> </ul>

	considerations (pump and turbine). However, the pressurisation alters the equilibrium point, which now occurs when $\Delta\pi = \Delta P$ , the applied pressure, and therefore limits the extractable energy.	
<i>El-Emam and Dincer (2014)</i>	<ul style="list-style-type: none"> <li>Investigated the effects of the operating recovery ratio of the plant, the seawater source salinity, the seawater feeding temperature value and the dead state temperature on the energetic and exergetic performances and the cost of the product water by varying the feed seawater temperature, while keeping all other parameters constants, has a very limited effect on the cost rate of product water.</li> </ul>	<ul style="list-style-type: none"> <li>The large irreversibility's occurred in the RO module of 67.8% and 17.16% of a high-pressure pump.</li> <li>Increasing the recovery ratio would decrease the water production cost.</li> <li>The exergy destruction by using a Pelton turbine as an energy recovery device has been reduced by about 35.5%, compared to the use of an expansion valve.</li> </ul>
<i>Haluch et al. (2017)</i>	<ul style="list-style-type: none"> <li>Evaluate the performance of a small capacity RO desalination systems on thermodynamic grounds for the semi-empirical proposed models. The osmotic pressure difference did not exceed the maximum pressure head provided by the pump due to the maximum feed concentration was 10 g l<sup>-1</sup>.</li> </ul>	<ul style="list-style-type: none"> <li>Increasing the feed water concentration caused an increase of exergy efficiency.</li> </ul>
<i>This work</i>	<ul style="list-style-type: none"> <li>The exergy losses and thermodynamic limitations of a multistage multi pass medium-sized spiral wound brackish water RO desalination plant of APC have been analysed.</li> <li>The exergy destruction distribution has investigated by incorporating both physical and chemical exergies of several units and compartments of the RO system.</li> </ul>	<ul style="list-style-type: none"> <li>The highest energy destruction explored at mixing permeate streams and mixing retentate streams of the first and second pass with about 62.28 % and 94.08 % and 71.18 % and 63.29 %, respectively.</li> </ul>

## 2.6 Modelling and Optimisation Software

gPROMS (general PROcess Modeling System) software is a potent modelling platform mainly used to carry out steady state and dynamic simulation, and primitive optimisation. However, a successful process simulation requires an accurate model with an applicable degree of freedom. gPROMS has several advantages of using its simple interface and its ability of handling steady state and dynamic processes of many algebraic, differential, and partial differential equations, sensitivity analysis and design of experiments. Moreover, the parameter estimation tool can be used to forecast the model parameters based on actual data. More importantly, the model equations of any studied model can be written in a random way without considering hierarchy model structures as the case of Matlab.

The gPROMS software has many merits including:

- Simple language and easy to be coded.
- Provides the degree of freedom that enables to characterise the full structure of the model.
- Several solvers are involved in the software and therefore complicated problems of high order differential and algebraic equations can be solved.
- Easy to be integrated with other software.
- Can be used to build both steady state and dynamic models.
- Can export the results to Excel sheets.
- Provides parameter optimisation to guess the values of constants.

### *2.6.1 Modelling and simulation in gPROMS*

The gPROMS suits has been used to simulate the simple and complicated designs of RO systems based on the model developed in Chapter 3. The model equations are coded and solved via gPROMS software. Afterwards, the variation of inlet parameters of RO system was achieved to systematically carry out the simulation and evaluate the variation of outlet parameters.

Fig. 2.2 depicts the platform of gPROMS Model Builder. Many entities can be seen including the variable types, models, processes, tasks, optimisation... etc.

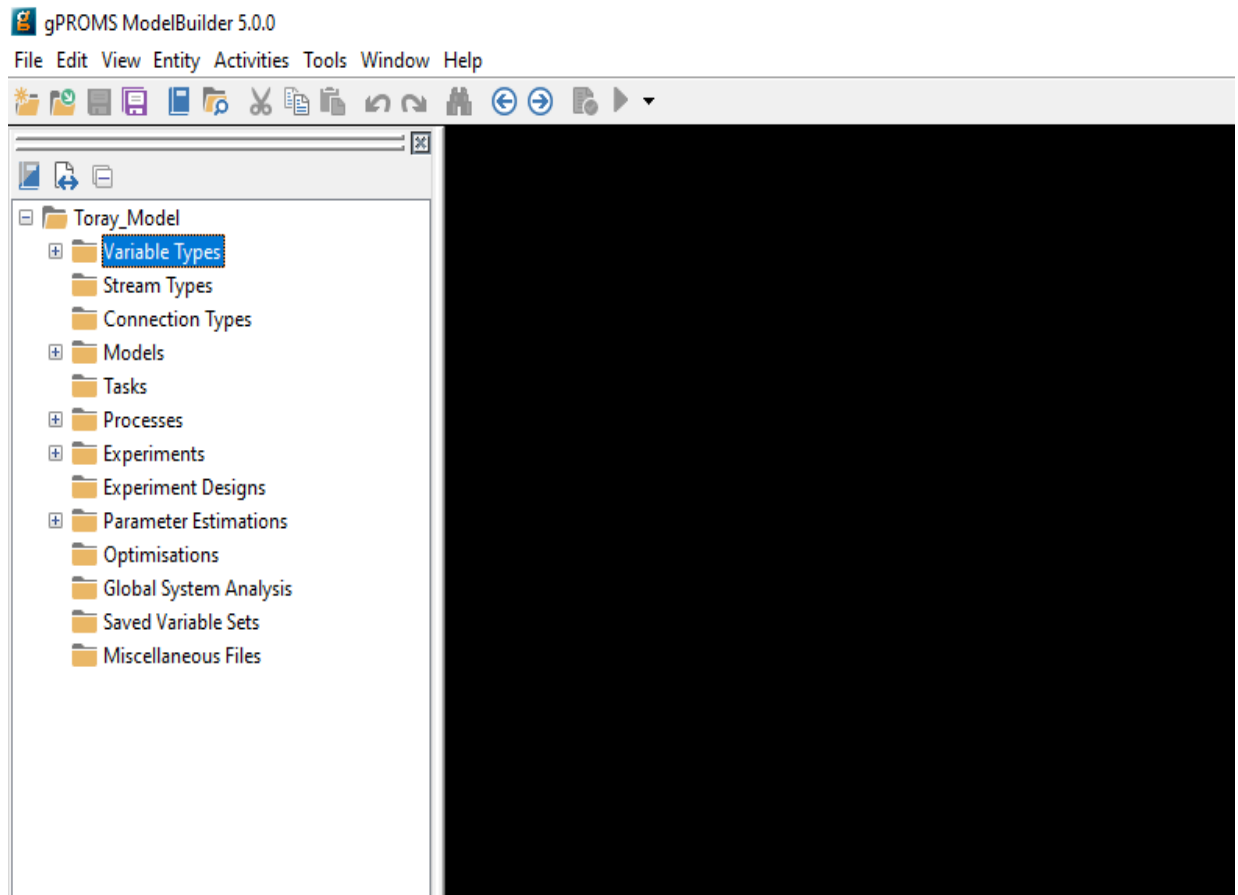


**Fig. 2.2.** Platform of gPROMS model builder

#### ***2.6.1.1 The model entity***

The model entity of any mathematical model contains three important components of parameters, variables, and equations. Occasionally, several algebraic and differential equations can form the model. Fig. 2.3 depicts the model entity. Furthermore, A snap of the model is given in Fig. 2.4.

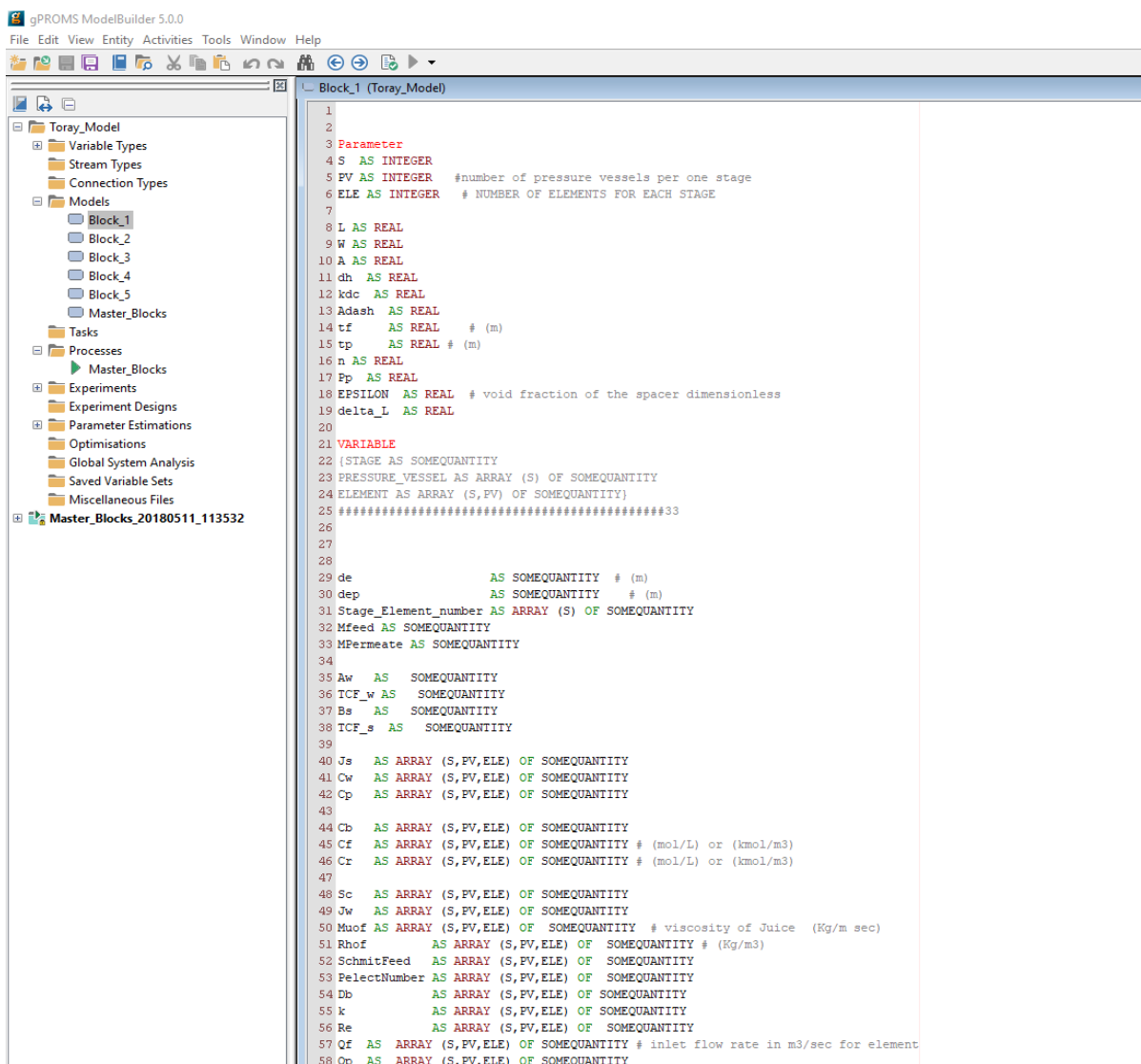


Fig. 2.3. The model entity

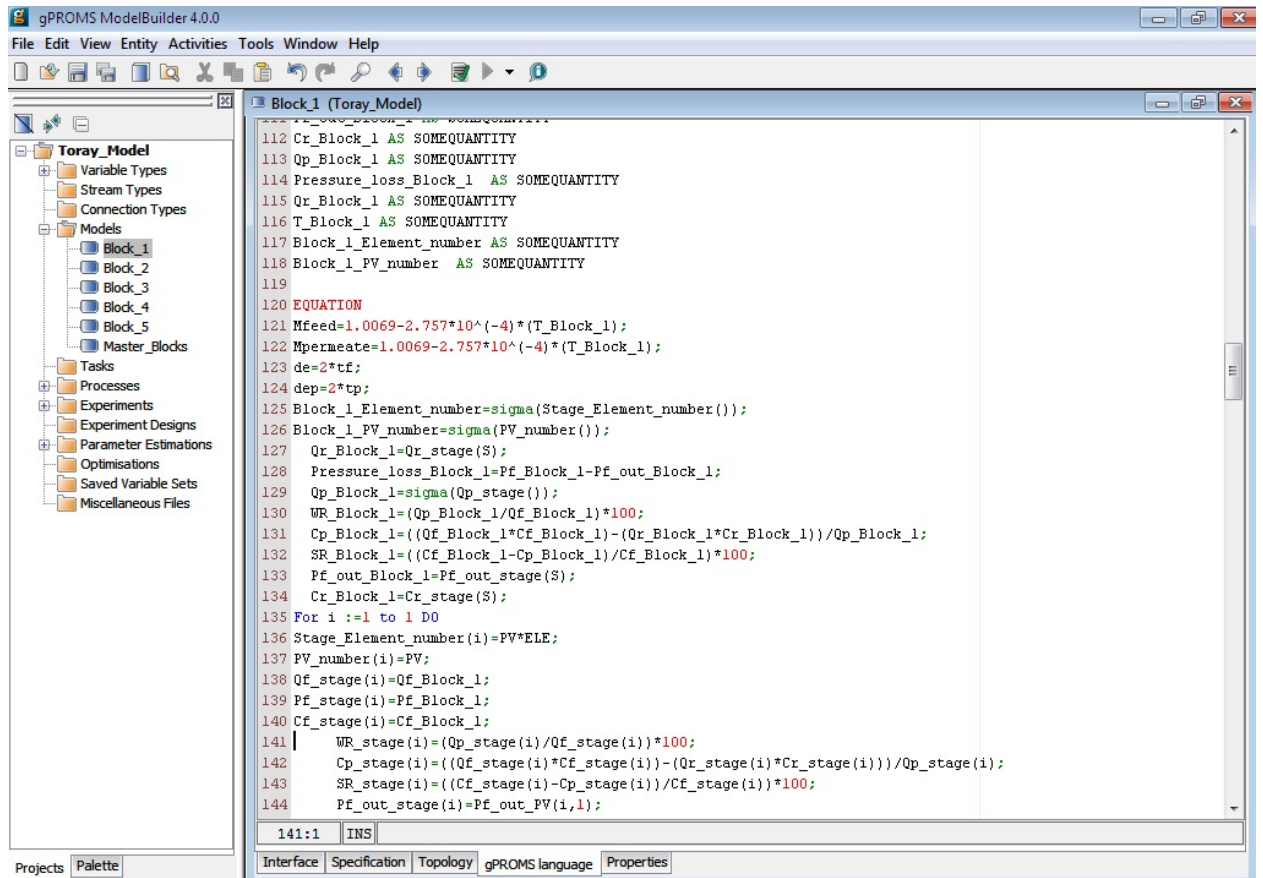
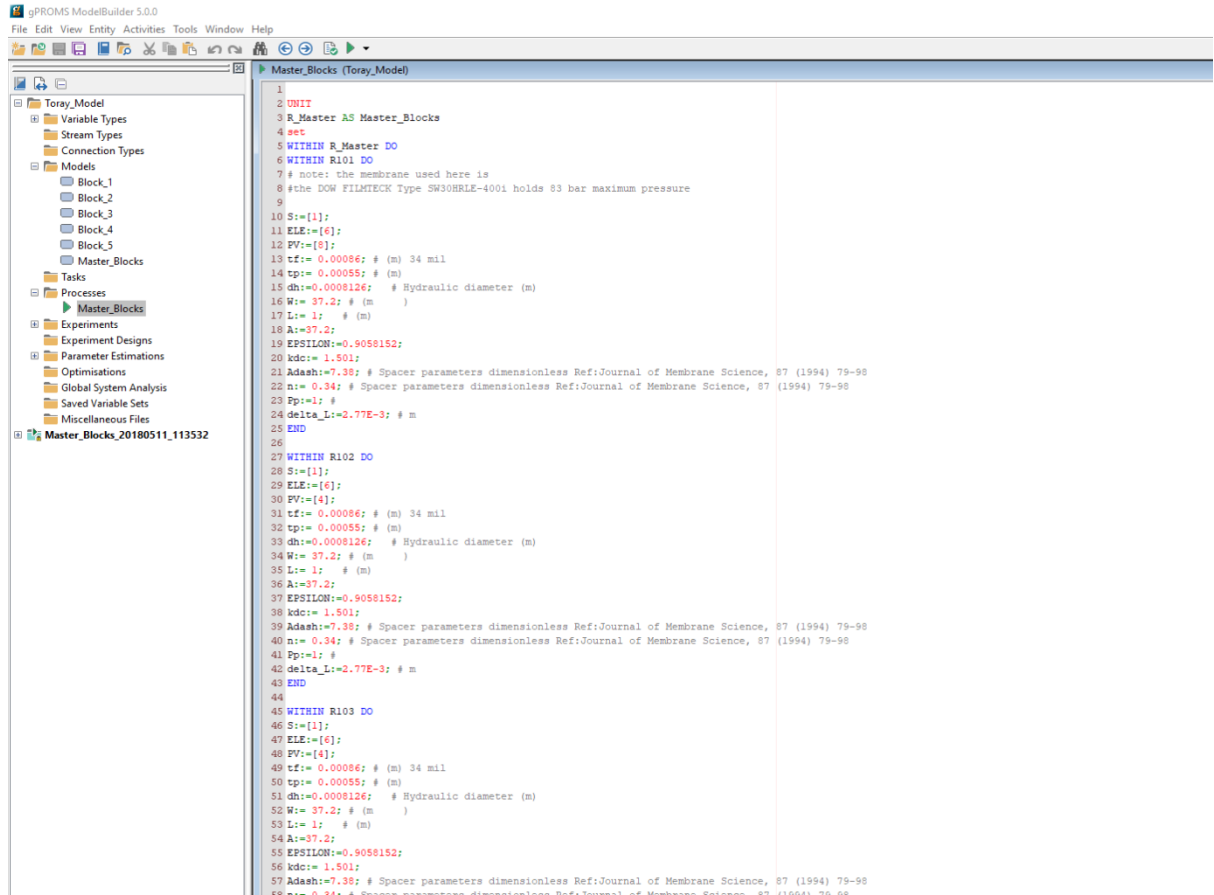


Fig. 2.4. The model equations

### 2.6.1.2 The process entity

The process entity comprises the important specifications to be assigned in order to solve the model equations and carry out the simulation. A snap of the process entity is given in Fig. 2.5. these specifications include the unit, set, assign, initial, solution parameters, and schedule.



**Fig. 2.5.** The process entity

### 2.6.1.3 Optimisation entity

There are three main components of optimisation entity including general, controls and constraints. These are important to formulate any optimisation problem based on selecting an objective function to be maximised or minimised. This is specifically determined in the general part. However, the upper and lower limits of variables can be assigned in the controls and finally the constraints can be used to constraint one or more control variables.

## 2.7 Conclusions

The criterion of this chapter has been designed to review the existed models developed for the RO process and its simulation, and optimisation studies carried out between 1965 and 2019. This is also included an extensive revision of the research done on thermodynamic restrictions of RO desalination process. The appraisal of the models

developed was explicitly showed evolution and a specific complexity that resulted in a lower convergence after comparing its prediction and plant observational data. In this regard, an approved maturity of simulation studies was also noticed due to advanced investigation of the inter-correlated variables. However, this chapter showed the deficiency of simulation of complex design of RO brackish water desalination system which is already considered one of the objectives of the recent research.

The optimisation studies have precisely analysed in this chapter and affirmed the optimal operational variables and process arrangement to guarantee the objective functions with respecting feasible process constraints. The thermodynamic limitations of RO process were also critically discussed based on minimising the specific energy consumption. Furthermore, the RO thermo-economic restrictions combine the exergy analysis and economic principles that provide a clear environment for the system designers to easily conceive the information of energy analysis and economic evaluations.

More importantly, the recent research would employ the model developed in chapter 3 to carry out the upcoming studies of this dissertation. The selection of this model is due to its robustness to forecast the performance indicators of multistage multi-pass RO system of APC.

## **CHAPTER THREE**

### **Modeling of a Spiral Wound Reverse Osmosis Desalination System**

#### **3.1 Introduction**

This chapter presents the development of a steady-state model for a spiral wound RO process that used to characterise the complete mathematical modelling of simple and complicated designs of multistage brackish water RO desalination plants. The model predictions for both simple and complicated designs of RO process are compared against the actual plant data and confirmed the consistency of the model developed. Afterwards, the model is utilised to explore the performance indicators of small-scale RO process against a considerable change in the inlet parameters via a comprehensive simulation.

#### **3.2 Modelling of a single spiral wound RO process**

Several assumptions were considered to build the model.

- The operation is steady state.
- The solution-diffusion model of the Lonsdale et al. (1965) is employed to express the transport phenomenon through the membrane for both solute and water.
- The membrane is quantified as a porous flat sheet with feed spacer.
- The dimensions of membrane and the height of channel are assumed constant.
- The concentration polarisation impact is identified by the film theory model.
- Constant pressure of 1 atm at the permeate channel and the pressure drop is ignored due to a very low velocity for permeate.
- Isothermal process, that means the temperature value is constant at the permeate and feed channels.
- The correlation of Da Costa et al. (1994) is used to estimate the pressure drop inside the feed channel. This includes the pressure drop caused by the feed spacer.

The solution-diffusion model is utilised to clarify the transport phenomenon of solute and permeate in the membrane. Eq. (3.1) is expressed the total water flux  $Q_p$  (m<sup>3</sup>/s).

$$Q_p = A_{w(T)} NDP_{fb} A_m \quad (3.1)$$

$A_{w(T)}$  (m/s atm): is the water permeability constant

$NDP_{fb}$  (atm): expresses the feed and brine Net Driving Pressure.

$A_m$  (m<sup>2</sup>): is the membrane area.

The process of RO is generally affected by operating temperature. Therefore, the estimation of the actual water transport parameter is depending on the reference value at 25 °C. Also, the temperature correction factor will be considered as

$$A_{w(T)} = A_{w(25\text{ }^\circ\text{C})} TCF_p F_f \quad (3.2)$$

$A_{w(25\text{ }^\circ\text{C})}$  (m/s atm): expresses the water permeability constant (at 25 °C).

$TCF_p$  (Dimensionless): The Temperature Correction Factor (at standard conditions).

$F_f$  (Dimensionless): The Fouling Factor.

The temperature correction factor is estimated by the following equations, which are proposed by the membrane manufacturer (Toray Membrane USA Inc.).

$$TCF_p = \exp [0.0343 (T - 25)] \quad ; \quad < 25\text{ }^\circ\text{C} \quad (3.3)$$

$$TCF_p = \exp [0.0307 (T - 25)] \quad ; \quad > 25\text{ }^\circ\text{C} \quad (3.4)$$

The driving pressure is quantified by Eq. (3.5)

$$NDP_{fb} = P_{fb} - P_p - \pi_b + \pi_p \quad (3.5)$$

**T (K) : is the temperature.**

$P_{fb}$  (atm): the pressure for feed brine.

$P_p$  (atm): the permeate pressure.

$\pi_b$  (atm): the osmotic pressure of bulk brine.

$\pi_p$  (atm): the osmotic pressure at the permeate channel.

$T$ (°C): the operating temperature.

$P_{fb}$  decreases along the feed channel length because of the pressure drop resulted from friction as illustrated in Eq. (3.6).

$$P_{fb} = P_f - \frac{\Delta P_{drop,E}}{2} \quad (3.6)$$

$P_f$  (atm): the operating feed pressure.

$\Delta P_{drop,E}$  (atm): represents the pressure drop through the length of membrane element.

$\Delta P_{drop,E}$  (atm) denotes the pressure difference between (the pressure for feed  $P_f$  (atm) and pressure for retentate  $P_r$  (atm)). Eq. (3.7) represents the effect of feed spacer on the pressure drop in the feed channel despite that the existence of feed spacer is important for increasing the mass transfer coefficient and promoting the turbulence rate inside the channel (Da Costa et al., 1994).

$$\Delta P_{drop,E} = \frac{9.8692 \times 10^{-6} A^* \rho_b U_b^2 L}{2 d_h Re_b^n} \quad (3.7)$$

$A^*$  and  $n$  (dimensionless): the feed spacer characteristic.

$\rho_b$  (kg/m<sup>3</sup>): expresses the bulk density.

$U_b$  (m/s): expresses the bulk velocity.

$L$  (m): is the length of membrane.

$d_h$ (m): the hydraulic diameter for feed spacer channel.

$Re_b$  (dimensionless): the Reynolds number.

$(\frac{A^*}{Re^n})$  denotes the total drag force based on the spacer characteristic and Reynolds number ( $Re_b$ ). Also, the  $Re_b$  and the bulk velocity are estimated from Eqs. (3.8) and (3.9), respectively.

$$Re_b = \frac{\rho_b d_h Q_b}{t_f W \mu_b} \quad (3.8)$$

$$U_b = \frac{Q_b}{W t_f \epsilon} \quad (3.9)$$

$Q_b$ (m<sup>3</sup>) represents the bulk flow rate which is calculated by the value of feed average  $Q_f$  (m<sup>3</sup>/s) and flow rates of retentate  $Q_r$  (m<sup>3</sup>/s).

$$Q_b = \frac{Q_f + Q_r}{2} \quad (3.10)$$

$W$ (m): is the membrane width.

$t_f$  (m): is the height of feed channel.

$\epsilon$  (dimensionless): feed spacer void fraction.

The proposed equation by the membrane manufacturer (Toray Membrane USA Inc.) is used to calculate the bulk and permeate osmotic pressures as illustrated in Eqs.(3.11) and (3.12), respectively.

$$\pi_b = 0.7994 C_b [1 + 0.003 (T - 25)] \quad (3.11)$$

$$\pi_p = 0.7994 C_p [1 + 0.003 (T - 25)] \quad (3.12)$$

$C_b(\text{kg/m}^3)$ : is the bulk salinity

$C_p(\text{kg/m}^3)$ : is the permeate salinity.

The bulk salinity  $C_b$  ( $\text{kg/m}^3$ ) can be estimated by take the average of feed salinity and retentate salinity.

$$C_b = \frac{C_f + C_r}{2} \quad (3.13)$$

Eq. (3.14) provides the formula to calculate the solute-flux within the membrane  $Q_s$  ( $\text{kg/m}^2 \text{ s}$ )

$$Q_s = B_{s(T)}(C_w - C_p) \quad (3.14)$$

$B_{s(T)}$  ( $\text{m/s}$ ): is the transport parameter of solute (at operating temperature), which illustrated in Eq. (3.15).

$C_w(\text{kg/m}^3)$ : denotes the concentration of solute (at the membrane surface).

The operating temperature impact on the solute transport parameter is estimated according to the reference value (at 25 °C).

$$B_{s(T)} = B_{s(25\text{ }^\circ\text{C})} TCF_s \quad (3.15)$$

$B_{s(25\text{ }^\circ\text{C})}$  ( $\text{m/s}$ ): represent the transport parameter of solute (at 25 °C).

$TCF_s$  (dimensionless): is the temperature correction factor of solute (at standard conditions).  $TCF_s$  is calculated according to both operating temperature and proposed correlation supplied by membrane manufacturer (Toray Membrane USA Inc.).

$$TCF_s = 1 + 0.05 (T - 25) \quad < 25\text{ }^\circ\text{C} \quad (3.16)$$

$$TCF_s = 1 + 0.08 (T - 25) \quad > 25\text{ }^\circ\text{C} \quad (3.17)$$

Michaels (1968) proposed the theory of analytical film to compute the concentration polarisation as a function of mass transfer coefficient  $k$  ( $\text{m/s}$ ). Therefore, the concentration at the membrane surface  $C_w$  ( $\text{kg/m}^3$ ) is considerably bigger than the bulk concentration  $C_b$  ( $\text{kg/m}^3$ ) because of the diffusion from the bulk flow.

$$C_w = C_p + \left( \frac{C_f + C_r}{2} - C_p \right) \exp \left( \frac{Q_p/A_m}{k} \right) \quad (3.18)$$

The equation of Da Costa et al. (1994) is used to estimate the mass transfer coefficient, which includes the Reynolds number  $Re$  (dimensionless), Schmidt number  $Sc$  (dimensionless), diffusivity parameter  $D_b$  ( $\text{m}^2/\text{s}$ ) and feed characteristics.

$$k = 0.664 k_{dc} Re_b^{0.5} Sc^{0.33} \left(\frac{D_b}{d_h}\right) \left(\frac{2d_h}{L_f}\right)^{0.5} \quad (3.19)$$

The model water equations of Koroneos et al. (2007) are used to estimate the physical properties are prophesied as follow.

$k_{dc}$  (dimensionless): is the feed spacer characteristic.

$d_h$  (m): represent the feed spacer channel hydraulic diameter.

$L_f$  (m): is the length of filament in the spacer mesh.

$\rho_b$  (kg/m<sup>3</sup>): express the bulk density.

$\mu_b$  (kg/m s): is the kinematic viscosity.

$$Sc = \frac{\mu_b}{\rho_b D_b} \quad (3.20)$$

$$\rho_b = 498.4 m_f + \sqrt{[248400 m_f^2 + 752.4 m_f C_b]} \quad (3.21)$$

$$m_f = 1.0069 - 2.757 \times 10^{-4} T \quad (3.22)$$

$$D_b = 6.72510^{-6} \exp\left\{0.154610^{-3} C_b - \frac{2513}{T + 273.15}\right\} \quad (3.23)$$

$$\mu_b = 1.234 \times 10^{-6} \exp\left\{0.0212 C_b + \frac{1965}{T + 273.15}\right\} \quad (3.24)$$

The total mass balance and solute balance for the complete unit is

$$Q_f = Q_r + Q_p \quad (3.25)$$

$$Q_f C_f - Q_r C_r = Q_p C_p \quad (3.26)$$

A new formula for the total recovery  $Rec$  (dimensionless) is developed as follows

$$Q_f C_f - Q_r C_r - Q_p C_r = Q_p C_p - Q_p C_r \quad (3.27)$$

$$Q_f C_f - C_r(Q_r + Q_p) = Q_p C_p - Q_p C_r \quad (3.28)$$

$$Q_f (C_f - C_r) = Q_p (C_p - C_r) \quad (3.29)$$

$$Rec = \frac{Q_p}{Q_f} = \frac{(C_r - C_f)}{(C_r - C_p)} \quad (3.30)$$

$Rej_{real}$  and  $Rej$  (dimensionless) represent the actual solute rejection and observed rejection, respectively, as specified in Eqs. (3.31) and (3.32).

$$Rej_{real} = \frac{C_w - C_p}{C_w} \quad (3.31)$$

$$Rej = \frac{C_f - C_p}{C_f} \quad (3.32)$$

A new expression for the water flux  $J_w$  (m/s) is also developed

$$J_w = \frac{B_s(T) Rej_{real}}{(1 - Rej)} \quad (3.33)$$

If  $Rej$  equals  $Rej_{real}$ , a new equation is given below for the solute rejection

$$Rej = \left(1 + \frac{B_s(T)}{J_w}\right)^{-1} \quad (3.34)$$

Based on the correlations proposed by Saltonstall Jr and Lawrence (1982), the average permeate salinity and retentate salinity can be calculated as

$$C_p = \frac{C_f}{Rec} [1 - (1 - Rec)^{(1 - Rej)}] \quad (3.35)$$

$$C_r = C_f [1 - Rec]^{-Rej} \quad (3.36)$$

The above steady-state model is developed for an individual spiral wound RO process would be utilised to create the full detailed model for any size of RO seawater desalination or brackish water desalination systems. In this regard, two comprehensive models were developed to characterise the properties of simple and complicated designs of brackish water RO desalination systems.

### **3.3 Model validation against two different sizes of brackish water RO desalination systems**

To represent the robustness of the model developed in this chapter, this section utilises the model validation against two different sizes of simple and complicated designs of RO system used to desalinate brackish water. To systematically carry out this validation, firstly, the description of each design of RO system will be thoroughly described. Secondly, the experimental results of two designs of RO system will be compared against the predictions of the model developed.

#### ***3.3.1 Description of a simple design of RO system***

A simple design of RO system, schematically presented in Fig. 3.1, was considered by Abbas (2005) to desalinate brackish water. This system is designed in three tapered stages with an arrangement (2:1:1) of four pressure vessels. Each pressure vessel contains three Dow/FilmTec BW30-400 spiral wound membranes in a series.

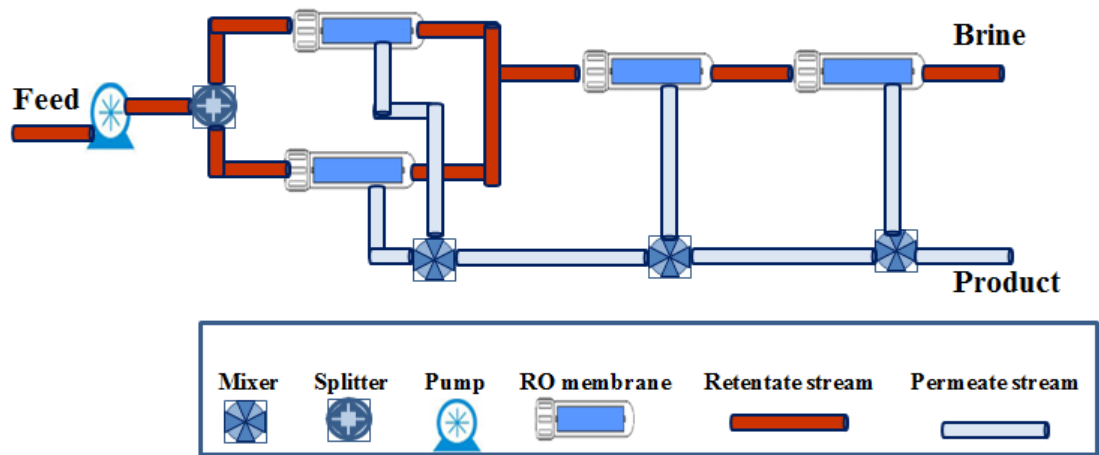


**Fig. 3.1.** Flowsheet of a simple design of RO brackish water desalination system

This design of RO system is characterised by feeding the first stage of two parallel membranes with an inlet feed flow rate of 20.4 m<sup>3</sup>/h of raw brackish water with total dissolved solids (TDS) of 2540 ppm. A high-pressure pump is used to deed the water inside the RO system. The retentate of the first stage is directly fed to the second stage of a single membrane and so on. The permeate of the first, second and third stages are collected to form the main product stream. Also, the retentate of the third stage represents the main brine stream of the RO system. Therefore, it can be said that the retentate reprocessing design is used to desalinate the simple RO brackish water desalination system.

### **3.3.2 Model validation**

The characteristics of feed brackish water to the RO system and the operating conditions are given in Table 3.1. Also, Table 3.2 presents the membrane specifications, and the water transport parameters.

**Table 3.1.** Design specification for a simple RO system

Operation condition		
Parameter	Unit	Value
Feed water salinity	ppm	2540
pH of feed water	-	6 - 6.5
Feed water flow rate	m <sup>3</sup> /h	20.4
Feed temperature	°C	28.8
Feed pressure	atm	12.04

**Table 3.2.** Specifications of the membrane element and transport parameters

Parameter	Value
Membrane and spacer characteristics	Membrane type Dow/FilmTec BW30-400 (spiral wound)
Feed and permeate spacer thickness $t_f, t_p$ (m)	8.6x10 <sup>-4</sup> (34 mils), 5.5x10 <sup>-4</sup>
Hydraulic diameter of the feed spacer channel $d_h$ (m)	8.126x10 <sup>-4</sup>
Effective membrane area $A$ (m <sup>2</sup> )	37.2
Membrane length $L$ and width $W$ (m)	1 and 37.2
Maximum operating pressure (atm)	40.464
Maximum feed flowrate (m <sup>3</sup> /h)	19.31
Maximum pressure drop per element (atm)	0.987
Maximum operating temperature (°C)	45
Minimum salt rejection (%)	97.60
$A_w(T_o)$ (m/ atm s) at 45 °C	9.5096x10 <sup>-7</sup>
$B_s(T_o)$ (NDMA) (m/s) at 45 °C	5.6459 x10 <sup>-8</sup>
Spacer type	NALTEX-129
length of filament in the spacer mesh $L_f$ (m)	2.77x10 <sup>-3</sup>
$A'$ (dimensionless)	7.38
$n$ (dimensionless)	0.34
$\varepsilon$ (dimensionless)	0.9058
$k_{dc}$ (-)	1.501

Table 3.3 presents the comparison between the experimental data of a simple design of RO system of Abbas (2005) and the model predictions. In this regard, a good accuracy can be confirmed where acceptable relative errors are noticed in the overall water recovery and salt rejection of 4.4% and -0.3 %, respectively.

**Table 3.3.** Comparison of simple design RO plant of Abbas (2005) and the model predictions of multistage model

Parameter	Abbas (2005) results	Model predictions	Error%
Permeate flow rate (m <sup>3</sup> /h)	11.954	11.287	5.5
Rejection (-)	98.90	99.205	-0.3
Recovery rate (-)	58.6	56.016	4.4

### ***3.3.3 Description of a complicated design of RO system***

The Arab Potash Company (APC) is the 8<sup>th</sup> largest potash producer worldwide by volume of production and the sole producer of potash in the Arab World. The RO plant of the APC (capacity of 1200 m<sup>3</sup>/day) is situated in Jordan near the Dead Sea with about 110 kilometres south of Amman and 200 kilometres north of Aqaba. APC is designed to comprise both retentate and permeate reprocessing designs (complicated design) that already built to ensure very low salinity of the product from brackish water resource. The raw water is pumped using high pressure pumps type Goulds; ITT to the RO system from groundwater salt wells at pH=7.45–7.59 and salinity of 1100 ppm. The RO system has 20 pressure vessels of 6 membranes in each. Spiral wound membranes of 37.2 m<sup>2</sup> type TMG20D-400 synthesised by Toray Membrane USA Inc., was stuffed in the pressure vessels. The 1<sup>st</sup> pass consists 2 stages arranged in parallel of 6 pressure vessels with configuration (4:2) and the 2<sup>nd</sup> pass consists 3 stages arranged in parallel of 4 pressure vessels with configuration (2:1:1). The high salinity retentate from the 1<sup>st</sup> pass is disposed into the drain system. The low-pressure permeates of the 1<sup>st</sup> pass are combined and pumped using two forwarding high pumps into the 2<sup>nd</sup> pass for further filtration, which produces very low salinity of produced water around 2 ppm. It is important to note that the feed water of the 1<sup>st</sup> pass consists of blending of two streams, i.e., the raw water stream and the low salinity retentate stream of the 2<sup>nd</sup> pass. In other words, the low salinity retentate stream from the 2<sup>nd</sup> pass is totally recycled back to be merged with the mainstream of raw water (with salinity 1098.62 ppm). The plant product stream is the collected permeates of 2<sup>nd</sup> pass of around 2 ppm.

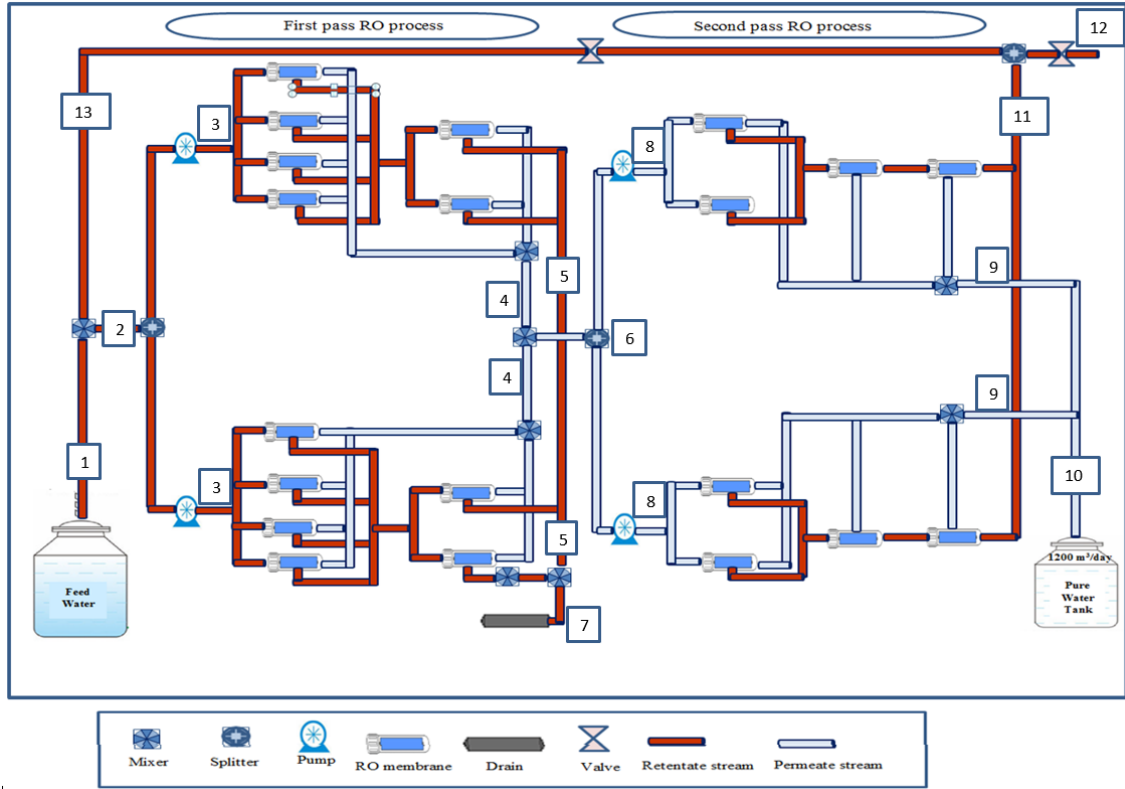


Fig. 3.2. Flowsheet of brackish water RO desalination plant of APC

### 3.3.4 Model validation

Due to the complexity of the RO system of APC, there is a necessity to develop new equations to relate the connected streams of the system and quantify the related retentate and permeate reprocessing designs throughout the RO system. Therefore, the following equations need to be integrated with the model developed in this chapter to maintain accurate calculations of the process performance indicators.

Eq. (3.37) expresses the feed flow rate of plant, where RR is the retentate ratio. Also, the inlet feed concentration is estimated by Eq. (3.38)

$$Q_{f(plant)} = RR Q_{r(plant)} + Q_{f(RW)} \quad (3.37)$$

$$Q_{f(plant)} C_{f(plant)} = RR Q_{r(plant)} C_{r(plant)} + Q_{f(RW)} C_{f(RW)} \quad (3.38)$$

The overall retentate flow rate of the RO system and retentate concentration are calculated in the counter of Eq. (3.39) and Eq. (3.40), respectively.

$$Q_{r(plant)} = Q_{r(pass = 2)} \quad (3.39)$$

$$C_{r(plant)} = C_{r(pass = 2)} \quad (3.40)$$

The product salinity permeate flow rate, constant temperature, and retentate pressure of the whole are represented in the context of the following equations.

$$C_{p(Plant)} = C_{p(pass = 2)} \quad (3.41)$$

$$Q_{p(Plant)} = Q_{p(pass = 2)} \quad (3.42)$$

$$T_{f(plant)} = T_{r(plant)} \quad (3.43)$$

$$P_{r(plant)} = P_{r(pass = 2)} \quad (3.44)$$

The feed salinity, feed flow rate, permeate flow rate, and permeate salinity of 1<sup>st</sup> pass are calculated as

$$C_{f(pass = 1)} = C_{f(plant)} \quad (3.45)$$

$$Q_{f(pass = 1)} = Q_{f(plant)} \quad (3.46)$$

$$Q_{p(pass = 1)} = \sum_{PV=1}^{10} Q_{p(PV)} \quad (3.47)$$

$$C_{p(pass = 1)} = \frac{\sum_{PV=1}^{10} C_{p(PV)} Q_{p(PV)}}{Q_{p(pass = 1)}} \quad (3.48)$$

The feed pressure, feed salinity, permeate flow rate, and permeate salinity of 2<sup>nd</sup> pass are calculated as

$$P_{f(pass = 2)} = 1.066x P_{f(pass = 1)} \quad (3.49)$$

$$C_{f(pass = 2)} = C_{p(pass = 1)} \quad (3.50)$$

$$Q_{p(pass = 2)} = \sum_{PV=1}^8 Q_{p(PV)} \quad (3.51)$$

$$C_{p(pass = 2)} = \frac{\sum_{PV=1}^{10} C_{p(PV)} Q_{p(PV)}}{Q_{p(pass = 2)}} \quad (3.52)$$

The characteristics of feed brackish water fed to the RO system and the operating conditions are given in Table 3.4. Table 3.5 presents the specifications of the membrane and transport parameters.

**Table 3.4.** Design specification for an industrial brackish water RO system of APC

Parameter	Unit	Value
Feed water salinity	ppm	1098.62
Conductivity	$\mu\text{S/cm}$	1983.06
pH of feed water	-	7.45 -7.55
Feed water flow rate	$\text{m}^3/\text{h}$	74
Feed temperature	$^{\circ}\text{C}$	25
Feed pressure to the 1st pass	atm	9.220
Feed pressure to the 2 <sup>nd</sup> pass	atm	9.832
Daily production capacity	$\text{m}^3/\text{day}$	1200
Average product salinity	ppm	1.96
Total system rejection	%	99.80

**Table 3.5.** Specifications of the membrane element and transport parameters (Adapted from Al-Obaidi et al., 2018a)

Parameter	Value	Parameter	Value
Membrane supplier	Toray Membrane USA Inc.	Membrane type and configuration	TMG20D-400, spiral wound
Spacer type	NALTEX-129	length of filament in the spacer mesh $L_f$ (m)	$2.77 \times 10^{-3}$
Feed spacer thickness ( $t_f$ ) (m)	$8.6 \times 10^{-4}$ (34 mils)	permeate spacer thickness ( $t_p$ ) (m)	$5.5 \times 10^{-4}$
Membrane length $L$ (m)	1	Membrane width $W$ (m)	37.2
Effective membrane area $A$ ( $\text{m}^2$ )	37.2	Minimum salt rejection (%)	99.5
$A_w(T_o)(\text{m}/\text{atm s})$ at 25 ( $^{\circ}\text{C}$ )	$9.6203 \times 10^{-7}$	$B_s(T_o)$ (NDMA) (m/s) at 25 ( $^{\circ}\text{C}$ )	$1.61277 \times 10^{-7}$
Hydraulic diameter of the feed spacer channel $d_h$ (m)	$8.126 \times 10^{-4}$	Maximum pressure drop per element (atm)	0.987
$A'$ (dimensionless)	7.38	$n$ (dimensionless)	0.34
$k_{dc}$ (dimensionless)	1.501	$\varepsilon$ (dimensionless)	0.9058
Maximum operating pressure (atm)	40.464	Maximum operating temperature ( $^{\circ}\text{C}$ )	45
Pump efficiency (-)	0.85%		

Table 3.6 depicts the high consistency of the model presented in this chapter. Low errors (maximum error of around 6%) are presented after comparing the experimental data of the RO system of APC against the model predictions for several performance indicators.

**Table 3.6.** Comparison of the experimental results of RO system of APC and the model predictions

1 <sup>st</sup> pass RO process					
Parameter	Position	Experimental results		Model	Error %
		Unit	Average		
Feed water salinity	1	ppm	1098.62	--	--
Feed flow rate	1	m <sup>3</sup> /h	74	--	--
Plant feed flow rate	2	m <sup>3</sup> /h	84	--	--
Plant feed salinity	2	ppm	997	--	--
Temperature	2	°C	25	--	--
Pressure	3	atm	9.220	--	--
Feed flow rate	3	m <sup>3</sup> /h	42	--	--
Salinity	3	ppm	997	--	--
Permeate flow rate	4	m <sup>3</sup> /h	29.233	29.423	-0.65
Retentate pressure	5	atm	8.3809	8.4420	-0.72
Retentate flow rate	5	m <sup>3</sup> /h	12.57	12.576	-0.05
Feed flow rate	6	m <sup>3</sup> /h	58.466	58.847	-0.65
Rejection	6	(-)	95.466	95.460	0.00
Recovery rate	6	(-)	70.08	70.056	0.03
Retentate flow rate	7	m <sup>3</sup> /h	25.14	25.152	-0.05
2 <sup>nd</sup> pass RO process					
Pressure	8	atm	9.832	--	--
Permeate salinity	9	ppm	1.96	2.0358	-3.86
Permeate flow rate	9	m <sup>3</sup> /h	24.57	24.131	1.78
Rejection	9	(-)	95.5	95.501	-1.59
Recovery rate	9	(-)	83.5	82.012	1.78
Permeate salinity	10	ppm	1.96	2.0358	-3.86
Permeate flow rate	10	m <sup>3</sup> /h	49.14	48.262	1.78
Retentate flow rate	11	m <sup>3</sup> /h	10	10.584	-5.84
Retentate salinity	11	ppm	246	242.31	1.49
Recycled salinity	13	ppm	245	242.31	1.09
Recycled flow rate	13	m <sup>3</sup> /h	10	10.584	-5.84

### 3.4 Further simulation for a simple design of RO system

This section utilises further simulation to investigate the influence of inlet parameters on the performance indicators. The simulation will be carried out on the simple design of RO process presented in Fig. 3.1.

#### 3.4.1 Impact of feed salinity

The impact of feed salinity on the performance indicators of RO process is carried out via increasing the feed salinity by 20% from the basic value of 2540 ppm to 3040 ppm in a

step increase of 100 ppm. However, fixed values of feed pressure, feed flowrate, and temperature are used as 12.04 atm, 20.4 m<sup>3</sup>/h and 28.8 °C, respectively. Fig. 3.3 indicates inconsiderable change in solute rejection of 0.04% from (99.205%–99.168%), and a significant decrease in water recovery of 19% from (56.02% -54.94%) as a response to the change of feed salinity. As the feed salinity increases, the bulk concentration and osmotic pressure will be increased that causes a decrease in the productivity of fresh water via the membrane. However, the change in the feed salinity was not enough to make a big change in the total solute rejection due to a simultaneous increase in both feed and permeate salinities. In this regard, Fig. 3.4 demonstrates an increase in permeate salinity of 25.2% from 20.19 ppm to 25.28 ppm due to increasing feed salinity. Also, a significant increase from 3210.5 ppm to 3790.8 ppm (18%) is deduced in retentate salinity as a response of increasing feed salinity.

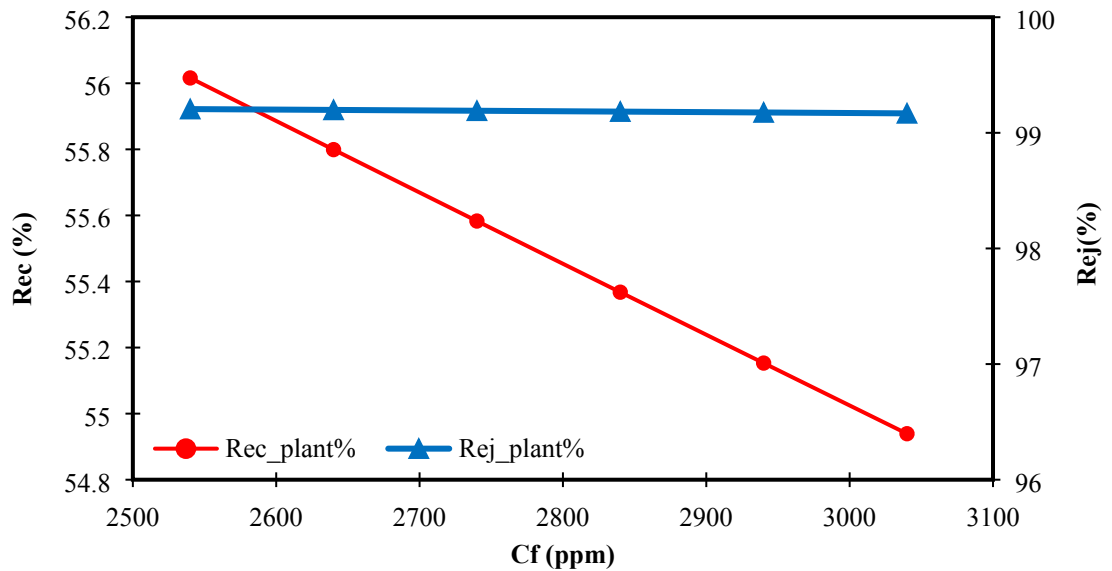


**Fig. 3.3.** Impact of feed water salinity on total recovery and solute rejection

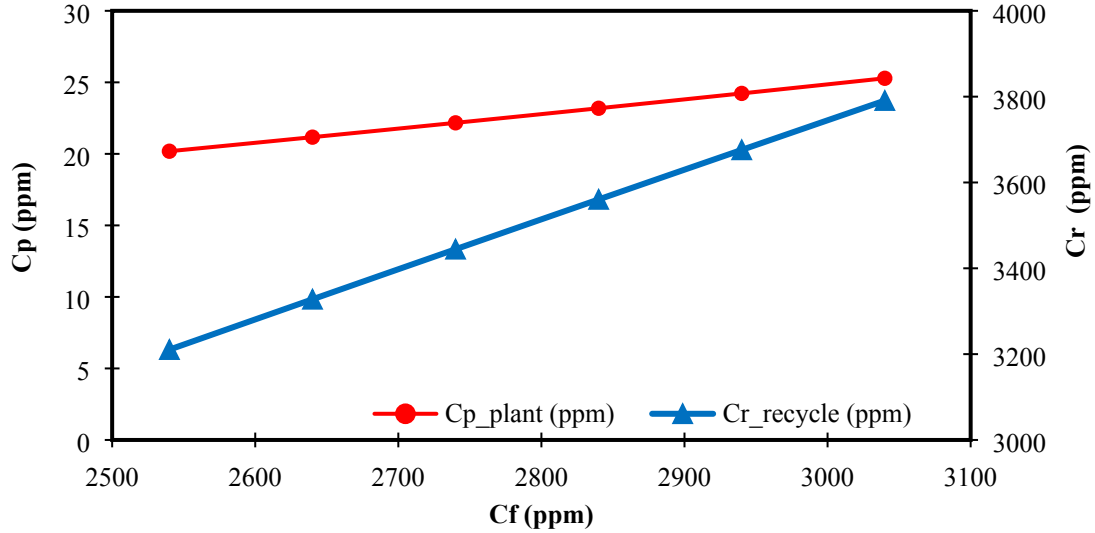


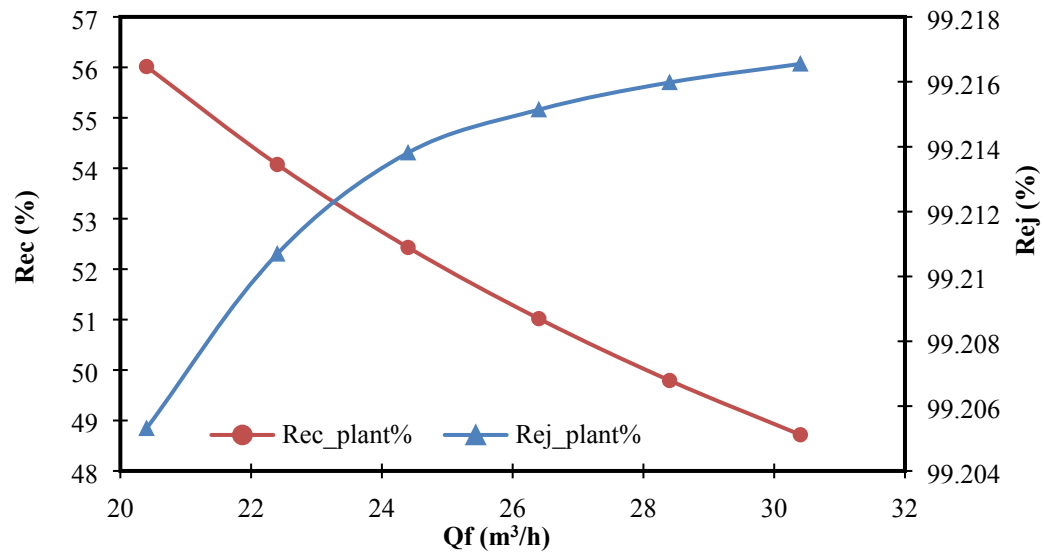
**Fig. 3.4.** Impact of feed water salinity on product and retentate salinities

### ***3.4.2 Impact of feed water flow rate***

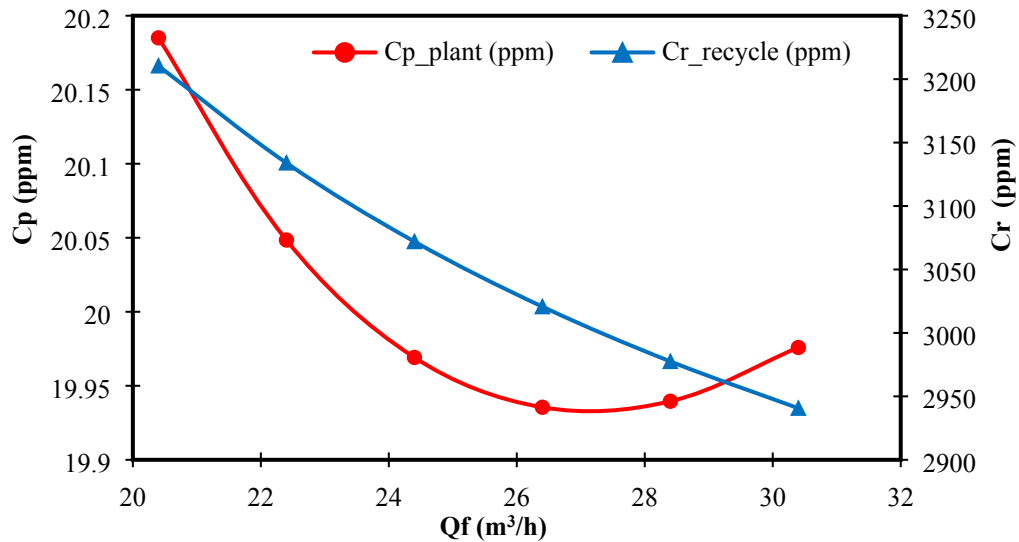
Figs. 3.5 and 3.6 present the behaviours of solute rejection, water recovery, permeate and retentate salinities, respectively, due to increasing the feed flow rate by 20% from 20.4 to 30.4 m<sup>3</sup>/h at fixed values of pressure, feed salinity, and temperature of 12.04 atm, 2540 ppm, and 28.8 °C, respectively. The solute rejection insignificantly increases by 0.011 % from (99.205–99.216%), while a decrease of 14.98% from (56.016%–48.718%) is noticed in water recovery.

Fig. 3.6 specifies exponential reductions of both permeate and retentate salinities due to increasing feed flow rate. Statistically, permeate and retentate salinities are reduced by 1.1% from 20.19 ppm to 19.97 ppm and 9.2% from 3210.5 ppm to 2940 ppm, respectively. Increasing feed flow rate simply means lowering the residence time of fluid inside the module that entirely means reducing the total productivity. Also, increasing feed flow rate has an advantage of reducing the wall membrane concentration and then reduces the solute flux through the membrane; reduces the permeate salinity. Furthermore, increasing feed flow rate would increase the turbulence and then reduces the salinity of outlet brine. More importantly, Fig. 3.6 shows a remarkable increase in water recovery at the low values of feed flow rate that followed by insignificant increase of water recovery at the high feed flow rate. Seemingly, the reason behind this phenomenon is that the gain due to the lower average osmotic pressure due to increasing feed flow rate is outweighed by the high

frictional pressure drop between the fluid and membrane surface and therefore, the net driving force of penetrating water through the membrane is retarded. Interestingly, Fig. 3.6 shows that there is an optimum value of feed flow rate that can maintain the lowest permeate salinity. Beyond this value, the permeate salinity starts to increase that might be caused due to increasing the solute flux after the optimum value of feed flow rate.



**Fig. 3.5.** Impact of feed flow rate on total recovery and solute rejection



**Fig. 3.6.** Impact of feed flow rate on product and retentate salinities

### 3.4.3 Impact of inlet feed pressure

An increase of 20% in feed pressure from 12.04 atm to 13.04 atm is considered to explore the influence of pressure on the performance indicators of the small-scale RO process (Fig. 3.1). the simulation is carried out at fixed feed salinity, feed flow rate, and temperature of 2540 ppm, 20.4 m<sup>3</sup>/h and 28.8 °C. As shown in Fig. 3.7, increasing feed pressure causes insignificant change in the salt rejection which increased by 0.067% from (99.205–99.272%), while a considerable increase of 40.94% from (56.016–58.31%) can be noticed in the water recovery. The higher water flux through the membranes attributed the increase of productivity and water recovery.

Fig .3.8 depicts a linear relationship between the permeate and retentate salinities and feed pressure at fixed other operating conditions. Statistically, the permeate salinity decreases by 9.18% from 20.19 ppm to 18.49 ppm with a decrease in the retentate salinity by 2.99% from 3306.4 ppm to 3210.8 ppm as a response to increasing the pressure.

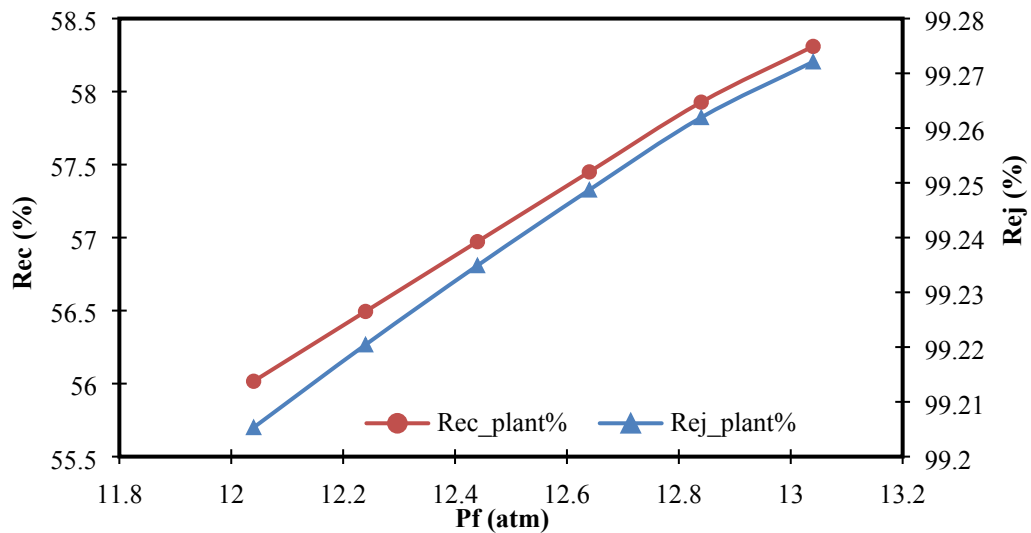


**Fig. 3.7.** Impact of feed pressure on total water recovery and solute rejection

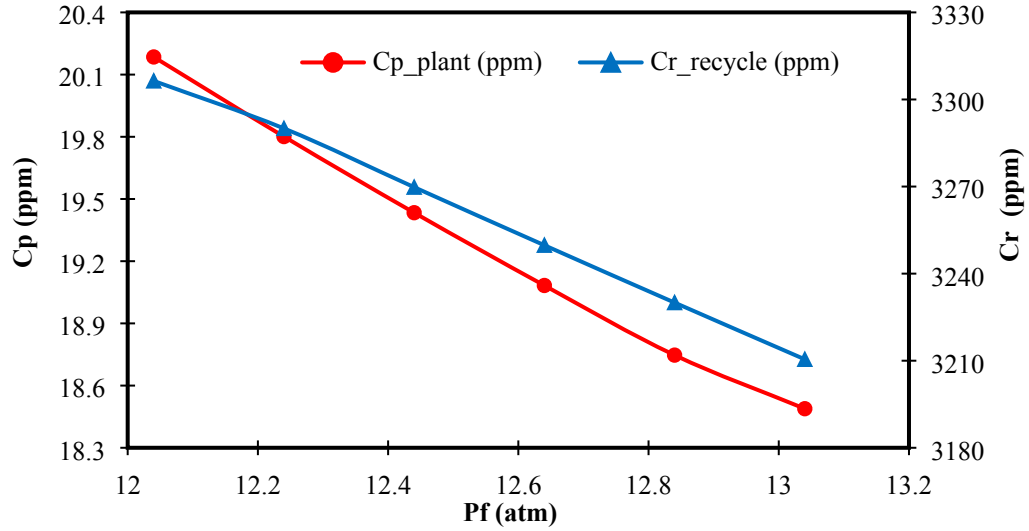


**Fig. 3.8.** Impact of feed pressure on product and retentate salinities

#### ***3.4.4 Impact of inlet feed temperature***

The influence of feed temperature variation from 28.8 to 33.8 °C on the performance indicators at fixed other operating parameters of feed water concentration 2540 ppm, feed water flow rate 20.4 m<sup>3</sup>/h and pressure 12.04 atm are investigated in this section.

Figs .3.9 indicates negligible influences of temperature on solute rejection (99.205–99.211%), and water recovery (56.016–56.073%). Also, Fig. 3.10 shows inconsiderable decreases of permeate salinity by 0.76 % from 20.19 ppm to 20.03 ppm and retentate salinity by 0.073% from 3210.5 ppm to 3212.8 ppm due to increasing temperature.

Increasing feed temperature means increasing of solute and water transport parameters of the membrane (directly related to temperature) that means increasing of both water and solute fluxes through the membranes. Also, increasing temperature would decrease water viscosity and density besides increasing the mobility of the membrane that aid to increase water productivity. This in turn would explain the phenomena presented in Figs. 3.7 to 3.10.

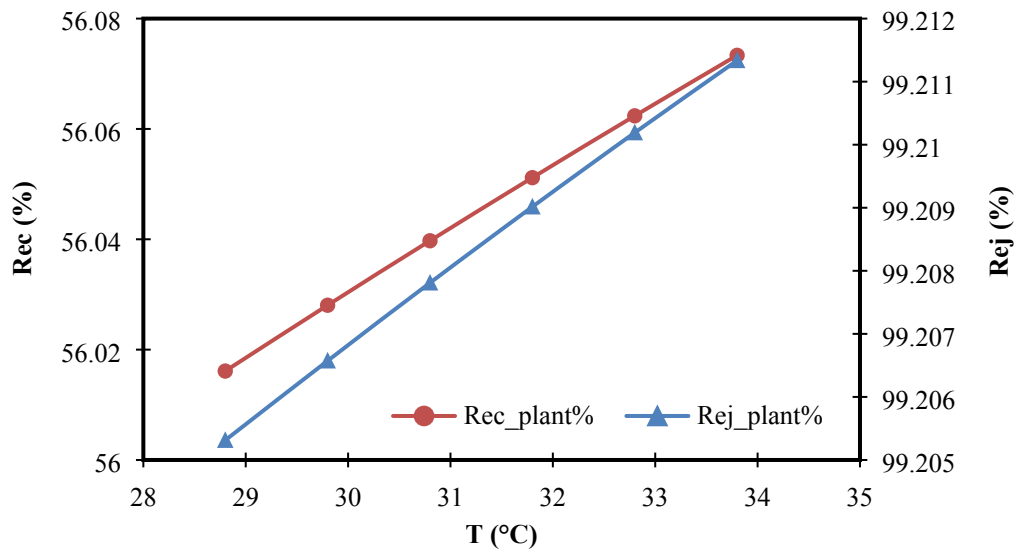


**Fig. 3.9.** Impact of feed temperature on water recovery and solute rejection

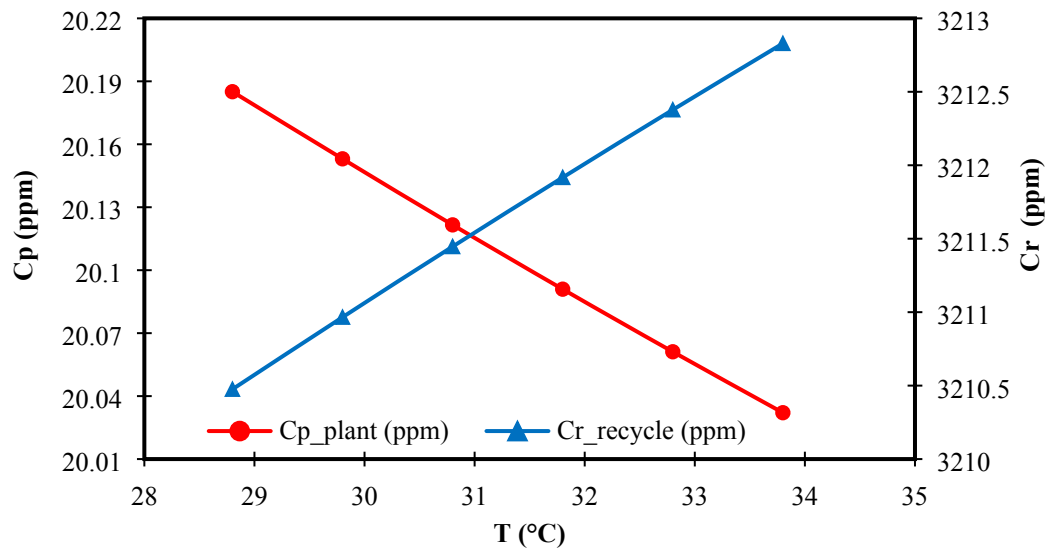


**Fig. 3.10.** Impact of feed temperature on product and retentate salinities

### 3.5 Conclusions

This chapter presents the development of a comprehensive model for the prediction of performance indicators of an individual spiral wound RO process. The model developed can include any number of stages, pressure vessels, membranes, in addition to its

capability of amending the stream connections in multistage RO process. Therefore, the model developed was upgraded to characterise two different sizes of RO process including the simple and complicated designs. To quantify the robustness of the model developed, two validation studies were carried out to examine the errors between the model predictions and experimental data of simple and complicated designs of RO process. The results showed the accuracy of the model and therefore it was used to carry out a comprehensive simulation to explore the influence of inlet parameters on the responses of the simple design of RO process. Furthermore, the model developed will be further used to improve the reliability of the simple and complicated designs of RO process as will be discussed in the upcoming chapters.

## CHAPTER FOUR

### Performance Evaluation of Reverse Osmosis Brackish Water Desalination Plant with Recycled Retentate Design

#### 4.1 Introduction

The RO process has stated its robustness as a foremost technology for desalting brackish water as a response to its high performance of salt rejection and water permeation (Ghaffour et al., 2015). Moreover, the application of RO process compared to other conventional thermal technologies is remarkably increased due to its high production with low cost and energy consumption (Al-Karaghoul and Kazmerski, 2013). The multistage RO process is eventually designed in several configurations to satisfy the qualifications of the produced water. One of the tested configurations of RO process in the open literature is the recycling of permeate stream or retentate stream into the feed stream. In this regard, the permeate and retentate recycling designs were employed by several researchers to improve the RO process performance and their influences on the response indicators were investigated. For instance, Al-Bastaki and Abbas (1999) utilised a retentate cyclic mode in a small-scale spiral wound RO water desalination plant to explore its contribution on the permeate flow rate and salt rejection. They demonstrated that implementing the cyclic mode would significantly reduce the concentration polarisation and enhance the permeate flux. Statistically, a cyclic operation led to a growth in the water flux of 6.5% beyond the one registered without retentate recycling.

Al-Bastaki and Abbas (2003) studied the impact of permeate recycling design on the performance of a small-scale spiral wound RO desalination plant. The permeate recycle percentage between 0% to 25% has limited the concentration polarisation that completely enhanced the product quality despite a reduction of the production rate. The product concentration was reduced by 15% (from 0.175 to 0.149 kg/m<sup>3</sup>) at 25% of permeate recycling percentage compared to the case of no recycle mode. However, the production rate was reduced by 22% from  $2.99 \times 10^{-3}$  to  $2.343 \times 10^{-3}$  m<sup>3</sup>/s compared to the case of no recycle mode as shown in Table 4.1.

**Table 4.1.** Effect of recycle ratio on the overall product flow rate and product salinity (Al-Bastaki and Abbas, 2003)

Recycle Ratio (%)	Cp (kg/m <sup>3</sup> )	Qp (m <sup>3</sup> /s) x10 <sup>3</sup>
4.97	20.964	2.719
5.79	17.336	2.667
7.07	14.571	2.589
10.18	11.790	2.481
12.31	10.238	2.418
14.65	8.239	2.362
20.62	7.116	2.259

A scenario of partial retentate recycle was tested on a small pilot-scale brackish water RO process by Sarkar et al. (2008). Increased retentate recycle requires an increase in the operating temperature to steadily maintain the performance at a fixed product flow rate. Table 4.2 depicts a comparison of specific energy consumption with recycle and without recycle modes. It can be stated that increasing feed salinity causes an increase in the specific energy consumption without retentate recycle mode. However, the specific energy consumption remains almost constant with retentate recycle mode.

**Table 4.2.** Specific energy consumption vs feed salinity (Sarkar et al., 2008)

Specific energy consumption without recycle (kWh/m <sup>3</sup> )	Specific energy consumption with recycle (kWh/m <sup>3</sup> )	Feed Salinity (ppm)
1.105	1.180	2611.3
1.12	1.186	3031.6
1.143	1.188	3453.1
1.208	1.192	4551.8
1.248	1.210	5250.9

Sharma et al. (2017) studied the performance of a batch closed-loop design RO membrane process with partial retentate recirculation and opened-loop design process without recirculation. The simulation results affirmed that the closed-loop design with recirculation of retentate consumes between 70% to 95% less power energy compared to

open-loop design. Moreover, implementing recirculation with an optimal ratio (maximum recirculation) can save up to 95% of energy power consumption.

Al-Obaidi et al. (2019) explored the influence of permeate, retentate and permeate-retentate streams recycling schemes on the rejection of chlorophenol from wastewater using model-based simulation. This study confirmed that the permeate recycling scheme has a considerable influence on the RO process performance compared to other tested schemes of retentate recycling and permeate-retentate recycling. The permeate recycling mode casus the highest reduction of phenol product concentration. Moreover, a continuous reduction in water recovery rate and an increase in energy consumption were registered as the water recycle ratio decreases as depicted in Table (4.3).

**Table 4.3.** Simulation results of three schemes of partial recycle on the product phenol concentration

Cp with both permeate and retentate recycling (kmol/m <sup>3</sup> ) x10 <sup>3</sup>	Cp with retentate recycling (kmol/m <sup>3</sup> ) x10 <sup>3</sup>	Cp with permeate recycling (kmol/m <sup>3</sup> ) x10 <sup>3</sup>	Partial recycle ratio (%)
1.113	1.12	1.14	0
1.059	1.115	1.05	10
1.059	1.095	1	20
1.018	1.097	0.97	30
0.983	1.096	0.9	40
0.956	1.11	0.8	50

This chapter intends to explore the influence of recycled retentate mode on the performance of brackish water RO desalination plant. In this regard, two case studies of retentate recycle mode for simple and complicated designs of brackish water RO desalination plants will be presented and the performance indicators will be discussed thoroughly.

## **4.2 Performance evaluation of retentate recycle mode for a simple design of brackish water RO process**

### ***4.2.1 Description of a simple design RO desalination plant with retentate recycle mode***

The simple design of RO process with retentate recycle mode is schematically given in Fig. 4.1. Occasionally, Fig. 4.1 shows the same simple design of RO process presented in chapter 3 (Fig. 3.1). In this regard, the retentate of the last stage is recycled to the feed

stream at different recycle ratios. The influence of retentate recycle scheme at various recycle percentage on the overall process performance indicators of the RO process will be discussed in the upcoming section.

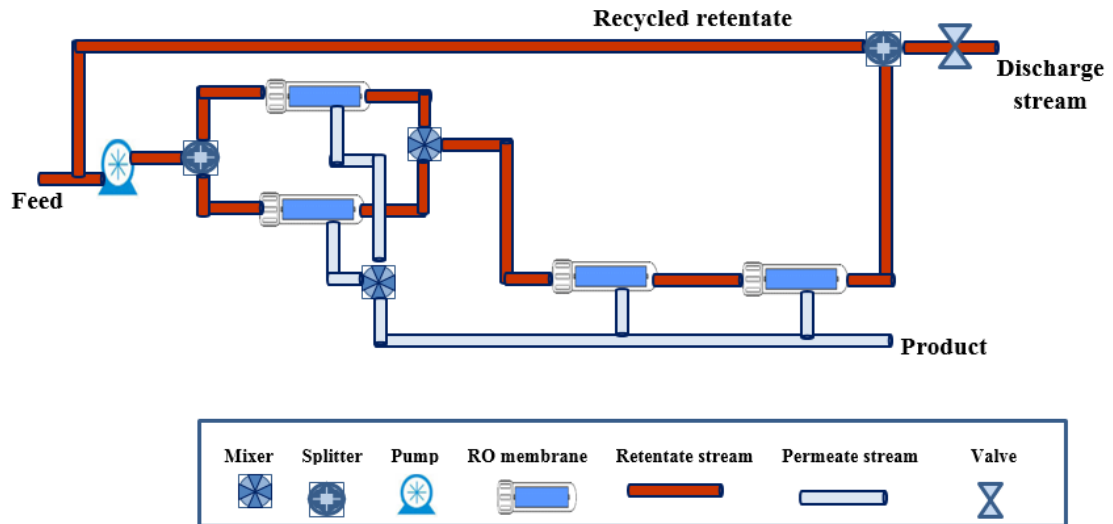


**Fig. 4.1.** Schematic diagram of a simple RO desalination plant

#### ***4.2.2 Impact of retentate recycling scheme on the RO process performance***

In this section, the performance of a simple RO plant is tested by implementing various percentages of retentate recycle of the last stage (Fig. 4.1) from 10% to 100% in a step change of 10%. Therefore, the performance indicators will be investigated based on this new scheme of recycling high salinity stream. The methodology applied here is a spontaneous recycling of the retentate stream which is quite different than employing a continuous operation of recycling the retentate stream, which would have a negative influence on the total process performance. In other words, this research intends to explore the feasibility of a spontaneous retentate recycling mode. The selected performance indicators of RO process are the water recovery (Rec), solute rejection (Rej), product and retentate concentrations ( $C_p$ ,  $C_r$ ), product and retentate flow rates ( $Q_p$ ,  $Q_r$ ), and specific energy consumption. It is important to note that this simulation is carried out at fixed feed salinity, feed flow rate, pressure, and temperature of 2540 ppm, 20.4 m<sup>3</sup>/h, 12.04 atm, and 28.8°C, respectively.

Fig. 4.2 depicts the influence of various percentages of retentate recycle on the solute rejection and water recovery. In this regard, the solute rejection is exponentially increased with the increase in the percentage of retentate recycle. However, this is an insignificant increase of 0.0046% in solute rejection that associated with a decrease of 3.55% in water recovery after applying 100% percentage of retentate recycle. However, the water recovery has noticed insignificant change along the tested percentages of the retentate recycle. The decrease of water recovery is essentially attributed to the reduction of productivity as the retentate recycle percentage increases.

Also, the solute rejection has noticed a clear variation throughout the variation of retentate recycle percentage. More importantly, the 80% of retentate recycle can attain the maximum value of solute rejection of 99.21%.

The influence of increasing the percentage of the retentate recycle on the product and retentate flow rates is depicted in Fig. 4.3. Consequently, it can be stated an insignificant decrease of product flow rate (water flux) and significant increase of retentate flow rate as the percentage of retentate recycle increases from 0% to 100%. It is well expected that increasing the inlet flow rate of the first stage due to an increase in the percentage of retentate recycle would increase the rate of turbulence inside the modules and therefore would cause a reduction of water flux, i.e., productivity. This is especially after applying the 10% retentate recycle that intensively reduces the product flow rate. However, it can be noticed that the product flow rate starts to upgrade after 20% retentate recycle that might be attributed to the growth of water flux as a result to increasing the rate of turbulence and increases mass transfer coefficient. Furthermore, the first depression of productivity at 10% might be ascribed to an instantaneous increase in pressure drop as a result to surprisingly increase the fluid velocity inside each module with the increase in percentage of retentate recycle. This is quite identical to the behaviour of water recovery (Fig. 4.2). Statistically, a decrease of 0.16% in the product flow rate and an increase of 12.3% in the retentate flow rate are recorded when the percentage of retentate recycle increases from 0% to 100%. Also, the reduction of retentate flow rate is expected since the product flow rate increases after applying the 20% retentate recycle and so on.

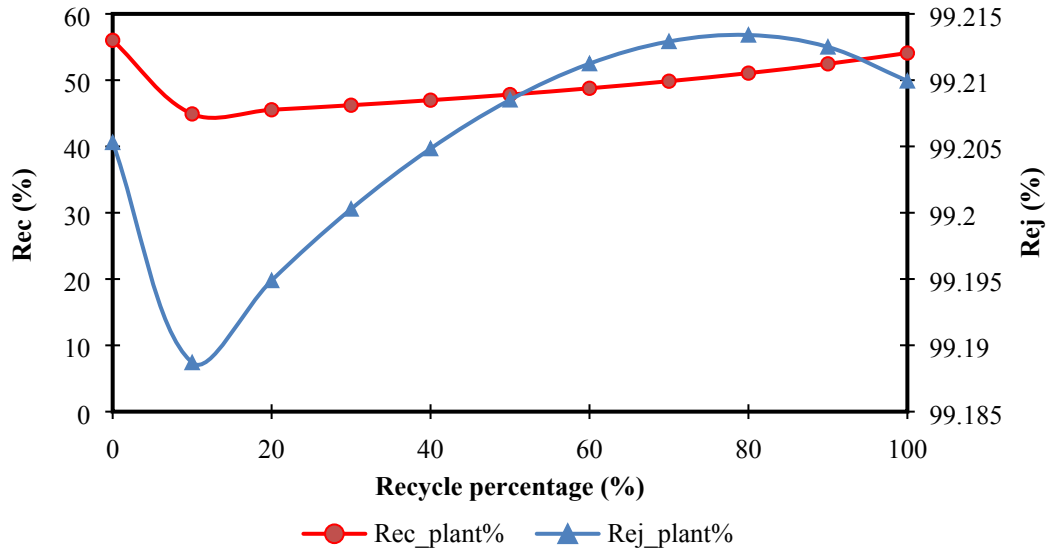


**Fig. 4.2.** Effect of retentate recycle percentage of the last stage on the water recovery and solute rejection

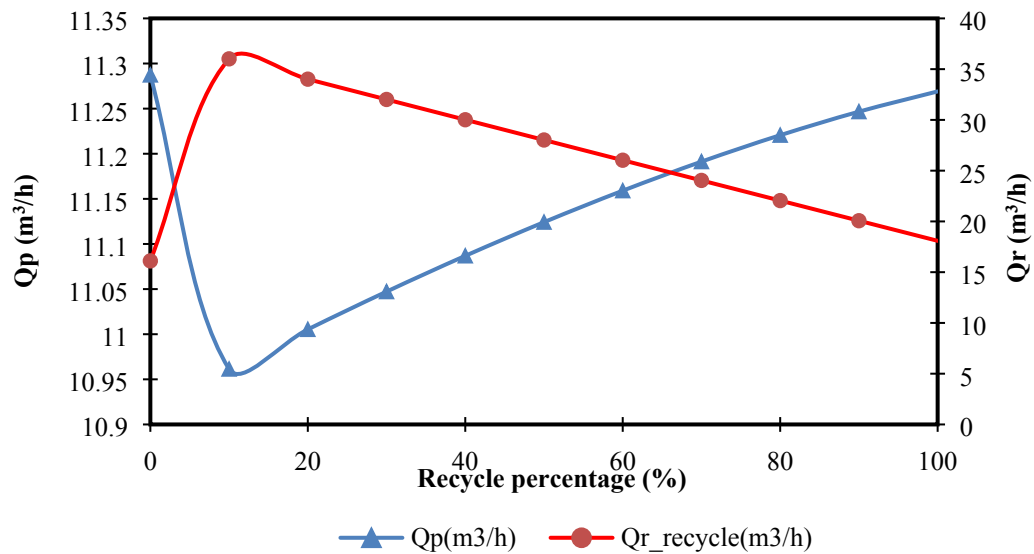


**Fig. 4.3.** Effect of retentate recycle percentage of the last stage on the product and retentate salinities on product and retentate flowrates

Fig. 4.4 presents that increasing of percentage of retentate recycle from 0 to 100% causes a marginal decrease in the product concentration and a significant decrease in the retentate concentration. This is specifically recorded 0.22%, and 2.1% increases in the product and retentate salinities, respectively. The increase of turbulence inside the modules due to increasing the percentage of retentate recycle would possibly reduce the solute flux through the membranes and therefore reduces the total product salinity. Fig. 4.3 showed an increase of productivity after applying 20% retentate recycle that consequently means

an improvement of product salinity. Also, the increase of turbulence would also reduce the retentate salinity.

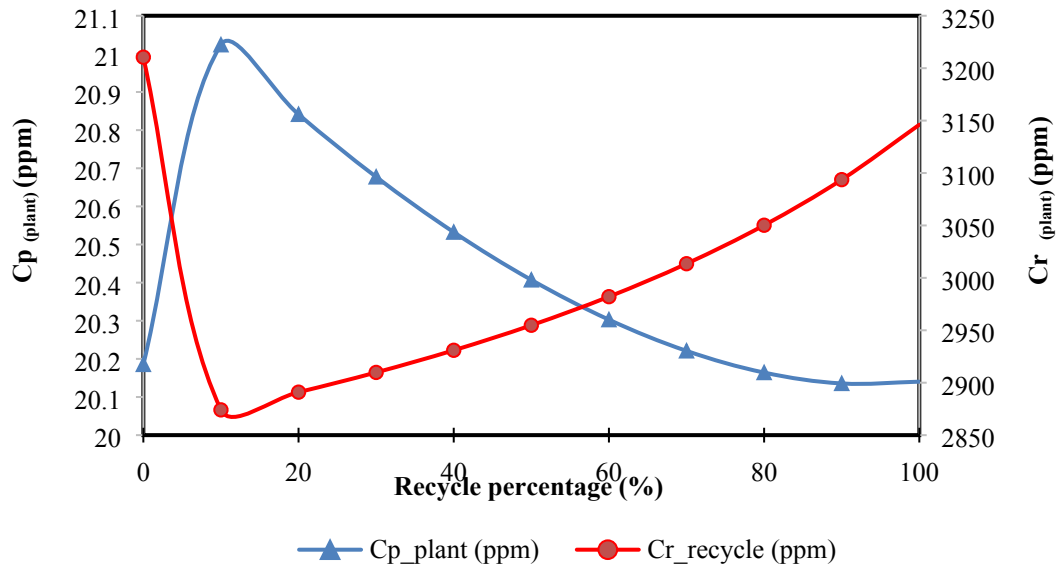


**Fig. 4.4.** Effect of retentate recycle percentage of the last stage on the product and retentate salinities

Due to the above behaviour of productivity (Fig. 4.3), it is expected to notice an increase in the specific energy consumption after applying the first increase of 10% in retentate recycle. However, a continuous depression of specific energy consumption is confirmed after applying 20% and so on. Fig. 4.5 pictures the influence of retentate recycle mode at different percentages on the specific energy consumption. It is therefore can be noted that any growth of productivity would reduce the specific energy consumption. Fig. 4.5 shows that the specific energy consumption is increased by 10% as a result to increasing the percentage of retentate recycle of the last stage from 0% to 100%.

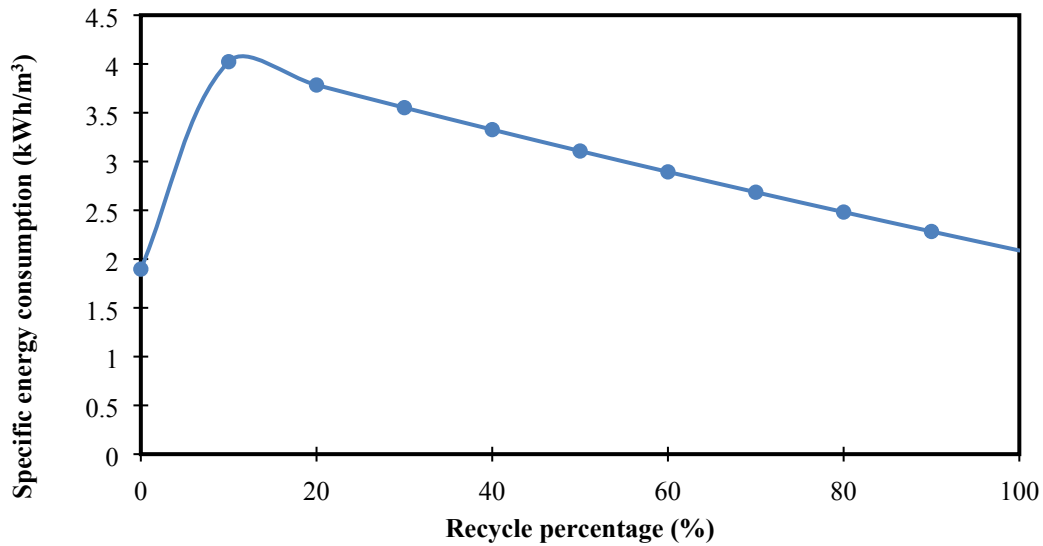


**Fig. 4.5.** Effect of retentate recycle percentage of the last stage on the specific energy consumption

To clarify the simulation results and comprehend the associated behaviours of the performance indicators of RO system, Table 4.4 shows the simulation results of several performance indicators with 80%, 100%, and without recycling mode for comparison purposes. It can be stated that recycle mode (100%) can keep the process at the lowest product salinity where the product salinity decreases from 20.185 to 20.140 ppm at the same operating conditions. Also, applying 100% retentate recycle mode would not considerably affect the solute rejection and requires 10% increase in the specific energy consumption if compared to no recycle mode. However, the no recycle mode of 0% would ensure the highest water recovery and product flow rate.

**Table 4.4.** Simulation results of process performance indicators with 0% (without recycle mode), 80% and 100% percentages of retentate recycle for simple RO system

Performance indicators at 0% recycle percentage		Performance indicators at 80% recycle percentage		Performance indicators at 100% recycle percentage	
Rej_plant (%)	99.205	Rej_plant (%)	99.213	Rej_plant (%)	99.209
Rec_plant (%)	56.016	Rec_plant (%)	51.064	Rec_plant (%)	54.094
Qp_plant (m <sup>3</sup> /h)	11.287	Qp_plant (m <sup>3</sup> /h)	11.220	Qp_plant (m <sup>3</sup> /h)	11.269
Qr_recycle from the last stage (m <sup>3</sup> /h)	16.112	Qr_recycle from the last stage (m <sup>3</sup> /h)	22.052	Qr_recycle from the last stage (m <sup>3</sup> /h)	18.088
Cp_plant (ppm)	20.185	Cp_plant (ppm)	20.164	Cp_plant (ppm)	20.140
Cr_recycle of the last stage (ppm)	3210.47	Cr_recycle of the last stage (ppm)	3050.20	Cr_recycle of the last stage (ppm)	3146.06
Specific energy consumption (kWh/m <sup>3</sup> )	1.897	Specific energy consumption (kWh/m <sup>3</sup> )	2.481	Specific energy consumption (kWh/m <sup>3</sup> )	2.087

### 4.3 Performance evaluation of retentate recycle mode for a complicated design of brackish water RO process

#### 4.3.1 Description of a complicated design of RO desalination plant of APC with retentate recycle mode

The full description of the original multistage multi pass RO system of APC was presented in Chapter 3. The recent modification is to upgrade the design of RO system by applying a retentate recycle mode on the first pass and recycle the high salinity stream (position 4) at different percentages to be merged with the inlet feed stream of the first pass. Therefore, the next section intends to test the feasibility of recycling the high salinity retentate stream of the first pass (that is originally disposed into the drain system) at different ratios between 10% to 100% to the feed water stream and explore its influence on the process operation. Consequently, the process performance indicators would be compared against

the original experimental data of no recycle mode that carried out at specified operating conditions to assess its contribution. Fig. 4.6 shows the multistage multi pass design of RO system with the retentate recycle mode of the first pass.

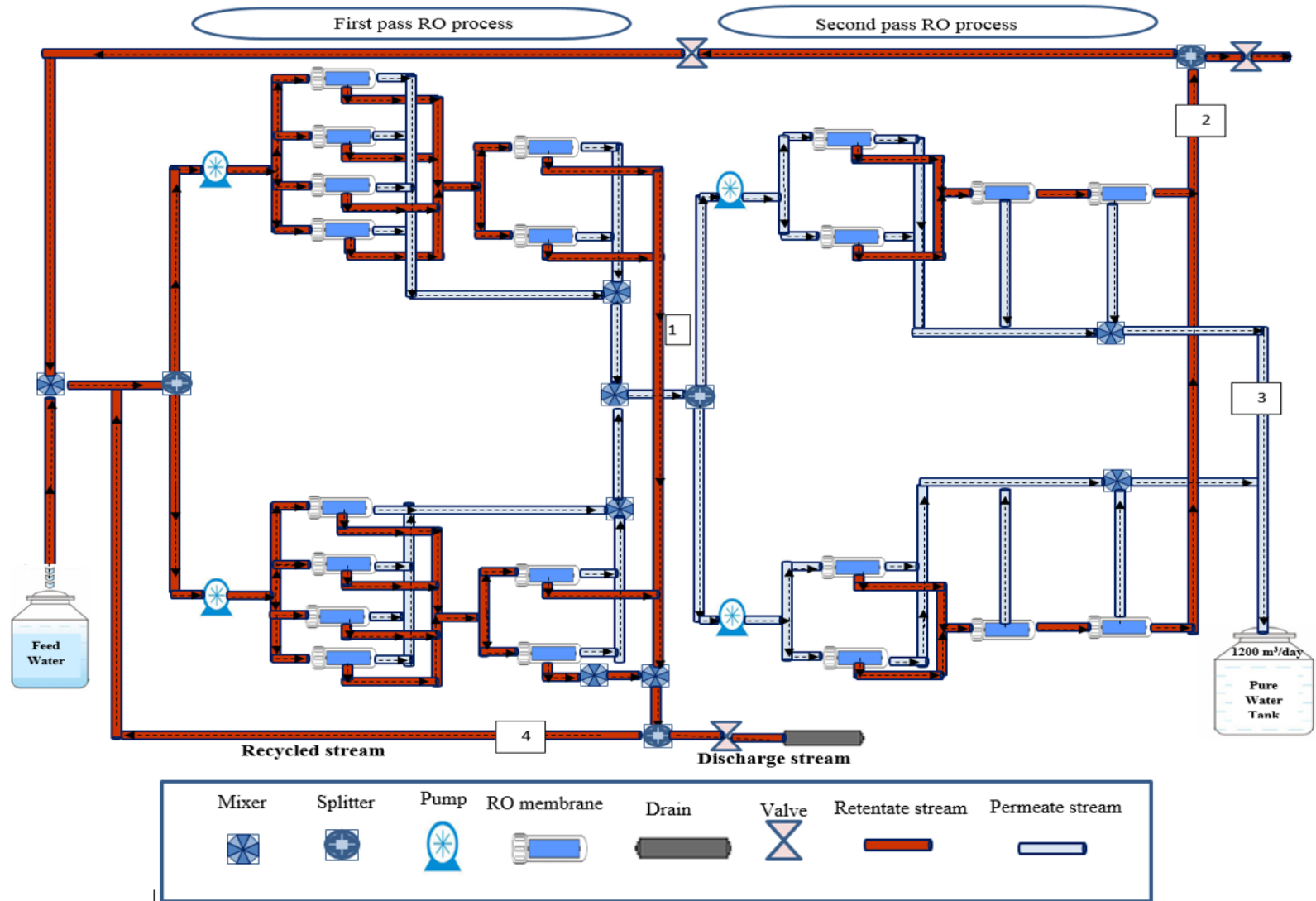


**Fig. 4.6.** Schematic diagram of brackish water RO desalination plant of APC with 1<sup>st</sup> pass retentate recycled mode (Adapted from Al-Obaidi et al., 2018a)

#### ***4.3.2 Impact of retentate recycling scheme of 1<sup>st</sup> pass on the RO process performance***

In this section, the performance of the brackish water RO process of APC plant is examined by varying the 1<sup>st</sup> pass retentate stream recycle percentage from 0% to 100% in a step change of 10%. The process performance indicators include the total plant recovery (Rec), total plant rejection (Rej), product flow rate and concentration (Q<sub>p</sub>, C<sub>p</sub>), retentate flow rate and concentration (Q<sub>r</sub>, C<sub>r</sub>), 1<sup>st</sup> and 2<sup>nd</sup> passes recovery, 1<sup>st</sup> and 2<sup>nd</sup> passes mass transfer coefficient, total energy consumption, and 1<sup>st</sup> pass permeate flow rate. Also, the current simulation is carried out at fixed values of 1098.62 ppm, 74 m<sup>3</sup>/h, 9.22 atm, and 25°C of raw water concentration, feed flow rate, operating pressure, and temperature, respectively.

Fig. 4.6 shows the influence of recycle percentage of the 1<sup>st</sup> pass retentate stream from 0 to 100% on the solute rejection and water recovery. An exponential relationship and a linear relationship represent the solute rejection and total plant recovery, against the increase of in the 1<sup>st</sup> pass retentate stream. Statistically, this is corresponding to a decrease of 0.003%, and an increase of 3% for solute rejection and plant water recovery, respectively. In this regard, it can be said that the optimal value of solute rejection can be attained at 40% of retentate recycled percentage. More importantly, the insignificant increase of plant water recovery can be attributed to an insignificant increase in the total plant permeate flow rate (at fixed raw water flow rate) due to an increase in the retentate recycle percentage of the 1<sup>st</sup> pass. As a result of this, the bulk velocities of all the membrane stages increase that accompanied with a reduction in the residence time of solution inside the feed channel. As a result of this, the bulk velocities of all the membrane stages in the 1<sup>st</sup> pass increases that corresponding to an increase in the concentration polarisation and entirely retard the permeated water through the membranes. Hence, the overall 1<sup>st</sup> pass permeate flow rate is decreased as a response to increasing the retentate recycle percentage of the 1<sup>st</sup> pass of high salinity stream (Table 4.5). However, an incremental increase of water recovery (around 3%) has been occurred due to a continual increase of total permeate flow rate of the 2<sup>nd</sup> pass (around 3%) as the percentage of retentate recycle increases (Table 4.5). This in turn has insignificantly increased the

overall water recovery as noticed in Fig. 4.7. It is also worth noting that any increase in the overall permeate flow rate  $Qp_{(plant)}$  means a lower necessity for energy consumption. Table 4.5 presents statistical values of the total permeate flow rate, total water recovery and energy consumption associated with different recycle percentages of the 1<sup>st</sup> pass.

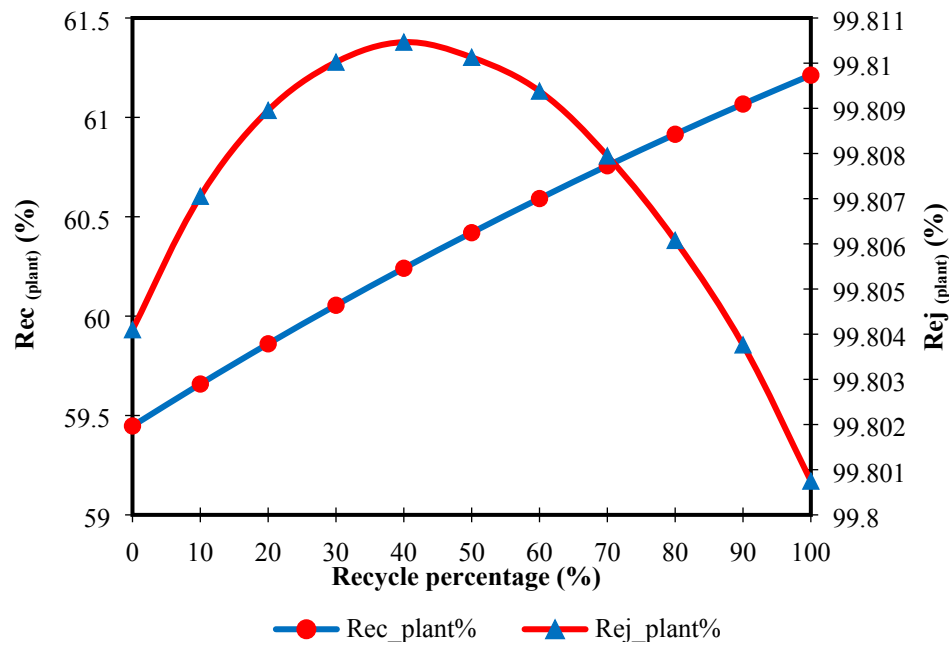


**Fig. 4.7.** Effect of different recycle percentage of the 1<sup>st</sup> pass retentate stream on plant recovery and solute rejection

The impact of increasing the 1<sup>st</sup> pass retentate recycle percentage from 0 to 100% on the plant product and retentate flow rates is shown in Fig. 4.8. It is clear that the product flow rate and retentate flow rate are considerably increased and decreased, respectively. Statistically, this is corresponding to an increase of 2.96% in the product flow rate and a decrease of 45.7% in the retentate flow rate. Increasing of product flow rate is ascribed to the variation of the product flow rate of the 1<sup>st</sup> pass. As illustrated above, increasing the recycle percentage of retentate stream of the 1<sup>st</sup> pass would decrease the total permeate flow rate of the 1<sup>st</sup> pass, which represents the feed flow rate of the 2<sup>nd</sup> pass. This means a lower velocity inside all the modules of the 2<sup>nd</sup> pass that resulted from decreasing the inlet feed flow rate of the 2<sup>nd</sup> pass with increasing the retentate recycled percentage of the 1<sup>st</sup>

pass. Therefore, it can be said that an increase in the total permeate flow rate of the 2<sup>nd</sup> pass is expected due to increasing the residence time of water inside the 2<sup>nd</sup> pass RO process. Relying on this point, this would also be related with a reduced retentate flow rate as noticed in Fig. 4.8 and increased water recovery of the 2<sup>nd</sup> pass. However, the overall water plant recovery keeps a marginal increase due to a high proceed of feed flow rate compared to an equivalent promotion of total product flow rate of the plant as illustrated in Fig. 4.7 and Table 4.5.

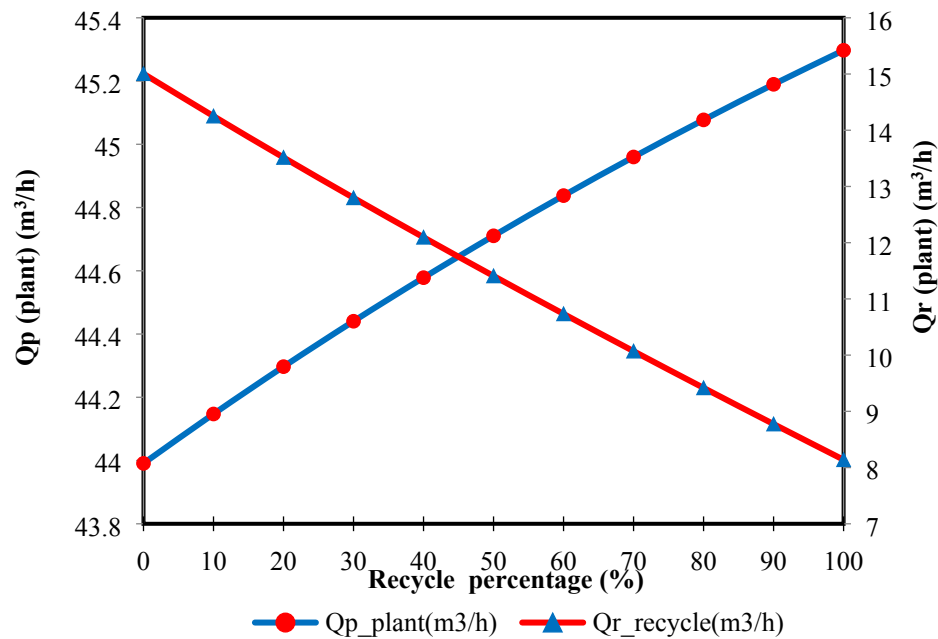


**Fig. 4.8.** Effect of different recycle percentage of the 1<sup>st</sup> pass retentate stream on product and retentate plant flowrate

The simulation results of Fig. 4.9 confirm that increasing of the 1<sup>st</sup> pass recycled retentate percentage from 0 to 100% causes an increase in the product concentration and a significant increase in the retentate concentration. This is specifically coming with 53.5%, and 117.8% of increasing in the product salinity and retentate salinity, respectively. This is attributed to increasing the plant feed water concentration due to increasing the recycle percentage of high salinity retentate stream. Furthermore, these results support the findings of Table 4.5 and Fig. 4.8 that associated with a continuous increase of permeate flow rate of the 2<sup>nd</sup> pass and total water recovery, respectively

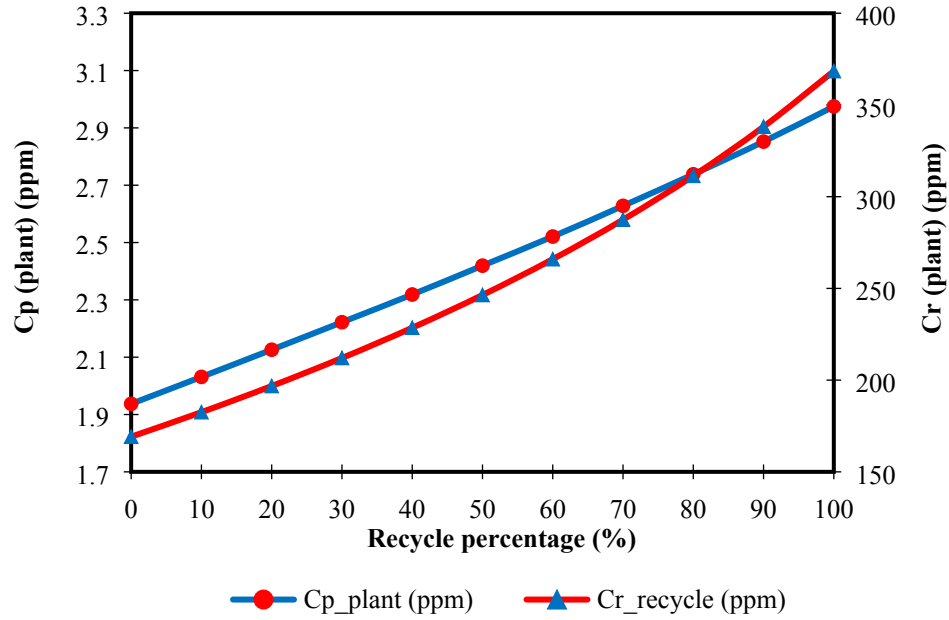


**Fig. 4.9.** Effect of different recycle percentage of the 1st pass retentate stream on product and retentate salinities

The model's predictions for the impact of changing the recycle percentage of the 1<sup>st</sup> pass from 0 to 100% on the water recovery is depicted in Fig. 4.10. This in turn confirmed a reduction of water recovery ratio of the 1<sup>st</sup> pass of around 27.7%. An increase in the plant feed flow rate would possibly explain this. Furthermore, increasing the feed concentration can raise the concentration polarisation that completely reduces the permeated water of each membrane. This also supports the reduction of total water recovery of the 1<sup>st</sup> pass. Consequently, the 1<sup>st</sup> pass permeate flow rate and water recover are dropped as a result of increasing the recycle retentate percentage. In the same aspect, increasing the recycle percentage of the 1<sup>st</sup> pass would increase the water recovery of the 2<sup>nd</sup> pass by about 12%. This is mainly attributed to a reduction of a total feed flow rate of the 2<sup>nd</sup> pass as a result to the growth of the recycle percentage of the 1<sup>st</sup> pass, which causes an insignificant increase of plant water recovery as a result to increasing the permeate flow rate of the 2<sup>nd</sup> pass (Table 4.5).

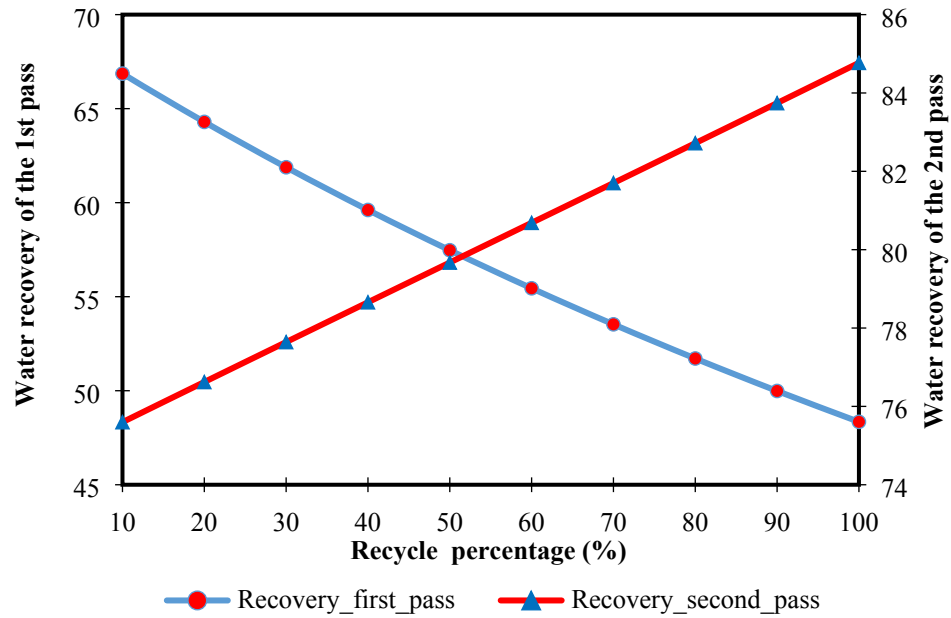


**Fig. 4.10.** Effect of different recycle percentage of the 1st pass retentate stream on the 1st and 2nd passes water recovery

To systematically understand, the transport phenomena inside each membrane in both the 1<sup>st</sup> and 2<sup>nd</sup> passes, it is vital to explore the variation of mass transfer coefficient as a result to increasing the retentate recycle percentage of the 1<sup>st</sup> pass. Basically, the mass transfer coefficient is a measure of water permeation through the membrane that related to the fluid physical properties such as diffusivity and fluid velocity inside the module. The concentration polarisation can be significantly determined by determining the mass transfer coefficient.

It can be seen from Fig. 4.11 that increasing the 1<sup>st</sup> pass retentate recycle percentage from 0 to 100% has a positive impact on the 1<sup>st</sup> pass mass transfer coefficient. Statistically, this is associated with an increase of 13%. This is ascribed to a significant increase of bulk velocity associated with increasing the solute diffusivity because of increasing feed concentration. In other words, the mass transfer coefficient is enhanced due to a higher turbulence in feed channel as a result to increasing the crossflow velocity. However, the quantity of water permeation through the membrane pores of the 1<sup>st</sup> pass has been decreased as a result to increasing the level of concentration polarisation. The retardation of permeate flow rate of the 1<sup>st</sup> pass has already presented in Table 4.5 due to an increase

in the recycle percentage. However, increasing the retentate recycle percentage from 0% to 100% has decreased the mass transfer coefficient of the 2<sup>nd</sup> pass as given in Fig. 4.11. This is specifically causing a reduction of 4.73% in the mass transfer coefficient. Interestingly, the reduction of mass transfer coefficient in the 2<sup>nd</sup> pass can be attributed to a noticeable reduction of permeate flow rate of the 1<sup>st</sup> pass that specifies the feed flow rate of the 2<sup>nd</sup> pass. Therefore, the bulk flow rate of each module in the 2<sup>nd</sup> pass will be decreased that accompany with a reduction of mass transfer coefficient (Fig. 4.11). However, the solution would have more residence time inside each module of the 2<sup>nd</sup> pass that would interpret the increase of permeate flow rate of the 2<sup>nd</sup> pass, as illustrated in Table 4.5.

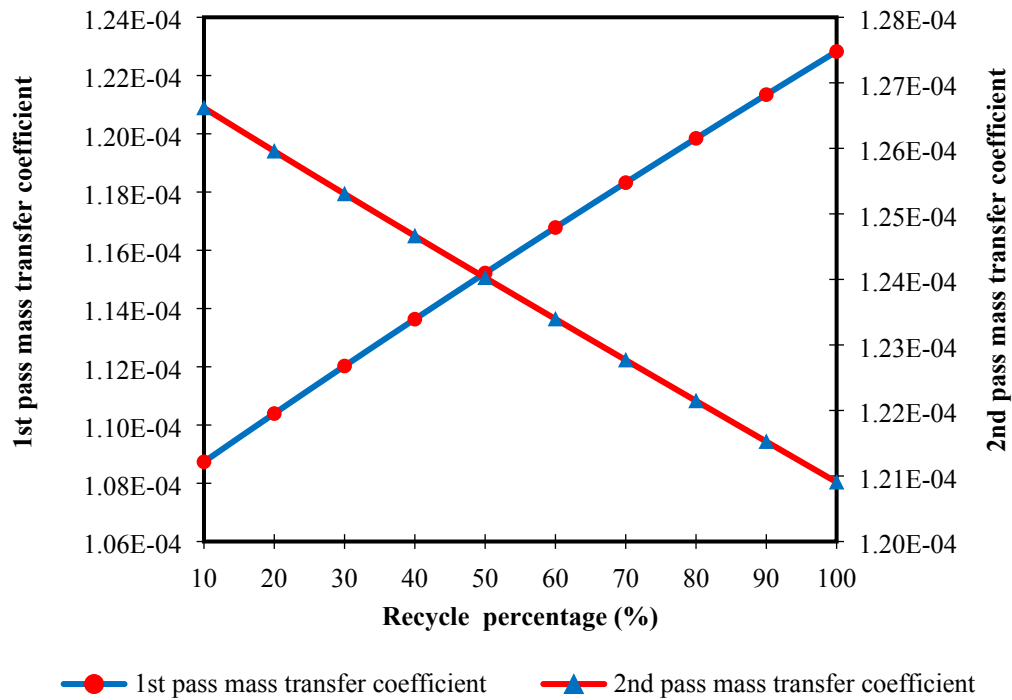


**Fig. 4.11.** Effect of different recycle percentage of the 1st pass retentate stream on the 1st and 2nd passes mass transfer coefficient

It is important to mention that the current simulation is conducted at fixed values of feed flow rate, pressure, temperature, and raw water salinity (Table 4.5). Fig. 4.12 and Table 4.6 depict that the total energy consumption of the plant is increased by 10.7% as a

response to an increase in the retentate recycle percentage of the 1<sup>st</sup> pass from 0% to 100%. Basically, the calculation of energy consumption of RO process of APC of power per cubic meter of fresh water is carried out for the 1<sup>st</sup> pass and 2<sup>nd</sup> pass where the pumps are located. Therefore, it is plausible to expect an increase in energy consumption as a response to an increase in the feed flow rate of the 1<sup>st</sup> pass ( $Q_{f(Raw\ water)} + Q_{r(1st\ pass)} + Q_{r(2nd\ pass)}$ ) despite the reduction of feed flow rate of the 2<sup>nd</sup> pass ( $Q_{f(Block\ 3)}$ ) as a percentage of the recycled stream of the 1<sup>st</sup> pass increases. Seemingly, the increase of the total permeate flow rate ( $Q_{p(plant)}$ ) is not comparable with the increase of feed flow rate of the 1<sup>st</sup> pass that would explain the growth of energy consumption. Occasionally, a marginal enhancement of the product flow rate was noticed due to increasing the retentate recycled percentage of the 1<sup>st</sup> pass (Table 4.5). On the other hand, a continuous increase of feed flow rate of the 1<sup>st</sup> pass has dominated the energy consumption. Statistical results of total energy consumption are embedded in Table 4.6.

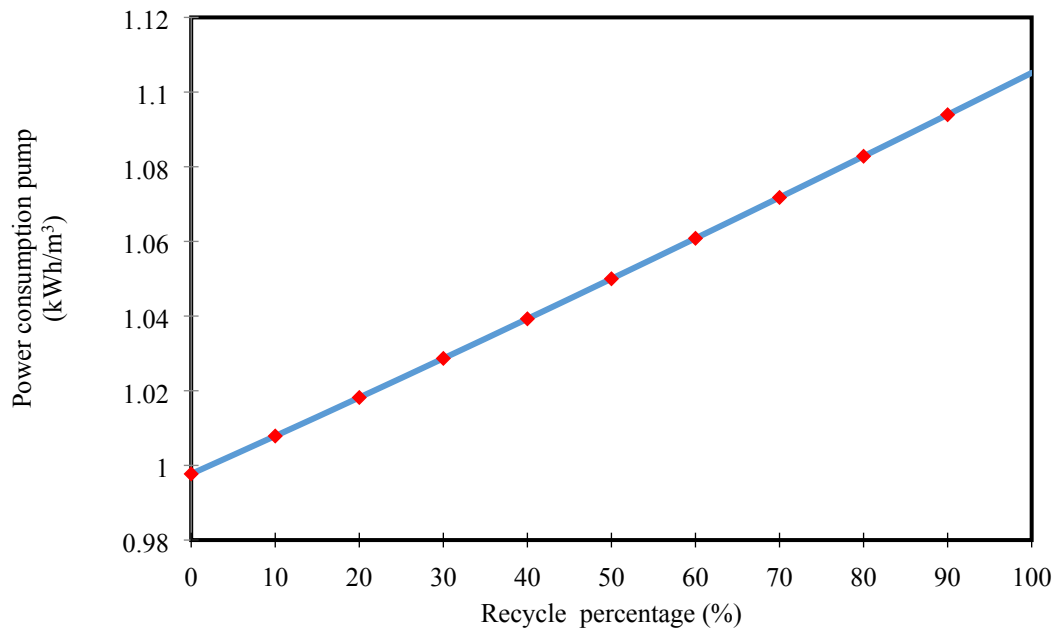


**Fig. 4.12.** Effect of different recycle percentage of the 1<sup>st</sup> pass retentate stream on the total energy consumption

Table 4.5 summarises all the simulation results that associated with the influence of varying the 1<sup>st</sup> pass retentate recycle percentage from 10 to 100% at fixed operating pressure and raw water salinity, raw feed flow rate, and temperature of raw water of 9.22

atm, 1098.62 ppm, 74 m<sup>3</sup>/h, and 25°C, respectively on several operating parameters including the 1<sup>st</sup> pass permeate flow rate, 2<sup>nd</sup> pass permeate flow rate, overall solute rejection and water recovery of the plant, mass transfer coefficient of the 1<sup>st</sup> pass, and mass transfer coefficient of the 2<sup>nd</sup> pass.

Basically, the 1<sup>st</sup> pass permeate flow rate fed to the 2<sup>nd</sup> pass is significantly decreased by about 9.4% as a response to this variation. This can be attributed to an increase in the retentate concentration with increasing the 1<sup>st</sup> pass retentate recycle percentage. Furthermore, increasing the feed salinity has entirely impacted the concentration polarisation, which reduces the permeated water through the membranes. Therefore, the total permeate flow rate of 1<sup>st</sup> pass is decreased dramatically due to increasing the retentate percentage.

**Table 4.5.** The simulation results of several operating conditions and process performance indicators with variable recycle percentage of the 1st pass retentate stream

<b>Recycle percentage</b>	<b>10%</b>	<b>20%</b>	<b>30%</b>	<b>40%</b>	<b>50%</b>
Total Qp of the 1 <sup>st</sup> pass (m <sup>3</sup> /h)	58.39	57.81	57.23	56.67	56.11
Total Qp of the 2 <sup>nd</sup> pass (m <sup>3</sup> /h)	44.147	44.296	44.440	44.578	44.7106
Total solute rejection of the plant (%)	99.80	99.80	99.81	99.82	99.80
Total water recovery of the plant (%)	59.65	56.86	60.05	60.24	60.41
Mass transfer coefficient of the 1 <sup>st</sup> pass (-)	1.09×10 <sup>-4</sup>	1.10×10 <sup>-4</sup>	1.12×10 <sup>-4</sup>	1.14×10 <sup>-4</sup>	1.15×10 <sup>-4</sup>
Mass transfer coefficient of the 2 <sup>nd</sup> pass (-)	1.27×10 <sup>-4</sup>	1.26×10 <sup>-4</sup>	1.25×10 <sup>-4</sup>	1.25×10 <sup>-4</sup>	1.24×10 <sup>-4</sup>
<b>Recycle percentage</b>	<b>60%</b>	<b>70%</b>	<b>80%</b>	<b>90%</b>	<b>100%</b>
Total Qp of the 1 <sup>st</sup> pass (m <sup>3</sup> /h)	55.57	55.03	54.49	53.96	53.44
Total Qp of the 2 <sup>nd</sup> pass (m <sup>3</sup> /h)	44.837	44.959	45.077	45.189	45.297
Total solute rejection of the plant (%)	99.80	99.80	99.80	99.80	99.80
Total water recovery of the plant (%)	60.591	60.756	60.915	61.07	61.21
Mass transfer coefficient of the 1 <sup>st</sup> pass (-)	1.17×10 <sup>-4</sup>	1.18×10 <sup>-4</sup>	1.20×10 <sup>-4</sup>	1.21×10 <sup>-4</sup>	1.23×10 <sup>-4</sup>
Mass transfer coefficient of the 2 <sup>nd</sup> pass (-)	1.23×10 <sup>-4</sup>	1.23×10 <sup>-4</sup>	1.22×10 <sup>-4</sup>	1.22×10 <sup>-4</sup>	1.21×10 <sup>-4</sup>

To comprehend the performance of multistage RO process with no recycle mode (0% retentate percentage), Table 4.6 presents the simulation results of several performance indicators with 40%, 100%, and without recycling mode for comparison purposes. Precisely, it can be noticed that no recycle mode (0%) can keep the process at the lowest

product concentration and lowest water recovery that corresponding with the lowest energy consumption. However, the highest overall product flow rate has been attained at 100% retentate recycle of the 1<sup>st</sup> pass, which involved a slight increase in product concentration from 1.937 to 2.974 ppm at the same operating conditions. Interestingly, the enhancement of the productivity of fresh water accompanied an increase of energy consumption by around 11% within almost fixed solute rejection. Up to the authors' knowledge, increasing the product flow rate for such RO desalination plant of APC by 3% will be profitable for the long-time of operation that needs to be applied in the original RO process design. Moreover, the improvement of energy consumption can be enlarged via the use of more-efficient pumps as the current pump efficiency was 85%.

**Table 4.6.** Simulation results of process performance indicators with 0% (without recycle mode), 40% and 100% percentages of retentate recycle

Without recycle mode (APC plant)		With recycle mode		With recycle mode	
Performance indicators of RO process at recycle percentage from 1 <sup>st</sup> pass = 0 %		Performance indicators of RO process performance at recycle percentage from 1 <sup>st</sup> pass = 40 %		Performance indicators of RO process performance at recycle percentage from 1 <sup>st</sup> pass = 100 %	
Rej_plant (%)	99.804	Rej_plant (%)	99.811	Rej_plant (%)	99.801
Rec_plant (%)	59.447	Rec_plant (%)	60.241	Rec_plant (%)	61.213
Q <sub>p(plant)</sub> (m <sup>3</sup> /h)	43.991	Q <sub>p(plant)</sub> (m <sup>3</sup> /h)	44.578	Q <sub>p(plant)</sub> (m <sup>3</sup> /h)	45.297
Q <sub>r_recycle</sub> from the 2 <sup>nd</sup> pass (m <sup>3</sup> /h)	15.005	Q <sub>r_recycle</sub> from the 2 <sup>nd</sup> pass (m <sup>3</sup> /h)	12.095	Q <sub>r_recycle</sub> from the 2 <sup>nd</sup> pass (m <sup>3</sup> /h)	8.139
C <sub>p_plant</sub> (ppm)	1.937	C <sub>p_plant</sub> (ppm)	2.319	C <sub>p_plant</sub> (ppm)	2.975
Cr_recycle of the 2 <sup>nd</sup> pass (ppm)	169.159	Cr_recycle of the 2 <sup>nd</sup> pass (ppm)	228.545	Cr_recycle of the 2 <sup>nd</sup> pass (ppm)	368.465
Power consumption pump (kWh/m <sup>3</sup> )	0.997	Power consumption pump (kWh/m <sup>3</sup> )	1.039	Power consumption pump (kWh/m <sup>3</sup> )	1.105

#### **4.4 Evaluation of retentate recycle mode on the performance of simple and complicated designs of brackish water RO desalination process**

A simple comparison of the simulation results presented in Table 4.4 and 4.5 confirms that the retentate mode in the simple design of brackish water multistage RO desalination process has a marginal contribution where almost all the process responses have not considerably affected. However, applying of retentate mode in the complicated design of brackish water multistage multi pass RO process of APC has entailed with an enhancement of the productivity of fresh water by around 3% in the case of recycling the retentate by 100% compared to no recycle mode. However, the penalty of this improvement is associated with an increase of specific energy consumption by more than 10%. Therefore, it can be stated that the retentate recycle mode is not a feasible option especially for the multistage retentate reprocessing design with a bit increase of productivity for the complicated design.

#### **4.5 Conclusions**

In this chapter, the viability of retentate recycle mode was tested on different sizes of simple and complicated brackish water RO systems. This in turn enabled to investigate the influence of retentate recycle at variable percentages on the performance indicators of the selected RO systems. The simulations have explored the variation of several performance indicators against the variation of input parameters. The simple brackish water RO system characterised by retentate reprocessing design while the complicated brackish water RO system characterised by retentate and permeate reprocessing designs of multistage multi pass RO system of APC. Moreover, each simulation has considered fixed feed flow rate, salinity, pressure, and temperature. The simulations of the simple and complicated RO systems were conducted using the model developed in Chapter 3.

The simulation results of the simple design highlighted the possibility of improving the product salinity due to applying 100% retentate recycle mode. Also, applying 100% retentate recycle mode would not significantly affect the solute rejection and necessitates 10% increase in the specific energy consumption if compared to no recycle mode.

The simulation of the complicated RO system of APC concluded that an implementing of a 100% recycle percentage can result in an increase in the production capacity (although with increased salinity of the product water and energy consumption) around 3% compared to 0% of no recycle mode that is currently used in the RO process of APC plant. Interestingly, increasing the 1<sup>st</sup> pass recycle percentage from 0% to 100% has increased the 1<sup>st</sup> pass mass transfer coefficient of 13%, which has a positive impact on the quantity of permeated water. Also, an increase of permeate flowrate of the 2<sup>nd</sup> pass by 7% has been deduced as a result to increase the residence time of water inside the 2<sup>nd</sup> pass RO modules. This also associated with an inconsiderable increase of the product water salinity of 2.975 ppm, which is still much below the recommended drinking water salinity limit of ~200 ppm set by various countries of the world. Clearly, the above results would plausibly confirm the insignificant progress of freshwater productivity of 3% and therefore the author would attempt different methodologies to raise the productivity at lower energy consumption and attaining similar product salinity. These attempts will be thoroughly discussed in the next chapters.

## **CHAPTER FIVE**

### **Evaluation and Minimisation of Energy Consumption of Reverse Osmosis Brackish Water Desalination Plant**

#### **5.1 Introduction**

Brackish water desalination is a well-known technology used to separate feed salinity water into low salinity water and concentrated brine. Basically, this technology requires vast quantities of energy, which is a function of incoming saline water parameters including the salinity, flow rate, pressure, and temperature (Wei and McGovern, 2017). In this respect, The RO process is one of the most common industrial applications deployed to produce reuse water from wastewater (Al-Obaidi et al., 2017a) and fresh water from brackish water resource (Anqi et al., 2015). This is economically and technically feasible due to recent improvements of RO membranes (Zhu et al., 2010). This in turn has resulted in a distinctive decrease in the total energy consumption compared to the other common technologies (e.g., thermal process of Multi Stage Flash) (Oh et al., 2009). It is noteworthy to know that the seawater RO process entails between 2 to 5 kWh/m<sup>3</sup> of power consumption based on the feed characteristics (Xevgenos et al., 2016). However, the total energy consumption of the BWRO process, which comprises the electrical energy consumption, ranges between 1.5 and 2.5 kWh/m<sup>3</sup> (Azevedo, 2014). In general, the downgrading in energy consumption of RO water desalination plants has been ongoing since the 1960s due to the development of energy recovery devices (ERDs). However, the research of mitigating the total energy consumption of RO desalination is still valid by investigating other feasible options, especially for medium and large size RO desalination plants (Pérez-González et al., 2012). In this regard, there are several designs that have been considered to decrease the energy consumption of water desalination plants besides suggesting further process improvements. For instance, Sassi and Mujtaba (2011) utilised a non-linear optimisation problem to minimise the specific energy consumption (SEC) of three-stages RO process at a fixed high-quality freshwater flow rate based on optimising the operating and design parameters. This in turn entailed a reduction of 20% in total energy consumption compared to the original process design. Also, Koutsou et al. (2015)

investigated the effect of alternative designs of RO process including membrane sheet number/width and feed-spacer geometry on the SEC at fixed recovery ratio. More importantly, the addition of ERD to the RO process has been conveyed by several researchers such as Al-Zahrani et al. (2012). This is evidenced by investigating the impact of different ERD efficiencies on energy consumption of seawater and brackish water RO desalination processes. However, it is necessary to run the RO process at high operating pressures to overcome the trans-membrane osmotic pressure that would significantly increase the pumping power. Moreover, the RO process performance in term of the water recovery and consuming energy is highly sensitive to several operating parameters as presented in many of steady-state and dynamic RO simulation and optimisation attempts (Villafafila and Mujtaba, 2003; Qi et al., 2012; Zhao et al., 2013; Al-Obaidi et al., 2017b, 2018a). For instance, Villafafila and Mujtaba (2003) implemented ERDs, and pressure exchangers in the optimisation target. Overall, they confirmed that the energy consumption could be dropped by more than half by implementing these devices on the plants. This improvement is mainly due to the fact that the energy can be absorbed from the high-pressure high-concentration retentate stream and deliver it efficiently to the raw water (Anderson et al., 2009). Basically, this is a surplus energy that can be regained by the ERD from the high salinity stream (brine stream) (Anderson et al., 2009; Al-Zahrani et al., 2012). Accordingly, the energy consumption can be considered as the most effective contributor to the total fresh water production cost of RO system (Geraldes et al., 2005; Qi et al., 2012; Mazlan et al., 2016a). Therefore, any reduction of energy consumption would afford a primitive effect on reducing the total fresh water production cost of RO process (Koroneos et al., 2007).

Several successful examples of reducing the total energy consumption in seawater and brackish water RO desalination process can be found in the open literature. To systematically realised the progress of reducing the energy consumption of the RO system, Table 5.1 demonstrates several examples of published studies that covered the mitigation of total energy consumption with explicitly highlighting the most advantages and disadvantages.

**Table 5.1.** Summary of studies on the energy consumption of RO process

No.	Author and year	Principle of the study	Features and advantages	Results	Shortcoming
1	Farooque (2008)	The specific energy consumption, percentage of energy saving, the efficiency of ERD and percentage of throttle loss are estimated using fundamental equations.	The influence of ERDs on the energy consumption of several seawater RO plants was investigated.	A max. energy saving of 27% can be achieved based on the max. power consumption of the high-pressure pump of 7.93 kWh/m <sup>3</sup> .	The influence of feed flow rate on the total energy consumption was not specifically analysed.
2	Sharif et al. (2009)	Presented an analytical method to estimate the specific energy consumption.	The influence of operating conditions and membrane area and water transport parameter on the energy consumption of seawater RO process was analysed.	The minimum specific energy consumption can be achieved at water recovery of 70% for a given feed salinity and membrane permeate flow rate of less than 2 m <sup>3</sup> /h.	The impact of several operating conditions on the energy consumption was not critically studied.
3	Li (2010)	Development of a constrained nonlinear optimisation framework.	Analyse the energy consumptions of three RO modules; a single stage, two stages, and a single stage with an ERD were optimised.	Increasing the number of stages as well as applying an ERD would enhance the reduction of energy consumption.	The calculations were specifically carried out at fixed retentate pressure.
4	Qi et al. (2012)	Development of a model for single and two-stages RO process considering the concentration polarisation issue.	The influence of operating conditions, ERD and pump efficiencies on the specific energy consumption was studied.	The optimised water recovery shifts to lower values because of the existence of ERDs.	The impact of operating conditions such as feed flow rate and temperature on the total energy consumption was not investigated.
5	El-Ghonymy (2012)	A primitive model equation was used to estimate the specific power consumption and total water recovery.	The performance of two-stage RO seawater desalination plant with two different ERDs on the energy consumption was analysed.	An energy saving between 41% to 42% was achievable for all the trains in the first stage due to the use of an ERD.	The impact of several operating conditions on the specific energy consumption was not analysed.
6	Kim et al. (2013)	Simple model equations were used to calculate the energy transfer efficiency, and specific energy consumption.	One centrifugal ERD and two isobaric ERDs (pressure exchanger and pressure exchanger for energy recovery were installed to an actual seawater RO plant of 1000 m <sup>3</sup> /day	Isobaric ERDs have higher efficiency than the centrifugal ERD.	Short-term experiments were carried out to recognise the performance of ERD system.

			and the energy consumption was assessed under various conditions.		
7	Wei et al. (2017)	A mass-balance model was presented to calculate the performance of RO system.	An optimal design and operation of a two-stage RO system were achieved and compared to a single-stage system with attaining a lower bound for the energy savings.	The highest energy savings are achieved with a two-stage RO system that has optimal configuration and pressure.	The model assumed perfect salt rejection. Also, the pressure dependence of density and osmotic pressure were ignored.
8	This work	Investigating the advantages of adding an ERD to simple and complicated designs of RO brackish water desalination systems.	The addition of an ERD causes a reduction of the specific energy consumption.	The specific energy consumption reduced by 47%-53.8% for the complicated design of RO process compared to the one calculated for the original design without an energy recovery device.	The importance of adding a booster pump in the simple design of RO system has not been explored.

This chapter intends to explore the viability of adding an energy recovery device (ERD) at different efficiencies to small and large sizes of RO brackish water desalination plants. Therefore, two case studies of multistage RO systems with and without an ERD will be presented and the associated water recovery and specific energy consumption will be thoroughly detailed.

The direction of travel of this research was to conduct a major advance in the multistage RO design of brackish water RO systems to elucidate an economically viable separation process.

## **5.2 Model development**

The model developed in Chapter 3 has successfully predicted the performance indicators of different sizes of multistage spiral wound RO process based on the philosophies of the solution diffusion model. Interestingly, the model developed considered the existence of concentration polarisation and signifies the impact of feed spacer on the pressure drop along the feed channel. The detailed equations of the model developed are given in Chapter 3.

The performance of any desalination process can be characterised based on evaluating one of the most significant parameters, i.e. the specific energy consumption (Semiat, 2008). Therefore, the model of Chapter 3 is currently modified by including energy consumption correlations. Furthermore, it is highly recommended to quantify the consequence of the variation of operating parameters on the total energy consumption and plant water recovery with and without the presence of an ERD. Therefore, the interest of this research has been directed to weight the possibility of decreasing the total energy consumption by investigating the impact of adding an ERD at different efficiencies and simulating the multistage RO process at a wide range of inlet conditions. Generally, the ERD and pump efficiencies are addressed as the two particular areas that can be employed to decrease the specific energy consumption for any RO desalination plant. The details of the three new equations added to the model developed in chapter 3 and specifically used to evaluate the total energy consumption of the whole plant are as follows.

The specific energy consumption of the high-pressure pump  $E_{HPP}$  (kWh/m<sup>3</sup>) is evaluated using Eq. (5.1) developed by Qi et al. (2012).

$$E_{HPP} = \frac{\frac{((P_{f(plant)}) \times 101325) (Q_{f(plant)})}{(Q_{p(plant)} \epsilon_{HP \text{ pump}})}}{36 \times 10^5} \quad (5.1)$$

$P_{f(plant)}$  is the operating feed pressure (atm),  $Q_{f(plant)}$  is the applied feed flow rate ( $m^3/s$ ),  $Q_{p(plant)}$  is the total flow rate ( $m^3/s$ ), and  $\epsilon_{HP \text{ pump}}$  is the high-pressure pump efficiency (dimensionless).

However, the specific energy consumption of RO system with the existence of an ERD (consists of a high-pressure pump (HPP), and an ERD) ( $E_{plant}$ ) ( $kWh/m^3$ ) is calculated using Eq. (5.2). It should be noted that one of the most important characteristics of an ERD is the recovery of energy from the high-concentration stream (retentate) to the inlet feed stream via the pressure exchangers. In this regard, the subtraction of the consumed energy of the pumps and the recovered energy by the ERD presents the net energy consumption per  $m^3$  of permeate of the RO process using an ERD.

$$E_{plant} = \frac{\frac{((P_{f(plant)}) \times 101325 \times) (Q_{f(plant)})}{(Q_{p(plant)} \epsilon_{HP \text{ pump}})} - \frac{((P_{r(stage \ 1)}) \times 101325 \times) (Q_{r(stage \ 1)}) (\epsilon_{ERD})}{(Q_{p(plant)})}}{36 \times 10^5} \quad (5.2)$$

$P_{r(stage \ 1)}$  is the retentate pressure of the first stage (atm),  $Q_{r(stage \ 1)}$  is the retentate flow rate for the first stage ( $m^3/s$ ), and  $\epsilon_{ERD}$  is the energy recovery device efficiency (dimensionless).

Furthermore, in case of using a booster pump (BP) after the ERD to systematically raise the pressure of the nominated stream same as the plant feed pressure, Eq. (5.3) can be used to calculate the specific energy consumption of the whole plant.

$$E_{plant} = \frac{\frac{((P_{f(plant)}) \times 101325 \times) (Q_{f(plant)})}{(Q_{p(plant)} \epsilon_{HP \text{ pump}})} + \frac{((P_{(B \text{ pump})}) \times 101325 \times) (Q_{f(stage \ 2)})}{(Q_{p(plant)} \epsilon_{B \text{ pump}})} - \frac{((P_{r(stage \ 1)}) \times 101325 \times) (Q_{r(stage \ 1)}) (\epsilon_{ERD})}{(Q_{p(plant)})}}{36 \times 10^5} \quad (5.3)$$

$P_{(B \text{ pump})}$  is the outlet booster pump pressure (atm),  $Q_{f(stage \ 2)}$  is the inlet feed flow rate of the second stage ( $m^3/s$ ),  $\epsilon_{B \text{ pump}}$  is the booster pump efficiency (dimensionless),

Hence, the outlet pressure of the ERD can be estimated based on the retentate pressure and the ERD efficiency, as highlighted in Eq. (5.4).

$$\epsilon_{ERD} = \frac{P_{out(ERD)}}{P_{out(Module)}} \quad (5.4)$$

$P_{out(ERD)}$  (atm) is the outlet pressure of the ERD and  $P_{out(MODULE)}$  (atm) is the retentate pressure of the membrane module. However, the booster pump pressure ( $P_{(BP)}$ ) (atm) can be obtained by Eq. (5.4).

$$P_{(BP)} = P_{f(plant)} - (P_{r_{stage 1}} \epsilon_{ERD}) \quad (5.5)$$

### 5.3 Case Study 1: Minimisation of energy consumption of a simple RO brackish water desalination plant

#### 5.3.1 Description of a simple RO brackish water desalination plant with an ERD

The full description of the original simple RO system was introduced in Chapter 3. The modified system with an ERD is schematically presented in Fig. 5.1. The importance of an ERD is to absorb the surplus energy from the brine stream of the first stage and deliver it to the low pressure permeate of the first stage. This in turn aids to further treating the permeate of the first stage in the second stage. Occasionally, the retentate of the first and third stages are blended to form the main brine stream. However, the permeate of the second and third stages are blended to form the main permeate stream.

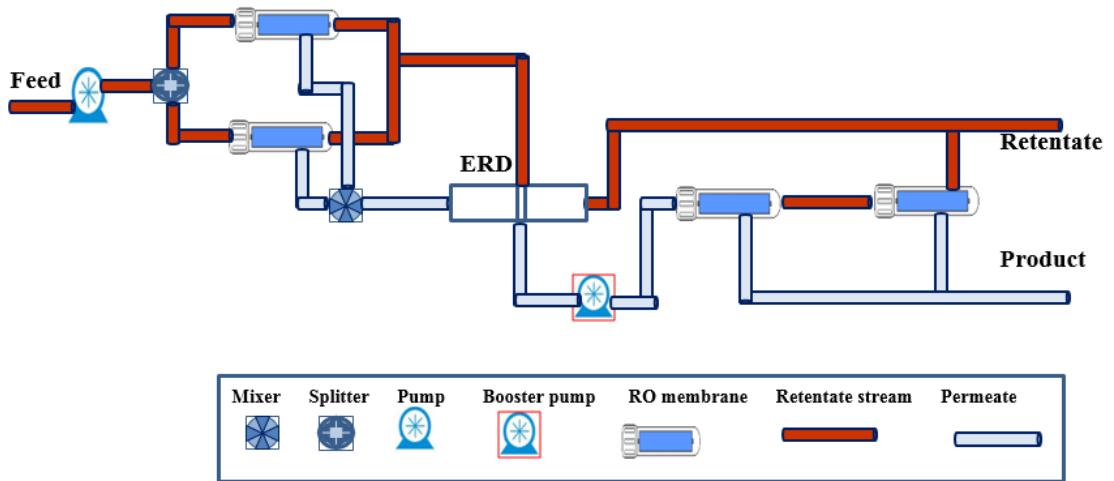


**Fig. 5.1.** Schematic diagram of multistage, multi pass simple BWRO desalination plant with adding of an ERD

### ***5.3.2 Process simulation: Impact of operating parameters of a simple multistage RO system***

In this section, the evaluation of specific energy consumption and plant water recovery of a simple design of brackish water RO system (Fig. 5.1) is carried out. Occasionally, these parameters are identified as the most important performance indicators that determine the feasibility of any industrial process. To systematically carry out this evaluation, the performance indicators are assessed with considering a wide range of operating feed flow rate, pressure, and temperature at three different ERD efficiencies of 80%, 85%, and 90%. Therefore, a variation of 20% in the inlet feed flow parameters of the RO system is selected. However, the inlet feed salinity of 2540 ppm is kept constant. The full details of each simulation and the gained results are discussed in the following sections. It is also important to mention that the model developed in Chapter 3 has been utilised to carry out the simulation of two case studies of simple and complicated designs of brackish water RO systems and upgraded by including the calculations of energy consumption with and without an ERD.

#### ***5.3.2.1 Impact of operating feed flow rate***

The influence of changing feed flow rate ( $Q_f$  plant) from 20.4 to 24.48 m<sup>3</sup>/h, at fixed feed salinity, pressure, and temperature of 2540 ppm, 12.04 atm, and 28.8 °C, respectively, on the specific energy consumption and water recovery with and without an ERD at different efficiencies is investigated in this section. Fig. 5.2 shows a maximum water recovery of 56.01% that can be achieved at the lowest feed flow rate of 20.4 m<sup>3</sup>/h and attains the lowest specific energy consumption of 1.897 kWh/m<sup>3</sup> without an ERD. Occasionally, lower feed flow rate means lower pressure drop along the feed channels of the membranes that permits higher water permeation through the membranes due to a higher time of residence inside the modules. On the other hand, adding an ERD would positively contribute the reduction of specific energy consumption. This is clearly noticed in Fig. 5.2. In addition, increasing the ERD efficiency from 80% to 85% and then to 90% would further reduce the specific energy consumption. Statistically, the reductions of 59.8%, 63.5%, and 67.2% in the specific energy consumption are registered for the addition of an ERD of 80%, 85%, and 90%, respectively at feed flow rate of 20.4 m<sup>3</sup>/h. Also, at feed

flow rate of 24.48 m<sup>3</sup>/h, the obtained reductions of specific energy consumption are 61.4%, 65.2%, and 69.1% for 80%, 85%, and 90%, respectively. Thus, it is fair to claim that adding as ERD would certainly reduce the specific energy consumption of the RO process.

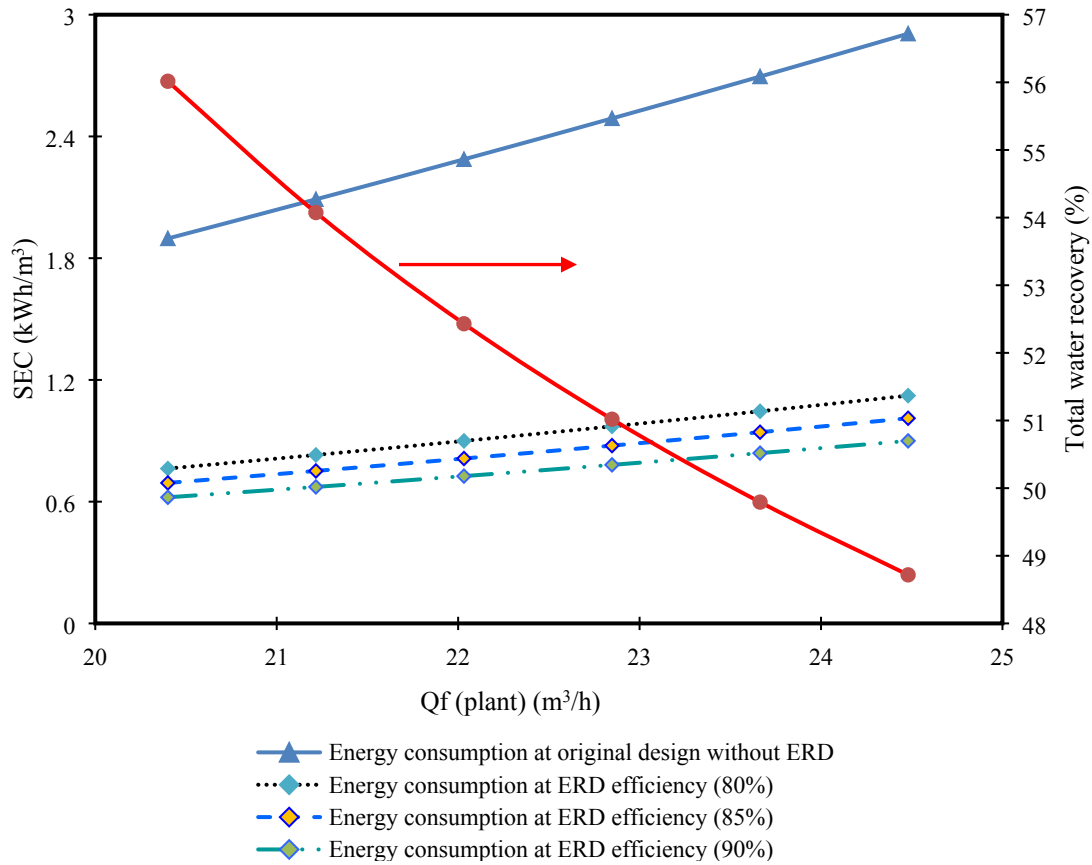


**Fig. 5.2.** Specific energy consumption and total water recovery of a small brackish water RO desalination plant with and without an ERD (at different efficiencies) against plant feed flow rate

### 5.3.2.2 Impact of operating feed pressure

The influence of feed pressure ( $P_{f(\text{plant})}$ ) on the performance indicators including the total water recovery and energy consumption of RO system has been studied by several researchers such as Avlonitis et al. (2003) and Dimitriou et al. (2015). Basically, the pressure is one of the most affected parameters on delivering high water permeation rate and high-quality water (Wei and McGovern, 2017; Karabelas et al., 2018).

Fig. 5.3 indicates that both water recovery and specific energy consumption are linearly related to feed pressure as it increases from 12.04 atm to 14.448 atm at fixed feed salinity,

flow rate, and temperature of 2540 ppm, 20.4 m<sup>3</sup>/h, and 28.8 °C, respectively. It can be stated that increasing feed pressure would positively increase the water recovery due to increasing the productivity at fixed feed flow rate. Therefore, the maximum water recovery of 58.31% is registered at the maximum tested feed pressure of 14.448 atm. Also, it can be stated that the maximum water recovery has gained the lowest specific energy consumption. Statistically, 14.448 atm of feed pressure causes the lowest specific energy consumption of 1.846 kWh/m<sup>3</sup> without an ERD. Interestingly, further reduction of specific energy consumption can be obtained as a result to adding an ERD where the maximum reduction can be attained with using the highest efficiency of an ERD and the reverse is correct. The reductions of 59.8 %, 63.5 %, and 67.2% in the specific energy consumption are registered for the addition of an ERD of 80%, 85%, and 90%, respectively at feed pressure of 12.04 atm. Also, at feed pressure of 14.448 atm, the obtained reductions of specific energy consumption are 59.1 %, 62.8 %, and 66.4% for 80%, 85%, and 90%, respectively. Overall, using 90% ERD can obtain promising reduction of specific energy consumption compared to 80% ERD.

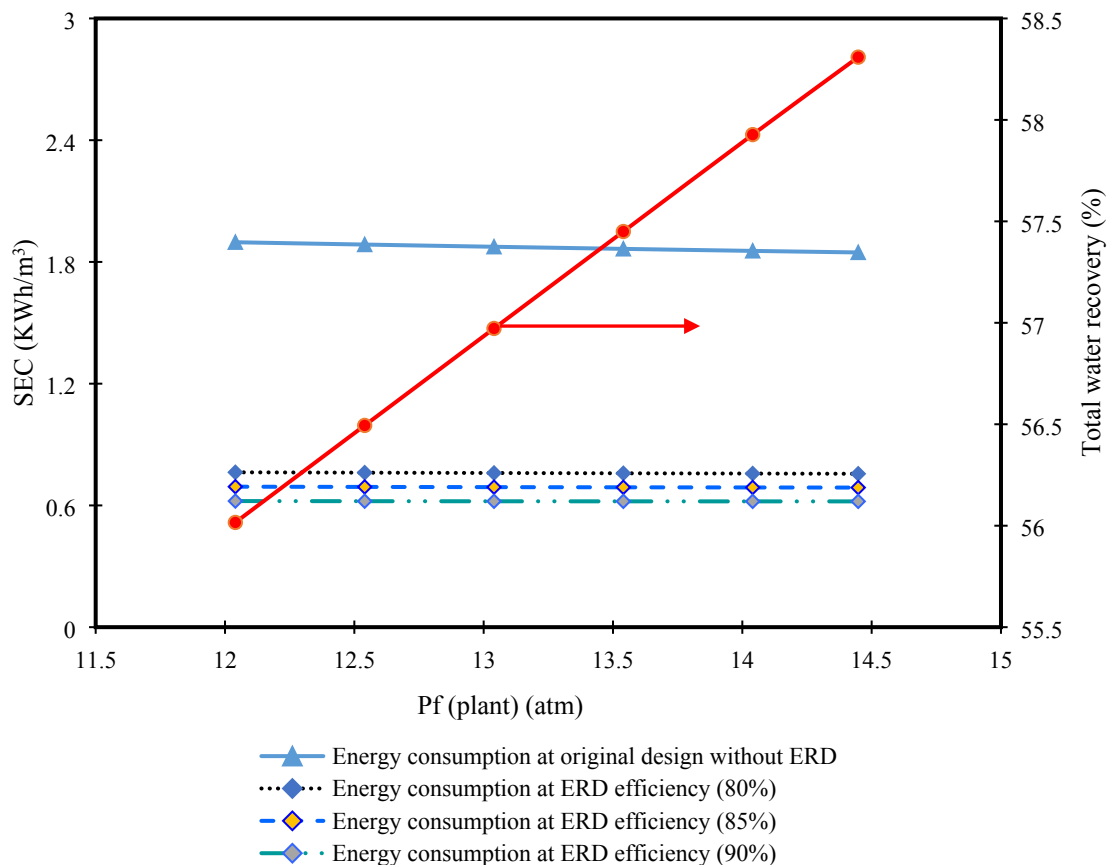


**Fig. 5.3.** Specific energy consumption and total water recovery of a small brackish water RO desalination plant with and without an ERD (at different efficiencies) against plant pressure

### 5.3.2.3 Impact of feed temperature

The influence of varying feed temperature by 20% from 28.8 °C to 34.56 °C on the water recovery and specific energy consumption of a small scale RO system (Fig. 5.1) at fixed values of feed salinity, pressure, flow rate of 2540 ppm, 12.04 atm, and 20.4 m<sup>3</sup>/h is illustrated in Fig. 5.4. In this regard, the maximum water recovery of 56.07% is obtained at the maximum feed temperature of 34.56 °C, which accompanied to the lowest specific energy consumption of 1.891 kWh/m<sup>3</sup> without an ERD. The reduction of specific energy consumption with the increase of temperature can be attributed to the increase in water productivity. Basically, increasing temperature would reduce the density and viscosity of the solution and therefore increases the mobility and water flux through the membrane pores. Furthermore, the addition of an ERD to the RO system causes a considerable

reduction of specific energy consumption. This reduction is increased with the increase in the ERD efficiency from 80% to 90%.

The reductions of 59.8 %, 63.5%, and 67.2% in the specific energy consumption are registered for the addition of an ERD of 80%, 85%, and 90%, respectively at feed temperature of 28.8 °C. Also, at feed temperature of 34.56 °C, the obtained reductions of specific energy consumption are 59.8%, 63.5%, and 67.2% for 80%, 85%, and 90%, respectively. overall, it can be noted that the lowest specific energy consumption of 0.619 kWh/m<sup>3</sup> can be obtained at the maximum tested temperature of 34.56 °C with the use of 90% efficiency of an ERD.

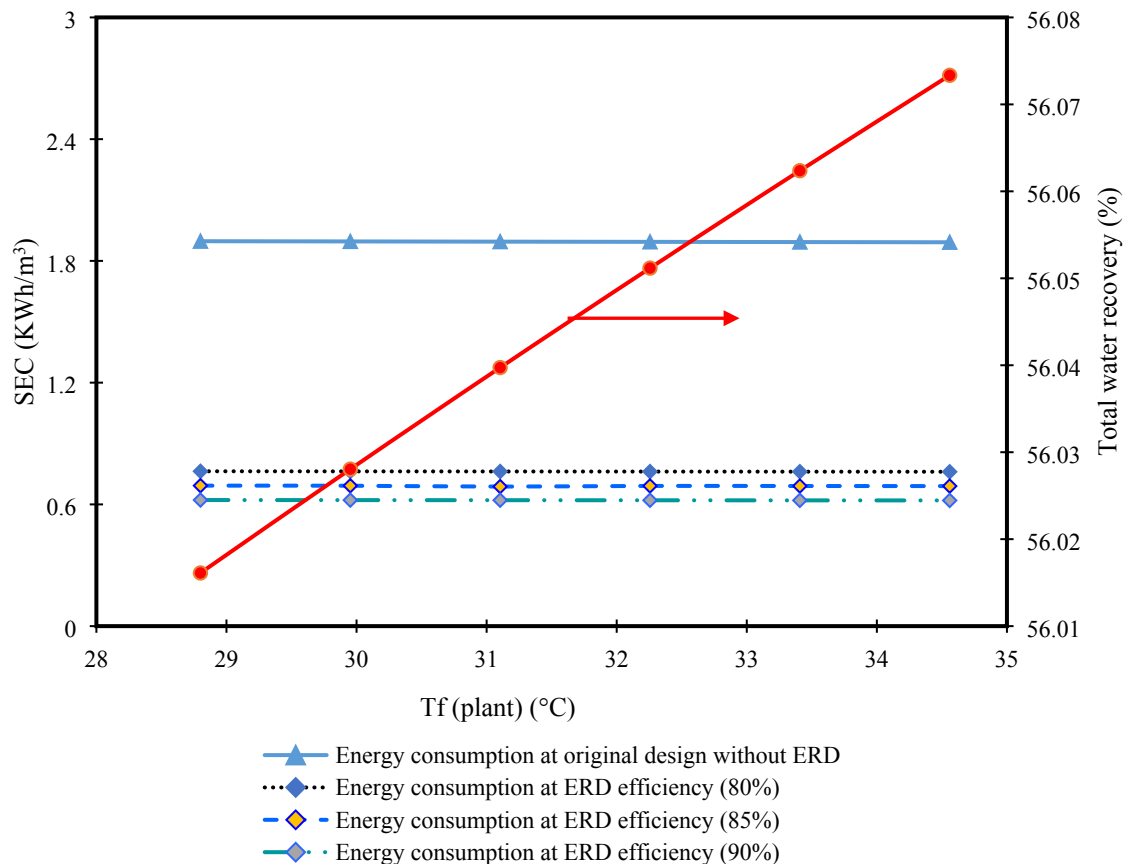


**Fig. 5.4.** Specific energy consumption and total water recovery of a small brackish water RO desalination plant with and without an ERD (at different efficiencies) against plant temperature

## **5.4 Case Study 2: Minimisation of energy consumption of a complicated RO brackish water desalination plant of APC**

The idea of employing an ERD at different efficiencies in the original design of RO system of Arab Potash Company (APC) constitutes the main target of this section. Also, it is fair to expect that the drop in energy consumption can be improved at high efficiencies of the ERD. This fact is clearly presented in the simulation results of the small-scale RO system (Fig. 5.1). To the best of the author's knowledge, the sensitivity analysis of the total plant water recovery and specific energy consumption with and without an ERD and also towards the variation of operating conditions (the feed flow rate, pressure and temperature) of a medium-sized industrial brackish water multistage multi-pass RO desalination plant of the Arab Potash Company APC has not been carried out. Mostly, it is hard to find comprehensive research in the open literature that discussed the influence of operating condition on the specific energy consumption of multistage multi-pass RO process. Therefore, in this section, a thorough analysis of the energy consumption and total water recovery of the RO process via simulation is carried out.

### ***5.4.1 Description of the complicated design of multistage brackish water RO desalination plant of APC with an ERD***

The full description of the original RO system of APC was introduced in Chapter 3. It is noteworthy to mention that a new design modification is employed in the current study by adding an ERD and booster pump after the first pass, as shown in the subfigure of Fig. 5.5. This also excluded the second high-pressure pump of the 2<sup>nd</sup> pass. The addition of an ERD is attributed to the possibility of reusing the hydraulic energy in the brine stream of the 1<sup>st</sup> pass of multistage RO plant, which has been already sent to the drainage system. This stream has a relative medium pressure of around 8.6 atm, that can be successfully transferred to low-pressure permeate stream of the 1<sup>st</sup> pass (1 atm). In other words, this research intends to recover the energy from the high-pressure retentate stream and deliver it to the next pass low-pressure stream by employing an ERD at different efficiencies. For instance, the 1 atm pressure can be converted into 7.9 atm when an ERD of 90% efficiency is deployed. Furthermore, the permeate pressure can be further increased into 9.2 atm by

applying a booster pump (Fig. 5.5). Accordingly, the booster pump is used to elevate the feed stream pressure of the 2<sup>nd</sup> pass to the same value of the operating plant pressure (9.2 atm). In this respect, the high-concentration stream of the 1<sup>st</sup> pass will be discharged out at atmospheric pressure (1 atm).

The next section will explore the contribution of the recent modification in the design of multistage multi-pass RO plant of APC by applying an ERD and booster pump at different efficiencies. The energy consumption of this set-up will be compared against the energy usage in the unmodified RO plant of APC. Also, the calculations of energy consumption would be estimated for an extensive range of variations in the main operating conditions.

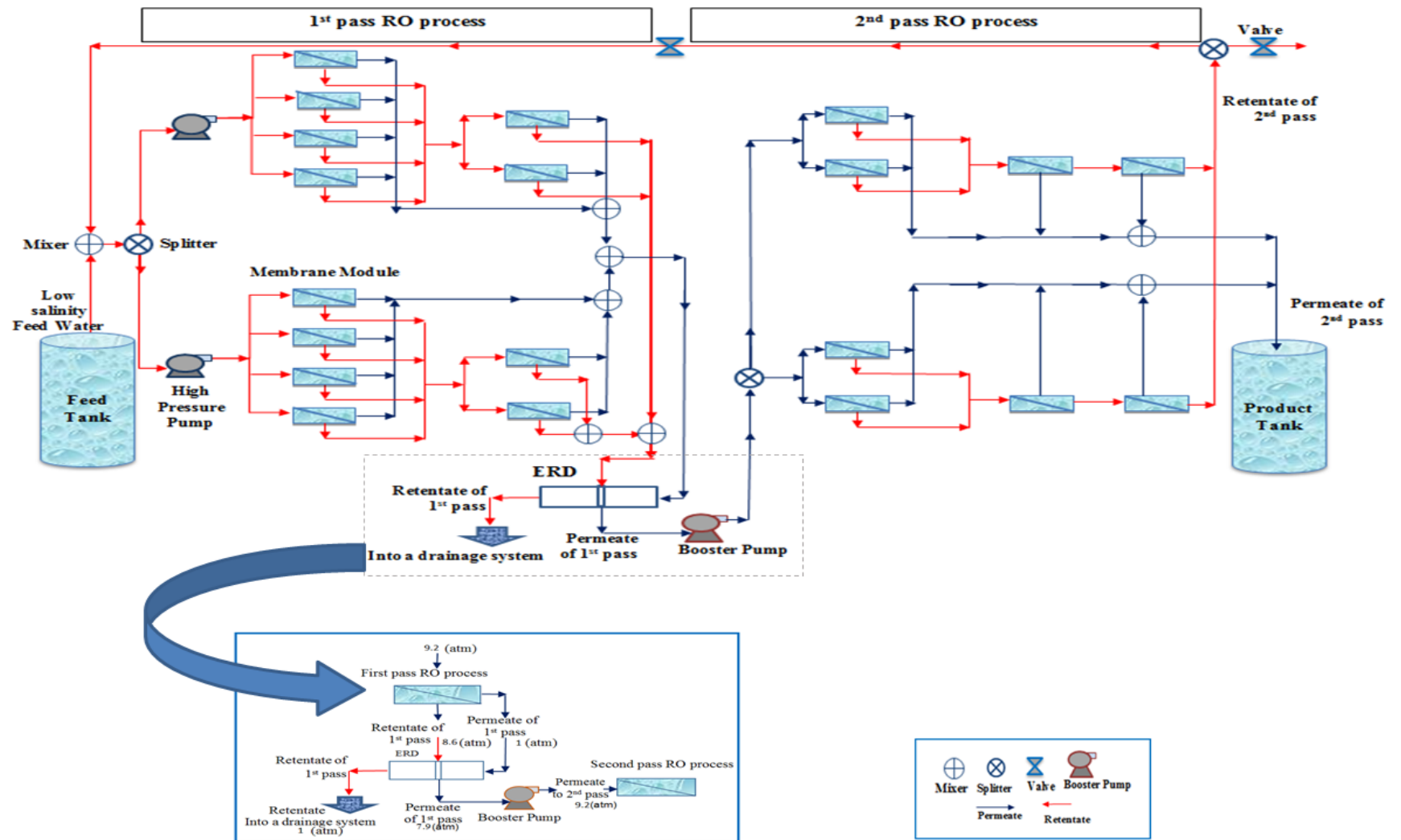


Fig. 5.5 Schematic diagram of multistage, multi-pass BWRO desalination plant of APC with adding of an ERD and booster pump

#### ***5.4.2 Process simulation: Impact of operating parameters***

In this section, the specific energy consumption and plant water recovery are identified as the most crucial performance indicators, which are evaluated for the RO system of APC considering a wide range of operating feed flow rate, pressure, and temperature at three different ERD efficiencies of 80%, 85%, and 90%. In other words, the impact of different operating conditions on the performance of RO desalination plant of APC has been judged by conducting a sensitivity analysis using gPROMS software suits. It is broadly speaking that the specific energy consumption is at least to some extent controlled by the feed fluid characteristics and operating conditions. Therefore, it is vital to comparatively analyse the contribution of these parameters on relevant water recovery and energy consumption. More importantly, the evaluation of these indicators is carried out at a fixed inlet feed concentration of 1098.62 ppm (actual concentration of brackish groundwater). However, it is decided to examine the effect of 20% variation of operating parameters of feed flow rate and pressure against the specific energy consumption and water recovery. Also, 20% variation of operating temperature from 25 °C to 30 °C is selected to represent the temperature variation of stored water in the feed tanks along summer and winter in the region of Dead Sea (Jordan). It is worth noting that high recoveries of freshwater can be produced as a result of using low feed concentration due to low osmotic pressure that exists in the RO modules (Al-Bastaki and Abbas, 2003).

##### ***5.4.2.1 Impact of operating feed flow rate***

This section demonstrates the effect of operating feed flow rate ( $Q_{f(\text{plant})}$ ) variation from 74 to 88.8 m<sup>3</sup>/h (20% increase), at constant feed salinity, pressure, and temperature of 1098.62 ppm, 9.22 atm, and 25 °C, respectively, on the total energy consumption and plant water recovery with and without the application of an ERD at different efficiencies. Fig. 5.6 shows a maximum water recovery of 65.84% that can be attained at the lowest feed flow rate of 74 m<sup>3</sup>/h and commensurate with the lowest energy consumption of 0.837 kWh/m<sup>3</sup> without an ERD inclusion. This is attributed to a lower pressure drop inside each RO module due to the practice of low feed flow rate, which elevates the water permeation through the membranes. In other words, the loss of pressure increases with increasing feed flow rate due to the growth in friction along the membrane length, which limits the

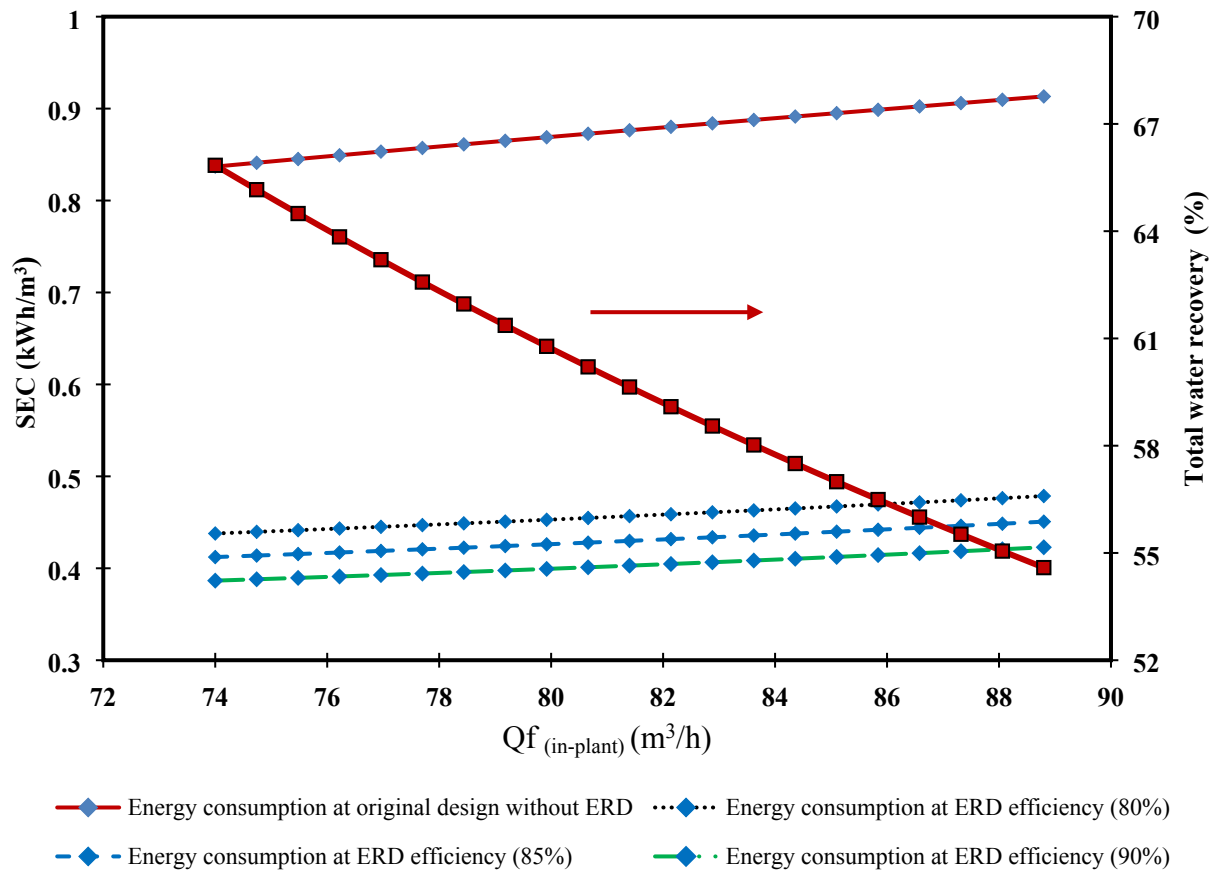
resultant water driving force. This played a weighty role in reducing the water permeation through the membranes despite the advantages of lowering the concentration polarisation and osmotic pressure due to increasing the feed flow rate (Villafafila and Mujtaba, 2003). In this regard, higher turbulence in the high concentration channel is an anticipated statement as a result to increasing the feed velocity in all the membranes situated in the 1<sup>st</sup> pass of the RO plant, which in turn increases the total retentate flow rate, decreases the retentate pressure and decreases the total permeate flow rate of the same pass. This can explain the noted reduction of total plant permeate flow rate and water recovery as a response to growing plant feed flow rate.

Fig. 5.6 also depicts an increase in the specific energy consumption due to increasing the feed flow rate; while keeping all the other operating conditions constant, due to a lower gain of fresh water penetrated the membranes. This is basically true due to an apparent reduction of water recovery and water permeation due to increasing the feed flow rate. Consequently, it is recommended to run the RO process at low values of feed flow rate to guarantee high values of water recovery at low values of energy consumption. In this respect, Al-Shayji (1998) provided a neural network model for simulation of a large-scale commercial Jeddah1 seawater RO Plant Phase II (the Kingdom of Saudi Arabia). The model used to appraise the influence of several operating conditions on the total consumption energy including water recovery. The simulation results showed an increase in the rate of production would reduce the energy consumption.

Fig. 5.6 also shows that increasing the ERD efficiency from 80% to 85% and then to 90% can result in a reduction of specific energy consumption by around 47.7%, 50.8%, and 53.8%, respectively, at inlet feed flow rate of 74 m<sup>3</sup>/h. However, the reductions of specific energy consumption are 47.6%, 50.7%, and 53.7% with ERD efficiency of 80% to 85% and 90%, respectively, at inlet feed flow rate of 88.8 m<sup>3</sup>/h. Therefore, it is concluded that an increase in ERD efficiencies would decrease the specific energy consumption of the RO process. More precisely, the energy consumption falls by a constant value of 6.6% for all feed flow rates when increasing the ERD efficiency from 80% to 85%. However, a reduction of a fixed value of 6.9% in energy consumption is noticed for all feed flow rates by elevating the ERD efficiency from 85% to 90%. Thus, it is suggested to implement a low feed flow rate with the presence of an ERD at the highest possible efficiency at fixed

pressure and temperature to guarantee lower energy consumption. Moreover, running the RO system at the highest feed flow rate requires a maximum specific energy consumption due to diminishing the water permeation through the membrane pores. It is noteworthy to mention that increasing the feed flow rate inside the membrane feed channel would increase the axial pressure drop that entirely reduces the water recovery. In this respect, Fig. 5.6 confirms the highest energy consumption for the case of without ERD, which stimulates the original design of multistage multi-pass RO system of APC.

The presented results of Fig. 5.6 are in a good agreement with the findings of Al-Obaidi et al. (2018c) over the range of feed flow rate for the removal of N-nitrosamine at a very low concentration from wastewater using multistage RO system.



**Fig. 5.6.** Specific energy consumption and water recovery of brackish water RO desalination plant of APC with and without an ERD (at different efficiencies) against plant feed flow rate

#### ***5.4.2.2 Impact of operating feed pressure***

This section aims to investigate the impact of increasing the plant pressure by 20% on the nominated performance indicators of total water recovery and specific energy consumption.

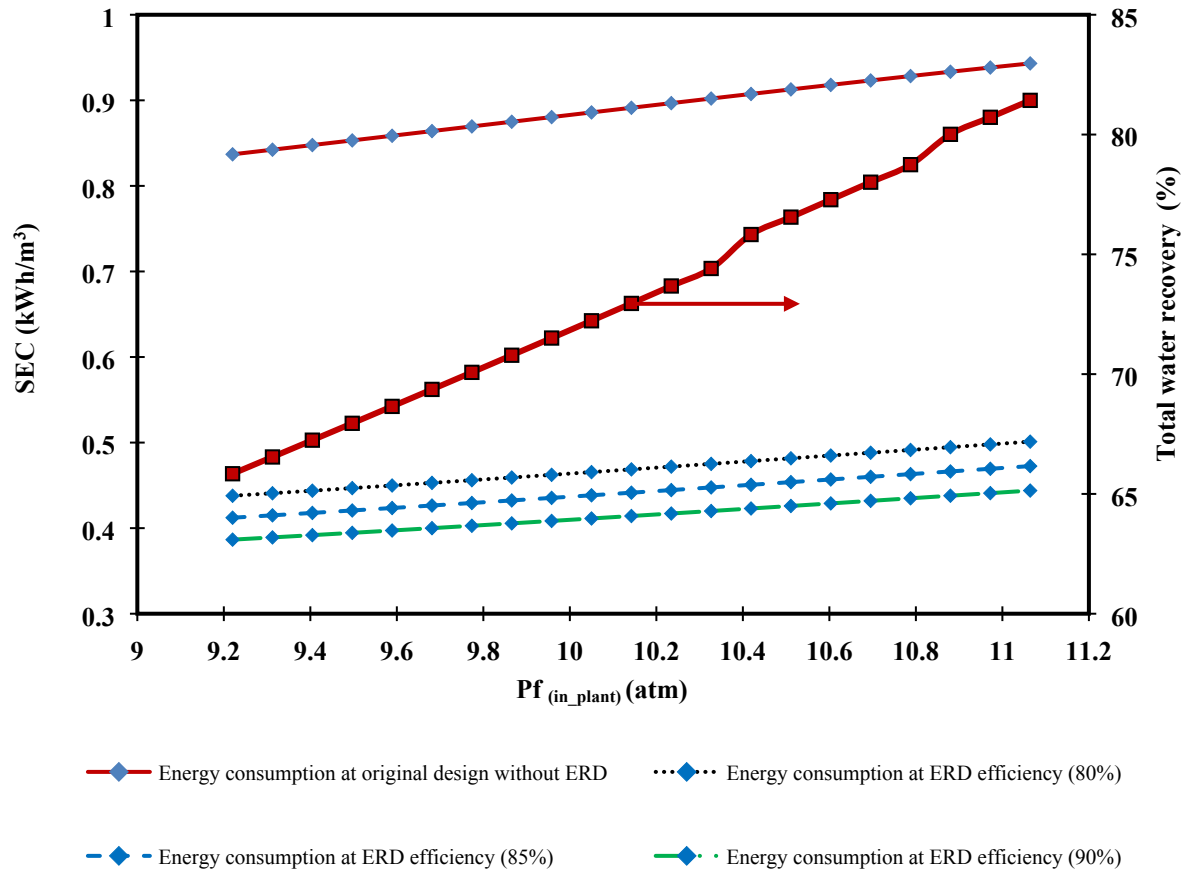
Linear correlations between the feed pressure and both specific energy consumption and water recovery are illustrated in Fig. 5.7 for the selected variation of operating pressure from 9.22 atm to 11.06 atm at fixed feed salinity, flow rate, and temperature of 1098.62 ppm, 74 m<sup>3</sup>/h, and 25 °C, respectively. However, an insignificant jump of water recovery is noticed close to 10.4 atm, which can be attributed to an insignificant increase of water permeation through the membrane texture. Specifically, any variation of feed pressure would directly affect both the water and solute flow rates through the membranes, which in turn alter the total water recovery (Thomson et al., 2003; Greenlee et al., 2009). More specifically, an increase in the applied pressure far away from osmotic pressure would enhance the driving force and hence water permeation through the membrane.

Fig. 5.7 presents that total water recovery with and without an ERD is significantly increased by increasing the operating pressure. This is agreed with a continuous reduction of the retentate flow rate of the 1<sup>st</sup> pass, an increase of fresh water flow rate of the 1<sup>st</sup> and 2<sup>nd</sup> passes of the RO plant, that guarantees the evolution of total plant permeation flow rate. Also, it is fair to expect the production of high-quality water as a result to increasing operating pressure. It should also be noted that a maximum selected operating pressure of 11.06 atm would attain a maximum water recovery of 81.42% at a maximum energy consumption of, 0.943 kWh/m<sup>3</sup> without an ERD (Fig. 5.7). This is comparable with the maximum water recovery achieved at the lowest feed flow rate (Fig. 5.6), which affirmed the superiority of feed pressure in the RO process. Also, this would reflect the advantages of the two-pass multistage of RO process of APC, which is critically designed to operate at high water recoveries that commensurate with low feed salinity. In this respect, Mazlan et al. (2016a) confirmed the feasibility of the RO process configuration to maintain the process at high water recoveries. This is specifically characterised by selecting a single stage (2:1) configuration of seawater RO system running at 50% of water recovery and a two-stage (3:2) configuration was nominated for running at 75% of water recovery.

In contrast, increasing of feed pressure has a considerable passive impact on the specific energy consumption, which is dramatically increased (Fig. 5.7). In other words, the RO system operating at high recoveries (high operating pressures) would require higher energy than those working at low recoveries and low water permeation (low operating pressures). The simulation results of this case confirm the authority of feed pressure to control the energy consumption compared to the incomparable impact of total permeate flow rate ( $Q_{p(\text{plant})}$ ). In other words, the progress of permeate flow rate due to an increased pressure was not sufficient to reduce the energy consumption. Therefore, the simulation results of Fig. 5.7 indicate that at the fixed feed flow rate, salinity, and temperature, the lower feed pressure results in lower water recovery and permeate flow rate, which generally sustain with lower specific energy consumption. The results obtained are also commensurate with the results of Stover (2007) and Sharif et al. (2009).

The specific energy consumption decreases, as expected when an ERD is used. As shown in Fig. 5.7, the lower energy consumption can be obtained by increasing the ERD efficiency from 80% to 85% and then to 90%. Apparently, the energy consumption dropped by a fixed value of 6% of all pressures with increasing the ERD efficiency from 80% to 85%. This is compared to 6.4% of energy reduction at all pressures, which is detected by increasing the ERD efficiency from 85% to 90%. Consequently, the specific energy consumption can be significantly decreased by around 47.7%, 50.8%, and, 53.8% in the case of adding an ERD in the original RO system of APC at the ERD efficiencies of 80%, 85%, and 90%, respectively, at an inlet pressure of 9.22 atm. Moreover, increasing the ERD efficiency from 80% to 85% and then to 90% can result in a reduction of specific energy consumption by 46.9%, 49.9%, and 52.9%, respectively, at inlet feed pressure of 11.06 atm. The recovery of the surplus energy of the high-pressure retentate stream of the 1<sup>st</sup> pass has quietly represented a substantial amount of hydraulic energy that can be saved for the studied RO system of APC. Furthermore, the maximum specific energy consumption is registered for the case of the original design of RO system of APC where only pumps are used (Fig. 5.7). The above results agree with the findings of Farooque (2008). Farooque (2008) investigated the influence of various ERDs of different efficiencies on the performance of seawater desalination RO plant in Saudi Arabia. This

is originally confirmed the possibility of 27% as a maximum energy saving based on the maximum power consumption of the high-pressure pump of 7.93 kWh/m<sup>3</sup>.



**Fig. 5.7.** Specific energy consumption and total water recovery of BWRO desalination plant of APC with and without an ERD (at different efficiencies) against operating feed pressure

#### 5.4.2.3 Impact of feed temperature

Jiang et al. (2015) reported that the feed temperature ( $T_{(plant)}$ ) (°C) has a considerable contribution on energy consumption and water recovery for any RO system. In this regard, the performance indicators of the brackish water RO desalination plant of APC (the total energy consumption and water recovery) are assessed in this section by imposing an increase in the applied temperature from 23 °C to 30 °C (within the feed water temperature variation due to seasonal variation in the plant area). Fig. 5.8 shows a growth in the water

recovery with the increased operating temperature at fixed feed salinity, flow rate, and pressure of 1098.62 ppm, 74 m<sup>3</sup>/h, and 9.220 atm, respectively. These results are in a good agreement with Agashichev and Lootahb (2003) and Saasi and Mujtaba (2012). It is well known that any increase in the applied temperature would enhance the water penetration through the membrane matrix as a result to affecting the membrane pore size (Malaeb and Ayoub, 2011). This is specifically attributed to enlarging the membrane pore size due to the thermal expansion of the membrane material, which would increase the water flux through the membrane texture. In this regard, Morin et al. (2004) deduced that increasing the pore size during buttermilk Microfiltration process causes an increase in the permeation flux. Moreover, Dang et al. (2014) experimentally affirmed an increase in the effective pore radius of NF membrane from 0.39 to 0.44 nm as a result to increasing the feed temperature from 20 to 40 °C. Apparently, increasing the operating temperature would decrease the water viscosity and density in addition to increase the water transport parameter. Consequently, this would increase the water permeation through the membrane pores. Therefore, it is fair to expect an improvement of water permeation and water recovery as a consequence of increasing temperature (Gude, 2011). Simulation carried out in this study show an increase in water recovery by around 12.7% due to increasing temperature from 25 °C to 30 °C. However, it is noteworthy to mention that increasing temperature would increase the solute diffusion through the membrane due to enlarging the membrane pore size. Therefore, it is also fair to expect that increasing temperature would slightly reduce the quality of permeated water at the permeate channel and reduce solute rejection. The simulation results affirmed an increase of freshwater concentration from 1.99 ppm at 25 °C to 3.58 ppm at 30 °C. This is in an agreement with the findings of Jin et al. (2009) who studied the effect of feed temperature of the RO process on both energy consumption and salt rejection. The results confirmed that increasing temperature could limit the concentration polarisation, which increases water and salt permeabilities. This in turn reduces the relevant salt rejection and specific energy consumption.

Fig. 5.8 approves a maximum water recovery of 75.45% has been achieved at the maximum tested temperature of 30 °C, which associated with the lowest energy consumption of 0.786 kWh/m<sup>3</sup>. Basically, Fig. 5.8 depicts that the specific energy consumption significantly decreases due to increasing temperature from 23 °C to 30 °C

with approximately 4.9% without an ERD (original design) and 2.3%, 4.8%, and 2.6% with an ERD efficiency of 80%, 85%, and 90%, respectively. Specifically, the specific energy consumption decreases by 47.7%, 50.8%, and 53.8% for the employment of 80%, 85%, and 90% of the ERD efficiency, respectively, at the feed temperature of 25°C, compared to the original design of APC (without an ERD). However, increasing the ERD efficiency from 80% to 85% and then to 90% can result in a reduction of specific energy consumption by around 46.3%, 49.3%, and 52.2%, respectively, at inlet feed temperature of 30°C.

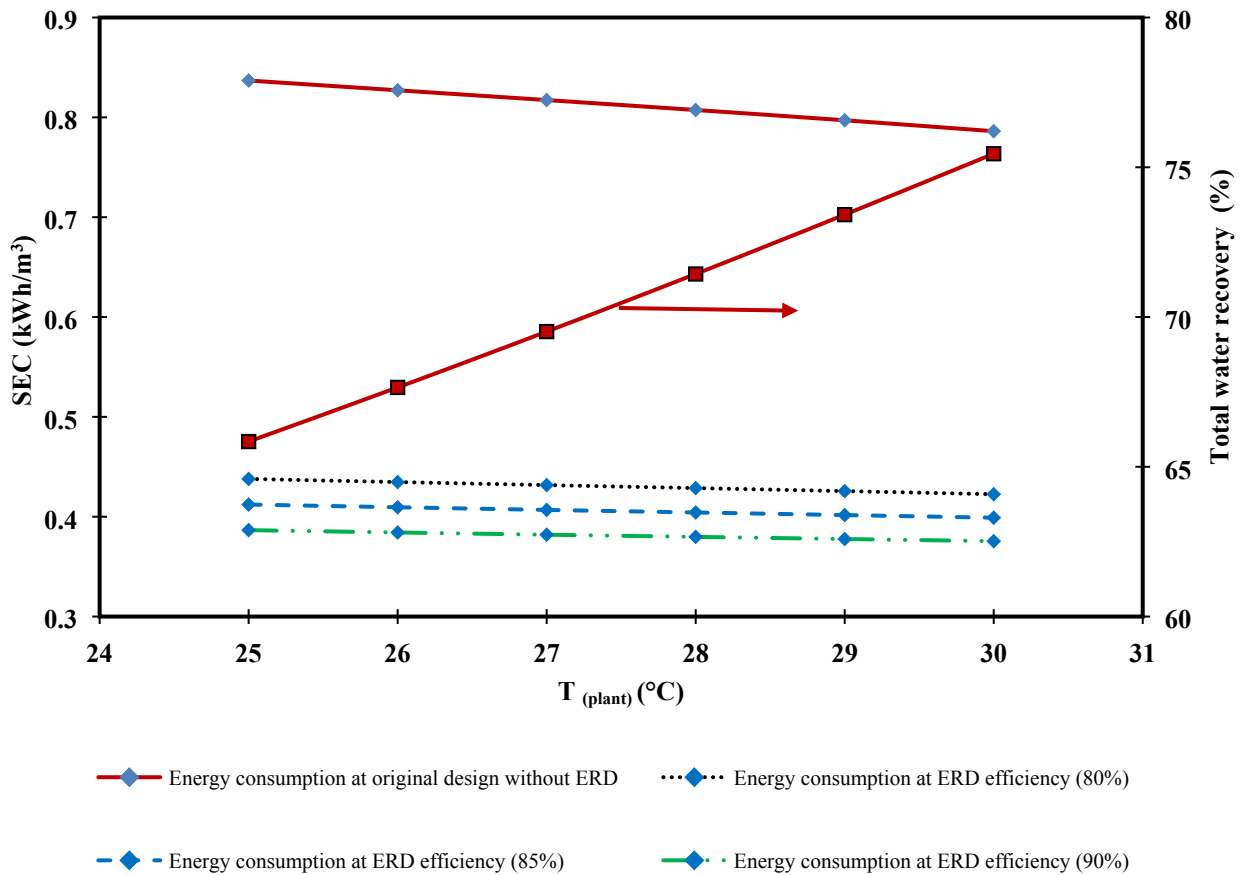


**Fig. 5.8.** Specific energy consumption and total recovery of brackish water RO desalination plant of APC without and with an ERD (at different efficiencies) against feed temperature

To summarise, the simulation results confirm that low values of feed flow rate and operating pressure reduces the energy consumption. Moreover, increasing operating

temperatures would reduce the energy consumption. It is also concluded that any increase of water permeation of the RO process would serve the minimisation of total energy consumption. The same trend of these simulation results is inconsistent with the simulation results of Stover et al. (2005) who presented the reduction of energy consumption of SWRO plant in Ghalilah (United Arab Emirates) as a response to increasing permeate flow rate.

This study has also affirmed the positive impact of employing an ERD in the actual design of the RO process of APC. Precisely, the implementation of an ERD plays a considerable role in mitigating the energy consumption over the range of operating conditions. Increased the ERD efficiency also results in higher energy savings. There is also a noticeable positive impact of increasing feed pressure and temperature on the water recovery rate. However, it is important to note that the outputs of this study are based on the assumption of 'high-performance' RO membranes of APC, which corresponds with the current upgraded membranes of infinite water permeation (Al-Obaidi et al., 2018b). This is originally proposed in the model developed in Chapter 3 which assumed fixed fouling factor of 1 (new synthesised membranes). Therefore, it is fair to expect that the simulation results of the current study would not accurately stimulate the process performance of a multistage multi-pass RO system of APC after a long time of operation. In other words, the evaluation of specific energy consumption and water recovery has been carried out based on fixed membrane permeability that would definitely vary (a prime concern) and affect the process performance due to fouling propensity. This in turn would result in a greater energy loss during the filtration process.

#### ***5.4.3 Expected merits of the advanced design of APC***

On the basis of simulation consideration, several expected merits of the implementation of an ERD in the multistage multi-pass RO system of APC can be drawn as follows:

- Installing an ERD in the multistage multi-pass RO design of APC would result in a decrease in the total energy consumption between 46.2% - 53.8% compared to the original design without an ERD. In this regard, Khawaji et al. (2007) presented a reduction of energy consumption from 6-8 kWh/m<sup>3</sup> without an ERD to 4-5 kWh/m<sup>3</sup> with an ERD for seawater RO desalination plant with capacity of

13.3 million gallons per day (MGD) located in the Kingdom of Saudi Arabia. Moreover, Stover (2007) affirmed the possibility of a dramatic improvement of seawater RO system as a result to use isobaric ERDs, which can diminish the energy consumption by as much as 60% compared to RO systems operating without ERD.

- Although the addition of an ERD and a booster pump is relatively expensive compared to the original design of RO system and would increase the fresh water production cost, it is expected that the benefit of this design will recover the capital cost of purchasing the ERD and booster pump. This is due to lower energy consumption over a prolonged operation time.
- Reducing the total energy consumption would aid to reduce the CO<sub>2</sub> gas emissions in the atmosphere. This is basically true since increasing the energy consumption means a higher necessity of fossil fuel combustion for electricity generation. In this aspect, the casual nexus between different sources of energy consumption and CO<sub>2</sub> gas emissions was explored by Palamalai et al. (2015). This in turn showed a statistically positive correlation that illustrates a high-level of energy consumption from the electricity sector would lead to high-gas emissions that passively impact the environment. Therefore, there are numerous publications that emphasised on energy saving.

Based on the above results, it is recommended to fine-tuning the original design of RO system of APC to comprise an ERD where a subsequent power saving can be achieved. Some attempts were made considering different aspects to minimise the total energy consumption of RO system that would be in a meaningful relationship with the recent study. For instance, Karabelas et al. (2018) analysed the contribution of several key design parameters to reduce the specific energy consumption of seven spiral wound modules in the pressure vessel for typical seawater and brackish water RO desalination processes. The assessed parameters were the retentate osmotic pressure, membrane permeability, friction losses in the feed and permeate channels, and the efficiency of ERD and high-pressure pumps. They demonstrated the importance of water permeability and efficiency of ERD and pumps to attain marginal reduction of specific energy consumption. Moreover, a superstructure optimisation methodology was used by Du et al. (2019), which

include all possible stream configurations in an RO network. In this regard, the optimal blending of different salinity streams could cause insignificant exergy destruction and lower total energy requirements. The effect of applying different membrane types of the original design of APC on the specific energy consumption will be investigated in the next chapter.

### **5.5 Critique of specific energy consumption of simple and complicated designs of brackish water RO process**

Based on the simulation results presented in the previous sections, Table 5.2 has been built. Table 5.2 is specifically presented the calculations of specific energy consumption of simple and complicated designs of brackish water multistage RO desalination systems. Simply, the energy saving of these systems within the existence of three efficiencies of an ERD are illustrated based on the variation of 20% in the inlet parameters of feed flow rate, pressure and temperature. Occasionally, the energy saving of RO system with the addition of an ERD is calculated based on the specific energy consumption of RO system without an ERD. Table 5.2 clearly indicates that the simple design of RO system of retentate reprocessing design has obtained higher energy saving with the existence of an ERD if compared to the complicated multistage multi pass RO system of APC in all the three inlet feed parameters of feed flow rate, pressure and temperature. However, it is important to noting that the complicated design of RO process of APC requires less specific energy consumption compared to the simple design of RO process. This is specifically attributed to the higher productivity of the complicated design. It can also be stated that the complicated design of RO system of APC contains two passes of higher number of pressure vessels where the second pass is responsible to further polishing the obtained permeate of the first pass. This in turn requires the instillation of other pumps to raise the pressure of the feed of the second pass. These pumps drive the permeate of low salinity at same operating pressure of the plant that maintains higher productivity compared to the simple design of RO process. In other words, the simple design of RO system has lower productivity of lower quality water (compared to the complicated design) and works at a higher operating pressure that interprets the necessity of a higher energy consumption.

**Table 5.2.** Simulation results of specific energy consumption of two different sizes of brackish water RO desalination systems

Case study	Variable type within 20% variation	Energy consumption without an ERD (kWh/m <sup>3</sup> )	Energy consumption with an ERD (kWh/m <sup>3</sup> )			Energy saving with an ERD (%)		
			Efficiency (80%)	Efficiency (85%)	Efficiency (90%)	Efficiency (80%)	Efficiency (85%)	Efficiency (90%)
Simple design of multistage RO system	Feed flow rate at 24.48 m <sup>3</sup> /h	2.906	1.123	1.011	0.899	61.355	65.209	69.064
	Pressure at 14.448 atm	1.847	0.756	0.688	0.619	59.068	62.750	66.486
	Temperature at 34.56 °C	1.892	0.761	0.690	0.619	59.778	63.530	67.283
Complicated design of multistage multi pass RO system	Feed flow rate at 88.8 m <sup>3</sup> /h	0.913	0.479	0.451	0.423	47.535	50.602	53.669
	Pressure at 11.06 atm	0.943	0.501	0.473	0.444	47.323	49.8401	52.916
	Temperature at 30 °C	0.786	0.423	0.399	0.375	46.183	49.236	52.290

## 5.6 Conclusions

The viability of adding an ERD at different efficiencies to two different sizes of brackish water multistage RO desalination systems with the possibility of saving energy is investigated in this chapter. This include the evaluation of the main performance indicators of specific energy consumption and water recovery of the brackish water multistage RO process of simple and complicated designs. To attain this goal, the model developed in Chapter 3 has been utilised and appropriately upgraded to estimate the specific energy consumption for with and without an ERD. The simulation studies covered the evaluation of the inlet feed conditions of brackish water RO process, including feed flow rate, pressure, and temperature, on the plant performance indicators at different efficiencies of an ERD. The results show that water recovery improves with increasing feed pressure and temperature but reduces with increasing feed flow rate. More importantly, lower energy consumption can be attained at lower values of feed flow rates and pressures and higher values of operating temperatures. Also, implementing an ERD would significantly reduce the specific energy consumption of the RO system when compared to the original design (without an ERD) for all the tested operating parameters. Specifically, this showed maximum reductions in specific energy consumption of the multistage multi pass RO system of APC of 47.5%, 50.6 %, and, 53.6% in line with 80%, 85%, and 90% of ERD efficiency, respectively. Also, the maximum energy savings of the simple design of RO process are 61.3%, 65.2%, and 69.0% in line with 80%, 85%, and 90% of an ERD efficiency, respectively. This in turn confirmed the feasibility of installing an ERD in the brackish water RO systems.

The simulation results of this chapter have utmost achieved the main targets of this dissertation where promising water recovery at low specific energy consumption were obtained. The next chapter would explore the viability of replacing the original membrane of RO system with other brand of membrane to quantify an upgraded performance of the system.

## **CHAPTER SIX**

### **Performance evaluation of a reverse osmosis brackish water desalination plant with different brands of membranes**

#### **6.1 Introduction**

The Reverse Osmosis (RO) process was first used in the 1950's and counted about 80% of the total desalination plant used worldwide (Anis et al., 2019). RO was designed to desalinate seawater and brackish water using an asymmetric cellulose acetate membrane. Membrane processes are more successful water desalination techniques compared to thermal ones. This is due to producing high-quality water at competitive low capital and operating costs (Goosen et al., 2005, Qasim et al., 2019). This also explains the popularity of membrane desalination plants around the world and especially in the Gulf countries that suffer from the lack of freshwater resources (Pearce and Kumar, 2003; Droogers et al., 2012). RO membranes are non-porous and semi-permeable and therefore exclude many particles of low-molecular weight such as salt ions and organic pollutants (Fujioka et al., 2018; Sagle and Freeman, 2004). Moreover, the low-energy consumption is a major advantage of RO technology due to the absence of an evaporation step (Van der Bruggen and Vandecasteele, 2002). However, low-productivity, concentration polarisation, and fouling are demonstrated as the main drawbacks of RO processes (Yang et al., 2013; Qasim et al., 2019). For instance, the concentration polarisation phenomena, causes solute buildup on the membrane surface and thus blocking the pores. This leads to a decrease in the filtration performance with time as it retards water permeation (Goosen et al., 2005). On top of this, the membrane fouling causes gel-layer formation and solute adhesion at the membrane surface, which requires periodic cleaning or replacing of the membranes (Pandey, 2014). Therefore, over the years, researchers have strived to improve the performance of RO processes by perform efficient and effective solute separation at low concentration polarisation and fouling propensities. Moreover, purified water standards issued by health organizations became more stringent, which forced scientists to

continually improve the design of water desalination plants (Sagle and Freeman, 2004). The enhancement of RO systems has been made in several aspects including membrane synthesis, structure, material and configurations of RO systems to obtain higher productivity and improved quality of freshwater besides attaining low-energy consumption and freshwater production cost at low fouling propensity. Therefore, several researchers focused on synthesizing new brands of membranes of high durability by using different polymers and liquids, polymeric structure, surface chemistry, bulk texture, morphology, and spacer's design (Du et al., 2012; Yan et al., 2019; Ruiz-García and de la Nuez Pestana, 2019). A wide variety of membranes were therefore developed with variable morphology, surface chemistry and production techniques. RO membranes are basically made from either cellulose acetate or polysulfone coated with aromatic polyamides (Sagle and Freeman, 2004). In this aspect, the manufactured membranes were sorted out based on the type of liquid to be treated, i.e., seawater, brackish water, and wastewater (Osada and Nakagawa, 1992; Khawaji et al., 2008). Recently, many polyamide RO membranes have been intensively used due to their high selectivity and good durability (Taniguchi and Kimura, 2000). On the other hand, the adaptation of an enhanced configuration of RO process and optimisation of membrane modules have mainly contributed to reduce the total energy consumption (Saif et al., 2008; Bartman et al., 2010). Due to the aforementioned advancements, the RO process has become more economical, adaptable and environmental friendly. This has made it a more attractive water desalination technology compared to the intensive-energy thermal technologies (Sagle and Freeman, 2004).

Although, the energy consumption has greatly improved from as much as 20 kWh/m<sup>3</sup> to nearly 2 kWh/m<sup>3</sup> at 50% recovery (Elimelech and Phillip, 2011), the interest of lowering the destructed energy due to the existence of intensive energy units such as pumps, is one of the most projected aims of recent research. This is due to a positive relationship between energy consumption and freshwater production cost; lower energy consumption means lowering freshwater production cost (Mazlan et al., 2016). Several successful studies can be found in the literature that provided a reliable RO system based on water desalination at low energy consumption. Some of these studies are now discussed.

Fethi (2003) upgraded the performance of brackish water at the Kerkennah Islands desalination plant by replacing the cellulosic acetate membranes with polyamide membranes stuffed in spiral wound modules. Improved productivity of freshwater at a high efficiency was obtained. The new brand of polyamide membrane required only 15 atm of pressure to generate the same production rate as that of acetate membranes operating at 29 atm. Therefore, a substantial energy saving of about 46% was obtained when using polyamide membranes compared to the original ones.

Pearce and Kumar (2003) utilised two new generation of brackish water RO membranes; ESPA 4 (Hydranautics, Inc, Oceanside, CA) and 4040 BL (Saehan Industries, South Korea) and their performances were compared against the old membranes of ESPA 2. The new membranes were more efficient due to improved rejection and water recovery. The total energy consumption was sufficiently reduced besides a substantial reduction in production cost.

Stover (2008) succeeded to reduce the total energy consumption of a large-scale desalination plant located in Singapore. They tested the Toray 8-inch TM820C of TFC spiral wound RO membrane and showed that the permeate flux, the salt rejection and the specific energy consumption were improved by 1.8%, 0.15%, and 1.7%, respectively.

The performance indicators of two large-scale seawater desalination plants with two different membrane types of SWC4+ 8-inch (Hydranautics) located in Spain and SW30HRLE 8-inch (DOW FILMTEC™) located in Australia were compared by Laine (2009). The results showed that the permeate flux, salt rejection and specific energy consumption of Hydranautics were 24.6 m<sup>3</sup>/day, 99.7-99.8 %, and 4.17 KWh/m<sup>3</sup>, respectively. However, 28 m<sup>3</sup>/day, 99.6-99.75 %, and 3.40 KWh/m<sup>3</sup> were recorded when using the DOW FILMTEC™ membrane. The DOW FILMTEC™ membrane thus reduces energy consumption by 18.5%.

Al-Obaidi et al. (2018b) assessed the possibility of lowering energy consumption of two configurations of RO systems (with and without energy recovery device, ERD) through altering the membrane dimensions. They tested the influence of membrane length, width and feed channel height on the energy consumption for the elimination of chlorophenol from wastewater. Their results showed up to 60% and 54% energy savings for the two configurations with and without ERD, respectively.

This chapter focuses on evaluating the performance of brackish water multistage RO process of two sizes (simple and complicated) via the implementation of different brands of membranes. The idea is to explore the most successful brand of membranes that can offer a higher performance of the RO process compared to the original one used. The performance indicators of the RO process including the solute rejection, water recovery, productivity and product salinity, and specific energy consumption will be under the focus for the two case studies of different sizes of RO brackish water desalination RO plants.

## **6.2 Case study 1. Performance evaluation of a simple multistage RO brackish water desalination plant with different brands of membranes**

This section intends to investigate the viability of changing the membrane's brand of a simple RO brackish water desalination plant. The simple design of multistage spiral-wound membrane type Dow/FilmTec BW30-400 of RO system was used to desalinate brackish water and presented by Abbas (2005). The full description of the RO system was presented in Fig. 3.1 in Chapter 3. In this regard, the performance of a simple multistage RO system is assessed against several brands of membranes and the associated results are compared against the original membrane's brand of Dow/FilmTec BW30-400. The performance indicators of the RO system including the water recovery, solute rejection, product salinity and most importantly the total energy consumption are considered. Therefore, this section will explore the appropriate brand of membrane that could be used in a simple RO system to attain the upgraded performance at the lowest energy consumption.

The proposal here, is that different spiral wound membranes will have differing water and solute transport parameters that directly influence the water and solute fluxes via the membrane's pores and therefore controlling the performance indicators of the process including solute rejection, water recovery, product salinity, productivity and more importantly the specific energy consumption. Therefore, the characteristic of the tested membranes including the water and solute transport parameters will be collected from literature. Moreover, the water and solute transport parameters of the original membrane (Dow/FilmTec BW30-400) are  $9.5096 \times 10^{-7}$  m/atm s, and  $5.646 \times 10^{-8}$  m/s, respectively, and the actual inlet parameters of the RO system are given in Table 6.1 as the base case.

**Table 6.1.** Input operating conditions of RO system of APC

Parameter	Operating feed flowrate (m <sup>3</sup> /h)	Operating temperature (°C)	Operating pressure (atm)	Salinity of brackish water (ppm)
Value	20.4	28.8	12.04	2540

### ***6.2.1 Simulation results and discussion***

This section discusses the simulation results (presented in Table 6.2) of applying several brands of membranes of the simple design of RO system. To assess the performance of RO system for these membranes, the simulation results of the original membrane type (base case) are also listed in Table 6.2. A simple comparison of the performance indicators shows that the membrane brand Filmtec BW30LE-440 can attain the best results of the total water recovery, productivity, and specific energy consumption.

**Table 6.2.** Simulation results of different brands of spiral wound membrane in a simple RO system with characterizing the performance indicators

No.	Membrane Types	Water permeability constant, $A_w$ (m/atm s)	Salt permeability constant, $B_s$ (m/s)	Rej_plant (%)	Rec_plant (%)	Cp_plant (ppm)	Qp_plant (m <sup>3</sup> /h)	Energy consumption (kWh/m <sup>3</sup> )	Reference
1	Dow/FilmTec BW30-400 ( <b>Base case</b> )	$9.5096 \times 10^{-7}$	$5.646 \times 10^{-8}$	97.791	56.330	56.112	4.351	1.869	<i>Al-Obaidi et al. (2018a)</i>
2	SW30XLE-400	$3.5463 \times 10^{-7}$	$3.2 \times 10^{-8}$	98.916	43.023	27.548	1.637	4.969	<i>(Lu et al. (2007), Du et al., 2012)</i>
3	SW30HR-380	$2.7357 \times 10^{-7}$	$3.2 \times 10^{-8}$	98.618	41.210	35.109	1.267	6.419	
4	SW30HR-320	$3.141 \times 10^{-7}$	$2.2 \times 10^{-8}$	99.161	42.112	21.306	1.451	5.606	
5	BW30-400	$7.599 \times 10^{-7}$	$6.2 \times 10^{-8}$	98.948	51.939	26.711	3.456	2.354	
6	Filmtec8I" SWC3	$5.07 \times 10^{-7}$	$5.6 \times 10^{-9}$	99.862	46.384	3.499	2.323	3.502	<i>Avlonitis et al. (2007)</i>
7	FilmTec spiral wound from DOW	$3.434 \times 10^{-7}$	$5.65 \times 10^{-8}$	98.047	42.788	49.597	1.589	5.119	<i>(Du et al. (2012), Sassi and Mujtaba, 2011)</i>
8	4" ROGA 4160-HRa	$2.112 \times 10^{-7}$	$1.444 \times 10^{-7}$	92.592	39.871	188.156	0.994	8.185	<i>Boudinar et al. (1992)</i>
9	FT 30 SW 2.5" FilmTec	$4.391 \times 10^{-7}$	$3.506 \times 10^{-8}$	99.025	44.903	24.755	2.0203	4.026	<i>(Avlonitis et al. (1991), Avlonitis et al., 1993)</i>
10	ROGA-4000	$1.985 \times 10^{-7}$	$2.3 \times 10^{-7}$	88.185	39.626	300.101	0.943	8.618	<i>Marriott and Sørensen (2003)</i>
11	FilmTec SW30HR-380	$2.360 \times 10^{-7}$	$2.21 \times 10^{-8}$	98.896	40.360	28.033	1.0934	7.438	<i>Geraldes et al. (2005)</i>
12	Spiral wound Qatar SWRO plant	$7.092 \times 10^{-5}$	$1 \times 10^{-5}$	93.592	40.871	198.156	1.0656	9.185	<i>Majali et al. (2008)</i>
13	FILMTEC SW30HR-380	$3.039 \times 10^{-7}$	$1.7 \times 10^{-8}$	99.329	41.881	17.023	1.4036	5.795	<i>Kaghazchi et al. (2010)</i>
14	Filmtec, SW30-4040	$9.058 \times 10^{-8}$	$2.11 \times 10^{-8}$	97.368	37.074	66.849	0.423	19.23	<i>Dimitriou et al. (2017)</i>
15	SW30-HR380	$2.533 \times 10^{-7}$	$2.5 \times 10^{-8}$	98.834	40.751	29.606	1.173	6.933	<i>Vince et al. (2008)</i>
16	<b>Filmtec BW30LE-440</b>	<b><math>1.215 \times 10^{-6}</math></b>	<b><math>15 \times 10^{-8}</math></b>	<b>98.283</b>	<b>61.594</b>	<b>43.615</b>	<b>5.425</b>	<b>1.499</b>	
17	TORAY SU 820	$1.136 \times 10^{-6}$	$2.264 \times 10^{-7}$	97.303	60.025	68.502	5.105	1.593	<i>Djebedjian et al. (2008)</i>
18	Filmtec8"RE 8040SN	$5.88 \times 10^{-7}$	$1.7 \times 10^{-8}$	99.635	48.172	9.263	2.687	3.027	<i>Avlonitis et al. (2007)</i>
19	Filmtec8I"SW30HR380	$4.56 \times 10^{-7}$	$6.8 \times 10^{-9}$	99.816	45.259	4.682	2.092	3.886	

To systematically drive the discussion and analyse the results of Table 6.2, it has been decided to formalise the simulation results in separate figures that would show the influence of using different brands of spiral wound seawater and brackish water membranes on each individual performance indicator with a thorough discussion.

The solute rejections of different membranes are given in Fig 6.1. This elaborates a trend of high solute rejection for most the tested membranes except the membrane 4” ROGA 4160-HRa, ROGA-4000, and Spiral wound Qatar SWRO plant (lines 8, 10, and 12, respectively). The seawater membrane type Filmtec8I" SWC3 (line 6 in Table 6.2) has attained the maximum solute rejection of 99.862 while the membrane Filmtec BW30LE-440 (line 16 in Table 6.2) has close and promising solute rejection of 98.283%. the improved solute rejection of the tested membranes can be ascribed to the high values of water transport parameters. The obtained results of these membranes are greater than the solute rejection of the base case membrane of Dow/FilmTec BW30-400 that achieves only 97.791%.

The increase of solute rejection of these membranes is attributed to their high values of water permeability coefficient compared to the base case membrane of Dow/FilmTec BW30-400. Simply, the membrane brand Filmtec BW30LE-440 has  $1.215 \times 10^{-6}$  (m/atm s) of water transport parameter compared to  $9.5096 \times 10^{-7}$  (m/atm s) for the Dow/FilmTec BW30-400 (base case). Furthermore, the solute transport parameter is an important indicator of the solute flux. In this regard, the maximum solute rejection of the membrane brand Filmtec8I" SWC3 has the lowest solute transport parameter of  $5.6 \times 10^{-9}$  (m/s) compared to the base case membrane brand of Dow/FilmTec BW30-400 of  $5.646 \times 10^{-8}$  (m/s). Occasionally, the lowest solute rejection of 88.185% of the membrane brand ROGA-4000 is due to the very high solute transport parameter of  $2.3 \times 10^{-7}$  m/s that intensively stimulates the solute passage. Furthermore, this membrane has one of the lowest water transport parameters. Therefore, it is fair to admit that both water and solute transport parameters can simultaneously affect the performance indicator of solute rejection.

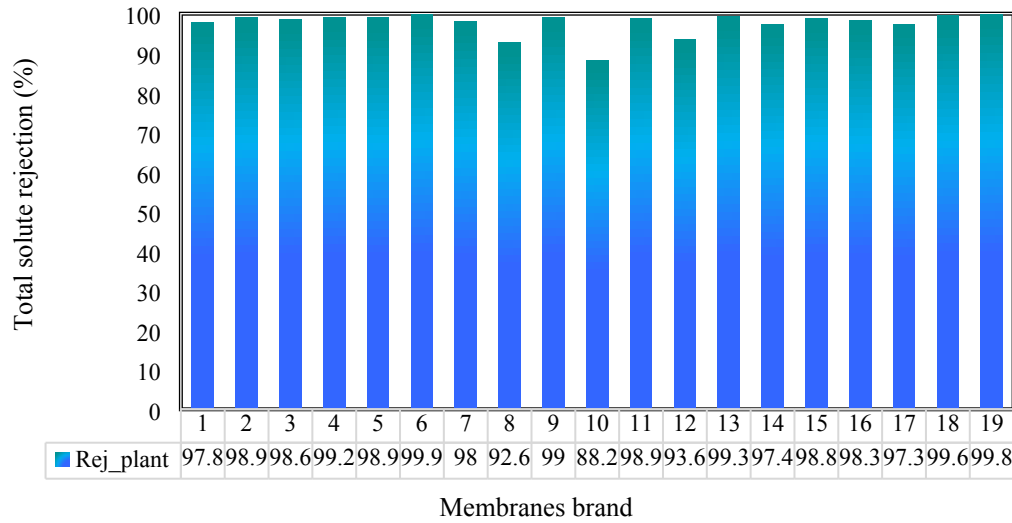


**Fig. 6.1.** Impact of membrane brands on solute rejection of a simple design of brackish water RO desalination system

Fig. 6.2 shows the water recovery of the simple design of RO system at various brands of spiral wound membrane applied for the operating condition presented in Table 6.1. The membrane brand of BW30LE-440 (line 16 in Table 6.2) has the maximum water recovery of 61.594 %. This is an improvement of 9.34% in water recovery compared to the base case of membrane brand Dow/FilmTec BW30-400. Occasionally, the membrane brand has the highest water transport parameter of  $1.215 \times 10^{-6}$  (m/atm s) compared to  $9.5096 \times 10^{-7}$  (m/atm s) of the membrane base case. Basically, the water transport parameter is a specified indicator of water flux. Therefore, high water transport parameter is an indication of high-water flux through the membrane pores and therefore high productivity. Fig. 6.2 shows that the membrane type Filmtec, SW30-4040 (line 14 in Table 6.2) has attained the lowest water recovery. This is due to the low water transport parameter of  $9.058 \times 10^{-8}$  (m/atm s). In other words, improving the water permeation tendency of the membrane is of high importance to gain high productivity.

The simulation results of Fig. 6.3 are supporting the results of Fig. 6.2 of maximum and minimum water recovery. In this regard, the membrane type of BW30LE-440 has **improved** the water permeation by 24.7% compared to the membrane base case. Statistically, BW30LE-440 gains 5.425 m<sup>3</sup>/hr of productivity compared to 4.351 m<sup>3</sup>/h of the base case. Again, the lowest water productivity of membrane brand Filmtec, SW30-

4040 of 0.423 m<sup>3</sup>/h is linked to the lowest water recovery. It is important to mention that the calculation of both water recovery and water productivity is conducted at a fixed feed flow rate of 20.4 m<sup>3</sup>/h (Table 6.1) for all the tested brands of membranes.

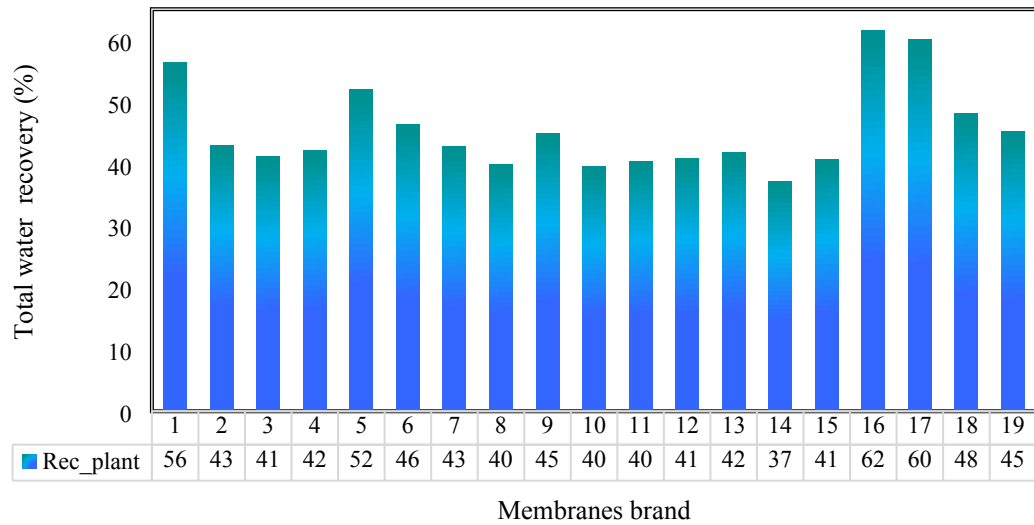


**Fig. 6.2.** Impact of membrane brands on total water recovery of a simple design of a brackish water RO desalination system

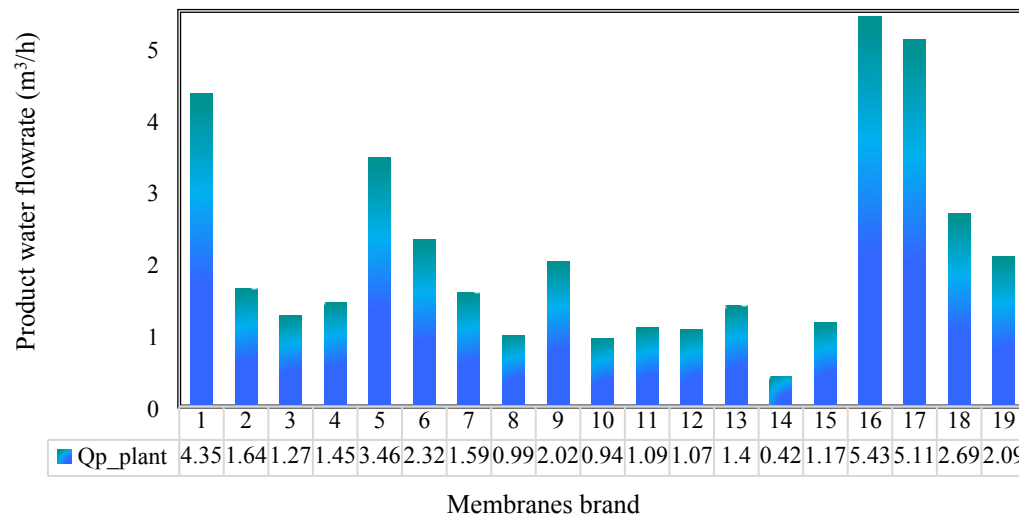


**Fig. 6.3.** Impact of membrane brands on total product flowrate of a simple design of brackish water RO desalination system

The simulation results of product salinity of different brands of membranes are presented in Fig. 6.4 at fixed operating conditions (given in Table 6.1). This specifically shows that membrane type Filmtec8I" SWC3 (line 6 in Table 6.2) has the optimum (lowest) product salinity of 3.499 ppm. This membrane has occasionally the lowest solute transport parameter. Moreover, the membrane type Filmtec BW30LE-440 (line 16 in Table 6.2) produces a lower product salinity of 43.615 ppm compared to the base case membrane type Dow/FilmTec BW30-400 of 56.112 ppm. This is specifically an improvement of 22.2% with **reduction** in the product salinity. This improvement can be attributed to the water and solute parameters of the corresponding membranes. For instance, the water transport parameter of Filmtec BW30LE-440 is higher than the base case membrane of Dow/FilmTec BW30-400. This in turn causes a higher possibility of water dilution in the permeate channel due to a higher water flux through the membrane pores.

The worse product salinity (maximum) of 300 ppm is linked to the membrane type ROGA-4000 (line 10 in Table 6.2) that has the maximum solute transport parameter compared to other tested membranes.

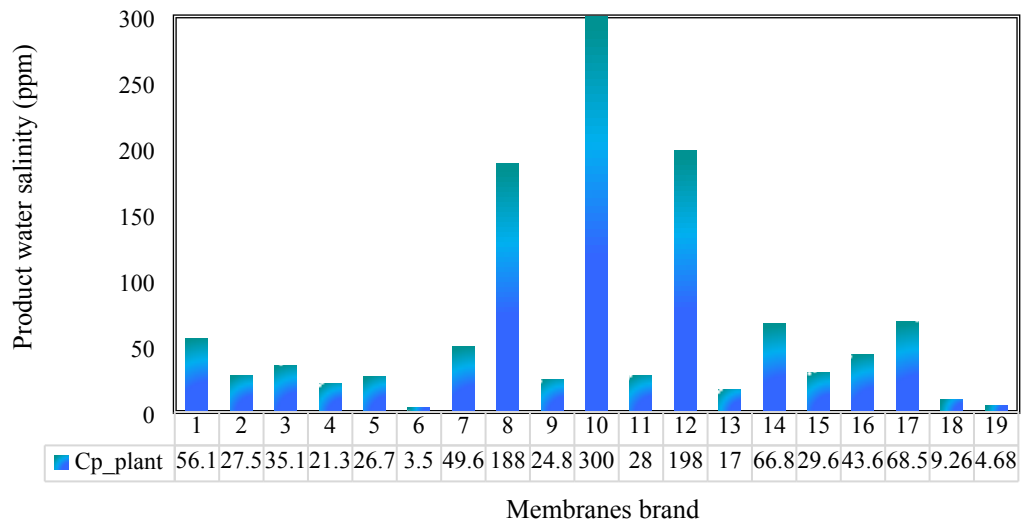


**Fig. 6.4.** Impact of membrane brands on total water salinity of a simple design of brackish water RO desalination system

Finally, the specific energy consumption is one of the most attractive indicators of the RO process. Fig. 6.5 shows that the Filmtec BW30LE-440 requires the lowest specific energy

consumption if compared to all the other tested membranes. Statistically, the membrane type Filmtec BW30LE-440 performs the brackish water desalination within 1.499 kWh/m<sup>3</sup> compared to 1.869 kWh/m<sup>3</sup> of the base case membrane type Dow/FilmTec BW30-400. This is specifically an improvement of 24.7%. In this regard, the simulation results of the productivity of Fig. 6.3 can interpret the results of Fig. 6.5 of the lowest specific energy consumption. Furthermore, the seawater membrane brand of SW30-4040 requires the maximum specific energy consumption of 19.23 kWh/m<sup>3</sup> due to the lowest water productivity if compared to the other tested membranes. Therefore, it can be said that the specific energy consumption of RO system is quite related to the water permeation. Due to simulating the membranes at a fixed set of operating conditions, the variation of membrane pores, design, and numbers, can interpret the variation of water flux through the membrane pores.

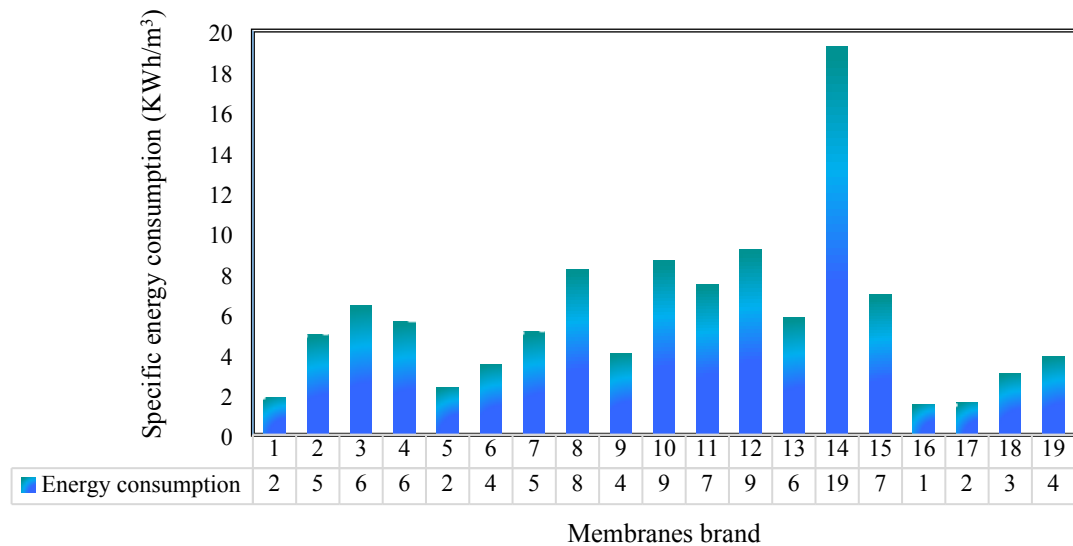


**Fig. 6.5.** Impact of membrane brands on plant energy consumption of a simple design of brackish water RO desalination system

### **6.3 Case study 2. Performance evaluation of a complicated multistage RO brackish water desalination plant of APC with different brands of membranes**

This section intends to improve the performance of a multistage multi-pass (complicated design) of brackish water RO system of the Arab Potash Company (APC) located in Jordan of a capacity of 1200 m<sup>3</sup>/h of potable water of 2 ppm salinity. The full description of RO system of APC was illustrated in Chapter 3 (Fig. 3.2). The plan is to test several brands of spiral-wound commercial membranes in the original RO plant and evaluating the performance indicators including water recovery, solute rejection, freshwater salinity and most importantly the specific energy consumption. The type of membrane currently used in the plant is TMG20D-400, Toray Membrane USA Inc. The performance results of the new membranes will be compared against the actual membrane used in the RO system. The water and solute transport parameters of the tested membranes will be collected from literature.

To gain fair results, the simulation based the new membranes will be carried out at fixed and same operating conditions of RO plant of APC including the brackish water salinity, flow rate and temperature. The model developed in Chapter 3 will be used to carry out this simulation using gPROMS suite software. Therefore, this research will identify the appropriate brand of membrane that could be used in the RO system of APC to perform the lowest specific energy consumption. In other words, this study would specify the best brand of membrane that integrates both performance metrics and lowest energy consumption.

The characteristics of the original membrane and water and solute transport parameters of the original membrane are given in Table 6.3 as the base case. Also, the actual inlet parameters of the RO system are provided in Table 6.4.

**Table 6.3.** Characteristics of the membrane used in the RO system of APC and transport parameters

Membrane brand		Transport parameters at 25 °C	
Parameter	Value	Parameter	Value
Membrane supplier	Toray Membrane USA Inc.	Water $A_w(T_o)$ (m/atm s)	$9.6203 \times 10^{-7}$
Membrane type and configuration	TMG20D-400, Ultra low pressure BWRO, spiral wound, polyamide thin-film Composite	Solute $B_s(T_o)$	$1.61277 \times 10^{-7}$
Dimensions		Characteristics of spacer	
Parameter	Value	Parameter	Value
Membrane area $A$ (m <sup>2</sup> )	37.2	Spacer type	NALTEX-129
Membrane length $L$ (m)	1	length of filament in the spacer mesh $L_f$ (m)	$2.77 \times 10^{-3}$
Membrane width $W$ (m)	37.2	Feed and permeate spacer thickness $t_f, t_p$ (m)	$8.6 \times 10^{-4}$ (34 mils), $5.5 \times 10^{-4}$
Limits of operating conditions		$A'$ (dimensionless)	7.38
Max. feed pressure (atm)	40.464	$n$ (dimensionless)	0.34
Max. pressure drop per membrane (atm)	0.987	$\varepsilon$ (dimensionless)	0.9058
Max. feed temperature (°C)	45	$k_{dc}$ (-)	1.501
Max. feed flowrate (m <sup>3</sup> /h)	18		

**Table 6.4.** Input operating conditions of a complicated RO system of APC

Parameter	Operating feed flowrate (m <sup>3</sup> /h)	Operating temperature (°C)	Operating pressure (atm)	Salinity of brackish water (ppm)
Value	74	25	9.22	1098.62

### 6.3.1 Simulation results and discussion

Here, the evaluation of applying different brands of spiral wound membrane on the performance of RO system of APC is carried out with a simple comparison against the simulation results of the original membrane (Toray Membrane USA Inc, TMG20D-400). The simulation results of employing different brands of membranes on the first and second passes of the RO system are shown in Table 6.5. In this regard, the simulation results of the original membrane type (base case) are also listed in Table 6.5 for comparison purposes. The Filmtec BW30LE-440 membrane shows the most promising results of the main performance indicators including the water recovery and specific energy consumption. Overall, this membrane also can remove salts from brackish water at very plausible product salinity.

**Table 6.5.** Simulation results of different brands of membranes in the complicated design of RO system with characterising the performance indicators

No.	Membrane Types	Water permeability constant, $A_w$ (m/atm s)	Salt permeability constant, $B_s$ (m/s)	Rej_plant (%)	Rec_plant (%)	Cp_plant (ppm)	Qp_plant (m <sup>3</sup> /h)	Energy consumption (kWh/m <sup>3</sup> )	Reference
1	Toray Membrane TMG20D-400	$9.6203 \times 10^{-7}$	$1.6127 \times 10^{-7}$	99.798	56.442	1.9879	48.133	0.8401	<i>Al-Obaidi et al. (2018a)</i>
2	SW30XLE-400	$3.5463 \times 10^{-7}$	$3.2 \times 10^{-8}$	99.964	25.379	0.3823	19.612	1.4107	<i>(Lu et al. (2007), Du et al., 2012)</i>
3	SW30HR-380	$2.7357 \times 10^{-7}$	$3.2 \times 10^{-8}$	99.945	19.924	0.5788	15.237	1.6967	
4	SW30HR-320	$3.141 \times 10^{-7}$	$2.2 \times 10^{-8}$	99.979	22.725	0.2209	17.460	1.5344	
5	BW30-400	$7.599 \times 10^{-7}$	$6.2 \times 10^{-8}$	99.963	20.514	0.2806	15.453	1.4126	
6	Filmtec8" SWC3	$5.07 \times 10^{-7}$	$5.6 \times 10^{-9}$	98.891	31.833	0.0508	15.762	1.9767	<i>Avlonitis et al. (2007)</i>
7	FilmTec spiral wound from DOW	$3.434 \times 10^{-7}$	$5.65 \times 10^{-8}$	99.882	24.537	1.2509	18.955	1.4435	<i>(Du et al. (2012), Sassi and Mujtaba, 2011)</i>
8	4" ROGA 4160-HRa	$2.112 \times 10^{-7}$	$1.444 \times 10^{-7}$	98.499	15.258	16.271	11.629	2.0687	<i>Boudinar et al. (1992)</i>
9	FT 30 SW 2.5" FilmTec	$4.391 \times 10^{-7}$	$3.506 \times 10^{-8}$	99.966	20.730	0.2694	15.460	1.4239	<i>(Avlonitis et al. (1991), Avlonitis et al., 1993)</i>
10	ROGA-4000	$1.985 \times 10^{-7}$	$2.3 \times 10^{-7}$	96.406	14.222	39.169	10.846	2.1696	<i>Marriott and Sørensen (2003)</i>
11	FilmTec SW30HR-380	$2.360 \times 10^{-7}$	$2.21 \times 10^{-8}$	99.968	17.349	0.3473	13.200	1.8966	<i>Geraldes et al. (2005)</i>
12	Spiral wound Qatar SWRO plant	$7.092 \times 10^{-5}$	$1 \times 10^{-5}$	99.872	13.788	1.3158	15.179	1.0425	<i>Majali et al. (2008)</i>
13	FILMTEC SW30HR-380	$3.039 \times 10^{-7}$	$1.7 \times 10^{-8}$	99.987	22.058	0.1333	16.922	1.5706	<i>Kaghazchi et al. (2010)</i>
14	Filmtec, SW30-4040	$9.058 \times 10^{-8}$	$2.11 \times 10^{-8}$	99.824	6.803	1.9171	5.089	4.2494	<i>Dimitriou et al. (2017)</i>
15	SW30-HR380	$2.533 \times 10^{-7}$	$2.5 \times 10^{-8}$	99.963	18.548	0.4002	14.144	1.7969	<b><i>Vince et al. (2008)</i></b>
16	<b>Filmtec BW30LE-440</b>	<b><math>1.215 \times 10^{-6}</math></b>	<b><math>15 \times 10^{-8}</math></b>	<b>99.829</b>	<b>68.998</b>	<b>1.6896</b>	<b>58.836</b>	<b>0.7593</b>	
17	TORAY SU 820	$1.136 \times 10^{-6}$	$2.264 \times 10^{-7}$	99.651	63.041	3.4136	54.931	0.7943	<i>Djebedjian et al. (2008)</i>
18	Filmtec8"RE 8040SN	$5.88 \times 10^{-7}$	$1.7 \times 10^{-8}$	98.919	28.567	0.0774	15.685	1.8197	<i>Avlonitis et al. (2007)</i>
19	Filmtec8"SW30HR380	$4.56 \times 10^{-7}$	$6.8 \times 10^{-9}$	98.823	31.101	0.0556	15.745	1.9419	

Fig. 6.6 shows the variation of solute rejection for the different brands of membranes. The simulation results of Fig. 6.6 indicate that almost all the membrane brands have succeeded to give high values of rejections except 4" ROGA 4160-HRa and ROGA-4000 (lines 8 and 10, respectively). In this regard, the brackish water membrane, Filmtec BW30LE-440, shows the most improvement of solute rejection. The Filmtec BW30LE-440 membrane (line 16 in Table 6.5, and Fig. 6.6) shows very promising solute rejection of 99.83% that exceeds the rejection of base case membrane (Toray TMG20D-400) which rejects solutes with efficiency of 99.8%. Therefore, the deployment of this membrane brand will positively influence the rejection parameter of the RO system of APC. However, the optimum solute rejection can be achieved using the seawater membrane FILMTEC SW30HR-380 (line 13 in Table 6.5 and Fig. 6.6) that results in an efficiency of 99.987%. The growth of solute rejection of these membranes is attributed to their high values of water permeability coefficient compared to the base case membrane. For instance, the water permeability coefficient of Filmtec BW30LE-440 is  $1.215 \times 10^{-6}$  (m/atm s) compared to the Toray Membrane TMG20D-400 (base case) of  $9.6203 \times 10^{-7}$  (m/atm s). Increasing the water permeability coefficient means an increased propensity of water permeation through the membrane pores that would reduce the salt concentration in the permeate channel and result in high rejection. It is also important to note that the solute transport parameter is related to solute flux through the membrane pores and therefore affects the solute rejection. For instance, the FILMTEC SW30HR-380 membrane obtains the optimum rejection due to its solute transport parameter of  $1.7 \times 10^{-8}$  (m/s), which is less than that of the Filmtec BW30LE-440 membrane of  $15 \times 10^{-8}$  (m/s). Moreover, the membrane ROGA-4000 has the lowest solute rejection due to its low water transport parameter of  $1.985 \times 10^{-7}$  (m/s atm) and high solute transport parameter of  $2.3 \times 10^{-7}$  (m/s) that triggers the propensity of solute passage. However, the membrane brand Spiral wound Qatar SWRO has the highest solute transport parameter and gained high solute rejection due to its  $7.092 \times 10^{-5}$  (m/s atm) water transport parameter that represents the highest value of the membranes.

From an engineering view, it can be said that the solute rejection of any membrane is affected by the combination of both water and solute transport parameters. Furthermore, the solute rejection is predominantly reliant on the membrane pore size, structure and their

intensity that would directly control the solute passage through the membrane pores. However, this study has not covered the membrane texture and pore design (beyond scope of this research) and therefore the results are interpreted based on the characteristics of water and solute transport parameters.

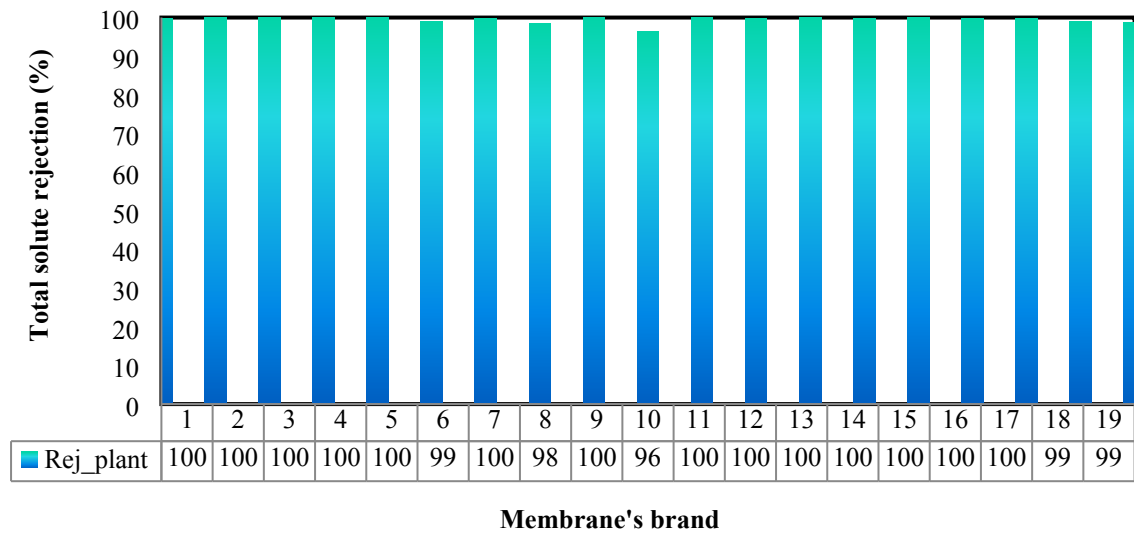
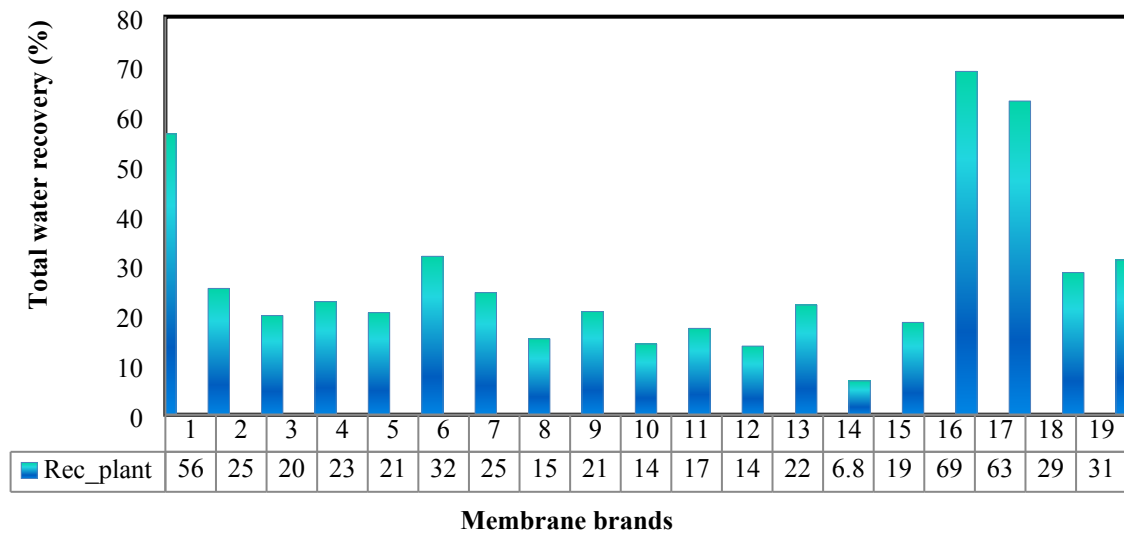


**Fig. 6.6.** Impact of membrane brands on solute rejection of a complicated brackish water RO desalination system

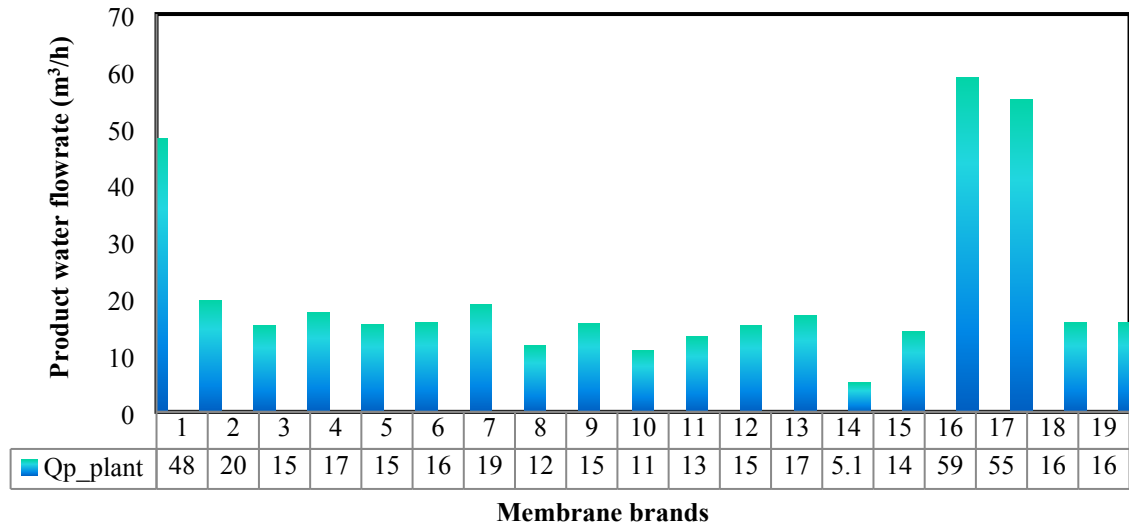
Fig. 6.7 and Table 6.5 show the total water recovery of the RO system for different brands of spiral wound membrane. In terms of water recovery, the results in Fig. 6.7 show that the best brand of membrane is Filmtec BW30LE-440 which has an optimal water recovery of 68.998 % followed by the TORAY SU 820 membrane (line 17 in Table 6.3) achieved a recovery of 63.041%. Statistically, the improvement of water recovery made by the Filmtec BW30LE-440 membrane is larger than the water recovery of base case (56.442%) by 22.2%. Again, the water flux is progressively increased with the Filmtec BW30LE-440 membrane due to its high-water transport parameter compared to the original membrane brand.

Fig. 6.7 confirms a considerable variation of water recovery for the tested membrane brands compared to the results of solute rejection (Fig. 6.6). This in turn explains the reason of recognising the water flux and associated water recovery for the RO system.

It is important to note that the simulation of the different membrane brands was carried out at the same operating conditions. Therefore, the trend of water recovery results would similarly reflect the results of total water productivity as illustrated in Fig. 6.8. In this regard, the maximum and minimum productivities obtained with the Filmtec BW30LE-440 and the Filmtec, SW30-4040 are 58.836 m<sup>3</sup>/hr, and 5.089 m<sup>3</sup>/hr, respectively. Furthermore, the productivity of the original membrane brand used in the RO of APC plant is 48.133 m<sup>3</sup>/h whereas the Filmtec BW30LE-440 membrane shows a productivity of 58.836 m<sup>3</sup>/hr i.e. an improvement in productivity of 22.2%.



**Fig. 6.7.** Impact of membrane brands on total water recovery of a complicated brackish water RO desalination system



**Fig. 6.8.** Impact of membrane brands on total product flow rate of a complicated brackish water RO desalination system

The product salinity is a paramount indicator of the performance of a RO process. Based on the simulation results shown in Fig. 6.9, the product salinity varies with the membrane brand. The data shows that the Filmtec BW30LE-440 membrane can generate product water with the lowest salinity compared to the original base case membrane brand. Statistically, the improved membrane brand attains high quality water of 1.689 ppm, compared to 1.988 ppm of the original membrane brand. The improvement percentage of product salinity of around 15% beyond the base case membrane is ascribed to an improved water flux of the new membrane that retards the product salinity. Interestingly, the result of product salinity comes with the tendency of reducing the product salinity that fits the required of distilled water to be used in the boilers. The Filmtec8I"SW30HR380 and 4" ROGA 4160-HRa membranes have constituted the best and worse product salinities of 0.055 ppm and 16.271 ppm, respectively, compared to other membrane brands. These results are derived due to the solute transport parameters that hit the maximum and minimum values of Filmtec8I"SW30HR380 and 4" ROGA 4160-HRa, respectively.

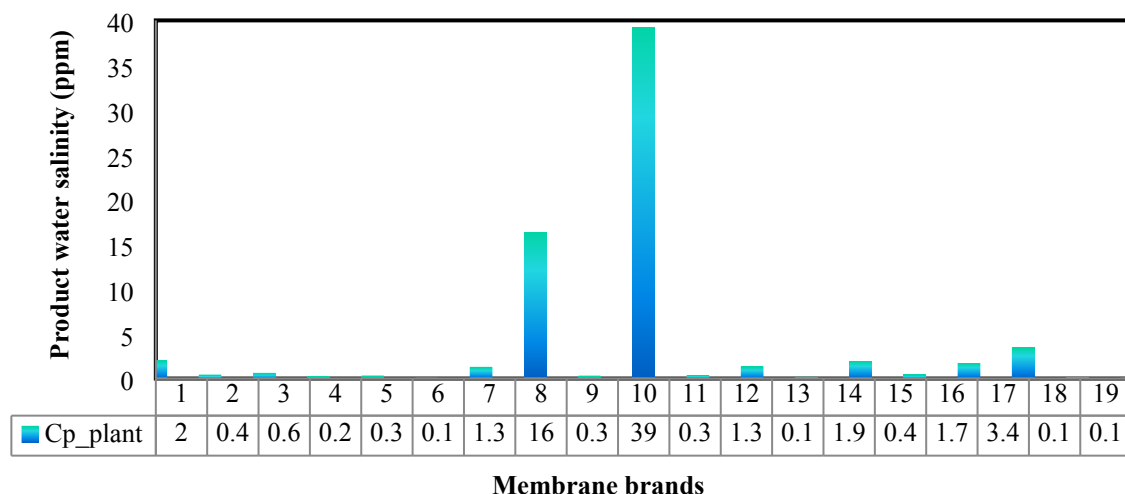


**Fig. 6.9.** Impact of membrane brands on product salinity of a complicated brackish water RO desalination system

One of the most important performance indicators of any industrial process is the specific energy consumption, which needs to be limited as much as possible since it relates the total production cost and gases emissions. Fig. 6.10 shows the specific energy consumption profile of different membrane brands deployed in the RO system of APC. It is clear from Fig. 6.10 that the Filmtec BW30LE-440 is the optimum membrane that can perform efficient filtration at the lowest specific energy consumption of 0.7593 kWh/m<sup>3</sup> compared to the original membrane's (Toray Membrane TMG20D-400) consumption of 0.8401 kWh/m<sup>3</sup>. This new membrane would reduce the energy consumption by 9.62%. This is due to the improvement of water flux that reduces the specific energy consumption. In this regard, Ettouney et al. (2002) confirmed the relationship between the feed salinity and total energy requirements of the RO system. The lower the water salinity, the higher the product purity, which permits the operation to be carried out at a lower specific energy consumption level. Furthermore, the Filmtec, SW30-4040 membrane is the worst one due to attaining the highest specific energy consumption of more than 4 kWh/m<sup>3</sup>.

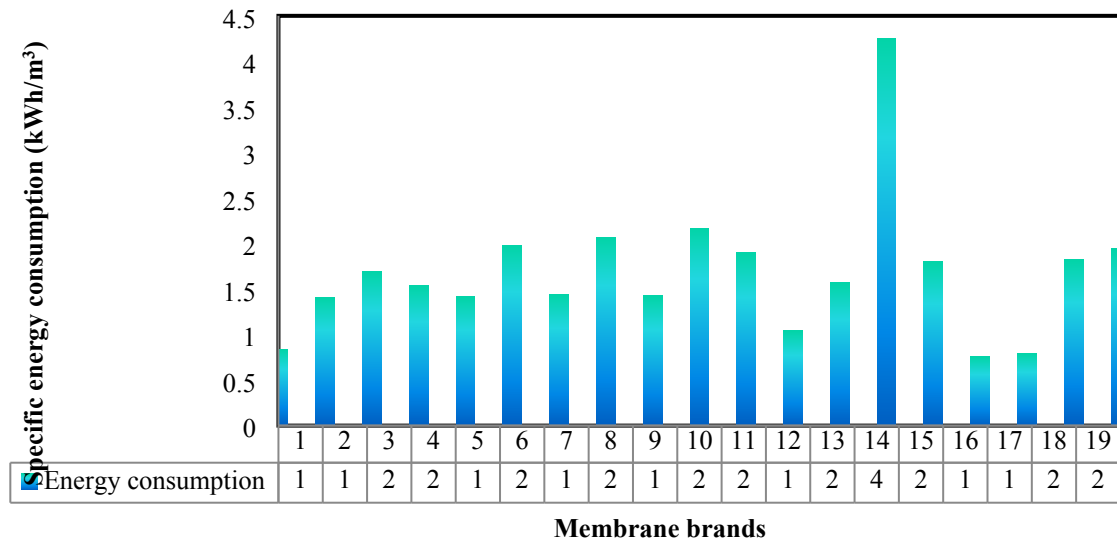


**Fig. 6.10.** Impact of membrane brands on plant energy consumption of a complicated brackish water RO desalination system

Overall, using membranes with high-water permeability parameter and low solute transport parameter would improve the treatment efficiency since there is a clear proportional relationship between these parameters and the performance metrics of RO system. Based on the results shown in Table 6.5 and Figs. 6.6 – 6.10, installing the Filmtec BW30LE-440 membrane in the RO system of APC would guarantee an improved operational performance compared to the existing membrane. Therefore, the improvements of the total plant water recovery, the total product flowrate and the energy saving at plausible product salinity are highlighted in this research.

#### **6.4 Critique of performance indicators of simple and complicated brackish water RO desalination systems based on the best brand of membranes**

This section focuses on comparing the performance indicators of the two selected case studies of simple and complicated RO brackish water desalination systems based on the best brand of membrane. Table 6.6 presents that the membrane type Filmtec BW30LE-440 is the best membrane type that can afford the best performance indicators for both the simple and complicated designs of brackish water RO desalination plants. However, the implementation of Filmtec BW30LE-440 in the complicated design of multistage multi pass RO process of APC has entailed promising performance indicators compared to the

implementation of Filmtec BW30LE-440 in the simple design. Specifically, the specific energy consumption of the complicated design of RO system is around the half of the simple design. This can be attributed to the high productivity of the complicated design compared to the simple one. Moreover, the product salinity of the complicated design of RO system is incomparable (lower) with the one obtained by the simple design. In other words, the replacement of the original membrane of RO system of APC would offer several merits compared to the same replacement of membrane for the simple design of RO system. The Filmtec BW30LE-440 membrane has been characterised by several promising advantages (Vince et al., 2008) that can support the results of this research as follows.

- High salt rejection and freshwater productivity.
- Sufficient to be instilled in the RO systems that work under low pressure to produce fresh water from brackish water resources. This membrane has been designed to produce the desired productivity with a significant saving of energy and low number of pumps.
- Adequate in managing high feed flowrate with a maximum limit of 18 m<sup>3</sup>/h.
- Large effective surface membrane area that would enhance the water productivity.
- Provides excellent structural stability.
- Fouling resistant.

**Table 6.6.** Comparison of performance indicators of two selected RO systems

Type of RO system	Best membrane type	Solute rejection %	Water recovery %	Productivity (m <sup>3</sup> /h)	Product salinity (ppm)	Specific energy consumption (kWh/m <sup>3</sup> )
Simple design	Filmtec BW30LE-440	98.283	61.594	43.615	5.425	1.499
Complicated design	Filmtec BW30LE-440	99.829	68.998	1.6896	58.836	0.759

## 6.5 Conclusions

This chapter focused on testing different brands of seawater and brackish water membranes from various suppliers on the multistage brackish water RO desalination

systems of simple and complicated designs to determine which brand of membranes gives the best performance indicators. Specifically, the performance indicators of solute rejection, water recovery, productivity, product salinity and specific energy consumption were used to compare the efficiency of these membranes and compared to the original one. The tested membranes were characterised by different values of water and solute transport parameters. Among the nineteen brands of membranes looked at, Filmtec BW30LE-440 has shown the best performance indicators for both simple and complicated designs of RO systems with the highest energy saving. In this regard, the Filmtec BW30LE-440 membrane shows an improvement of 22.24% in water recovery, 15% in product salinity and 9.62% in the specific energy consumption compared to the original membrane of the complicated design of RO system of APC. However, the Filmtec BW30LE-440 membrane shows an improvement of 9.34% in water recovery, 22.2% in product salinity, and 24.7% in the specific energy consumption compared to the original membrane of the simple design of RO system. Therefore, the Filmtec BW30LE-440 membrane is recommended as the best choice to be used in the RO system of both designs. The simulation results of this chapter have confirmed a considerable improvement of water recovery and associated specific energy consumption. However, the next chapter would discuss the optimisation of the simple and complicated designs of RO system to investigate the possible operating conditions that can entail the lowest specific energy consumption of each RO design.

## **CHAPTER SEVEN**

### **Optimisation of energy consumption in a reverse osmosis brackish water desalination plant**

#### **7.1 Introduction**

Fresh water is becoming rare in some regions of the world that associated with progressive people worldwide demands due to the increase in population growth and change of their lifestyle. Therefore, several desalination processes were invented. In this regard, the desalination of brackish water offers a feasible solution to tackle the water shortage.

Membrane technology has been used very effectively to produce fresh water from different resources of water (Tsiourtis, 2001). Specifically, RO process is a pressure-driven process and considered as one of the commercially attractive membrane technologies available for desalting brackish and seawater (Peñate and García-Rodríguez, 2012). The RO membrane can differentiate, and selectively separate salts and water based on the operating conditions such as feed salinity, applied pressure, flow rate and temperature (Tsiourtis 2001). The simple design of RO process and high quality of water produced are the main reasons why it is widely accepted throughout the world compared to other technologies such as the thermal desalination processes. However, the RO process consumes a considerable amount of energy that needs to be reduced considerably. Therefore, several studies have been carried out to minimise the specific energy consumption and accordingly the freshwater production cost, which in turn make this process more affordable. In this regard, the optimisation of the RO system has been successfully used to attain these goals. For this, the RO process market has seen a steady increase due to a primitive advancement in RO operation that is associated with lower energy consumption and reduced freshwater production cost (Shenvi et al., 2015). Some comments on the most successful research are reported below.

Zhu et al. (2008) minimised the energy consumption of RO membrane process via constraining the thermodynamic feed flow rate or permeate flow rate. Results showed that lowering of osmotic pressure would limit the energy consumption. The optimisation of energy consumption of two-pass RO seawater desalination unit and a single pass

membrane desalination unit, by considering the goal of product recovery and salt rejection, was investigated by Zhu et al. (2009b). This affirmed the optimal operational conditions need to be applied to lowering the energy consumption. Their studies showed that the two-pass process performs better than the single-pass RO one. Bartman et al. (2010) used an energy optimisation methodology of multiple RO system variables to estimate the optimal operating conditions that minimise the specific energy consumption. The results showed that increasing water recovery would lower the energy consumption with reduced salt rejection. Li (2010) implemented a constrained nonlinear optimisation framework to minimise the total energy consumption of single-stage, two-stage, and single-stage RO modules with an energy recovery device (ERD). The results showed that the two-stage module is better than one stage based on specific energy consumption and water recovery.

This chapter focuses on investigating the possibility of reducing the specific energy consumption via optimising the main control variables of two case studies of simple and complicated brackish water RO desalination systems. Finally, this chapter will compare the optimisation results of the two designs of RO systems and discuss the main outputs.

## **7.2 Case Study 1: Optimisation of energy consumption of a simple RO brackish water desalination plant**

The full details of the simple design of brackish water RO desalination process was provided in Section 3.3.1 in Chapter 3. Also, the detailed of the membrane used in the RO system was presented in Table 3.2 in Chapter 3. To systematically optimise this RO system, a steady-state operation model presented in Chapter 3 is coded to represent the configuration of RO system and then embedded within an optimisation framework. Typically, the optimisation problem is expressed as a Nonlinear Programming problem to attain the lowest specific energy consumption (objective function), as well as optimising the decision variables of operating flow rate and pressure for a given feed concentration and temperature. The fixed feed water characteristics of 2540 ppm and 28.8 °C of feed water salinity and temperature respectively are considered. Moreover, the optimisation problem has been associated with upper and lower limits of decision variables as characterised by the membrane manufacturer. Also, to quantify the high standards of the

filtration process, feasible constraints of the upper and lower bound of feed flow rate of each membrane are considered. To represent the viability of the optimisation, the optimisation results will be compared against the simulation results of the simple design of RO system.

### 7.2.1 Mathematical optimisation problem

Given: Feed water conditions, RO module specifications.

Optimise: The optimisation variables of feed pressure, and flow rate.

Minimise: The specific energy consumption of RO system.

Subject to: Equality and inequality constraints of the process model and limits of optimisation variables, respectively. Hence, the optimisation problem is mathematically fashioned as

$$\text{Min} \quad E_{consumption}$$

$$P_{f(plant)}, Q_{f(plant)}$$

Subject to: Equality constraints: RO process model

Inequality constraints:

a) Lower and upper limits of feed flow rate of RO system

$$(7.2 \text{ m}^3/\text{h}) \quad Q_{f(plant)}^L \leq Q_{f(plant)} \leq Q_{f(plant)}^U (396 \text{ m}^3/\text{h})$$

$$(10 \text{ atm}) \quad P_{f(plant)}^L \leq P_{f(plant)} \leq P_{f(plant)}^U (40.464 \text{ atm})$$

b) Lower and upper limits of feed flow rate of each membrane module

$$(3.6 \text{ m}^3/\text{h}) \quad Q_{f(membrane)}^L \leq Q_{f(membrane)} \leq Q_{f(membrane)}^U (198 \text{ m}^3/\text{h}).$$

### 7.2.2 Optimisation results

Table 7.1 shows the simulation values as the base case (not optimised) of the simple design brackish water RO desalination process at given feed salinity and temperature. Also, Table 7.1 represents the optimisation results including the performance indicators. The ratio of energy-saving of RO system is calculated by subtraction of simulated and optimised values. It can be clearly seen that the optimisation framework has entailed a gain of energy

saving of 37.3% based on the optimum feed flow rate of 14.46 m<sup>3</sup>/h and pressure of 24.62 atm. Also, the water recovery has been improved by 22.4% due to applying the optimal operating conditions. In this regard, the water productivity has reduced by 12.2% that associated with a reduction of **retentate flow rate by 50.1%** and causes an improvement of product salinity by 35.66 %.

**Table 7.1.** Simulation and optimisation results of a simple RO system at base case conditions

Feed conditions			Optimised feed conditions	
Parameter	Value	Unit	Parameter	Value
Plant feed pressure	12.04	Atm	Optimal operating pressure	24.62
Plant feed flow rate	20.4	m <sup>3</sup> /h	Optimal feed flow rate	14.46
Feed operating salinity	2540	ppm	Feed operating salinity	2540
Feed operating temperature	28.8	°C	Feed operating temperature	28.80
Simulation results		Unit	Optimised results	
Plant water recovery	56.016	%	Plant water recovery	68.548
Plant salt rejection	99.205	%	Plant salt rejection	99.488
Produced water flow rate	11.290	m <sup>3</sup> /h	Produced water flow rate	9.912
Produced water salinity	20.190	ppm	Produced water salinity	12.990
Retentate flow rate	<b>9.110</b>	m <sup>3</sup> /h	Retentate flow rate	<b>4.548</b>
Specific energy consumption	1.897	kWh/m <sup>3</sup>	Specific energy consumption	1.189
<b>Energy-saving = 37.3%</b>				

### 7.3 Case Study 2: Optimisation of energy consumption of a complicated RO brackish water desalination plant of APC

The RO process has been employed to produce potable water from brackish water resources in the APC. However, the RO process still operates at an elevated level of energy consumption, in kWh per m<sup>3</sup> of product water, due to the use of high-pressure pumps. The description of the complicated multistage multi pass RO system of APC is provided in Chapter 3 in section 3.3.3. Also, the feed operating conditions and characteristics of the membrane used are included in Tables 3.4 and 3.5, respectively, in Chapter 3. To the best of the author's knowledge, the lowering of the specific energy consumption of RO system of APC via optimisation cannot be found in the open literature. Therefore, the current section attempts to optimise the decision variables of feed pressure and flow rate for a considered feed salinity of 1098.62 ppm and temperature 25 °C to explore the lowest

energy consumption. The model developed in Chapter 3 is characterised to predict the performance indicators of the complicated configuration of RO system of APC. Afterwards, the model is embedded within an optimisation framework to attain the lowest specific energy consumption. To formalize a safe operation of the RO system, the optimisation has considered the upper and lower limits of decision variables as characterised by the membrane manufacturer. Also, to quantify the high standards of the filtration process, feasible constraints of the pressure loss along the x-axis of membrane length and upper and lower bound of feed flow rate of each membrane are considered. To affirm the viability of the optimisation, the simulation results of the RO process are compared against the optimisation results to explore the total energy saving and the improvements of performance indicators.

The original simulation of the multistage multi pass RO plant of APC is achieved under the base operating conditions are listed in Table 7.2.

### ***7.3.1 Mathematical optimisation problem***

The main goal of this optimisation is to optimise the RO system of APC, i.e., to target the objective function of minimising the specific energy consumption by forecasting the best-operating conditions (optimal values) of the process, which include feed pressure and feed flow rate at fixed salinity and temperature. The fixed feed water characteristics of 988.93 ppm and 25 °C of feed water salinity and temperature respectively are considered. The mathematical expression of the optimisation is as follows.

Given: Feed water conditions, RO module specifications.

Optimise: The optimisation variables of feed pressure, and flow rate.

Minimise: The specific energy consumption of RO system.

Subject to: Equality and inequality constraints of the process model and limits of optimisation variables, respectively.

Hence, the optimisation problem is mathematically fashioned as

$$\text{Min} \quad E_{consumption}$$

$$P_{p(plant)}, Q_{f(plant)}$$

Subject to: Equality constraints: RO process model

Inequality constraints:

a) Lower and upper limits of feed flow rate of RO system

$$(29.04 \text{ m}^3/\text{h}) \quad Q_{f(\text{plant})}^L \leq Q_{f(\text{plant})} \leq Q_{f(\text{plant})}^U (154.48 \text{ m}^3/\text{h})$$

$$(5 \text{ atm}) \quad P_{f(\text{plant})}^L \leq P_{f(\text{plant})} \leq P_{f(\text{plant})}^U (20 \text{ atm})$$

b) Lower and upper limits of feed flow rate of each membrane module

$$(3.63 \text{ m}^3/\text{h}) \quad Q_{f(\text{membrane})}^L \leq Q_{f(\text{membrane})} \leq Q_{f(\text{membrane})}^U (19.31 \text{ m}^3/\text{h}).$$

### 7.3.2 Optimisation results

Table 7.2 displays the simulation values as the base case (not optimised) of the RO process at given feed salinity and temperature. More importantly, the optimisation results including the performance indicators are presented in Table 7.2. The ratio of energy-saving of RO system is accounted by subtraction of simulated and optimised values. It can be clearly seen that the optimisation framework has entailed a gain of energy saving of 35% based on the optimum feed flow rate of 61.66 m<sup>3</sup>/h and pressure of 7.574 atm. Moreover, there is a considerable enhancement of water recovery by 12.8%, which contributes to improving the produced water salinity by 13.5%. Furthermore, the produced water flow rate is reduced by 17.9% whilst at the same time reducing the retentate flow rate by 39.7%.

**Table 7.2.** Simulation and optimisation results of RO system of APC at base case operating conditions

Feed conditions			Optimised feed conditions	
Parameter	Value	Unit	Parameter	Value
Plant feed pressure	9.220	atm	Optimal operating pressure	7.574
Plant feed flow rate	84.760	m <sup>3</sup> /h	Optimal feed flow rate	61.660
Feed operating salinity	988.930	ppm	Feed operating salinity	988.930
Feed operating temperature	25	°C	Feed operating temperature	25
Simulation results		Unit	Optimised results	
Plant water recovery	57.205	%	Plant water recovery	64.545
Plant salt rejection	99.797	%	Plant salt rejection	99.922
Produced water flow rate	48.490	m <sup>3</sup> /h	Produced water flow rate	39.790
Produced water salinity	2.0052	ppm	Produced water salinity	1.734
Retentate flow rate	36.27	m <sup>3</sup> /h	Retentate flow rate	21.87
Specific energy consumption	0.9977	kWh/m <sup>3</sup>	Specific energy consumption	0.6478
Energy-saving = 35%				

#### 7.4 Evaluation of optimisation of two different sizes of brackish water RO desalination systems

This section utilises a comparative assessment of the obtained optimisation results of simple and complicated designs of brackish water RO desalination systems. A precise look at the optimisation results of the two case studies presented in Tables 7.1 and 7.2 will confirm that the complicated design of RO process requires less specific energy consumption compared to the simple design one.

The optimised lower feed pressure used in the complicated design associated with the higher productivity of fresh water are the main reasons behind the necessity of a lower specific energy consumption. Furthermore, the feed salinity of the complicated design of RO process is almost less than half the feed salinity of the simple design. In this regard, Karabelas et al. (2018) asserted that seawater desalination is associated with a higher specific energy consumption compared to brackish water desalination. This is due to much smaller feed salinity and lesser osmotic pressure for the brackish water desalination. However, Tables 7.1 and 7.2 show that the simple design of RO process has entailed with a higher energy saving after optimising the decision variables of the process compared to the complicated design of RO process.

Obviously, the multistage multi pass of retentate and permeate reprocessing design of RO process of APC requires higher feed flow rate due to the existence of higher number of pressure vessels in the first column of the first stage compared to the simple design of retentate reprocessing design of RO process. However, lower feed pressure is applied in the complicated design compared to the necessity of a higher operating pressure in the simple design of RO process. Again, the high salinity of simple design of RO process requires a higher feed pressure. Another advantage of the complicated design is the producing of very low salinity of fresh water at a higher productivity compared to the simple design of RO process.

## 7.5 Conclusions

In this chapter, a single optimisation framework was developed to mitigate the total energy consumption of two different sizes of simple and complicated brackish water RO desalination systems. This is basically carried out within allowed operational limits of the operating conditions to maintain a safe process. In general, the manipulation of control variables via optimisation has a positive influence on raising the water recovery of simple and complicated RO design processes by 22.4% and 12.8%, respectively. Furthermore, the optimisation caused a reduction of the specific energy consumption by 37.3 and 35% for the simple and complicated designs when compared with the original simulation value of consumed energy. Also, the product water salinity has been improved by 35.66% and 13.5% for the simple and complicated designs. Therefore, it can be said that the optimisation used in this chapter has economically upgraded the RO systems with a substantial improvement in the process performance. The optimisation results of this chapter introduced a noticeable improvement of several performance indicators. Therefore, it is fair to claim the consistency of using the optimisation to upgrade the performance of RO system especially for the hypothesis of adding an ERD in the RO system. Furthermore, the specific energy consumption is quite related to the energy losses in the compartments of RO system. Therefore, the next chapter will attempt to investigate the locations of the highest destruction exergy and thermodynamic limitations in a detailed study specialized for the complicated design of RO process of APC.

## **CHAPTER EIGHT**

### **Thermodynamic limitations and exergy analysis of reverse osmosis brackish water desalination plant**

#### **8.1 Introduction**

Due to the scarcity of freshwater resources, the improvement of water desalination technologies is by far the most important target for current researchers aiming to deliver clean, safe, and healthy water (El-Emam and Dincer, 2014). Furthermore, there is an exponential growth of water need for domestic, agricultural, industrial, and other usages. The main desalination processes used to desalinate water are the Reverse Osmosis (RO) and multi-stage flash (MSF) processes which counting about 90% of the total fraction of fresh water produced in the world. However, the other water desalination technologies of multiple effect desalination (MED), Electrodialysis, and vapor compression are sharing the remaining fraction of 10% of freshwater produced (Kim, 2011).

The seawater and brackish water desalination using the RO process has dominated the membrane technologies due to producing freshwater at reduced energy consumption. Indeed, the simple design of compact size and modularity of RO units and ease of operation at ambient temperature have added other merits and introduced the RO process on the top list of water desalination technologies (Ahmad and Schmid, 2002). Interestingly, the flexibility in capacity expansion of RO process with short construction periods, low investment costs and low periodical maintenance enable the construction of RO desalination plants of different sizes in the rural areas of water shortage. However, the performance capacity of RO process is directly related to the inlet conditions and therefore it varies based on the seawater quality, site location and the start-up and shut-off (Herold et al., 1998; Latorre et al., 2015).

The main principle of RO process is to treat poor quality (high salinity) water and produce high quality freshwater and disposed brine. This is originally occurring due to using higher pressure than the osmotic pressure that serves water passage through the membrane pores from the high concentration side into the low concentration side complemented by the rejection of majority salts (Goh et al., 2016; Al-Obaidi et al., 2018a). However, the RO process and especially the large-scale RO systems require a vast amount of energy to operate the pumps. In other words, the RO process consumes a considerable amount of energy due to the exergy destruction in several units of the process especially in large scale RO desalination systems. In this regard, the necessity of energy is directly related to the operating conditions where an increase in the feed salinity or pressure would cause an increase in the supplied energy (Patel et al., 2020; Alsarayreh et al., 2020; Al-Obaidi et al., 2018b). Although, water desalination based RO process has been proved to expense less than the half of energy needed for thermal processes (Bouguecha et al., 2004), the research on improving the existed water desalination plants is important to introduce the RO process as the most reliable, efficient and economical option compared to other involved water treatment technologies (Cerci, 2002). In this regard, the brackish RO and seawater water desalination consume about 1 kWh/m<sup>3</sup>, and 1.5 to 2.5 kW h/m<sup>3</sup>, respectively. However, the MSF and MED thermal processes require 4 to 6 kW h/m<sup>3</sup>, 1.5-2.5 kW h/m<sup>3</sup>, respectively. Therefore, it is expected to notice several articles in the open literature that interested on improving the RO desalination plants. The main intention of

these articles was to investigate the most reliant parts of energy dissipation. The exergy based on thermodynamic properties was on top of other methodologies used to explore the energy losses in actual RO desalination plants (Al-Zahrani et al., 2012). Exergy is quite different than energy, where exergy is always destroyed and not conserved like energy in the process. More importantly, the thermodynamic imperfections of any industrial process cannot be measured by energy calculations (first law of thermodynamic) unlike the exergy that signifies the causes of energy losses and justifies the irreversibilities such as chemical reactions, heat transfer through a finite temperature difference, friction, mixing, and unrestrained via the second law of thermodynamic (Aljundi, 2009).

The exergy and energy analysis have gradually attracted the attention to achieve the requirements for thermodynamic calculations with high accuracy. This attributed to the complexity of power-generating units, which significantly increased and necessitated the operation of power plants in the most efficient manner, as a result to depletion the rate of fossil fuel reserves and the environmental impacts. Interestingly, the most aim of exergy analysis is to improve the thermodynamic performance of the process by offering an option to reduce the supplied electrical energy and therefore making the desalination plant more cost effective. In other words, investigating the main sources of exergy dissipation would conceivably reduce the total energy consumption (Villafafila and Mujtaba, 2003; Qi et al., 2012; Zhao et al., 2013)

Aljundi (2009) stated that the exergy analysis is a potential tool to determine the inefficiencies of the RO process, which can aid to improve the overall performance. The exergy enables the evaluation of maximum work that can be extracted from a certain system relative to the surrounding environment (El-Emam and Dincer, 2014). The following present some successful examples of these articles.

Cerci (2002) conducted the exergy analysis of RO desalination plant in California with capacity 7250 m<sup>3</sup>/d using actual plant operation data. The exergy destruction distribution is evaluated, and the results showed that in the membrane modules the largest exergy destruction is occurred with about 74.07% of the total exergy input. Moreover, the mixing chamber has got the smallest exergy destruction of 0.67% of the total exergy input.

Kahraman et al. (2005) examined the exergy destruction rates and exergy flow rates in a brackish water RO desalination plant. They showed that the most exergy destruction can

be found in motor, pump, and separation units. Statistically, 39.7% of the total exergy is destructed in the pump/motor of the RO unit. This also showed that the cost of desalination can be reduced drastically using high efficiency pumps and motors. Moreover, the Second Law efficiency of RO system is about 8% which is very low.

Aljundi (2009) evaluated the exergy flow rates and the exergy destruction rates thermodynamically throughout the RO plant of Al-Hussein thermal power station located in Jordan. He showed that the exergy destruction occurred within the throttling valves and in the pumps and motors with rates 56.8%, 21%, and 19.6%, respectively. However, the second law efficiency was very low and accounted about 4.1%. Therefore, Aljundi (2009) highlighted the importance of employing high-efficiency pump/motor with energy recovery devices with replacing the existed throttling valves.

El-Emam and Dincer (2014) investigated the RO seawater desalination plant performance based on the first and second laws of thermodynamics. The results showed that the largest amount of irreversibility occurs within the high-pressure pump of 17.16% and in the RO module of 67.8%. However, the overall system exergy efficiency is about 5.82 %, and the exergy destruction reduced by 35.5% by using a Pelton turbine as energy recovery compared with using an expansion valve.

The above research confirmed the possibility of mitigating the thermodynamic limitations of RO systems where several researchers focused on delivering feasible options to resolve this issue. Most importantly, the intention was to specify the most units responsible to dissipate energy. However, no attempts can be found in the open literature to analyse the exergy losses and thermodynamic limitations of the RO system of Arab Potash Company (APC). More specifically, the sensitivity analysis of exergy at the thermodynamic restrictive limit of a medium-sized industrial RO brackish water desalination plant of APC has not been yet investigated. Therefore, this chapter comes to resolve this challenge by carrying out a thorough exergy analysis based on chemical and physical exergies for all the main parts of the RO desalination plant. It is fair to expect that this study would be a successful tool to determine the parts of RO system of APC to be considered for further improvement. Furthermore, it is well expected that the consequences of this study would aid to attain the aim of this dissertation and improve the performance of brackish water desalination via the multistage RO process.

## **8.2 Thermodynamic limitations and exergy analysis of brackish water RO desalination plant of APC**

This section focuses on analysing the thermodynamic limitations and exergy destruction of the multistage multi pass brackish water RO desalination system of Arab Potash Company (APC). The examined parts of RO system include (1) the RO membrane modules in which the saline water is separated into the permeate and retentate, (2) the throttling valve where the pressure of liquid is reduced, (3), mixing zones where the permeates or retentate streams are mixed, (4) and various process components such as pumps, disposal water stream, and product water stream. To carry out this study, a sub-model of exergy analysis was collected from literature and embedded in the original RO model developed in Chapter 3.

### ***8.2.1 General overview of the RO system of APC and tested locations***

The RO desalination system of APC was mainly constructed to desalinate the brackish water of feed salinity 1098.62 ppm and flow rate 74 m<sup>3</sup>/h. The pure produced water is demineralized by ion exchangers and directly fed to the boilers. The RO plant produces 1200 m<sup>3</sup>/d equivalent to 13.85 kg/s of pure water with salinity around (2 ppm).

At this point it is worth to noting that there are two groups (A, and B) in first and second passes of RO process, which have the same number of RO membranes and arranged in parallel. The flow diagram of the plant is shown in Fig. 8.1. At position (0) the brackish raw water fed to the plant with a total flow rate 1776.00 m<sup>3</sup>/day which contains 1536 m<sup>3</sup>/day raw feed water mixed with a recycled retentate of plant 240 m<sup>3</sup>/day. The mass feed flow rate is divided into two parallel streams (group A and group B) called stages and then pumped with high pressure pump (1-2) to the RO membrane modules (3-10). The membrane modules require high operating pressure to overcome the osmotic pressure and fluid friction that occurs across the membranes. The high-pressure pump is used to raise the feed water from 923.071 kPa at position (3) to 934.22 kPa at position (4). The retentate water results from the RO module (6,8, 10 and 12) are mixed and fed to the next stage in the first pass of RO process to produce a retentate at (14,16) and then is dis-charged to the a drainage system at position (18). However, the permeate water streams (5, 7, 9, and 11)

collected with permeate from next parallel stage (13, 15) at position (17). Then, this permeate is fed into the membrane modules in first stage of second pass RO process by high pressure pumps (19, 20). Next, the result permeates from all RO modules of second pass (21, 23, 26, and 28) are mixed and collected in a product tank at position (30) with salinity of around 2 ppm at a relatively daily production capacity of 1200m<sup>3</sup>/day. The retentate results from the first stage composed of two RO modules (22, 24) is fed to second stage (one RO module) and then fed to the third final stage (25) of one RO module. Finally, the retentates result from the third final stage of second pass (27) of group A is mixed with retentate of group B at position (29) and recycled back to couple with plant feed raw water. The recycled flow passes through a throttling valve (31).

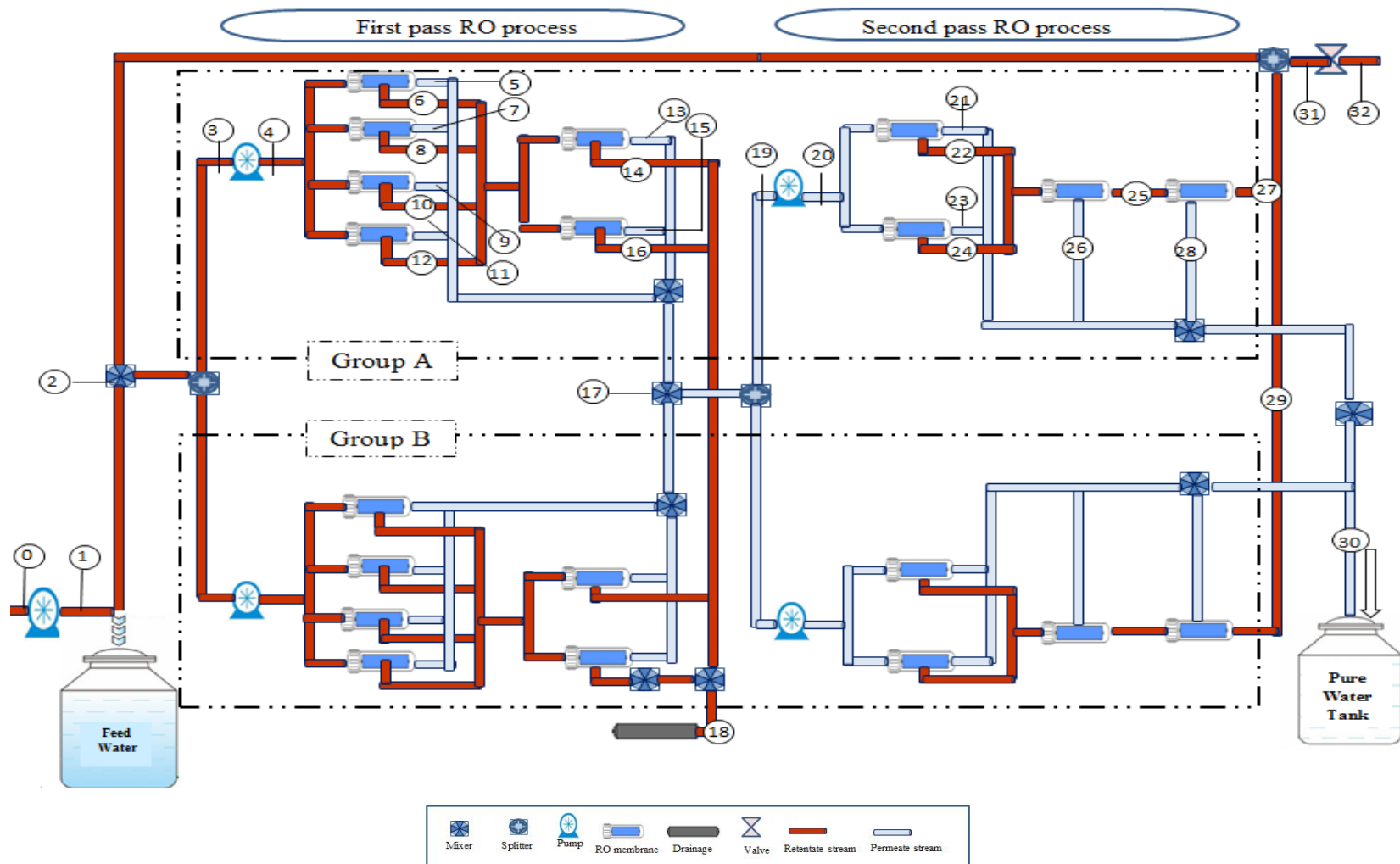


Fig. 8.1. Schematic diagram of the multistage RO desalination plant of APC

### 8.2.2 Exergy analysis

The RO brackish water desalination plant of APC performs an efficient separation process in which the incoming brackish water is separated into retentate water (brine) and product water (low salinity water). Based on this, the analysis of salt and pure water properties must be considered. Salinity is usually expressed in part per million (ppm) and defined. The mole fraction of salt  $x_s$  is determined from the following relations (Cengel et al., 1999)

$$mf_s = \frac{m_s}{m_{mix}} = \frac{N_s M_s}{N_{mix} M_{mix}} = x_s \frac{M_s}{M_{mix}} \quad (8.1) \quad mf_w$$

$$= x_w = 1 - mf_s \quad (8.2)$$

$$Mf_w = \frac{M_w}{M_{mix}} \quad (8.3)$$

$mf$ ,  $M$ ,  $N$ , and  $x$  are the mass fraction, molar mass, number of moles, and the mole fraction, respectively. Also, the subscripts  $s$ ,  $w$ , and  $mix$  represent the salt, water, and mixture of saline water, respectively.

The molar mass of the saline water can be expressed as

$$M_m = \frac{m_m}{N_m} = \frac{N_s M_s + N_w M_w}{N_m} = x_s M_s + x_w M_w \quad (8.4)$$

Combining Eqs. (8.1), (8.2), (8.3) and (8.4) yields Eq. (8.5), and (8.6) to convert the mass fractions into mole fractions. The molar masses of water and NaCl are 18.0 kg/kmol, and 58.5 kg/kmol, respectively.

$$x_w = \frac{M_s}{M_w \left( \frac{1}{mf_w} - 1 \right) + M_s} = \frac{58.5}{18 \left( \frac{1}{mf_w} - 1 \right) + 58.5} = 1 - x_s \quad (8.5)$$

$$x_s = \frac{M_w}{M_s \left( \frac{1}{mf_s} - 1 \right) + M_w} = \frac{18}{58.5 \left( \frac{1}{mf_s} - 1 \right) + 58.5} = 1 - x_w \quad (8.6)$$

Also, the summation of salt and water mole fractions equal one ( $x_w + x_s = 1$ ).

The salinity of brackish water of APC plant is 1098.62 ppm is corresponding to salt and water mass fractions of  $mf_s = 0.001098$  and  $mf_w = 0.99890138$  as  $PPM = mf_s \times 10^6$ , respectively. Also, the mole fractions are calculated from Eqs. (8.5), and (8.6) to be  $x_s = 3.383 \times 10^{-4}$  and  $x_w = 0.9997$ , respectively.

The average salinity of brackish water of APC is 0.109862% and therefore it can be considered as diluted solution since the salinity is lower than 4%. The diluted solution can approximately behave as an ideal solution where it is reasonable to ignore the effect of dissimilar molecules (molecules of salt and water) on each other.

The extensive properties per unit mass of a mixture can be represented by enthalpy  $h$  (kJ/kg) and entropy  $s$  (kJ/kg K). These properties can be determined by the sum of each individual component in a mixture at specified temperature and pressure (Klotz, 1964) as depicted in the following expressions

$$h = \sum m f_i h_i = m f_s h_s + m f_w h_w \quad (8.7)$$

$$s = \sum m f_i s_i = m f_s s_s + m f_w s_w \quad (8.8)$$

$h_s, s_s, h_w, s_w$ , are the specific enthalpy of salt (kJ/kg), specific entropy of salt (kJ/kg K), the specific enthalpy of water (kJ/kg), and specific entropy of water (kJ/kg K), respectively.

The inlet conditions of brackish water are presented in Table 8.1. These values will be taken as the properties at the dead state.

**Table 8.1.** The dead state operating conditions of RO desalination plant of APC

Temperature	Pressure	Salinity	Flow rate
25 (°C) (298.15 K)	9.22 (atm) (934.217 kpa)	1.0986 (kg/m <sup>3</sup> ) (1098.62 ppm)	0.0205 (m <sup>3</sup> /s) (20.49 kg/s)

The enthalpy and entropy of salt and water at a given temperature  $T$  (K) can be determined from the following relations (Cerci, 2002, Kahraman and Cengel, 2005)

$$h_s = h_{s0} + C p_s (T - T_o) \quad (8.9)$$

$$s_s = s_{s0} + C p_s \ln \left( \frac{T}{T_o} \right) \quad (8.10)$$

$$h_w = h_{w0} + C p_w (T - T_o) \quad (8.11)$$

$$s_w = s_{w0} + C p_w \ln \left( \frac{T}{T_o} \right) \quad (8.12)$$

It is worth to mention that the enthalpy and entropy are dependent on temperature but independent of pressure (Cerci, 2002). The specific heat of salt  $C_{p_s}$  at 25 °C is 0.8368 (kJ/kg K), while the specific heat of water  $C_{p_w}$  at 25 °C (dead state) is 4.1816 (kJ/kg K). Moreover, the enthalpy and entropy of salt and water at 25 °C are  $h_{s0} = 21.0455$  (kJ/kg) and  $s_{s0} = 0.07328$  (kJ/kg K),  $h_{w0} = 104.86$  (kJ/kg) and  $s_{w0} = 4.180$  (kJ/kg K), respectively (El-Emam and Dincer, 2014).

The entropy of saline water per unit mass in an ideal solution at a specified temperature  $T$  (K) and pressure  $P$  (kpa) is determined by

$$s = mf_s \times s_s(T,P) + mf_w \times s_w(T,P) - R(x_s \ln x_s - x_w \ln x_w) \quad (8.13)$$

$R$  represent the gas constant and equals 8.314 (kJ/kmol K)

The exergy  $Ex_{gy}$  (kJ/kg) of a flow stream is given as (Cengel and Boles, 2007; El-Emam and Dincer, 2014; Cerci, 2002; Kahraman and Cengel, 2005)

$$Ex_{gy} = (h - h_o) - T_o(s + s_o) \quad (8.14)$$

Also, the rate of exergy flow associated with a fluid stream is given by Eq. (8.15)

$$\dot{X} = \dot{m} Ex_{gy} = \dot{m} [(h - h_o) - T_o(s + s_o)] \quad (8.15)$$

The model equations presented above is coded and solved within gPROMS software suite and used to evaluate the specific exergy and exergy flow rates of various locations throughout the RO system. Afterwards, the exergy flow rates of the specified locations will be used to evaluate the exergy destructed within any selected unit, component, and stream via the evaluation of exergy balance.

### ***8.2.3 Discussion of exergy distribution of the RO system***

The specific exergy, exergy rate and the rate of exergy change at all major states for each component of RO desalination plant are evaluated. The results are listed in Table 8.2. The selected locations of the states for each component are numbered in the schematic diagram of the RO desalination plant in Fig. 8.1.

The exergy at position (0) is zero since no energy consumption at this point. However, at position (1), the high-pressure pump provides the system with energy to work at the dead state, (25 °C, 9.22 atm, 950.16 ppm, and 17.72 kg/s). Point (1) presents the feed brackish raw water stream of plant before connected with retentate plant stream at point (2), where the exergy rate is 25.163 kJ/kg. Occasionally, this pump has not been involved in the RO

system of APC since it only used to draw water from well and pumping it into the RO system. The RO system contains four high pressure pumps, two in the first pass and two in the second pass.

It is worth to note that the exergies of retentate (brine) streams are negative because of higher salinity than the dead state level.

The input brackish water stream enters the RO system at temperature 30 °C and pressure 9.22 atm, and the output streams are the permeate and retentate that exit at the same temperature and pressure but with different salinities. As shown in Table 8.1, there is a total of 9.432 kW exergy input to the system through the pumps. About 67.8% of the exergy destroyed by the group A of first pass RO process at position (3, and 4) and the remaining 32.2% is contributed by the high pressure pumps of group A of second pass RO process at position (19, and 20).

The exergy of raw brackish water at position (2) which presents a mixing point will be assigned as zero since it indicates the dead state (Cerci, 2002). However, Fig. 8.1 shows that the feed raw water relates to a recycled retentate stream of 2.77 kg/s. At the connection point, the measured temperature confirmed an increase from 25 °C to 30°C that causes an increase in the exergy rate by 16.699 kJ/kg, that associated with an increase in the raw water salinity to 1098.62 ppm and the total feed plant flow rate to 20.49 kg/s. A total 9.31% of the input exergy is destroyed (Table 8.2) due to the mixing of recycled stream of the second pass and the feed raw water at location (2). This is not surprising statement because a mixing dot has a potential to produce work when solutions of different concentrations are mixed reversibly. Location (2) represents a reversible mixing point where low salinity water is mixed with high salinity water, and therefore a reversible work could be delivered, but it is not. Thus, the exergy destroyed during the mixing process represents the work that would be produced if the mixing process occurred reversibly (Wark, 1995) .

The positions (5-16) represent the 1<sup>st</sup> pass RO membrane components where the feed brackish water separates to the permeates at (5, 7, 9, 11, 13, and 15) and the retentates at positions (6, 8, 10, 12, 14, and 16) at which the exergy destroyed with 28.26 % by RO permeate streams, and 41.33% by RO retentate streams of total exergy input. Table 8.2 indicates that the pressure drops from 9.22 atm to 8.94 atm in the separation process (the

first pass). The decreases in brine pressure causes an increase in the dissipated exergy and that means the exergy destroyed by retentate lines more than exergy destroyed by permeate lines.

Regarding the second pass of RO system, the permeate product from the first pass is pumped by high pressure pumps to the second pass at positions 21 to 28. Then, this point indicates the total input exergy. The fed permeate water is processing in the second stage and produces the high quality water at positions 21, 23, 25, and 27 and retentates at positions 22, 24, 26, and 28. This is reasoned a dissipated exergy of the total exergy input of 69.39 % caused by the permeate streams and 71.36 % by retentate streams. This can be attributed to a decrease in the brine pressure, which results in an increase in the exergy destroyed in retentate lines than the permeate lines. The outgoing retentate at position 29 leaves the system at dead state of system 25 °C and 9.22 atm with a high salinity of 409.2 ppm and has a negative exergy rate of -0.087 kW. The negative sign is an evidence that the work input to the brine is essential to drive the brine into its dead state. It is worth to noting that this point considers as a mixing point of retentate. However, the product permeate water at position 30 has a positive exergy rate of 6.04 kW and has a potential to produce work relative to the dead state. The difference between the exergies of the retentate and the product water is the net exergy discharge from the system, which is equal to 2.91 kW. This quantity is the minimum work requirement to extract product water with a salinity of 2 ppm at a mass flow rate of 13.85 kg/s from the incoming saline water of 1098.62 ppm flowing at a mass flow rate of 20.49 kg/s.

The net exergy discharge is another feasible tool to represent the net salinity exergy discharge due to its relation to the salinity variation. Table 8.2 shows positive and negative values of the rate of exergy change of components. This is also a clear indication of transferred exergy to component (positive) and destroyed exergy by component (negative).

Table 8.2 indicates that the largest exergy loss occurs in the desalination process at position (17) of mixed permeate streams, and mixed products at position (30) with rate of 5.88 kW, and 9.03 kW, respectively. This accounts for 62.28%, and 95.74% of the total exergy input. Furthermore, the disposed retentate stream at position (18) and the mixing point of retentate streams of plant at position (29) with rate of 7.57 kW, and 6.13 kW,

respectively. This accounts for 71.18 %, and 64.95 % of the total exergy input, respectively.

The disposal retentate at position (18) has a negative exergy rate of -4.33 kW , this attributed to the work input to the retentate is required to bring it to the dead state 25 °C and 9.22 atm from 29.9 °C and 8.68 atm, besides the high salinity of discharged retentate water of 4426.27 ppm.

Table 8.2 also shows that the brine pressure in throttling valve at position (31, and 32) decreased from 13.8 atm to the dead state pressure 9.22 atm, resulting in a total 2.99 kW of exergy destruction, which amounts to 31.71% of the exergy input.

The second law of efficiency of the RO desalination plant is determined by dividing the net salinity exergy by the total exergy input provided by the first and second passes pumps. It gives

$$\text{Efficiency} = \frac{\text{Net Exergy rate}}{\text{Total Exergy Input}} \quad (8.16)$$

From the above relation, the efficiency of the first pass of RO system is 1.86% of the total input energy, while the second pass is 2.63%. This indicates that the RO system at specified rates could be accomplished using only 4.48 kW of exergy instead of 9.43 kW. In a fact, most of the exergy input to the RO system is destroyed in the components, and the remaining exergy is discharged from the system. The exergy destruction occurs due to the pressure drops in the mixing points, the membrane modules, the brine transmission streams, and the throttling valve. Based on this, it can be said that the different results of exergies for outgoing streams depend on the salinities different.

**Table 8.2** Rate of exergy change of major components of RO of APC desalination plant

Component	Location	Temperature (°C)	Pressure (kpa)	Mass rate (kg/s)	Salinity (ppm)	Chemical Exergy (kJ/kg)	Physical Exergy (kJ/kg)	Specific Exergy Ex (kJ/kg)	Exergy rate X (kJ/kg)	Rate of exergy change $\Delta X$ (kW)	$\Delta X$ (kW)
Pump for tank	0	25	101.325	17.72	950.16	0	0	0	0	25.1624	25.1624
Pump for tank	1	25	934.22	17.72	950.16	-0.08	1.5	1.42	25.1624	-17.577002	--
Mixing with opening valve	2	30	934.22	20.49	1098.62	-0.1037	0.4739	0.3702	7.585398	-0.877798	0.8778
Before 1 <sup>st</sup> pass pump 1 <sup>st</sup> stage	3	25	923.07	10.25	549.31	-0.0531	0.7075	0.6544	6.7076	0.003075	0.0031
After 1 <sup>st</sup> pass pump 1 <sup>st</sup> stage	4	30	934.22	10.25	549.31	-0.0529	0.7076	0.6547	6.710675	-6.3939653	6.3939
Permeate of RO membrane	5	29.6	934.22	0.213	60.49	-0.0062	1.4931	1.4869	0.3167097	-0.5500203	0.5500
Retentate of RO membrane	6	29.6	905.85	1.142	2414.17	-1.495	1.2907	-0.2043	-0.2333106	0.3826236	0.3826
Permeate of RO membrane	7	25	934.22	0.213	60.49	-0.0061	0.7071	0.701	0.149313	-0.3833088	0.3833
Retentate of RO membrane	8	30	905.85	1.142	2414.17	-1.5767	1.3718	-0.2049	-0.2339958	0.3833088	0.3833
Permeate of RO membrane	9	25	934.22	0.213	60.49	-0.0061	0.7071	0.701	0.149313	-0.3831946	0.3832
Retentate of RO membrane	10	29.9	905.85	1.142	2414.17	-1.5561	1.3513	-0.2048	-0.2338816	0.3831946	0.3832
Permeate of RO membrane	11	25	934.22	0.213	60.49	-0.0061	0.7071	0.701	0.149313	-0.3831946	0.3832
Retentate of RO membrane	12	29.9	905.85	1.142	2414.17	-1.5561	1.3513	-0.2048	-0.2338816	0.3354292	0.3354
Permeate of RO membrane	13	25	934.22	0.147	163.55	-0.0163	0.7071	0.6908	0.1015476	-0.482988	0.4829
Retentate of RO membrane	14	29.9	879.5	1.221	4426.27	-1.5575	1.2451	-0.3124	-0.3814404	0.482988	0.4829
Permeate of RO membrane	15	25	934.22	0.147	163.55	-0.0163	0.7071	0.6908	0.1015476	-0.482988	0.4829
Retentate of RO membrane	16	29.9	879.5	1.221	4426.27	-1.5575	1.2451	-0.3124	-0.3814404	1.9309266	1.9309
Mixing of permeate stream	17	30	934.22	4.258	106.89	-0.0109	0.3748	0.3639	1.5494862	-5.87445	5.8745
Mixing of retentate stream and disposal	18	25	934.22	4.882	4426.27	-1.006	0.1201	-0.8859	-4.3249638	7.5659405	7.5659

**Table 8.2.** Rate of exergy change of major components of RO of APC desalination plant (continued)

Component	Location	Temperature (°C)	Pressure (kpa)	Mass rate (kg/s)	Salinity (ppm)	Chemical Exergy	Physical Exergy	Specific Exergy Ex (kJ/kg)	Exergy rate X (kJ/kg)	Rate of exergy change $\Delta X$ (kW)	$\Delta X$ (kW)
Before 2 <sup>nd</sup> pass pump 1 <sup>st</sup> stage	19	30	879.5	2.129	534.46	-0.0529	1.5752	1.5223	3.2409767	0	0
After 2 <sup>nd</sup> pass pump 1 <sup>st</sup> stage	20	30	996.03	2.129	534.4586	-0.0529	1.5752	1.5223	3.2409767	-3.0352979	3.0353
Permeate of RO membrane	21	25	934.22	0.291	2.008113	-0.0002	0.707	0.7068	0.2056788	1.8753876	1.8754
Retentate of RO membrane	22	30	933.2	2.104	106.23672	-1.5748	2.5639	0.9891	2.0810664	-1.4882412	1.4883
Permeate of RO membrane	23	25	934.22	0.291	2.008113	-0.0002	2.0374	2.0372	0.5928252	2.0590564	2.0591
Retentate of RO membrane	24	30	933.2	2.104	106.23672	-1.3035	2.5639	1.2604	2.6518816	0.5678768	0.5679
Retentate of RO membrane	25	30	856.19	2.568	172.2393	-1.3035	2.5573	1.2538	3.2197584	-2.68605654	2.6861
Permeate of RO membrane	26	25	934.22	0.262	3.662468	-0.00037	2.0374	2.03703	0.53370186	1.98910134	1.9891
Retentate of RO membrane	27	30	856.19	2.568	172.2393	-1.5749	2.5573	0.9824	2.5228032	-1.98842014	1.9884
Permeate of RO membrane	28	25	923.07	0.262	3.662468	-0.00037	2.04	2.03963	0.53438306	-0.62100926	0.6210
Mixing of retentate stream	29	30	934.22	2.118	409.19554	-1.5545	1.5136	-0.0409	-0.0866262	6.1266112	6.1266
Mixing of permeate stream or product	30	30	934.22	13.85	2.000186	0.0109	0.4252	0.4361	6.039985	-9.0308128	9.0308
Throttling valve	31	30	1400	2.118	409.19554	-1.4528	0.0407	-1.4121	-2.9908278	2.9908278	2.9908
Throttling valve	32	30	1400	2.118	409.19554	0	0	0	0	0	--

### 8.3 Conclusions

This chapter focused on the calculations of exergy analysis based on thermodynamic limitations of the multistage multi pass brackish water RO desalination plant of APC of a daily production rate of 13.85 kg/s. The exergy calculations have considered both physical and chemical exergies of the RO desalination plant. To carry out this aim, a comprehensive set of thermodynamic equations was embedded in the model of RO system (developed by the same authors) to precisely carrying out the analysis of exergy destruction. In this regard, a computational code was developed using gPROMS software to analyse the system and asses its performance.

Several locations throughout the RO system were selected and subjected to the calculations of exergy destruction to investigate the most locations of the highest energy loss. The results of this study indicated that the mixing location of permeate of the first pass and the product stream at positions (17, and 30) are responsible of exergy rate of 5.88 kW, and 9.03 kW, respectively. These are causing the highest exergy destruction in the RO system. Statistically, these results account 62.28 %, and 95.8% of the total exergy input. Also, the disposed retentate stream causes an exergy rate of 7.57 kW, and mixing retentate of plant with rate 6.13 kW at positions (18, and 29). These account 71.18 %, and 64.95 % of the total exergy input, respectively.

Interestingly, the study introduced several opportunities to improve the thermodynamic performance of the plant due to investigating the locations of high exergy destruction. The obtained results of this study are in a full agreement with the findings of other studies carried out on different RO desalination systems. In this regard, the RO system has a second law efficiency of 4.48%, which is close to the second law efficiency presented in Cerci (2002). However, it is vital to realise that all the exergy calculations are carried out based on the hypothesis of ideal solutions of water and salt (brackish water).

## **CHAPTER NINE**

### **Conclusions and Recommendations for Future Work**

#### **9.1 Introduction**

This chapter summaries the research progress toward modelling, simulation and optimisation of multistage brackish water RO desalination system. More specifically, two different sizes of multistage brackish water RO desalination systems were considered including simple and complicated designs. The main conclusions of this research and recommendations for the future work are presented in the following.

#### **9.2 Conclusions**

RO process is considered as one of the most successful technologies for the commercial production of large quantities of fresh water from brackish and seawater at low energy consumption compared to alternative thermal processes. The main goal of this research is to generate a reliable brackish water desalination process via introducing several methods of improvements. In this regard, saving energy has a fundamental role in the cost reduction of water production in a desalination process which is the main objective of this research. Several contributions were made in this research as summarised below.

- A comprehensive mathematical model was developed for an individual spiral wound RO process and then used to generate successful models to predict the performance of two different case studies of simple and complicated designs of brackish water RO desalination systems. The robustness of the model developed was confirmed via two validation studies against experimental data of the two sizes of brackish water desalination RO process.
- A new mode of recycling the retentate stream was suggested for the multistage brackish water RO desalination process. The viability of this mode was investigated for both simple and complicated designs of RO process. More specifically, the retentate of the last stage of the simple design (retentate reprocessing design) to be linked to the feed stream was applied. Furthermore, the

design of multistage multi pass RO system of APC was improved by presuming the recycling of the high salinity retentate stream of the 1<sup>st</sup> pass to be mixed with the inlet feed stream. The simulation results confirmed the inconsistency of the retentate mode on the improvement of performance indicators of the simple design of RO process. In this regard, the product salinity has been slightly improved at 100% retentate recycle mode. However, 100% retentate recycle mode has insignificant impact on solute rejection and requires an increase of 10% in the specific energy consumption if compared to no recycle mode. On the other hand, the simulation results of the complicated design of RO process confirmed the possibility of increasing the productivity by around 3% with 100% recycle ratio of the high salinity retentate stream as a response of retentate recycle mode of the first pass.

- Another vital improvement of the multistage simple and complicated designs of RO process was achieved via adding an energy recovery device (ERD) to the RO process. The simulation results affirmed that the specific energy consumption could be reduced at low values of feed flow rates and pressures and high values of temperatures. More importantly, there is an opportunity to reduce the specific energy consumption between 47%-53.8% for the complicated design of RO process compared to the one calculated for the original design without an energy recovery device. On the other hand, the simple design of RO process has entailed a higher energy saving with the existence of an ERD if compared to the complicated multistage multi pass RO system of APC in all the three inlet feed parameters of feed flow rate, pressure and temperature. This has specifically achieved 61.3%, 65.2%, and 69.0% of energy saving for 80%, 85%, and 90% of an ERD efficiency, respectively. However, it is important to noting that the complicated design of RO process of APC requires less specific energy consumption compared to the simple design of RO process. Moreover, increasing pressure and temperature are positively affecting water recovery of RO process.
- The performance of multistage brackish water RO desalination system of two different designs (simple and complicated) has also improved by testing several brands of spiral-wound commercial membranes in the original RO plant. The

improvement was clarified via evaluating the performance indicators including water recovery, solute rejection, freshwater salinity and most importantly the specific energy consumption. The simulation results showed that the Filmtec BW30LE-440 membrane brand has shown the best performance indicators with the highest energy saving for both the simple and complicated designs of RO process. Specifically, the specific energy consumption of the complicated design of RO system is around the half of the simple design. This was attributed to the high productivity of the complicated design compared to the simple one. In this regard, the Filmtec BW30LE-440 membrane shows an improvement of 22.24% in water recovery, 15% in product salinity and 9.62% in the specific energy consumption of the complicated design of RO process compared to the original membrane.

- The optimisation framework has been developed for simple and complicated designs of multistage brackish water RO desalination process and its contribution on mitigating the specific energy consumption was presented. The optimisation results confirmed that the specific energy consumption can be reduced by 35% for the complicated design of RO process when compared with the original simulation value of consumed energy. In this regard, the product water salinity has been enhanced by 13.5% to fulfil the requirements of high-quality water. On the other hand, the simulation results show that the simple design of RO process has entailed with a higher energy saving after optimising the decision variables of the process compared to the complicated design of RO process. Statistically, the optimisation caused a reduction of the specific energy consumption by 37.3 for the simple design when compared to the original simulation value of consumed energy. Also, the product water salinity has also been improved by 35.66%.
- The exergy losses and thermodynamic limitations of a multistage multi pass medium-sized spiral wound brackish water RO desalination plant of APC have been analysed. In this regard, the exergy destruction distribution has investigated by incorporating both physical and chemical exergies of several units and compartments of the RO system. The simulation results explored the most sections that cause the highest energy destruction. Specifically, it is confirmed the largest

exergy destruction occurred in the mixing permeate streams and mixing retentate streams of the first pass and second pass of 62.28 % and 94.08 % and 71.18 % and 63.29 %, respectively.

### 9.3 Recommendations for Future Work

- Justifying the influence of critical membrane fouling by amending the model developed in Chapter 3 to comprise the fouling propensity that would measure the deterioration of the membranes for a long time of operation.
- Investigating the possibility of refining the design of brackish water RO desalination process via the application of complicated optimisation methods such as the Mixed Integer **Non-Linear programming optimisation** Problem that can predict the best design of multistage RO system to satisfy any required fresh water salinity and productivity.
- Implementing different practical methodologies of process modelling and optimisation such as artificial neural network and response surface methodology is vital to be investigated as they shown high accuracy of predicting the model parameters.
- The possibility of developing the dynamic version of the model developed in Chapter 3 to characterise the dynamic variation of the operating conditions and predict the process responses for any specified operating time.
- A comprehensive optimisation study is important to be carried out to investigate the viability of combining the proposed improvement methods of this research in one run. The optimisation needs to be built to simultaneously explore the feasible operating conditions, the best membrane type, the optimal retentate recycle ratio, and the optimum efficiency of an ERD. This would introduce the best methodology to upgrade the performance indicators of the complicated design of brackish water RO desalination process of APC.

## References

- Abbas, A. (2005) Simulation and analysis of an industrial water desalination plant. *Chemical Engineering and Processing: Process Intensification* 44 (9), 999-1004.
- Abbas, A. and Al-Bastaki, N. (2001) Performance decline in brackish water Film Tec spiral wound RO membranes. *Desalination* 136 (1-3), 281-286.
- Abbas, A. and Al-Bastaki, N. (2005) Modeling of an RO water desalination unit using neural networks. *Chemical Engineering Journal* 114 (1-3), 139-143.
- Abdallah, S., Abu-Hilal, M. and Mohsen, M. (2005) Performance of a photovoltaic powered reverse osmosis system under local climatic conditions. *Desalination* 183 (1-3), 95-104.
- Agashichev, S. P. and Lootahb, K. N. (2003) Influence of temperature and permeate recovery on energy consumption of a reverse osmosis system. *Desalination* 154 (3), 253-266.
- Ahmad, G. and Schmid, J. (2002) Feasibility study of brackish water desalination in the Egyptian deserts and rural regions using PV systems. *Energy Conversion and Management* 43 (18), 2641-2649.
- Al-bahou, M., Al-Rakaf, Z., Zaki, H. and Ettouney, H. (2007) Desalination experience in Kuwait. *Desalination* 204 (1-3), 403-415.
- Al-Bastaki, N. and Abbas, A. (1999) Improving the permeate flux by unsteady operation of a RO desalination unit. *Desalination* 123 (2-3), 173-176.
- Al-Bastaki, N. and Abbas, A. (2003) Permeate recycle to improve the performance of a spiral-wound RO plant. *Desalination* 158 (1-3), 119-126.
- Al-Karaghoul, A. and Kazmerski, L. L. (2013) Energy consumption and water production cost of conventional and renewable-energy-powered desalination processes. *Renewable and Sustainable Energy Reviews* 24, 343-356.
- Al-Obaidi, M., Kara-Zaitri, C. and Mujtaba, I. M. (2017a) Scope and limitations of the irreversible thermodynamics and the solution diffusion models for the separation of binary and multi-component systems in reverse osmosis process. *Computers & Chemical Engineering* 100, 48-79.
- Al-Obaidi, M., Kara-Zaitri, C. and Mujtaba, I. M. (2019) Performance evaluation of multi-stage reverse osmosis process with permeate and retentate recycling strategy for the removal of chlorophenol from wastewater. *Computers & Chemical Engineering* 121, 12-26.
- Al-Obaidi, M., Li, J.-P., Kara-Zaitri, C. and Mujtaba, I. M. (2017b) Optimisation of reverse osmosis based wastewater treatment system for the removal of chlorophenol using genetic algorithms. *Chemical Engineering Journal* 316, 91-100.
- Al-Obaidi, M. A., Alsarayreh, A. A., Al-Hroub, A. M., Alsadaie, S. and Mujtaba, I. M. (2018a) Performance analysis of a medium-sized industrial reverse osmosis brackish water desalination plant. *Desalination* 443, 272-284.
- Al-Obaidi, M. A., Kara-Zaitri, C. and Mujtaba, I. M. (2018b) Significant energy savings by optimising membrane design in multi-stage reverse osmosis wastewater treatment process.
- Al-Obaidi, M., Li, J.-P., Alsadaie, S., Kara-Zaitri, C. and Mujtaba, I. M. (2018c) Modelling and optimisation of a multistage Reverse Osmosis processes with permeate reprocessing and recycling for the removal of N-nitrosodimethylamine from wastewater using Species Conserving Genetic Algorithms. *Chemical Engineering Journal* 350, 824-834.
- Al-Shayji, K. A. M. (1998) *Modeling, simulation, and optimization of large-scale commercial desalination plants*. Virginia Tech.
- Al-Zahrani, A., Orfi, J., Al-Suhaibani, Z., Salim, B. and Al-Ansary, H. (2012) Thermodynamic analysis of a reverse osmosis desalination unit with energy recovery system. *Procedia engineering* 33, 404-414.

- Alghoul, M., Poovanaesvaran, P., Sopian, K. and Sulaiman, M. (2009) Review of brackish water reverse osmosis (BWRO) system designs. *Renewable and Sustainable Energy Reviews* 13 (9), 2661-2667.
- Aljundi, I. H. (2009) Second-law analysis of a reverse osmosis plant in Jordan. *Desalination* 239 (1), 207-215.
- Alsarayreh, A. A., Al-Obaidi, M., Al-Hroub, A., Patel, R. and Mujtaba, I. (2020) Evaluation and minimisation of energy consumption in a medium-scale reverse osmosis brackish water desalination plant. *Journal of Cleaner Production* 248, 119220.
- Anderson, W., Stover, R. and Martin, J. (2009) Keys to High Efficiency, Reliable Performance and Successful Operation of SWRO Processes. *Proceedings of the IDA World Congress, Dubai UAE*.
- Andrew Maddocks, R. s. y. a. P. R. (2015) *Ranking the World's Most Water-Stressed Countries in 2040*. World Resources Institute. <https://www.wri.org/blog/2015/08/ranking-world-s-most-water-stressed-countries-2040>
- Anis, S. F., Hashaikeh, R. and Hilal, N. (2019) Functional materials in desalination: A review. *Desalination* 468, 114077.
- Anqi, A. E., Alkhamis, N. and Oztekin, A. (2015) Numerical simulation of brackish water desalination by a reverse osmosis membrane. *Desalination* 369, 156-164.
- Avlonitis, S., Hanbury, W. and Boudinar, M. B. (1991) Spiral wound modules performance. An analytical solution, part I. *Desalination* 81 (1-3), 191-208.
- Avlonitis, S., Hanbury, W. and Boudinar, M. B. (1993) Spiral wound modules performance an analytical solution: Part II. *Desalination* 89 (3), 227-246.
- Avlonitis, S., Kouroumbas, K. and Vlachakis, N. (2003) Energy consumption and membrane replacement cost for seawater RO desalination plants. *Desalination* 157 (1-3), 151-158.
- Avlonitis, S., Pappas, M. and Moutesidis, K. (2007) A unified model for the detailed investigation of membrane modules and RO plants performance. *Desalination* 203 (1-3), 218-228.
- Azevedo, F. D. A. S. M. (2014) *Renewable energy powered desalination systems: technologies and market analysis*.
- Baker, R. W. and ProQuest (2012) *Membrane technology and applications*. 3rd edition. Wiley.
- Banchik, L. D. and Lienhard, J. H. (2012) Thermodynamic analysis of a reverse osmosis desalination system using forward osmosis for energy recovery. *ASME 2012 International Mechanical Engineering Congress and Exposition*. American Society of Mechanical Engineers.
- Bartman, A. R., Zhu, A., Christofides, P. D. and Cohen, Y. (2010) Minimizing energy consumption in reverse osmosis membrane desalination using optimization-based control. *Journal of Process Control* 20 (10), 1261-1269.
- Bennett, A. (2013) 50th Anniversary: Desalination: 50 years of progress. *Filtration+ Separation* 50 (3), 32-39.
- Bhattacharyya, D. and Williams, M. E. (1992) Reverse Osmosis: Theory. *IN: Membrane Handbook*. Van Nostrand Reinhold, New York. 1992. p 269-280. 6 fig, 26 ref.
- Boudinar, M. B., Hanbury, W. and Avlonitis, S. (1992) Numerical simulation and optimisation of spiral-wound modules. *Desalination* 86 (3), 273-290.
- Bouguecha, S., Hamrouni, B. and Dhahbia, M. (2004) Operating analysis of a direct energy coupled desalination family prototype. *Desalination* 168, 95-100.
- Burgi, P. H., Cabrera, E., Arregui, F. and Leiden, A. (2010) Water challenges in the 21<sup>st</sup> century. *Water Engineering and Management through Time-Learning from History*. CRC Press/Balkema. 303-334.
- Cengel, Y., Cerci, Y. and Wood, B. (1999) Second law analysis of separation processes of mixtures. *Proceedings of the ASME advanced energy systems division*. Vol. 39.

- Cengel, Y. A. and Boles, M. A. (2007) *Thermodynamics: An Engineering Approach 6th Edition (SI Units)*. The McGraw-Hill Companies, Inc., New York.
- Cerci, Y. (2002) Exergy analysis of a reverse osmosis desalination plant in California. *Desalination* 142 (3), 257-266.
- Cerci, Y., Cengel, Y., Wood, B., Kahraman, N. and Karakas, E. (2003) *Improving the thermodynamics and economic of desalination plants: Minimum work required for desalination and case studies of four working plants*. Technical report.
- Costa, M. L. and Dickson, J. (1991) Modelling of modules and systems in reverse osmosis. Part I: Theoretical system design model development. *Desalination* 80 (2-3), 251-274.
- Da Costa, A., Fane, A. and Wiley, D. (1994) Spacer characterization and pressure drop modelling in spacer-filled channels for ultrafiltration. *Journal of membrane science* 87 (1-2), 79-98.
- Dang, H. Q., Price, W. E. and Nghiem, L. D. (2014) The effects of feed solution temperature on pore size and trace organic contaminant rejection by the nanofiltration membrane NF270. *Separation and Purification Technology* 125, 43-51.
- Dimitriou, E., Boutikos, P., Mohamed, E. S., Koziel, S. and Papadakis, G. (2017) Theoretical performance prediction of a reverse osmosis desalination membrane element under variable operating conditions. *Desalination* 419, 70-78.
- Dimitriou, E., Mohamed, E. S., Karavas, C. and Papadakis, G. (2015) Experimental comparison of the performance of two reverse osmosis desalination units equipped with different energy recovery devices. *Desalination and Water Treatment* 55 (11), 3019-3026.
- Djebedjian, B., Gad, H., Khaled, I. and Rayan, M. A. (2008) Optimization of reverse osmosis desalination system using genetic algorithms technique. *Twelfth International Water Technology Conference, IWTC12, Alexandria, Egypt*.
- Droogers, P., Immerzeel, W., Terink, W., Hoogeveen, J., Bierkens, M., Van Beek, L. and Debele, B. (2012) Water resources trends in Middle East and North Africa towards 2050. *Hydrology and Earth System Sciences* 16, 3101-3114.
- Du, Y., Liang, X., Liu, Y., Xie, L. and Zhang, S. (2019) Exergo-economic analysis and multi-objective optimization of seawater reverse osmosis desalination networks. *Desalination* 466, 1-15.
- Du, Y., Xie, L., Wang, Y., Xu, Y. and Wang, S. (2012) Optimization of reverse osmosis networks with spiral-wound modules. *Industrial & engineering chemistry research* 51 (36), 11764-11777.
- Edgar, T. F., Himmelblau, D. M. and Lasdon, L. S. (2001) *Optimization of chemical processes*. 2<sup>nd</sup> edition. London;Boston;: McGraw-Hill.
- El-Dessouky, H. T. and Ettouney, H. M. (2002) *Fundamentals of salt water desalination*. Elsevier.
- El-Emam, R. S. and Dincer, I. (2014) Thermodynamic and thermoeconomic analyses of seawater reverse osmosis desalination plant with energy recovery. *Energy* 64, 154-163.
- El-Ghonemy, A. (2012) Waste energy recovery in seawater reverse osmosis desalination plants. Part 1. *Renewable and Sustainable Energy Reviews* 18 (C), 6-22.
- El-Manharawy, S. and Hafez, A. (2001) Water type and guidelines for RO system design. *Desalination* 139 (1-3), 97-113.
- Elimelech, M. and Phillip, W. A. (2011) The future of seawater desalination: energy, technology, and the environment. *science* 333 (6043), 712-717.
- Eltawil, M. A., Zhengming, Z. and Yuan, L. (2009) A review of renewable energy technologies integrated with desalination systems. *Renewable and Sustainable Energy Reviews* 13 (9), 2245-2262.
- Farhat, A., Ahmad, F., Hilal, N. and Arafat, H. A. (2013) Boron removal in new generation reverse osmosis (RO) membranes using two-pass RO without pH adjustment. *Desalination* 310, 50-59.

- Farooque, A., Jamaluddin, A., Al-Reweli, A., Jalaluddin, P., Al-Marwani, S., Al-Mobayed, A. and Qasim, A. (2008) Parametric analyses of energy consumption and losses in SWCC SWRO plants utilizing energy recovery devices. *Desalination* 219 (1-3), 137-159.
- Feinberg, B. J., Ramon, G. Z. and Hoek, E. M. (2013) Thermodynamic analysis of osmotic energy recovery at a reverse osmosis desalination plant. *Environmental science & technology* 47 (6), 2982-2989.
- Fethi, K. (2003) Optimization of energy consumption in the 3300 m<sup>3</sup>/d RO Kerkennah plant. *Desalination* 157 (1-3), 145-149.
- Fritzmann, C., Löwenberg, J., Wintgens, T. and Melin, T. (2007) State-of-the-art of reverse osmosis desalination. *Desalination* 216 (1-3), 1-76.
- Fujioka, T., Ishida, K. P., Shintani, T. and Kodamatani, H. (2018) High rejection reverse osmosis membrane for removal of N-nitrosamines and their precursors. *Water research* 131, 45-51.
- Geraldes, V., Pereira, N. E. and Norberta de Pinho, M. (2005) Simulation and optimization of medium-sized seawater reverse osmosis processes with spiral-wound modules. *Industrial & engineering chemistry research* 44 (6), 1897-1905.
- Ghaffour, N., Bundschuh, J., Mahmoudi, H. and Goosen, M. F. (2015) Renewable energy-driven desalination technologies: A comprehensive review on challenges and potential applications of integrated systems. *Desalination* 356, 94-114.
- Gilau, A. M. and Small, M. J. (2008) Designing cost-effective seawater reverse osmosis system under optimal energy options. *Renewable Energy* 33 (4), 617-630.
- Goh, P. S., Matsuura, T., Ismail, A. F. and Hilal, N. (2016) Recent trends in membranes and membrane processes for desalination. *Desalination* 391, 43-60.
- Goosen, M., Sablani, S., Al-Hinai, H., Al-Obeidani, S., Al-Belushi, R. and Jackson, a. (2005) Fouling of reverse osmosis and ultrafiltration membranes: a critical review. *Separation science and technology* 39 (10), 2261-2297.
- Greenlee, L. F., Lawler, D. F., Freeman, B. D., Marrot, B. and Moulin, P. (2009) Reverse osmosis desalination: water sources, technology, and today's challenges. *Water research* 43 (9), 2317-2348.
- Gude, V. G. (2011) Energy consumption and recovery in reverse osmosis. *Desalination and water treatment* 36 (1-3), 239-260.
- Guria, C., Bhattacharya, P. K. and Gupta, S. K. (2005) Multi-objective optimization of reverse osmosis desalination units using different adaptations of the non-dominated sorting genetic algorithm (NSGA). *Computers and Chemical Engineering* 29 (9), 1977-1995.
- Hadadin, N., Qaqish, M., Akawwi, E. and Bdour, A. (2010) Water shortage in Jordan — Sustainable solutions. *Desalination* 250 (1), 197-202.
- Haluch, V., Zanoelo, E. F. and Hermes, C. J. (2017) Experimental evaluation and semi-empirical modeling of a small-capacity reverse osmosis desalination unit. *Chemical Engineering Research and Design* 122, 243-253.
- Hatfield, G. B. and Graves, G. W. (1970) Optimization of a reverse osmosis system using nonlinear programming. *Desalination* 7 (2), 147-177.
- Herold, D., Horstmann, V., Neskakis, A., Plettner-Marliani, J., Piernavieja, G. and Calero, R. (1998) Small scale photovoltaic desalination for rural water supply-demonstration plant in Gran Canaria. *Renewable Energy* 14 (1-4), 293-298.
- Hoek, E. M. and Elimelech, M. (2003) Cake-enhanced concentration polarization: a new fouling mechanism for salt-rejecting membranes. *Environmental science & technology* 37 (24), 5581-5588.
- Hyung, H. and Kim, J.-H. (2006) A mechanistic study on boron rejection by sea water reverse osmosis membranes. *Journal of Membrane Science* 286 (1-2), 269-278.
- I.W.M.I. (2001) *Projected Water Scarcity in 2025*. International Water Management Institute. <http://www.waternunc.com/gb/pws2025.htm> Accessed 14/6/2019.

- Islam, M., Sultana, A., Saadat, A., Shammi, M. and Uddin, M. (2018) Desalination technologies for developing countries: A review. *Journal of Scientific Research* 10 (1), 77-97.
- Jiang, A., Wang, J., Biegler, L. T., Cheng, W., Xing, C. and Jiang, Z. (2015) Operational cost optimization of a full-scale SWRO system under multi-parameter variable conditions. *Desalination* 355, 124-140.
- Jin, X., Jawor, A., Kim, S. and Hoek, E. M. (2009) Effects of feed water temperature on separation performance and organic fouling of brackish water RO membranes. *Desalination* 239 (1-3), 346-359.
- Jones, E., Qadir, M., van Vliet, M. T., Smakhtin, V. and Kang, S.-m. (2018) The state of desalination and brine production: A global outlook. *Science of the Total Environment*.
- Kaghazchi, T., Mehri, M., Ravanchi, M. T. and Kargari, A. (2010) A mathematical modeling of two industrial seawater desalination plants in the Persian Gulf region. *Desalination* 252 (1-3), 135-142.
- Kahraman, N. and Cengel, Y. A. (2005) Exergy analysis of a MSF distillation plant. *Energy Conversion and Management* 46 (15-16), 2625-2636.
- Kahraman, N., Cengel, Y. A., Wood, B. and Cerci, Y. (2005) Exergy analysis of a combined RO, NF, and EDR desalination plant. *Desalination* 171 (3), 217-232.
- Karavelas, A., Koutsou, C., Kostoglou, M. and Sioutopoulos, D. (2018) Analysis of specific energy consumption in reverse osmosis desalination processes. *Desalination* 431, 15-21.
- Khan, S. U.-D., Khan, S. U.-D., Haider, S., El-Leathy, A., Rana, U. A., Danish, S. N. and Ullah, R. (2017) Development and techno-economic analysis of small modular nuclear reactor and desalination system across Middle East and North Africa region. *Desalination* 406, 51-59.
- Khawaji, A. D., Kutubkhanah, I. K. and Wie, J.-M. (2007) A 13.3 MGD seawater RO desalination plant for Yanbu Industrial City. *Desalination* 203 (1-3), 176-188.
- Khawaji, A. D., Kutubkhanah, I. K. and Wie, J.-M. (2008) Advances in seawater desalination technologies. *Desalination* 221 (1-3), 47-69.
- Kim, D. H. (2011) A review of desalting process techniques and economic analysis of the recovery of salts from retentates. *Desalination* 270 (1-3), 1-8.
- Kim, S. and Hoek, E. M. V. (2005) Modeling concentration polarization in reverse osmosis processes. *Desalination* 186 (1), 111-128.
- Kim, Y., Kang, M. G., Lee, S., Jeon, S. G. and Choi, J.-S. (2013) Reduction of energy consumption in seawater reverse osmosis desalination pilot plant by using energy recovery devices. *Desalination and Water Treatment* 51 (4-6), 766-771.
- Kim, Y. M., Kim, S. J., Kim, Y. S., Lee, S., Kim, I. S. and Kim, J. H. (2009) Overview of systems engineering approaches for a large-scale seawater desalination plant with a reverse osmosis network. *Desalination* 238 (1-3), 312-332.
- Klotz, I. M. (1964) Chemical thermodynamics; basic theory and methods.
- Koroneos, C., Dompros, A. and Roumbas, G. (2007) Renewable energy driven desalination systems modelling. *Journal of Cleaner Production* 15 (5), 449-464.
- Kotb, H., Amer, E. and Ibrahim, K. (2015) Effect of operating conditions on salt concentration at the wall of RO membrane. *Desalination* 357, 246-258.
- Kotb, H., Amer, E. H. and Ibrahim, K. A. (2016) On the optimization of RO (Reverse Osmosis) system arrangements and their operating conditions. *Energy* 103, 127-150.
- Koutsou, C., Karabelas, A. and Kostoglou, M. (2015) Membrane desalination under constant water recovery—The effect of module design parameters on system performance. *Separation and Purification Technology* 147, 90-113.
- Laine, J. (2009) Design & Operation Considerations: Two Large-Scale Case Studies, in. *Suez Environment*.
- Latorre, F. J. G., Báez, S. O. P. and Gotor, A. G. (2015) Energy performance of a reverse osmosis desalination plant operating with variable pressure and flow. *Desalination* 366, 146-153.

- Lee, C.-J., Chen, Y.-S. and Wang, G.-B. (2010) A dynamic simulation model of reverse osmosis desalination systems. *The 5th International Symposium on Design, Operation and Control of Chemical Processes, PSE ASIA, Singapore*.
- Lee, S. and Lueptow, R. M. (2001) Rotating reverse osmosis: a dynamic model for flux and rejection. *Journal of membrane science* 192 (1-2), 129-143.
- Li, M. (2010) Minimization of energy in reverse osmosis water desalination using constrained nonlinear optimization. *Industrial & Engineering Chemistry Research* 49 (4), 1822-1831.
- Lohman, E. (1994) Operating report of the largest reverse osmosis desalting plant. *Desalination* 96 (1-3), 349-358.
- Lonsdale, H., Merten, U. and Riley, R. (1965) Transport properties of cellulose acetate osmotic membranes. *Journal of applied polymer science* 9 (4), 1341-1362.
- Lu, Y.-Y., Hu, Y.-D., Zhang, X.-L., Wu, L.-Y. and Liu, Q.-Z. (2007) Optimum design of reverse osmosis system under different feed concentration and product specification. *Journal of membrane science* 287 (2), 219-229.
- Mabrouk, A. A., Nafey, A. and Fath, H. (2007) Thermoeconomic analysis of some existing desalination processes. *Desalination* 205 (1-3), 354-373.
- Majali, F., Ettouney, H., Abdel-Jabbar, N. and Qiblawey, H. (2008) Design and operating characteristics of pilot scale reverse osmosis plants. *Desalination* 222 (1-3), 441-450.
- Malaeb, L. and Ayoub, G. M. (2011) Reverse osmosis technology for water treatment: state of the art review. *Desalination* 267 (1), 1-8.
- Mallevalle, J., Odendaal, P. E. and Wiesner, M. R. (1996) *Water treatment membrane processes*. American Water Works Association.
- Mancosu, N., Snyder, R. L., Kyriakakis, G. and Spano, D. (2015) Water scarcity and future challenges for food production. *Water* 7 (3), 975-992.
- Mane, P. P., Park, P.-K., Hyung, H., Brown, J. C. and Kim, J.-H. (2009) Modeling boron rejection in pilot-and full-scale reverse osmosis desalination processes. *Journal of membrane science* 338 (1-2), 119-127.
- Marriott, J. and Sørensen, E. (2003) A general approach to modelling membrane modules. *Chemical engineering science* 58 (22), 4975-4990.
- Maskan, F., Wiley, D. E., Johnston, L. P. and Clements, D. J. (2000) Optimal design of reverse osmosis module networks. *AIChE Journal* 46 (5), 946-954.
- Mason, E. and Lonsdale, H. (1990) Statistical-mechanical theory of membrane transport. *Journal of Membrane Science* 51 (1-2), 1-81.
- Mazlan, N. M., Peshev, D. and Livingston, A. G. (2016a) Energy consumption for desalination—A comparison of forward osmosis with reverse osmosis, and the potential for perfect membranes. *Desalination* 377, 138-151.
- Mazlan, N. M., Peshev, D. and Livingston, A. G. (2016b) Energy consumption for desalination — A comparison of forward osmosis with reverse osmosis, and the potential for perfect membranes. *Desalination* 377, 138-151.
- Mehdizadeh, H. (2006) Membrane desalination plants from an energy–exergy viewpoint. *Desalination* 191 (1-3), 200-209.
- Miller, S., Shemer, H. and Semiat, R. (2015) Energy and environmental issues in desalination. *Desalination* 366, 2-8.
- Mohsen, M. S. and Jaber, J. O. (2001) A photovoltaic-powered system for water desalination. *Desalination* 138 (1-3), 129-136.
- Morin, P., Jiménez-Flores, R. and Pouliot, Y. (2004) Effect of temperature and pore size on the fractionation of fresh and reconstituted buttermilk by microfiltration. *Journal of dairy science* 87 (2), 267-273.
- Nair, M. and Kumar, D. (2013) Water desalination and challenges: the Middle East perspective: a review. *Desalination and Water Treatment* 51 (10-12), 2030-2040.

- Nemeth, J. E. (1998) Innovative system designs to optimize performance of ultra-low pressure reverse osmosis membranes. *Desalination* 118 (1-3), 63-71.
- Nooijen, W. and Wouters, J. (1992) Optimizing and planning of seawater desalination. *Desalination* 89 (1), 1-19.
- Oh, H.-J., Hwang, T.-M. and Lee, S. (2009) A simplified simulation model of RO systems for seawater desalination. *Desalination* 238 (1), 128-139.
- Osada, Y. and Nakagawa, T. (1992) *Membrane science and technology*. CRC Press.
- Pais, J. A. G. and Ferreira, L. M. G. (2007) Performance study of an industrial RO plant for seawater desalination. *Desalination* 208 (1-3), 269-276.
- Palamalai, S., Ravindra, I. and Prakasam, K. (2015) Relationship between energy consumption, CO<sub>2</sub> emissions, economic growth and trade in India. *Srinivasan P, Inder SR and Karthigai P. (2015), Relationship between Energy Consumption, CO<sub>2</sub> Emissions, Economic Growth and Trade in India, International Journal of Economics* 2 (1), 1-17.
- Pandey, S. R. (2014) *Evaluation of pre-treatments for minimizing membrane fouling in water recovery*. Deakin University.
- Patel, S. K., Ritt, C. L., Deshmukh, A., Wang, Z., Qin, M., Epsztein, R. and Elimelech, M. (2020) The relative insignificance of advanced materials in enhancing the energy efficiency of desalination technologies. *Energy & Environmental Science*.
- Pearce, W. and Kumar, M. (2003) Evaluation of new generation brackish water reverse osmosis membranes. *Proc of Membrane Technology Conference, American Water Works Association*.
- Peñate, B. and García-Rodríguez, L. (2012) Current trends and future prospects in the design of seawater reverse osmosis desalination technology. *Desalination* 284, 1-8.
- Pérez-González, A., Urtiaga, A., Ibáñez, R. and Ortiz, I. (2012) State of the art and review on the treatment technologies of water reverse osmosis concentrates. *Water research* 46 (2), 267-283.
- Qasim, M., Badrelzaman, M., Darwish, N. N., Darwish, N. A. and Hilal, N. (2019) Reverse osmosis desalination: A state-of-the-art review. *Desalination* 459, 59-104.
- Qi, B., Wang, Y., Xu, S., Wang, Z. and Wang, S. (2012) Operating Energy Consumption Analysis of RO Desalting System: Effect of Membrane Process and Energy Recovery Device (ERD) Performance Variables. *Industrial & Engineering Chemistry Research* 51 (43), 14135-14144.
- Rao, S. M. (2011) Reverse Osmosis. *Resonance* 16 (12), 1333-1336.
- Ruiz-García, A. and de la Nuez Pestana, I. (2019) Feed Spacer Geometries and Permeability Coefficients. Effect on the Performance in BWRO Spiral-Wound Membrane Modules. *Water* 11 (1), 152.
- Ruiz-García, A., Melián-Martel, N. and Mena, V. (2018) Fouling characterization of RO membranes after 11 years of operation in a brackish water desalination plant. *Desalination* 430, 180-185.
- Ruiz-Saavedra, E., Ruiz-García, A. and Ramos-Martín, A. (2015) A design method of the RO system in reverse osmosis brackish water desalination plants (calculations and simulations). *Desalination and Water Treatment* 55 (9), 2562-2572.
- Sagle, A. and Freeman, B. (2004) Fundamentals of membranes for water treatment. *The future of desalination in Texas* 2 (363), 137.
- Saif, Y., Elkamel, A. and Pritzker, M. (2008) Optimal design of reverse-osmosis networks for wastewater treatment. *Chemical Engineering and Processing: Process Intensification* 47 (12), 2163-2174.
- Sarkar, P., Goswami, D., Prabhakar, S. and Tewari, P. (2008) Optimized design of a reverse osmosis system with a recycle. *Desalination* 230 (1-3), 128-139.

- Sassi, K. M. and Mujtaba, I. M. (2011) Optimal design and operation of reverse osmosis desalination process with membrane fouling. *Chemical engineering journal* 171 (2), 582-593.
- Sassi, K. M. and Mujtaba, I. M. (2012) Effective design of reverse osmosis based desalination process considering wide range of salinity and seawater temperature. *Desalination* 306, 8-16.
- Saltonstall Jr, C. and Lawrence, R. (1982) Calculation of the expected performance of reverse osmosis plants. *Desalination* 42 (3), 247-253.
- Semiat, R. (2008) Energy issues in desalination processes. *Environmental science & technology* 42 (22), 8193-8201.
- Senthilmurugan, S., Ahluwalia, A. and Gupta, S. K. (2005) Modeling of a spiral-wound module and estimation of model parameters using numerical techniques. *Desalination* 173 (3), 269-286.
- Sharif, A., Merdaw, A., Al-Bahadili, H., Al-Tae, A., Al-Aibi, S., Rahal, Z. and Derwish, G. (2009) A new theoretical approach to estimate the specific energy consumption of reverse osmosis and other pressure-driven liquid-phase membrane processes. *Desalination and water treatment* 3 (1-3), 111-119.
- Sharma, A., Jelemenský, M., Paulen, R. and Fikar, M. (2017) Modeling and optimal operation of batch closed-loop diafiltration processes. *Chemical Engineering Research and Design* 122, 198-210.
- Shenvi, S. S., Isloor, A. M. and Ismail, A. F. (2015) A review on RO membrane technology: Developments and challenges. *Desalination* 368, 10-26.
- Song, L., Hu, J., Ong, S., Ng, W., Elimelech, M. and Wilf, M. (2003a) Emergence of thermodynamic restriction and its implications for full-scale reverse osmosis processes. *Desalination* 155 (3), 213-228.
- Song, L., Hu, J., Ong, S., Ng, W., Elimelech, M. and Wilf, M. (2003b) Performance limitation of the full-scale reverse osmosis process. *Journal of Membrane Science* 214 (2), 239-244.
- Sourirajan, S. (1970) *Reverse osmosis*. London, UK: Logos Press Ltd.
- Sourirajan, S. and Matsuura, T. (1985) Reverse osmosis/ultrafiltration process principles.
- Speth, T. F., Gusses, A. M. and Summers, R. S. (2000) Evaluation of nanofiltration pretreatments for flux loss control. *Desalination* 130 (1), 31-44.
- Staudé, E. (1992) Marcel Mulder: Basic Principles of Membrane Technology, Kluwer Academic Publishers, Dordrecht, Boston, London, 1991, ISBN 0-7923-0978-2, 363 Seiten, Preis: DM 200,—. *Berichte der Bunsengesellschaft für physikalische Chemie* 96 (5), 741-742.
- Stover, R. (2008) Low energy consumption SWRO. *submitted to Proceedings of Clean Technology*.
- Stover, R. L. (2007) Seawater reverse osmosis with isobaric energy recovery devices. *Desalination* 203 (1-3), 168-175.
- Stover, R. L., Ameglio, A. and Khan, P. (2005) The Ghalilah SWRO plant: an overview of the solutions adopted to minimize energy consumption. *Desalination* 184 (1-3), 217-221.
- Subramani, A., Badruzzaman, M., Oppenheimer, J. and Jacangelo, J. G. (2011) Energy minimization strategies and renewable energy utilization for desalination: A review. *Water Research* 45 (5), 1907-1920.
- Taniguchi, M. and Kimura, S. (2000) Estimation of transport parameters of RO membranes for seawater desalination. *AIChE journal* 46 (10), 1967-1973.
- Tanvir, M. S. and Mujtaba, I. M. (2008) Optimisation of design and operation of MSF desalination process using MINLP technique in gPROMS. *Desalination* 222 (1), 419-430.
- Temperely, T. (1995) The coming age of desalination. *Proceeding of the IDA World Congress on Desalination and Water Sciences, Abu Dhabi Publishing Co., Abu Dhabi, United Arab Emirates*. Vol. 1.

- Thomson, M., Miranda, M. S. and Infield, D. (2003) A small-scale seawater reverse-osmosis system with excellent energy efficiency over a wide operating range. *Desalination* 153 (1-3), 229-236.
- Toray Membrane USA Inc., m. t. s. O., Maintenance and Handling Manual. (2015) <http://www.toraywater.com/> Accessed 10/3/2018.
- Tran, T., Bolto, B., Gray, S., Hoang, M. and Ostarcevic, E. (2007) An autopsy study of a fouled reverse osmosis membrane element used in a brackish water treatment plant. *Water Research* 41 (17), 3915-3923.
- Tsiourtis, N. X. (2001) Desalination and the environment. *Desalination* 141 (3), 223-236.
- Van der Bruggen, B. and Vandecasteele, C. (2002) Distillation vs. membrane filtration: overview of process evolutions in seawater desalination. *Desalination* 143 (3), 207-218.
- Van der Meer, W. and Van Dijk, J. (1997) Theoretical optimization of spiral-wound and capillary nanofiltration modules. *Desalination* 113 (2-3), 129-146.
- Veza, J. M. (2001) Desalination in the Canary Islands: an update. *Desalination* 133 (3), 259-270.
- Villafafila, A. and Mujtaba, I. (2003) Fresh water by reverse osmosis based desalination: simulation and optimisation. *Desalination* 155 (1), 1-13.
- Vince, F., Marechal, F., Aoustin, E. and Bréant, P. (2008) Multi-objective optimization of RO desalination plants. *Desalination* 222 (1-3), 96-118.
- Wark, K. (1995) *Advanced thermodynamics for engineers*. McGraw-Hill New York.
- Wei, Q. J. and McGovern, R. K. (2017) Saving energy with an optimized two-stage reverse osmosis system. *Environmental Science: Water Research & Technology* 3 (4), 659-670.
- WHO (2003) *Atrazine in drinking-water: background document for development of WHO guidelines for drinking-water quality*. World Health Organization.
- WHO (2018) *2.1 billion people lack safe drinking water at home, more than twice as many lack safe sanitation*. World Health Organization. <https://www.who.int/news-room/detail/12-07-2017-2-1-billion-people-lack-safe-drinking-water-at-home-more-than-twice-as-many-lack-safe-sanitation>
- Wiley, D. E., Fell, C. J. and Fane, A. G. (1985) Optimisation of membrane module design for brackish water desalination. *Desalination* 52 (3), 249-265.
- Wilf, M. and Klinko, K. (1994) Performance of commercial seawater membranes. *Desalination* 96 (1-3), 465-478.
- Wilf, M. and Bartels, C. (2005) Optimization of seawater RO systems design. *Desalination* 173 (1), 1-12.
- Wilf, M. and Schierach, M. K. (2001) Improved performance and cost reduction of RO seawater systems using UF pretreatment. *Desalination* 135 (1-3), 61-68.
- Winzeler, H. B. and Belfort, G. (1993) Enhanced performance for pressure-driven membrane processes: the argument for fluid instabilities. *Journal of Membrane Science* 80 (1), 35-47.
- Xevgenos, D., Moustakas, K., Malamis, D. and Loizidou, M. (2016) An overview on desalination & sustainability: renewable energy-driven desalination and brine management. *Desalination and Water Treatment* 57 (5), 2304-2314.
- Yan, W., Shi, M., Wang, Z., Zhou, Y., Liu, L., Zhao, S., Ji, Y., Wang, J. and Gao, C. (2019) Amino-modified hollow mesoporous silica nanospheres-incorporated reverse osmosis membrane with high performance. *Journal of Membrane Science* 581, 168-177.
- Yang, X., Wang, R., Fane, A. G., Tang, C. Y. and Wenten, I. (2013) Membrane module design and dynamic shear-induced techniques to enhance liquid separation by hollow fiber modules: a review. *Desalination and Water Treatment* 51 (16-18), 3604-3627.
- Zhang, Y., Zhang, L., Hou, L., Kuang, S. and Yu, A. (2019) Modeling of the variations of permeate flux, concentration polarization, and solute rejection in nanofiltration system. *AIChE Journal* 65 (3), 1076-1087.

- Zhao, L., Chang, P. C.-Y. and Ho, W. W. (2013) High-flux reverse osmosis membranes incorporated with hydrophilic additives for brackish water desalination. *Desalination* 308, 225-232.
- Zhu, A., Christofides, P. D. and Cohen, Y. (2008) Effect of thermodynamic restriction on energy cost optimization of RO membrane water desalination. *Industrial & Engineering Chemistry Research* 48 (13), 6010-6021.
- Zhu, A., Christofides, P. D. and Cohen, Y. (2009a) Energy Consumption Optimization of Reverse Osmosis Membrane Water Desalination Subject to Feed Salinity Fluctuation. *Industrial & Engineering Chemistry Research* 48 (21), 9581-9589.
- Zhu, A., Christofides, P. D. and Cohen, Y. (2009b) Minimization of energy consumption for a two-pass membrane desalination: effect of energy recovery, membrane rejection and retentate recycling. *Journal of Membrane Science* 339 (1-2), 126-137.
- Zhu, A., Rahardianto, A., Christofides, P. D. and Cohen, Y. (2010) Reverse osmosis desalination with high permeability membranes—cost optimization and research needs. *Desalination and Water Treatment* 15 (1-3), 256-266.

## List of Publications

The publications out of the author's PhD student project can be listed as follow.

### Journals

1. Al-Obaidi, M.A., Alsarayreh, A.A., Al-Hroub, A.M., Alsadaie, S. and Mujtaba, I.M., 2018. **Performance analysis of a medium-sized industrial reverse osmosis brackish water desalination plant.** *Desalination*, 443, pp.272-284.
2. Alsarayreh, A.A., Al-Obaidi, M.A., Al-Hroub, A.M., Patel, R. and Mujtaba, I.M., 2019. **Performance Evaluation of Reverse Osmosis Brackish Water Desalination Plant with Different Recycled Ratios of Retentate.** In *Computer Aided Chemical Engineering* (Vol. 46, pp. 181-186). Elsevier.
3. Alsarayreh, A.A., Al-Obaidi, M.A., Al-Hroub, A.M., Patel, R. and Mujtaba, I.M., 2019. **Evaluation and minimisation of energy consumption in a medium-scale reverse osmosis brackish water desalination plant.** *Journal of Cleaner Production*, p.119220.
4. Alsarayreh, A.A., Al-Obaidi, M.A., Patel, R. and Mujtaba, I.M., 2020. **Scope and Limitations of Modelling, Simulation, and Optimisation of a Spiral Wound Reverse Osmosis Process-Based Water Desalination.** *Processes*, 8(5), p.573.
5. Alsarayreh, A.A., Al-Obaidi, M.A., Farag, S.K., Patel, R. and Mujtaba, I.M., **Performance evaluation of a medium-scale industrial reverse osmosis brackish water desalination plant with different brands of membranes. A simulation study.** *Desalination*, 503, p.114927.
6. Alsarayreh, A.A., Al-Obaidi, M.A., A.M., Patel, R. and Mujtaba, I.M., 2020. **Thermodynamic limitations and exergy analysis of reverse osmosis brackish water desalination plant of Arab Potash Company.** *Will be submitted soon.*

### **Conferences**

- 1- Alsarayreh, A.A., Al-Obaidi, M.A., Al-Hroub, A.M., Patel, R. and Mujtaba, I.M., 2019. **Performance Evaluation of Reverse Osmosis Brackish Water Desalination Plant with Different Recycled Ratios of Retentate.** In Computer Aided Chemical Engineering. **Accepted and Published in ESCAPE 29.**
- 2- Alsarayreh, A.A., Al-Obaidi, M.A., Al-Hroub, A.M., Patel, R. and Mujtaba, I.M., 2019. **Optimisation of energy consumption in a medium-scale reverse osmosis brackish water desalination plant.** **Accepted and Published in ESCAPE 30.**
- 3- Alsarayreh, A.A., Al-Obaidi, M.A., A.M., Patel, R. and Mujtaba, I.M., 2020. **Enhancement of energy saving of reverse osmosis system of Arab Potash Company via a wind energy system.** **Accepted in ESCAPE 31.**

**Paper (1)**



Get Access

Share

Export



**Desalination**

Volume 443, 1 October 2018, Pages 272-284



# Performance analysis of a medium-sized industrial reverse osmosis brackish water desalination plant

M.A. Al-Obaidi <sup>a, b</sup>, A.A. Alsarayreh <sup>a</sup>, A.M. Al-Hroub <sup>c</sup>, S. Alsadaie <sup>d</sup>, I.M. Mujtaba <sup>a</sup>

Show more

<https://doi.org/10.1016/j.desal.2018.06.010>

[Get rights and content](#)

## Highlights

- A detailed model is developed for a medium sized industrial desalination plant.
- The effect of several operating parameters on the plant performance is evaluated.
- Several conceptual suggestions are made to enhance the RO plant performance.
- The multistage RO plant model is capable of extending to large scale RO plant.

## Abstract

The implementation of **Reverse Osmosis** (RO) technology is noticeably increased to produce freshwater from brackish and seawater resources. In this work, performance analysis of a **multistage** multi pass medium-sized spiral wound

## Paper (2)

[Get Access](#)[Share](#)[Export](#)

Computer Aided Chemical Engineering

Volume 46, 2019, Pages 181-186



# Performance Evaluation of Reverse Osmosis Brackish Water Desalination Plant with Different Recycled Ratios of Retentate

A.A. Alsarayreh <sup>a</sup>, M.A. Al-Obaidi <sup>a, b</sup>, A.M. Al-Hroub <sup>c</sup>, R. Patel <sup>a</sup>, I.M. Mujtaba <sup>a</sup>

[Show more](#)

<https://doi.org/10.1016/B978-0-12-818634-3.50031-X>

[Get rights and content](#)

## Abstract

Reverse Osmosis (RO) process can be considered as one of the most widely utilised technologies for brackish water desalination due to its capabilities of retaining salts and producing high-quality water. This paper focuses on the retentate recycle design of an industrial medium-sized spiral wound brackish water RO desalination plant (1200 m<sup>3</sup>/day) of Arab Potash Company (APC) located in Jordan. The plant is essentially designed as a multistage and multi pass RO system including a low salinity retentate recycle stream from the 2<sup>nd</sup> pass and a high salinity retentate disposal from the 1<sup>st</sup> pass. However, in this work, we have considered recycle of high salinity retentate stream from the 1<sup>st</sup> pass and explored the impact of different recycled ratio on the process performance indicators such as the fresh water salinity, overall recovery rate, and specific energy consumption. The simulation is carried out using the model developed earlier by us for the specified RO plant using

## Paper (3)

[Get Access](#)[Share](#)[Export](#)

Journal of Cleaner Production

Available online 13 November 2019, 119220

In Press, Corrected Proof



# Evaluation and minimisation of energy consumption in a medium-scale reverse osmosis brackish water desalination plant

Alanood A. Alsarayreh <sup>a</sup>, M.A. Al-Obaidi <sup>b</sup>, A.M. Al-Hroub <sup>c</sup>, R. Patel <sup>a</sup>, I.M. Mujtaba <sup>a</sup>

[Show more](#)

<https://doi.org/10.1016/j.jclepro.2019.119220>



[Get rights and content](#)

## Highlights

- The energy consumption of BWRO desalination plant was weighed with and without ERD.
- An proper model was used to predict RO process performance and energy consumption.
- The energy consumption reduced between 47% and 53.8% due to the existence of ERD.
- Increasing pressure and temperature are positively affecting water recovery of RO process.
- It is confirmed the feasibility of installing an ERD in the original design of APC.

Review

# Scope and Limitations of Modelling, Simulation, and Optimisation of a Spiral Wound Reverse Osmosis Process-Based Water Desalination

Alanood A. Alsarayreh <sup>1</sup>, Mudhar A. Al-Obaidi <sup>2</sup> , Raj Patel <sup>1</sup> and Iqbal M. Mujtaba <sup>1,\*</sup> 

<sup>1</sup> Department of Chemical of Engineering, Faculty of Engineering and Informatics, The University of Bradford, Bradford BD7 1DP, UK; A.A.M.Alsarayreh@bradford.ac.uk (A.A.A.); r.patel@bradford.ac.uk (R.P.)

<sup>2</sup> Middle Technical University, Technical Institute of Baquba, Baquba 00964, Iraq; dr.mudhar.alaubedy@mtu.edu.iq

\* Correspondence: I.M.Mujtaba@bradford.ac.uk; Tel.: +44-012-7423-3645

Received: 30 March 2020; Accepted: 26 April 2020; Published: 12 May 2020



**Abstract:** The reverse osmosis (RO) process is one of the best desalination methods, using membranes to reject several impurities from seawater and brackish water. To systematically perceive the transport phenomena of solvent and solutes via the membrane texture, several mathematical models have been developed. To date, a large number of simulation and optimisation studies have been achieved to gauge the influence of control variables on the performance indexes, to adjust the key variables at optimum values, and to realise the optimum production indexes. This paper delivers an intensive review of the successful models of the RO process and both simulation and optimisation studies carried out on the basis of the models developed. In general, this paper investigates the scope and limitations of the RO process, as well as proving the maturity of the associated perspective methodologies.

**Keywords:** water desalination; reverse osmosis process; spiral wound (SW) module; modelling; simulation; optimization



# Performance evaluation of a medium-scale industrial reverse osmosis brackish water desalination plant with different brands of membranes. A simulation study

Alanood A. Alsarayreh <sup>a</sup>, Mudhar A. Al-Obaidi <sup>b</sup>, Shekhah K. Farag <sup>a</sup>, Raj Patel <sup>a</sup>, Iqbal M. Mujtaba <sup>a</sup>

Show more

+ Add to Mendeley Share Cite

<https://doi.org/10.1016/j.desal.2020.114927>

[Get rights and content](#)

## Highlights

- Different membrane brands are applied on the original design of RO system of APC.
- An accurate mathematical model was used to carry out an intensive simulation.
- The performance metrics of the membrane brands are compared vs the original one.
- The most suitable membrane brand for a RO plant is explored.
- The energy consumption is improved using the Filmtec BW30LE-440 membrane brand.

**Abstract**

In this work, the performance for multistage and multipass of an industrial medium-sized spiral wound brackish water RO desalination plant (1200 m<sup>3</sup>/day) of Arab Potash Company (APC) located in Jordan with different recycled ratios of 1st pass retentate (high salinity) is investigated via simulation. The impact of different recycled ratios is explored on the process performance indicators such as the fresh water salinity, overall recovery rate, and specific energy consumption.

**Introduction**

The application of RO process is interestingly increased due to its low cost and energy consumption compared to other conventional thermal technologies (Al-Karaghouli and Kazmerski, 2013). The influence of different ratios of retentate stream recycle (that combined with raw water stream) on the process performance indicators is investigated via simulation. The simulation is carried out using the model developed earlier by Al-Obeidi et al. (2018) for the specified RO plant using gPROMS software. The performance of RO process with 10% to 100% high salinity retentate stream of the 1st pass has been investigated. Then, the process performance has been compared against the original experimental data with no recycle mode operation carried out at specified operating conditions.

**Description of BWRO desalination plant of APC**

The low-pressure permeates of 1st pass (position 1) are combined and pumped to the 2nd pass. Therefore, two forwarding high pumps are used to drive the water through the membranes in the 2nd pass. However, the high salinity retentate from the 1st pass is discharged into drain system (position 4). The permeate streams of 2nd pass are gathered to form the plant product stream, which is collected in product tank with salinity around 2 ppm (position 3). However, the low salinity retentate stream from the 2nd pass (position 2) is recycled back to be coupled with the main stream of raw water (with salinity 1098.62 ppm). Fig. 1 depicts the configuration of BWRO plant which contains 120 membranes, 20 pressure vessels (6 membranes in each) and includes two passes with retentate reprocessing design. The 1st pass comprises 2 stages arranged in parallel of 6 pressure vessels with configuration (4:2) and the 2nd pass comprises 3 stages of 4 pressure vessels with configuration (2:1:1).

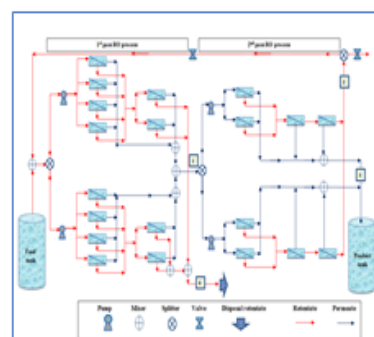


Fig. 1. Schematic diagram of BWRO desalination plant of APC.

**Results and discussions**

Table 1 presents the simulation results of energy consumption with the tested recycle ratio of the 1<sup>st</sup> pass retentate at fixed operating pressure and raw water concentration. The results indicate the possibility of increasing the product capacity by around 3% with 100% retentate recycle ratio of the 1<sup>st</sup> pass which involved a slight increase of product concentration from 1.937 to 2.974 ppm at the same operating conditions. Basically, the energy consumption is significantly increased by around (15%) as a response to this variation. Table 2 presents the simulation results of several performance indicators with 40% and without recycle mode for comparison purposes.

Table 1. The energy consumption simulation results with variation of recycled retentate

Recycle ratio	10%	20%	30%	40%	50%
Power consumption (kW/m <sup>3</sup> )	0.980	0.972	0.967	0.960	0.914
Recycle ratio	60%	70%	80%	90%	100%
Power consumption (kW/m <sup>3</sup> )	0.929	0.944	0.959	0.975	0.992

Table 2. The simulation results of process performance indicators with 100%, 40%, and without recycle mode.

Process performance at recycle ratio from 1 <sup>st</sup> pass = 0% (APC plant)	Process performance at recycle ratio from 1 <sup>st</sup> pass = 40 %	Process performance at recycle ratio from 1 <sup>st</sup> pass = 100 %	
Rec_plant (%)	99.804	99.811	99.801
Rec_plant (%)	51.898	46.828	40.981
Co_plant (m <sup>3</sup> /h)	42.991	44.578	45.237
Co_recycle from 2 <sup>nd</sup> pass (m <sup>3</sup> /h)	15.005	12.095	8.126
Co_plant (ppm)	1.937	2.219	2.975
Co_recycle (ppm)	169.139	228.545	268.465
power consumption pump (KWh/m <sup>3</sup> )	0.948	0.900	0.991

**Conclusions**

The simulation is carried out at fixed raw water flow rate, concentration, pressure, and temperature. This in turn explored that 100% retentate recycle can result in the increased production capacity (although with increased salinity of the product water and energy consumption) compared to no recycle mode that is currently being used in the RO process of APC plant. However, note that the product water quality (2.975 ppm) is still much below the recommended drinking water salinity limit (~200 ppm) set by various countries of the world.

**References**

- Al-Obeidi, M. A., Alsarayreh, A. A., Al-Hroub, A. M., Alsadaie, S. & Mujtaba, I. M. 2018. Performance analysis of a medium-sized industrial reverse osmosis brackish water desalination plant. Desalination, 443, 272-284.